DEVELOPMENT OF IN-SITU COATED LACTOSE PARTICLES DURING SPRAY DRYING

A thesis presented in fulfilment

of the requirements for a degree of

Doctor of Philosophy

in Chemical and Process Engineering

University of Canterbury

New Zealand

MICHAEL BRECH

JULY 2014

LOGIC BRINGS YOU FROM A TO B;

IMAGINATION BRINGS YOU EVERYWHERE.

-Albert Einstein-

ABSTRACT

Lactose is used in many food/pharmaceutical products, despite powders containing amorphous lactose being difficult to handle because they tend to be sticky and are prone to crystallization and powder caking. There is therefore a market for lactose powder with improved functionality to facilitate powder handling. In this work, spray-dried lactose powders containing low concentrations of edible additives were produced in order to investigate the ability of these additives to accumulate at the droplet surface during drying to form a coating that improves powder functional properties and limits powder caking. This thesis presents the results of the trials necessary to develop this "one-step spray coating" process and, by way of experiments and numerical modelling, elucidates how the additives were able to improve the functionality of the lactose powder.

Lactose/sodium caseinate (Na-Cas) powders were made by spray drying solutions with various ratios, feed and spray dryer conditions, and it was found that lowering TS and using a pH closer to the isoelectric point (pI) of the protein resulted in higher protein accumulation at the particulate surface. When the protein concentration exceeded 5wt% in the bulk, its surface concentration plateaued at around 70 to 80% due to the aqueous surface becoming saturated with protein, and lactose binding to adsorbed proteins. Changing the drying rate by changing the spray dryer air inlet temperature and droplet size (via nozzle air pressure), did not change the surface composition of the dried particulates, which indicates protein adsorption and saturation of the droplet surface occurred well before the droplet solidified, even at shorter drying times (higher drying air temperatures or smaller droplets). Using sugars more soluble than lactose (sucrose or maltose) did not affect the surface accumulation of the protein. No crystallization was observed for any of the spray-dried powders, which shows that, irrespective of the sugar tested, a glass was formed that allowed protein mobility well above the solubility limit of the sugar.

The surface compositions of spray-dried lactose/Na-Cas powders were compared with those of thin (slowly) dried films of the same composition to investigate the effect of different drying systems on the surface accumulation of surface active proteins. Higher Na-Cas surface concentrations were found for spray-dried particles, compared with dried films. Results indicate that during film and spray drying, surface-active molecules, such as proteins, accumulate at the droplet surface due to their surface activity, but only during spray drying

can they be further packed above their saturation concentration due to other effects, such as moisture content gradients or a possible Peclet number effect, capable of driving further solute segregation between lactose and protein. Moreover, the reducing surface area of drying droplets may have caused a further packing of adsorbed proteins.

Other surface active additives, such as whey protein (WPI), gelatine, hydroxylmethyl cellulose (HPMC) and lecithin were also investigated as coating additives for lactose. It was found that all of these enriched at the droplet surface during spray drying and dominated the particulate surface. When large added molecules, such as Na-Cas, gelatine, WPI or HPMC, accumulate at the particulate surface and bind to lactose, they raise the glass transition temperature there. The higher glass transition temperature decreased particle stickiness, which resulted in increased spray dryer yields and less agglomerated powders with improved flowability, particularly for HPMC. Higher glass transition temperature also reduced surface crystallization for Na-Cas and HPMC-coated lactose powder when the surface was exposed to a humid environment, as shown by SEM, and therefore prevented neighbouring particles from caking together which preserved the powder flowability after crystallization (10 and 20 dry wt% of HPMC or Na-Cas, respectively, were required). Lactose crystallization was delayed in lactose powders containing lecithin, milk fat, WPI, Na-Cas, gelatine and HPMC as additives. This effect increased with higher additive bulk concentration, in particular for large, polar molecules, such as gelatine, HPMC and Na-Cas, that can form more and larger complexes with lactose; moreover, when HPMC and Na-Cas were present in the bulk the particulate structure was retained upon lactose crystallization because the particles remained rigid as the powders absorbed moisture.

Large, flexible additives, such as HPMC, gelatine or Na-Cas, confer elasticity to the particle wall, which then stretches during drying due to the formation of vapour vacuoles within the particles. As a result, larger particles of lower density were produced, in particular when using HPMC as additive. Powders with larger particles flowed more easily, but the lower particulate density meant that wetting ability was reduced. Moreover, the reorientation of non-polar parts of a protein or polymer upon adsorption made the particulate surface less polar, which further contributed to poor powder wetting, in particular with HPMC-containing powders, which had the lowest density and tended to form a viscous gel-layer upon dissolution. Changes in the total solid content (TS), feed pH or air inlet drying temperature did not have an obvious effect on the powder functional properties, lactose crystallization or caking of lactose/Na-Cas powders, while a lower atomization pressure produced larger

particles with improved powder flows. It was found that wettability, dissolution and also powder flow were significantly improved when the powders were produced by a larger scale spray dryer and when the TS content of the starting solutions was increased, probably due to the formation of larger, more dense, agglomerated particles. The presence of two surface active additives was found to be useful to tailor powder properties, for example, HPMC ensures good powder flow while lecithin ensures instant wetting. HPMC was the only additive capable of displacing other surface active molecules, such as proteins (Na-Cas or WPI) or lecithin, completely from the drying droplet surface during spray drying. Furthermore, when lactose was spray-dried together with a protein and HPMC, the release of the protein in water was delayed with increasing HPMC concentrations, particularly when using HPMC with higher molecular weight. This could have useful applications in the production of coated powders or tablets with a delayed, controlled drug release.

ACKNOWLEDGEMENTS

First of all, I want to express my sincere gratitude for the constant support and help of my supervisor Justin Nijdam, who didn't mind having lengthy meetings and discussions in order to help me out wherever possible. Thank you very much Justin for your encouragement and enthusiasm for this project, together with the many laughs, which made the whole experience very exciting and fun. Thank you for your excellent supervision, which was always characterized by respect, warmth and openness.

I also want to thank my co-supervisors David Pearce, Payel Bagga and Lu Zhang from Fonterra Research and Development Centre (FRDC) for their support throughout my Ph.D, for their always helpful conversations and advice, and for all the exciting meetings and catch-ups at FRDC. Thank you so much for the open and warm supervision, for giving me direction and for helping out wherever possible. Thanks are also due to Sue Adams, for her support in the scale-up spray drying run at FRDC. I gratefully acknowledge the financial support I received from the FRDC, who provided a Ph.D scholarship enabling research in this area.

I want to thank the whole CAPE technical staff, in particular Michael Sandrige, Leigh Richardson, Bob Gordon, Tim Moore, Stephen Beuzenberg, Stephen Hood, Tony Allen and Glenn Wilson, for great support and advice and for the many laughs we had. You did a great job in helping out and I appreciated your always friendly, cheerful and respectful manner. Special thanks go to Michael Sandrige for the personal advice and for helping out so frequently with the analytical instruments, and to Leigh Richardson for fixing my spray dryer whenever it was becoming grumpy, and for always having a cheerful word.

I also want to express my gratitude to the CAPE academic staff for the administrative support. Thanks to you, in particular, Ranee Hearst; you did an absolutely great job. Thanks also to Ken Morison, Richard Jordan, Garrick Thorn, Gabriel Visnovsky, Aaron Marshal, Simone Dimartino and Peter Gustomski for the support and help, good conversations and laughs.

I also want to thank the technical staff from other departments of the University of Canterbury, in particular Neil Andrews (Biological Sciences) and Matthew Polson (Chemical Sciences) for their technical support in SEM and XRD, and Rob McGregor (Chemical Sciences), for cutting many of my glass plates free of charge. Thanks also to the staff of other

New Zealand universities, in particular Colin Doyle and Catherine Hobbis (Auckland University, Research Centre for Surface and Material Sciences) for their assistance with XPS and SEM, and Warwick Johnson and Ivan Simpson (Massey University) for helping out with the homogenization of my fat-lactose solutions, free of charge. Thanks to Formula Foods Corporation for their assistance in carrying out the vapour sorption analysis of the powders. Thanks to DFE Pharma (Germany), in particular Gerald Hebbink (Scientist) and Wouter Noordman (Project Manager) for their project cooperation in testing one of my polymer-coated lactose powders in pharmaceutical tablets. Thanks also to Rocky Hudson for helping out in proofreading my Ph.D thesis.

Lastly, I want to thank my family back in Germany, in particular my mother and father, for their constant support and unconditional love and for believing in me, often more than I did myself. Thanks to all my sisters and brothers for cheering me up in difficult times. I love you all and look forward to soon being united with all of you.

TABLE OF CONTENTS

NOMENCLATURE

Roman Symbols

Symbol	Explanation	Units
A	Surface area	m^2
$A_{film}^{(0)}$	(Initial) Film area	m^2
a_w	Water activity	-
$c_{w,sat}$	Partial concentration of water vapour at its saturated surface	kg/m^3
$c_{w,\infty}$	Partial concentration of water vapour in the air	kg/m^3
$d/dt(N_w)$	Convective molar flux of water	mol/s
D_i	Diffusion coefficient of solute i	m^2/s
D_W	Fickian diffusion coefficient	m^2/s
D_W^s	Fickian diffusion coefficient (solute-fixed coordinate)	m^2/s
$\dot{E}$	Evaporation velocity of film	m/s
h	Heat transfer coefficient	$W/(m^2.K)$
H	Initial film thickness	m
i	Number of nodes (for numerical modelling)	-
j_W^S	Water flux at air-water boundary	kg/s
k	Material specific constant	-
kT	Thermal energy	W
k_c	Convective mass transfer coefficient	m/s
K_B	Boltzmann constant	-
L	Characteristic length	m
m	Boundary nodes (distance grids) across drying film	m
$\dot{m}_w$	Evaporation rate of water (area specific)	$kg/(m^2.s)$
M_W	Molar mass of water	kg/kmol
n	Time grids across drying film	s

p	Pressure	$kg/(m.s^2)$
p_{atm}	Atmospheric air pressure	$kg/(m.s^2)$
$p_{w,sat}$	Partial water vapour pressure at its saturated surface	$kg/(m.s^2)$
$p_{w,\infty}$	Partial water vapour pressure in the air	$kg/(m.s^2)$
Pe_i	Peclet number of component i	-
R	Universal gas constant	J/(mol.K)
R_i	Hydrodynamic radius of molecule i	m
R_{cond} / R_{conv}	Resistance to heat conduction versus heat convection	-
t	Time	s
T	Temperature	K
T_{air}	Air temperature	°C
T_{WB}	Wet bulb temperature	°C
T_g	Glass transition temperature	°C
T_{g1}	Glass transition temperature of component 1	°C
T_{g2}	Glass transition temperature of component 2	°C
T_{surf}	Surface temperature of a material	°C
v	Velocity	m/s
V	Volume	m^3
$V_{film}^{(0)}$	(Initial) Film volume	m^3
$w_{1(2)}$	Mass fraction of component 1 (2)	kg/kg total
x_i	Mass fraction of component i	kg/kg total
x_s	Mass fraction of the solute	kg/kg total
$X_W^{(0)}$	(Initial) Water content (dry)	kg /kg dry
$\overline{X}_W$	Average water content across aqueous film (dry)	kg /kg dry
y	Spatial variable (distance across wet film)	m
y_{max}	Initial wet film thickness	m
z	Spatial variable (distance across dry film)	m
z_{max}	Dry film thickness	m

Greek Symbols

Symbol	Explanation	Units
γ	Surface tension	mN/m
Δy	Cell sizes across wet film	m
Δz	Cell sizes across dry film	m
Δt	Time steps	s
η	Kinematic viscosity	m^2/s
κ	Shrinkage rate of drying droplet surface	m^2/s
λ	Wavelength	m
μ	Dynamic viscosity	Pa.s
ρ_i	Density of component i	kg/m^3
ρ_s	Density of dry film containing multiple components	kg/m^3
$\rho_{sol}^{(0)}$	(Initial) Density of solution containing multiple components	kg/m^3
ρ_W	Density of water	kg/m^3
φ_s	Volume fraction of the solute	m^3/m^3

Abbreviations

A_{280}	UV absorbance at 280 nm
AMF	Anhydrous milk fat
Bi	Biot number
BSA	Bovine Serum Albumin
Da	Dalton
DSC	Differential Scanning Calorimetry
DVS	Dynamic Vapour Sorption
HPMC	Hydroxylpropyl methylcellulose
Na-Cas	Sodium caseinate
J	Joule
O/W	Oil in water (emulsion)
N	Newton
pI	Isoelectric point
PPI	Pea protein isolate
Pe	Peclet (number)
RH	Relative humidity
SDS	Sodium dodecyl sulfate
SEM	Scanning Electron Microscopy
SSL	Sodium stearoyl lactylate
Tween-80	Polysorbate 80
TS	Total solid (content)
vdW	Van der Waals
WB	Wet bulb
WPI	Whey protein isolate
wt%	Weight %
XRD	X-ray Diffraction
XPS	X-ray Photoelectron Spectroscopy

1. INTRODUCTION

1.1. RATIONALE

The dairy industry is the biggest industry in New Zealand and represents around a quarter of all New Zealand merchandise exports. New Zealand's largest company is Fonterra, a cooperative owned by more than 10,000 New Zealand farmers. Fonterra is the world's largest milk processor as well as one of the leading export dairy companies worldwide. It produces more than 2 million metric tons per year of dairy ingredients and consumer products, 95% of which are exported. To improve the durability and storage of milk and other dairy products, dairy powders are commonly produced by spray drying, which transforms a concentrated solution, for example liquid milk, into a dried powder form (Pisecky, 1997). This facilitates the export of the dairy products significantly and saves transport costs (Masters, 1979). A basic flow diagram of a spray drying system (open-cycle) is illustrated in Figure 1.1. A concentrated solution is commonly atomized into small droplets by using appropriate nozzles, located at the top of the spray dryer. The heated air supplied through the inlet stream provides the energy for drying the droplets and transforming them into particles, which are separated from the moist air by efficient particle separators, such as cyclones (Masters, 2002; Pisecky, 1997). Industrial-scale spray dryers commonly also include a bag filter system to separate the fines from the air (Masters, 2002; Pisecky, 1997).

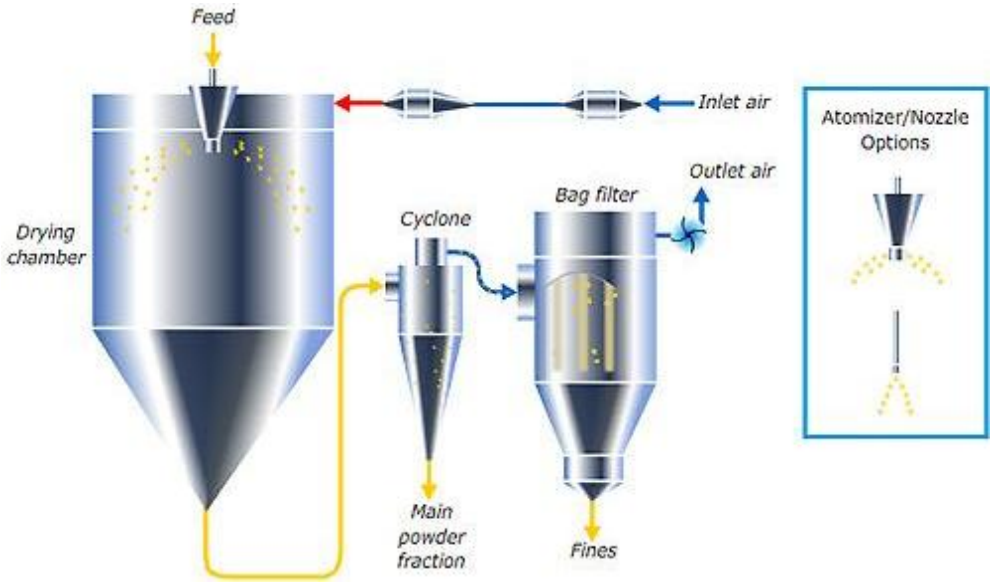

Figure 1.1: Flow diagram of a spray dryer: Open-cycle system, with bag filter attached to separate the fines (GEA, Niro).

Lactose, a natural component in milk, is a disaccharide carbohydrate (milk sugar), which exists in many varieties of dairy products, ranging from yoghurt and cheese to ice cream and dairy drinks (Ganzle et al., 2008; Lifran et al., 2000). The amount of lactose in a food product depends on the nutritional, calorific and functional properties required (Ganzle et al., 2008). Lactose has unique value as a food component because it provides sweetness and calorific energy, and more importantly, is a very good flavour-binding agent and fat replacer (Holsinger & Kligerman, 1991; Listiohadi et al., 2005; McSweeney & Fox, 2009). However, lactose manifests in different states and has temperature-dependant physicochemical properties (Ganzle et al., 2008). Over time and given sufficient moisture, amorphous lactose within a food product will crystallize and the resultant lactose crystals will grow in size. This can introduce an undesirable gritty texture in the food system (Ganzle et al., 2008). Moreover, when not stored properly in a dry environment, spray-dried dairy powders tend to cake, mainly because amorphous lactose has a high degree of stickiness, and this caking is followed by lactose crystallization (Listiohadi et al., 2005). Hence, it has been a formulation challenge for dairy researchers to manipulate lactose in food systems so as to reduce the gritty texture and prevent powder caking induced by lactose crystallization.

The aim of the proposed project is to coat lactose particles with other food components (for example proteins, polymers or fat) during spray drying in order to produce a value-added, free-flowing and non-caking lactose powder that can be easily blended into other dairy products, such as dry-powder soups or drinks, and non-dairy products such as chocolate bars. The principle of particle coating during spray drying (*in-situ coating*), which exploits the phenomenon of solute segregation of different components within the drying droplet, was used for the purpose of producing such powders. Several authors have stated that, during the spray drying of milk or protein/sugar solutions, the surface active proteins preferentially adsorb at the droplet surface at the expense of the sugar, and this results in an accumulation of proteins on the surface of spray-dried particles (Fäldt & Bergenståhl, 1994; Gaiani et al., 2011; Kim et al., 2002, 2009a; Nijdam & Langrish, 2006; Wang & Langrish, 2010). Several other components, such as surfactants, fat, large carbohydrates and polymers, have also been found to enrich at droplet surfaces during spray drying, at the expense of smaller, non-surface active components such as lactose (Adhikari et al., 2009b; Elversson & Millqvist-Fureby, 2006; Jayasundera et al., 2010a; Kim et al., 2009b; Millqvist-Fureby & Smith, 2007; Nijdam & Langrish, 2005).

This "spray coating" process can be used as particle coating technique in the dairy industry in order to alter surface properties and thereby allow manufacturers to create powders with desirable properties such as flowability, wettability or dispersibility (Sollohub & Cal, 2010; Wan et al., 1992b). The accumulation of larger molecules, such as proteins or polymers, on the surface of a drying droplet has been shown to reduce the stickiness of spray-dried, sugar-containing food powders due to the higher glass-transition temperature of the adsorbed larger molecules, and this results in better powder recoveries (Adhikari et al., 2009b; Wang & Langrish, 2010). Hence, a suitable coating could presumably increase the powder yield, improve powder flow and protect the amorphous lactose against re-crystallization and excessive caking. This coating process also has potential to be used in the pharmaceutical industry to protect sensitive active drugs and/or to effect a retarded drug-release (Elversson & Millqvist-Fureby, 2006; Takeuchi et al., 1998).

1.2. SIGNIFICANCE OF THESIS

This novel technique of "spray coating" has the potential to add significant value to dairy product formulations with lactose content. Most of the dairy companies in New Zealand will benefit from this technique. It has been forecast that by 2015 Fonterra will produce up to 120,000 million ton per year of excess permeate solids, the main component of which is lactose. The current high demand for lactose is driven by the allowance of standardising of the milk proteins by addition of lactose solids to reduce the protein content (in New Zealand) or by addition of milk retentate to boost the protein content (in parts of Europe) (D. Pearce, Fonterra Cooperative Group Ltd, Personal Communication, 2014). The added value coated lactose powder will increase the market need and add value to lactose by transforming it from a commodity to a functional food ingredient. If successful, this value-added opportunity could deliver an additional USD 35-70 million per annum in revenue (estimated by Fonterra).

Besides the high market potential of coated lactose powder for the New Zealand dairy industry, a successful spray-dried lactose powder with non-gritty, non-reactive functionality will also be sought after by other (non-dairy) food companies, such as confectionary and chocolate producers and pharmaceutical companies, who will benefit from the unique spray coating process presented in this thesis. Caking of lactose (or other sugar-containing) powders could be prevented by efficiently protecting the unstable amorphous sugar beneath the coating layer. The product quality of sugar-containing food products could be

significantly increased by preventing the "sandiness" effect, caused by the crystallization of the sugar when crystals grow to sizes of over 10 to 16 microns (Ganzle et al., 2008). When the coating material consists of large, high-molecular-weight molecules with a higher glass transition temperature than the main "inner" component, particle stickiness could be reduced due to the overall increase in glass transition temperature of the particle surface. This could result in higher product yields as well as improved powder flowability for coated as opposed to non-coated powders, and therefore would reduce the cost of spray-dried products.

The development of a one-step spray coating process for producing stable, amorphous lactose powder might additionally offer a cheaper alternative to the expensive crystallization process currently employed. Regardless of whether the spray-dried material is to be used in the food, chemical or pharmaceutical industry, a coating on the surface of any sticky particles could generally be exploited to protect the active material against environmental impacts such as moisture or oxygen uptake, or to prevent direct contact with the human skin. Spray-dried lactose powders coated with hydrophilic polymers during spray drying could be used, for example, as pharmaceutical excipient in oral solid dosage formulations such as controlled-release tablets, hence obviating the coating of the whole tablet following pressing (Ré, 2006), thus saving production costs. A one-step spray coating process could be also used to develop multi-layered coatings, which might be used, for example, to place an active component such as a catalyst at the particle surface (Trueman 2012). Furthermore, particle characteristics could be changed and thus functional properties of the powder altered (Sollohub & Cal, 2010; Wan et al., 1992). Because particle size and density are highly dependent on the physical properties of the adsorbing species during drying (Vehring, 2008), powder bulk density, powder flow, wetting properties and dissolution of the powder can be affected and, in the best case, controlled.

A good understanding of the mass transfer of different solutes within the drying droplet is therefore necessary to control the surface accumulation of different species and therefore create custom powders with unique properties. Different particles could be specifically "engineered" for different purposes, for example where an improved powder flow, improved powder dispersibility or a controlled drug release is desirable. Hence, this Ph.D thesis aimed to further contribute to a deeper understanding of solute segregation phenomena during spray drying, in order to increase the current knowledge of how the particle surface composition and thus particle and final powder properties can be controlled.

1.3. SCOPE OF THESIS

During this Ph.D project, the mechanism of *in-situ coating* was exploited to produce protective coatings for spray-dried amorphous lactose powder by using small fractions of additives with the ability to enrich at the air-water interface during spray drying. The goal of this project was to identify edible protective barriers for lactose particles that effectively protect the encapsulated amorphous lactose against excessive stickiness and powder caking. Different surface active proteins, fats, polymers and other suitable materials were investigated to determine their effectiveness as a protective barrier in terms of surface coverage as well as limitation of moisture sorption and subsequent lactose crystallization. The mechanisms of solute segregation during spray drying were investigated in order to understand how the surface composition of spray-dried powders might be controlled. Identification of promising composites for coating the lactose was within the scope of the thesis, in order to prevent the presence of amorphous lactose on the surface of the particles. The aim was for the coating material to give a 100% surface coverage. In that case, the coating would prevent lactose crystallization on the surface of the particles which, in turn, should prevent the caking of the powder. Even in the case of lactose crystallization within the particles, the lactose crystals of neighbouring particles should not be able to grow together due to the protective physical barrier of the coating, hence powder caking could be possibly prevented.

Optimal flowability, stability (against lactose crystallization and powder caking) and wettability were further desirable qualities of the coated lactose powders. An important approach was to therefore develop a coating that would stabilize a powder and enhance its shelf-life by delaying moisture from absorbing into the particles in order to limit—or, in the best case, prevent—lactose crystallization. A non-hygroscopic material would be the most suitable for that purpose. A hydrophobic coating, such as a fat layer, might delay sorption of water vapor into the particle. Thus, milk fat was tested as a possible coating additive. Other additives that were investigated as edible coatings for lactose included milk proteins, lecithin and other suitable wall-materials such as gelatine and bio-polymers.

In addition to investigating suitable edible coating materials, the optimal spray dryer configuration and operating conditions needed to be developed to ensure an optimal surface enrichment of the coating material. A good understanding of the mass transfer within the drying droplets was necessary in order to be able to control surface enrichment. Although

different theories abound in the literature, there is currently no consistent agreement on how components within a drying droplet segregate, due to the high complexity of the topic and differences in the behaviours of different coating additives. This Ph.D thesis aimed to contribute towards a deeper understanding of the mechanisms involved in solute segregation during drying by 1) making comparisons between the surface enrichment of an additive in two very different drying systems — very fast drying droplets (via spray drying) and slow drying thin films of aqueous lactose/additive, 2) modeling possible moisture gradients within drying films and 3) investigating competitive adsorption between different competing species (protein, surfactant, polymer) that vary in molecular size and surface activity. Moreover, the study used two different spray dryers, a laboratory spray dryer and also a pilot-scale spray dryer (located at Fonterra Research and Development Centre (FRDC)), in order to compare the surface accumulation of the coating additive, as well as powder stability and powder functional properties, between small and larger scale spray drying.

It was highly desirable to use this acquired knowledge about solute segregation to develop a coated lactose product for food or pharmaceutical applications. Hence, the one-step spray coating process was exploited to produce a polymer coated lactose powder with potential applications in the pharmaceutical industry, for example in oral solid formulations such as capsules or tablets. Lactose is commonly used in pharmaceutical tablets as a filler and binder (Gohel & Jogani, 2005; Gonnissen et al., 2007). The one-step coating process, presented in this thesis, aimed to produce a coated pharmaceutical powder consisting of the active pharmaceutical ingredient (API, for example a protein) and lactose, both encapsulated by a polymer matrix such as hydroxypropyl methylcellulose (HPMC). This facilitated process may therefore offer an alternative method for producing tablets, which are conventionally manufactured by blending the API and lactose (non-coated), and then pressing them (together with other additives) into a tablet (Gohel & Jogani, 2005; Gonnissen et al., 2007), which often needs post-treatment coating with HPMC to achieve the desired retardation in drug release (Gao et al., 1996; Tahara et al., 1995).

1.4. STRUCTURE OF THESIS

Chapter 2 is a literature review which serves to provide the reader with the necessary background information, summarize the literature relevant to the *in-situ coating* of spray-dried powders, and set this Ph.D thesis in the context of other research done in the area of microencapsulation / coating during spray drying.

In Chapter 3, experiments are described in which the milk proteins Na-caseinate (Na-Cas) and whey protein (WPI) were used as model proteins to explore the following: A) protein surface enrichment during spray drying, B) powder functional properties, such as powder flowability, wettability, and powder bulk density, C) powder morphology and D) powder moisture sorption, lactose crystallization and powder caking. For this purpose, various parameters were manipulated such as lactose/protein ratios, total solids (TS) content, solution pH and different spray drying parameters (namely the inlet and outlet air temperature and the atomization pressure).

The first part of Chapter 4 investigates the relevance of different solute segregation mechanisms proposed in the literature for spray drying involving microencapsulation, focusing on Na-Cas as the coating additive. A numerical model was established to help elucidate the effect of moisture content gradients on solute segregation. A spray drying versus film drying study was performed in order to compare solute segregation between protein and lactose in different drying systems (droplet versus film). This helped to differentiate different mechanisms for solute segregation. Lactose/Na-Cas ratio, total solid content and film drying temperature were varied in this study. The second part of the chapter looks at the effect of process scale-up on the Na-Cas surface enrichment. Powders from a laboratory-scale and a pilot-scale spray dryer were compared. In addition to surface protein concentration, this study considered the powder stability—with regards to lactose crystallization and powder caking—as well as the powder functional properties and powder morphology of spray-dried lactose/Na-Cas powders produced on these two different scales.

Chapter 5 investigates the potential of different coating additives, such as gelatine, lecithin, HPMC polymer and milk fat, to enrich on droplet surfaces during spray drying of aqueous lactose solutions. The coating ability of these additives could then be compared with that of the previously tested milk proteins Na-Cas and WPI. The effect of the different coating additives on powder functional properties, powder moisture sorption, lactose

crystallization delay, powder caking and powder morphology was also investigated in order to determine which of the tested additives is the most promising coating additive for spray-dried lactose powder. The second part of the chapter describes a competitive absorption study in which two different coating additives, differing in molecular weight and surface activity, were simultaneously spray-dried together with lactose as the main component. This study aimed to build on the information about solute segregation phenomena obtained through the work described in Chapter 4, and also to investigate the effect of binary coating additives on powder functional properties and powder morphology.

Chapter 6 investigates the unique properties of the polymer HPMC as a coating additive. The first part of the study looked at the effect of the molecular weight of HPMC on surface enrichment during drying, powder morphology and powder functional properties. The second part of the study looked at possible applications of a lactose/protein/polymer powder, produced via the one-step spray coating process, in pharmaceutical applications, for example in tablets. The ability of HPMC to retard the release of the protein Na-Cas out of the particle into water upon powder dissolution was investigated. HPMC at various concentrations was spray-dried together with Na-Cas (representing the API) and lactose (the bulk component). As an excipient in oral dosage applications, such as tablets, this powder would have the advantage of affecting a controlled, delayed release of the API.

The thesis finishes with an overall conclusion and recommendations (Chapter 7).

2. LITERATURE REVIEW

2.1. LACTOSE

This work used lactose as the main component of solutions to be spray-dried. Various other additives, such as proteins, lipids or polymers, were also added to the solutions to coat the lactose powder during spray drying. This section describes basic information about the properties and material behaviour of lactose, its industrial manufacture, and its use.

2.1.1. Properties and applications

Lactose, also known as milk sugar, is the most abundant component in the milk of most mammals, and exists in a variety of different food products such as yoghurt, cheese, ice cream, dairy drinks and chocolate snacks (Ganzle et al., 2008; McSweeney & Fox, 2009). Lactose reduces sweetness, enhances texture and flavour, provides calorific energy and extends the shelf life of many food products, but also has its special uses as a flavour-binder, a fat replacer and as a pharmaceutical excipient for oral-solid formulations (Holsinger & Kligerman, 1991; Listiohadi et al., 2005; McSweeney & Fox, 2009).

Lactose is a disaccharide composed of one glucose molecule bound to a galactose molecule by a glycosidic linkage (Listiohadi et al., 2005), as illustrated in Figure 2.1. This glycosidic linkage is common to all carbohydrates. Aqueous solutions of lactose contain two isomeric forms, α- and β-lactose, which have different physicochemical properties (Shawqi Barham et al., 2006). The difference between the two forms of lactose is the configuration of the terminal hydroxyl group of the glucose moiety, as illustrated in Figure 2.1. In solution, both forms are in equilibrium and change into one another continuously. This mutarotation is dependent on the temperature, with slightly higher transformation into the α form with increasing temperatures, but is independent of the pH (McSweeney & Fox, 2009).

Table 2.1: Application and uses of lactose in food and pharmaceutical products (Lifran et al., 2000)

Application	**Use for**
Infant formulae	Nutritional balance, energy source
Baked goods	Enhanced shortening emulsification, controlled browning, flavour and colour carrier
Beer	Flavour and colour carrier
Confectionery, syrups, fruit pie, canned fruits, honey powder	Increased osmotic pressure and viscosity, improved texture, enhanced aroma, improved smoothness and chewiness, extended shelf life
Sweetened condensed milk, frozen dessert, ice-cream and other dairy products	Price advantage
Frozen and concentrated milk, coffee whiteners	Stabilisation of proteins
Dry soups and sauces, instant noodles, spices and flavourings	Enhanced flavour, reduced sweetness, extended shelf life, dispersibility
Salad dressing and mustard	Reduced sweetness, extended shelf life, price advantage
Fruit beverages, instant drinks	Health aspects, enhanced aroma and dispersibility
Cocoa, chocolate milk	Reduced sweetness, enhanced aroma, improved texture, viscosity and cost
Meat and sausages	Reduced sweetness, extended shelf life and price advantage
Table and capsule excipient	Filler and drug carrier, artificial sweeteners carrier
Instantised pharmaceutical powders	Dispersing agent

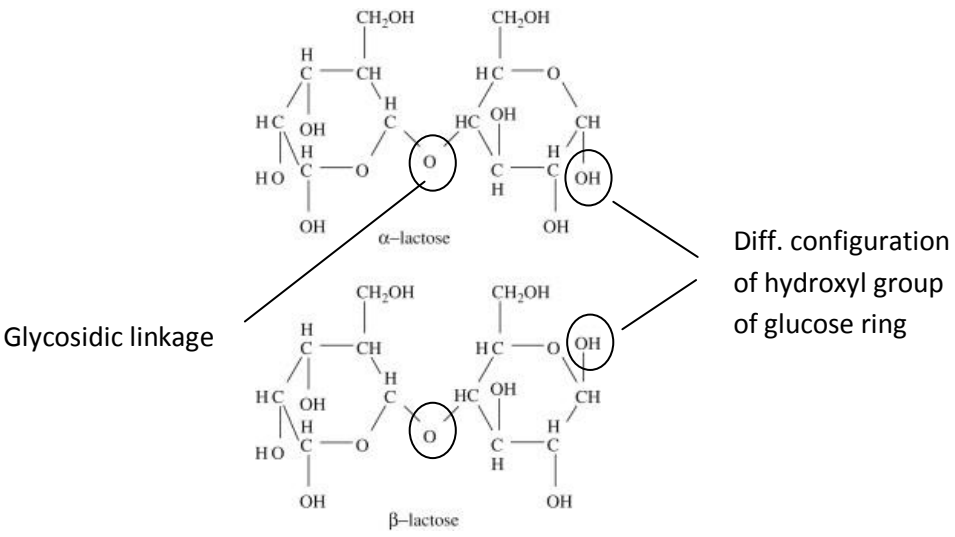

Figure 2.1: Molecular structure of α- and β-lactose (Ganzle et al., 2008).

Figure 2.2 shows the solubility profile of lactose in water, with varying water temperature. The solubility of lactose is low compared to other sugars such as glucose or sucrose (Ganzle et al., 2008; Listiohadi et al., 2005). The dissolution speed of lactose powder depends on its particle size and its isomeric form. Generally, β-lactose dissolves more readily than α-lactose due to its higher initial solubility. However, the final solubility of α- and β-lactose is the same due to the mutarotation equilibrium which occurs automatically within solution (Fox, 1985).

Lactose in the solid state exists either as an amorphous "unstable" powder, where molecules are captured in a highly viscous, glassy state, or as a crystalline "stable" powder, in which the molecules are highly organized, being closely packed into their lowest possible energy state. The manufacture of both these powder forms is described in Section 2.1.2. Amorphous lactose tends to transform over time into the crystalline state, given sufficient moisture (Fitzpatrick et al., 2004). This phase transformation occurs above the glass transition temperature, which is explained in Section 2.1.3.

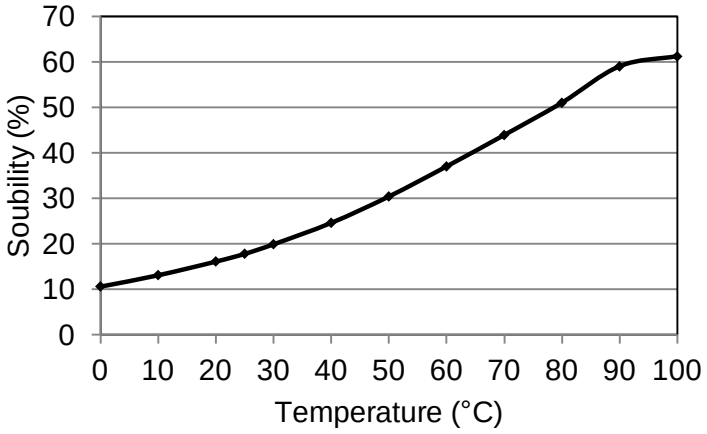

Figure 2.2: Lactose solubility in water as a function of the water temperature

2.1.2. Lactose origin and manufacture

Lactose is a by-product of cheese and casein manufacture. It enriches in the cheese whey during cheese production together with the whey proteins, while the casein proteins remain in the thickening cheese solution (Jelen, 2009). Due to its physical stability, crystalline lactose powder, produced via crystallization, is the preferred form of powdered lactose. Crystallization is induced either directly from the cheese whey or after protein removal by ultrafiltration or heat coagulation (McSweeney & Fox, 2009). There are three basic steps involved in the crystallization process: A) condensing of the whey by a multi-stage evaporation to approximately 50 to 70 % total solids, B) crystallization, either spontaneous or initiated by seeding with fine crystals and C) separation of the crystals from the mother liquor by centrifugation and cleaning of the crystals (McSweeney & Fox, 2009). Lactose solutions can become supersaturated before crystallization occurs (Ganzle et al., 2008). Due to its lower initial solubility, α-lactose crystallizes at lower temperatures than β-lactose. At temperatures below 93.5 °C lactose crystallizes into α-lactose monohydrate, in which a single water molecule is bound to each lactose molecule, while the anhydrous crystalline form of β-lactose only forms at temperatures above 93.5 °C (Listiohadi et al., 2005; Pisecky, 1997). β-lactose is less hygroscopic than the α-form and has a different structure once crystallized (Listiohadi et al., 2005).

For the production of amorphous lactose, spray drying or freeze drying are commonly used techniques. Both methods rely on the removal of water from a solution of lactose in a way that prevents lactose crystallization occurring. During freeze drying, the solution is

frozen and the solvent is removed by sublimation. The frozen, immobilized matrix hinders the rearrangement of lactose molecules into a crystalline structured state (Bhandari & Howes, 1999; Haque & Roos, 2005). Spray drying is a more economical process for the production of pharmaceutical lactose powder. It involves the rapid removal of moisture upon drying, and the sudden increase in viscosity limits the molecular mobility of lactose, so that it is unable to enter an organized, crystalline state (Roos, 2002). However, other authors reported that lactose crystallization during spray drying is sometimes possible, and largely depends on the spray drying conditions such as drying temperature and relative air humidity (Chiou et al., 2008; Islam & Langrish, 2010; Islam et al., 2010a; Islam et al., 2010b). These authors report that high air drying temperatures and high air humidities favour lactose crystallization during spray drying because these conditions reduce the glass transition temperature of lactose and therefore increase its crystallization rate. The principles of spray drying are described in detail in Section 2.3.

Generally, it is not very common to produce a 100% amorphous powder via spray drying, mainly due to the high degree of hygroscopicity and instability of the final amorphous powder and the low solubility of lactose. The latter prevents the spray drying of solutions with high total solids, in which the solubility limit is exceeded. A high total solids content is desirable because this reduces the process costs, since less water must be evaporated. When lactose is to be used as a pharmaceutical excipient in oral solid forms, it usually needs to be converted to a partly amorphous/crystalline lactose powder with a spherical particle form (Sollohub & Cal, 2010). This spray-dried powder, which is made by spray drying a solution in which refined lactose crystals have been only partially dissolved, consists of lactose crystals which are bound together by the continuous matrix of the amorphous lactose. Due to its spherical shape, this spray-dried powder has improved final flowability, compressibility and binding properties, compared with the non-treated crystalline α-lactose monohydrate. Thus, this modified powder has the properties required for direct compression into a tablet. (DMV-Fonterra Excipients GmbH & Co.KG, Technical paper: Directly compressible lactose).

Amorphous lactose is very common in dairy powders such as milk powders, milk protein powders and other powders derived from milk (Jelen, 2009; Pisecky, 1997). The solutions are commonly concentrated via evaporation, to increase the total solids content, and then spray-dried (Pisecky, 1997). The amorphous lactose within those spray-dried powders has

implications for powder stability, as it tends to re-crystallize into the crystalline form and therefore causes powder stickiness and caking, as explained in more detail in Sections 2.1.3 to 2.1.5.

2.1.3. Glass transition and stickiness

The glass transition of a molecule describes the reversible transition of an amorphous solid from a highly viscous, glassy state to a sticky, rubbery state. An amorphous solid is a non-crystalline solid that is formed at non-equilibrium conditions by a fast dehydration process such as freeze drying, spray drying or roller drying (Bhandari & Howes, 1999). It is generally defined as glass when its viscosity exceeds 10^{12} Pa s (Bhandari & Howes, 1999; Roos, 2002). A glass is in a meta-stable state, which tends to convert into the crystalline state, depending on the temperature and moisture content (Bhandari & Howes, 1999; Flink, 1983; Roos, 2002). The glass transition is related to molecular mobility (Champion et al., 2000; Roudaut et al., 2004). The high viscosity within a glass freezes the amorphous solids so that they exhibit only molecular vibrations and side chain rotation while overall molecular mobility is highly restricted (Bhandari & Howes, 1999; Roos, 2002). During the glass transition, the molecular mobility increases due to a plasticization which allows the translational movement and reorientations of molecules necessary for an orderly re-alignment of molecules into a crystalline state (Haque & Roos, 2004a, 2004b; Roos, 2002; Shrestha et al., 2007).

The glass transition temperature is defined as the critical temperature at which this glass transition occurs. Above the glass transition temperature, there is a sharp decrease in viscosity (*rubbery state*) due to the plasticization of the molecules, where the viscosity falls from around 10^{12} Pa s to a range between 10^{6} and 10^{8} Pa s (Bhandari & Howes, 1999; Champion et al., 2000). The glass transition temperature can be measured experimentally by using differential scanning calorimetry (DSC), which measures a change in heat capacity that occurs over the glass transition temperature range (Bhandari & Howes, 1999). The glass transition temperatures T_g of a binary mixture with various ratios can be expressed by the *Gordon-Taylor Equation* (Equation 2.1) (Gordon & Taylor, 1952).

$$T_g = \frac{w_1 T_{g1} + k w_2 T_{g2}}{w_1 + k w_2} \qquad (2.1)$$

where w_1 is the mass fraction of component 1 (here lactose), w_2 is the mass fraction of component 2 (here water), T_{g1} is the glass transition temperature of component 1, T_{g2} is the glass transition temperature of component 2, and k is a material specific constant (6.4 for lactose) (Jouppila & Roos, 1994b).

Figure 2.3 shows the glass transition temperatures of lactose with varying water content, calculated using Equation 2.1. Amorphous "glass" is characterized by its unstable hygroscopic behaviour in which it tends to absorb moisture from humid air. Anhydrous lactose has a glass transition temperature T_g of around 105 °C (Haque & Roos, 2004a), which decreases as soon as the powder absorbs moisture from the air. As long as the glass transition temperature is above the surface temperature of the product T_{surf}, the powder is in the *glassy state* and is stable as long as it is kept dry and cool. However, if the relative humidity of the air is high enough, the powder will continue to absorb moisture due to its high hygroscopicity.

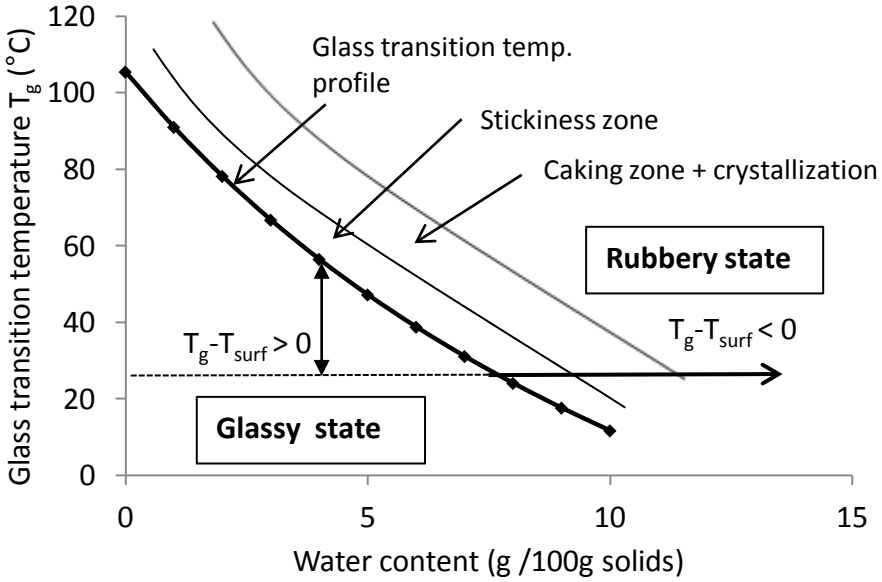

Figure 2.3: Glass transition temperature profile, stickiness and caking zone of amorphous lactose with varying water contents.

Over time and given sufficient moisture, amorphous materials, such as amorphous lactose, plasticize and become sticky. This behaviour occurs when the glass transition temperature T_g of the hygroscopic material has fallen below the surface temperature of the material (T_g - T_{surf} < 0), as shown for lactose in Figure 2.3. This is characterized by a glass transition from the *glassy state* into the *rubbery state*. The *sticky point* is defined as the point where the surface of the lactose becomes sufficiently sticky to allow particles to stick

together. For lactose, this point lies approximately 10 to 20°C above the glass transition temperature (T_{surf} - $T_g \geq 20$°C) (Roos & Karel, 1991a). Powder caking and lactose crystallization start to occur at this point.

Stickiness and glass formation during spray drying of lactose

During the spray drying of a solution of a low-molecular-weight sugar, such as lactose, stickiness of the spray-dried powder can occur near the end of the dehydration process, where the moisture content and temperature of the freshly formed particles are still high (Bhandari & Howes, 1999). This can cause particles to adhere to the spray dryer wall with consequent low powder yields (Adhikari et al., 2007b).

After atomization, the droplet surface is fully saturated and thus the surface water activity is unity. Upon initial dehydration in the upper part of the dryer, a plastic surface is formed due to glass formation during drying, which results in a large increase in solution viscosity. As long as the surface temperature does not rise more than 10-20 °C above the T_g, no stickiness occurs. Further dehydration in the middle part of the spray dryer causes the temperature of the particle surface (T_{surf}) to increase significantly due to the water activity falling below unity once a crust has been formed and saturated surface conditions (and evaporative cooling) can no longer be maintained (Bhandari & Howes, 1999), as explained in Section 2.3.3. When the glass viscosity is below a critical level of 10^7 Pa s, the particle surface becomes sticky, which can cause agglomeration with other particles when they collide with each other and particle adhesion at the dryer wall (Bhandari & Howes, 1999). In the lowest part of the spray dryer, the water content further decreases upon dehydration. Then the glass transition temperature T_g can again rise above the sticky point temperature of the amorphous material and as a result the viscosity of the glass increases above the critical level of 10^7 Pa s, causing the particle surface to become non-sticky (Bhandari & Howes, 1999).

Effect of high-molecular-weight additives on the glass transition temperature of lactose

Bhandari and Howes (1999) state that the glass transition temperature of a mixture of various solutes (including water) is a non-linear function of the glass transition temperatures of the individual solutes. The *Gordon-Taylor Equation* (Equation 2.1) is typically applied to estimate the T_g of a binary mixture, for example lactose-protein. The presence of molecules of higher molecular weight, such as proteins, within a sugar matrix increases the total glass

transition temperature (Roos and Karel (1991b). During spray drying of an aqueous sugar/protein solution, proteins have been shown to enrich at the droplet surface (Adhikari et al., 2009a; Fäldt & Bergenståhl, 1994; Wang & Langrish, 2010). Sugar-protein interactions occur, as described in more detail in Section 2.2.5. This increases the total glass transition temperature of the particulate surface during drying, resulting in higher spray dryer yields due to the particles being less sticky than those of pure spray-dried sugar powders, as shown by Adhikari et al. (2009a) and Wang and Langrish (2010).

2.1.4. Crystallization of amorphous lactose

A time-dependent phase transition from the unstable amorphous state to the stable crystalline state occurs above the glass transition temperature. Due to plasticization of amorphous lactose above the glass transition temperature, lactose molecules attain higher mobility, which allows them to re-organize themselves into a much more organized, lower energy state (Ganzle et al., 2008). Roos (2002) reports that most of the crystals formed are anhydrous β-lactose, but that an increasing amount of α-lactose monohydrate is formed at higher humidities. Other authors also report that a mixture containing various ratios of α-lactose/β-lactose is formed, with the relative proportions depending on crystallization conditions such as temperature and relative humidity (Bushill et al., 1965; Ibach & Kind, 2007; Listiohadi et al., 2005).

The crystallization rate is a function of T_{surf} - T_g. It increases with higher relative humidity and/or higher ambient air temperatures because these conditions promote faster plasticization and thus faster re-organizations of the molecules (Bhandari & Howes, 1999; Haque & Roos, 2005; Jouppila & Roos, 1994a). The different hygroscopicities of amorphous and crystalline lactose mean that most of the absorbed moisture is lost upon crystallization (Bronlund & Paterson, 2004; Haque & Roos, 2004a; Roos, 2002; Shrestha et al., 2007). This is illustrated schematically in a moisture sorption isotherm—a relationship between equilibrium moisture content of the powder and the air humidity (*RH*) the powder is exposed to—of lactose (Figure 2.4), which shows a sudden decrease in water content upon lactose crystallization. Roos (2002) reported that at room temperature, the critical relative humidity, where a phase transition from the glassy to the rubbery state occurs, is at around 37% RH, while lactose crystallization was reported to occur at RH of above 43% and water contents of

around 9 to 10 kg/kg dry (Bronlund & Paterson, 2004; Foster et al., 2005; Haque & Roos, 2004a; Shawqi Barham et al., 2006; Shrestha et al., 2007).

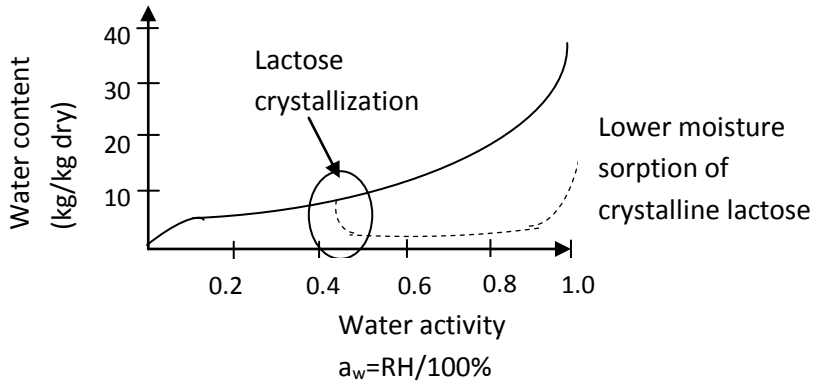

Figure 2.4: Schematic moisture sorption isotherm (25 °C) of amorphous lactose (solid line) and crystalline lactose (dashed line) after lactose crystallization.

Lactose can also crystallize over time within a food product given sufficient moisture, and the crystals can grow in size causing a "gritty" or "sandy" texture on the tongue when the food is eaten (Ganzle et al., 2008). This is highly undesirable, as it makes a product unpleasant to eat and therefore limits its quality. Various crystal shapes can be formed upon lactose crystallization, depending on crystallization conditions and whether crystallization occurs from a supersaturated solution or from an initial glass state (Ganzle et al., 2008; Listiohadi et al., 2005). The most common crystalline shapes are the pyramid, tomahawk, diamond and prism. Prism crystals are commonly formed when the crystallization rate is high, as occurs in supersaturated solutions. Decreasing the crystallization rate of lactose causes a change from the prism shape to diamond-shaped plates, and then to pyramids and tomahawks (Ganzle et al., 2008).

Several authors have reported that, compared to a pure amorphous lactose powder, lactose crystallization in milk powders and other dairy powders, such as whey powders, is delayed, which means that higher RH are required to initiate crystallization of lactose (Berlin et al., 1968; Foster et al., 2005; Ibach & Kind, 2007; Jouppila & Roos, 1994a). Moreover, Haque and Roos (2004a, 2004b) studied the water sorption, plasticization behaviour and lactose crystallization of various lactose/protein mixtures and found that glass transition temperatures and crystallization temperatures of lactose were both increased in the presence of high-molecular-weight proteins. They spray-dried aqueous solutions of 15wt% lactose/protein mixtures at a solid weight ratio of 3:1, and compared WPI, Na-caseinate,

albumin and gelatine with regards to their effectiveness in increasing the glass transition and crystallization temperatures of amorphous lactose. They postulated that the more protein-lactose binding within the matrix, the higher the glass transition and crystallization temperature. All proteins successfully delayed lactose crystallization during storage, with gelatine and Na-Cas being more effective than WPI and albumin. Haque and Roos (2004a, 2004b) postulated that Na-cas and gelatine were the most effective in delaying lactose crystallization because they could interact with lactose to a greater extent.

2.1.5. Powder caking

The caking of an amorphous powder is a time-dependent phenomenon (Bhandari & Howes, 1999) which is difficult to define. Caking and powder agglomeration are often indicated by stickiness and the formation of lumps or a general loss of powder flowability (Listiohadi et al., 2005). Generally, amorphous powders such as lactose become sticky and begin to cake as the viscosity of the glass surface decreases and particles start to adhere to each other, which causes agglomeration. This behaviour starts to occur at the sticky point, which is around 10-20°C above the glass transition temperature (Roos, 2002), as mentioned in Section 2.1.3. A rubbery, sticky cake will form due to the formation of liquid bridges between the particles, which stops the powder from flowing freely. Further plasticization then causes a further reduction in the viscosity of the adhesive particles up to a point where particles become joined, as illustrated in Figure 2.5. This can cause a complete collapse of the particulate structure (Listiohadi et al., 2005). Upon lactose crystallization, the viscous liquid bridges transform into solid crystalline bridges (Listiohadi et al., 2005), in which case a very hard and brittle cake is formed. Within the context of this Ph.D thesis, powder caking is defined as having occurred only when lactose crystallization has transformed the initially flowable powder into a cake. To avoid caking of lactose-containing powders such as dairy powders, the powders need to be stored in such a way so as to protect them from normal environmental conditions, for example, by using vacuum-sealed packaging. Once the packaging is opened, storage in a cool and dry place is required to prevent moisture sorption and thus lactose crystallization.

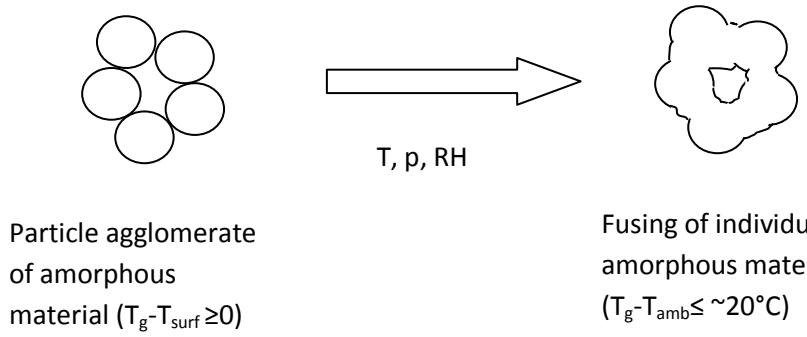

Figure 2.5: Development of powder caking of amorphous material above the glass transition temperature.

2.2. PROPERTIES OF PROTEINS

In the work described in this thesis, proteins were used as the main coating additives within aqueous spray-dried lactose solutions. Their adsorption behaviour during spray drying and their ability to form a non-sticky coat on the surface of spray-dried lactose particles was investigated. Hence, this section of the literature review will provide the reader with an overview of basic protein properties, including their structure, solubility, surface activity and adsorption behaviour at fluid interfaces.

2.2.1. Protein structure

Proteins are polypeptides consisting of chains of amino acids connected by peptide bonds into definite sequences. The chain (the primary structure) is organized into regular substructures known as *α-helix* and *β-sheet* (the secondary structure), which are stabilized by intra-molecular bonds such as disulfide and hydrogen bonds (Haynes & Norde, 1994; Yampolskaya & Platikanov, 2006). Further folding of the polypeptide chain takes place, and the result is a compact, three-dimensional form (the tertiary structure), which is held together by hydrogen bonding, disulfide bonds, and van der Waals (vdW), hydrophobic and electrostatic forces. Different proteins in the tertiary form may organize themselves into a multi-protein complex containing different domains (quaternary structure) (Haynes & Norde, 1994). High temperature, high ionic strength and extremes in pH cause protein denaturation (Magdassi, 1996). During denaturation, the protein structure collapses, causing the intramolecular bonds to break and the hydrophobic protein residues to be exposed towards

the surface (Haynes & Norde, 1994; Magdassi, 1996). Protein denaturation is mostly irreversible and results in protein insolubility and strong aggregation.

2.2.2. Protein functionality and solubility

Proteins are large, complex, amphipathic molecules, which contain ionic, polar and hydrophobic regions (Magdassi, 1996). Many properties of protein solutions are determined by the molecular structure of the protein, which is controlled by its amino acid sequence. Solubility and other related physical and chemical properties such as protein-protein interactions (aggregation), self-association in the bulk and at interfaces (adsorption phenomena), solute binding, surface activity, water absorption and emulsifying activity depend on the extent and distribution of hydrophobic and polar residues exposed to the exterior (Yampolskaya & Platikanov, 2006).

Protein solubility is highly dependent on the pH of the solution, because the pH affects the protonation status of each amino acid (Haynes & Norde, 1994). Amino acids have a central carbon atom to which is attached two functional groups (an amino group and a carboxyl group), a hydrogen atom and a particular side chain. They can be categorized according to their polarity and side chain group type. Hydrophobic amino acids are mainly protected within the core of the folded protein, while the polar amino acids are mostly extended at the exterior, and this gives a protein solubility in a polar solvent such as water (Haynes & Norde, 1994). The higher the quantity of hydrophobic amino acids on the surface of a protein, the lower its solubility in water and the more likely protein aggregation will occur.

Figure 2.6 shows a schematic diagram of the effect of pH on the protein charge. Most proteins are negatively charged at neutral pH. The electrostatic repulsion between identically charged proteins prevents intermolecular interactions, which means they tend to be soluble in polar solvents such as water. Lowering the pH of the solution decreases the negative charge on the protein until the overall protein surface charge becomes zero. This pH is also called the *isoelectric point (pI).* Due to the lack of electrostatic repulsion of neutrally charged proteins at their *pI,* protein-protein interactions are more likely to occur. Hence, the solubility of the protein is minimized when the pH approaches the *pI* of the protein, and, depending on the type of protein, aggregation is more likely to occur (Magdassi, 1996).

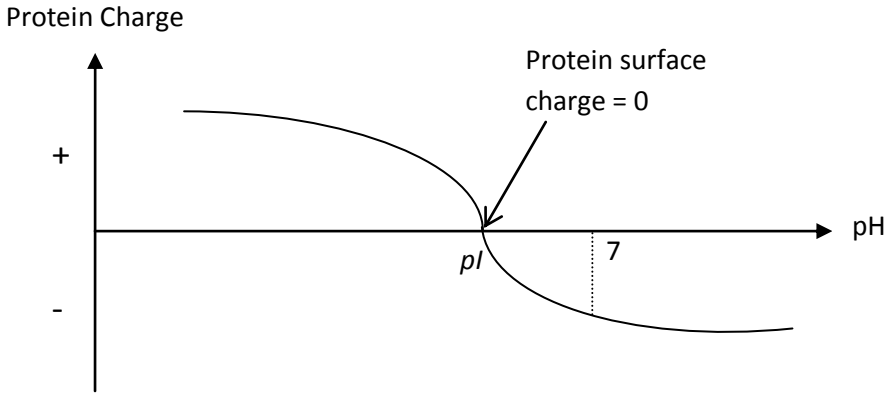

Figure 2.6: Effect of pH on protein charge

2.2.3. Surface activity

Because proteins have both polar and non-polar amino acids exposed on their surfaces, they are surface active, which leads to their adsorption to hydrophobic-hydrophilic interfaces such as air-water or oil/water interfaces. The surface activity of a protein is related to its size, structure, surface charge and hydrophobicity (Dickinson, 1999; Norde, 1992). The size of a protein is important, because proteins form multiple contacts with the surface. Larger molecules can expose a higher number of hydrophobic residues towards the air phase, which makes protein desorption more difficult (Dee et al., 2003).

The charge and its distribution within the protein molecule also strongly influence the surface activity. Proteins with a lower overall charge have higher adsorption rates because there is less electrostatic repulsion and therefore the energy barrier to adsorption is lower (Atkinson et al., 1995b; Magdassi, 1996). Hence, proteins near their *pI* have increased surface activity and increased adsorption rates (Magdassi, 1996). Proteins with higher surface hydrophobicity also show higher surface activity, because they are capable of more interaction with the hydrophobic interface and this reduces the overall energy of the system (Magdassi, 1996). Another reason for increased surface activity is protein flexibility. With the more flexible proteins, there is a greater degree of protein rearrangement upon adsorption, which allows higher numbers of hydrophobic residues to interact with the hydrophobic interface (Magdassi, 1996).

2.2.4. Adsorption and molecular reorientations at the air-water interface

Surface activity is assumed to be one of the main reasons why surface active species such as proteins accumulate at an air-water interface (Adhikari et al., 2009a; Fäldt & Bergenståhl, 1994; Kim et al., 2009a; Wang & Langrish, 2010). This process involves molecular diffusion towards and adsorption at the surface (Graham & Phillips, 1979a; Landström et al., 2003). Generally, protein adsorption is thermodynamically driven: the main driving force is the removal of non-polar and hydrophobic parts of the molecule from the polar aqueous environment, which occurs when they become orientated towards the non-polar air phase (Dickinson, 1999; Thompson et al., 2009). Another force driving protein adsorption is their unfolding and reorganization upon adsorption, which is due to interactions with the interface (Thompson et al., 2009). This reduces the free energy of the system and hence the interfacial tension, resulting in an overall increase in entropy (Norde, 1992).

Generally, the structural orientations of proteins at interfaces depend on protein properties such as size, structure, stability and hydrophobicity (Graham & Phillips, 1979a; Yampolskaya & Platikanov, 2006), and therefore can be altered by changes in the environment of a protein, such as alterations in pH and ionic strength (Brash & Horbett, 1995). It was stated by Graham and Phillips (1979a, 1979b, 1979c), who performed adsorption studies of different proteins at flat water surfaces, that the initial stage of protein adsorption, which includes the transport of proteins towards the water surface, is diffusion-controlled and the activation energy for adsorption is zero.

Higher surface coverage of protein increases the energy barrier to adsorption, hence the ability of the protein to penetrate and re-arrange at the surface might be rate-determining and therefore depends mainly on the protein's surface activity (Graham & Phillips, 1979a; Landström et al., 2003). When the maximum possible protein concentration for a given protein is obtained at the air-water surface, the surface becomes saturated with proteins (Graham & Phillips, 1979a). The protein concentration in this saturated monolayer often depends on the structure, size, hydrophobicity and surface charge of the protein, with the latter being influenced by the pH of the solution.

Several authors performed adsorption studies of proteins at flat surfaces and demonstrated that a pH closer to the *pI* of the protein can result in higher protein surface concentrations and surface pressures due to denser protein packing (Atkinson et al., 1995b; Caessens et al., 1999; Paulsson & Dejmek, 1992). Paulsson and Dejmek (1992) observed

increased surface pressures for different globular proteins as the pH approached the pI of the protein, while Atkinson et al. (1995b) observed a thicker and denser protein layer for adsorbed β-casein when the pH was lowered towards its *pI*. When the overall protein charge is close to the *pI* of the protein, electrostatic repulsion in interfacial layers is minimized (Magdassi, 1996). Hence, proteins can approach each other more closely and higher surface concentrations can be expected (Atkinson et al., 1995b). Additionally, there is a decreased electrostatic barrier for protein adsorption at a pH close to the *pI* of the protein (due to the lower overall charge), as mentioned in Section 2.2.3, hence faster protein adsorption rates can be expected (Dee et al., 2004; Magdassi, 1996).

2.2.5. Protein-sugar interactions

There is considerable literature that reports on protein-polysaccharide (Dickinson, 2008; Rodríguez Patino & Pilosof, 2011) and protein-disaccharide interactions (Arakawa & Timasheff, 1982; Belyakova et al., 2003; Fäldt & Bergenståhl, 1995; Lee & Timasheff, 1981) within aqueous solutions and at fluid interfaces. Depending on the type of polysaccharide and protein, various possible interactions can occur, for example, electrostatic, hydrophobic, van-der-Waal and hydrogen bonding. The rate, extent and strength of these interactions is highly dependent on environmental conditions such as temperature, pH, ionic strength and mechanical forces (Dickinson, 2008; Rodríguez Patino & Pilosof, 2011).

Protein interactions with sugars such as lactose are of great importance during spray drying, as they may 1) affect solute segregation between these two species, 2) stabilize adsorbed proteins against molecular rearrangement and unfolding at the surface and 3) increase the surface activity of the protein (Belyakova et al., 2003; Fäldt & Bergenståhl, 1995). Fäldt and Bergenståhl (1995) reported that, when sugars such as lactose bind to adsorbed proteins, they act as a "water-replacer" upon dehydration, and thus keep proteins solubilised. Interactions between low-molecular-weight sugars, such as lactose or sucrose, and proteins are mainly limited to hydrogen bonding—where hydroxide groups of the sugar attract the polar groups of a protein—due to the absence of a positive or negative charge on the sugar molecules (Arakawa & Timasheff, 1982). Those hydrogen bonds will have the effect of hydrating and therefore solubilizing and stabilizing proteins adsorbed at the droplet surface.

Belyakova et al. (2003) investigated the extent of interactions between sucrose and sodium caseinate, and found that those interactions may affect the self-association of sodium caseinate sub-micelles, depending on the solution pH and the ratio of protein to sucrose. A high sugar concentration supported protein-sugar interactions and thereby increased the solubility of the protein and minimized its aggregation. Protein-sugar interactions were lower at a pH closer to the *pI* of the protein, resulting in increased protein self-aggregation due to the proteins having a lower overall charge. The presence of sucrose influenced the hydrophobic-hydrophilic balance of the protein surface and thus affected the affinity of the proteins for the aqueous medium and for each other (Belyakova et al., 2003). Lee and Timasheff (1981) reported that the stabilization of the protein by the sugar can be also explained by an exclusion effect, in which the sugar is excluded from the protein domain, which consequentially increases the free energy of the system.

2.3. SPRAY DRYING

Spray drying is a well-established process used in the food, chemical and pharmaceutical industries to transform a concentrated solution, suspension or paste into dried powder for improved stability, storage and transport (Masters, 1972). Spray drying uses convective drying principles and is the most widely used industrial process involving liquid spraying, droplet drying, particle formation, powder handling and collection (Masters, 2002). Spray drying is used to dry pharmaceuticals, chemicals, foods, dairy products, fruit juice, blood plasma, organic and inorganic materials, ceramic powders, detergents, proteins (Mujumdar, 2006) and other products, listed in Table 2.2. The major advantages of spray drying over other convective drying methods are the simple process control and the low operation temperature, which reduces energy consumption and also enables the drying of heat-sensitive materials such as proteins. Furthermore, product characteristics such as particle size, morphology, density and residual moisture content can be controlled by the spray drying process, which can often be adjusted to produce powders with particular functional properties (Kim et al., 2009b; Nijdam & Langrish, 2006; Pisecky, 1997). Spray drying is also commonly used for microencapsulation of fat and volatile substances, such as aromas and flavours, in order to prevent their loss, which would reduce the quality of the end-product (Vignolles et al., 2007). The transformation from a droplet into a particle within a spray dryer is complex and depends on the drying conditions and the properties of the dissolved components within the medium.

Table 2.2: Industrial applications of spray drying (GEA Niro A/S, Denmark, 2005)

Industrial Branch	Industrial Application	
Food and Diary	- Baby food - Cheese and whey products - Coconut milk - Coffee and coffee substitutes - Coffee whitener - Eggs - Flavours - Maltodextrines	- Milk - Soup mixes - Soy-based food - Spices/herb extracts - Sugar-based food - Tea - Tomato - Vegetable protein
Pharmaceutical	- Analgesics - Antibiotics - Enzymes - Plasma and plasma Substitutes	- Vaccines - Vitamins - Yeasts
Chemical	- Catalysts - Detergents - Dyestuffs - Fine (in)organic chemicals - Tannins	- Chelates - Fungicides - Herbicides - Insecticides
Polymer	- ABS - E-PVC - PMMA - UF/MF resins	
Ceramic	- Advanced ceramic formulations - Carbides - Ferrites - Nitride	- Oxides - Silicates - Steatites - Titanates

2.3.1. Spray drying principle

Spray drying consists of three main process stages, namely atomization, droplet/air mixing resulting in water evaporation from the droplets in the drying chamber, and powder separation from the air. A basis flow diagram of a spray dryer system is illustrated in Figure 2.7. The fluid is atomized using a rotary atomizer or appropriate nozzles such as a pressure or two-fluid nozzle (Masters, 2002). Using a suitable air disperser, the droplets are then vigorously mixed with a flow of hot, dry air, which supplies the energy for the water evaporation. Due to the increase in surface area upon atomization and the stream of heated air flowing through the drying chamber, high rates of heat and mass transfer take place, causing fast water evaporation and particle formation (Masters, 2002). Relatively high air drying temperatures of around 180-220°C are usually used within a spray dryer (Masters, 2002). The rapid evaporation and hence evaporative cooling results in the droplet temperature being between the temperature of the surrounding air and its wet bulb temperature, which is below 100 °C at the start of the drying when the water activity of the droplet surface is close to 1 (Pisecky, 1997). Crust formation at the droplet surface causes particles to heat up (see Section 2.3.3). Spray drying time is very short compared to other drying methods, mainly due to the high surface area to volume ratio of the spray (Masters, 1972, 1979, 2002). The time required for transformation from a droplet into a particle usually lies in the range of milliseconds (laboratory-scale) to seconds (pilot- and industrial-scale), depending on the spray dryer dimensions (Vehring, 2008).

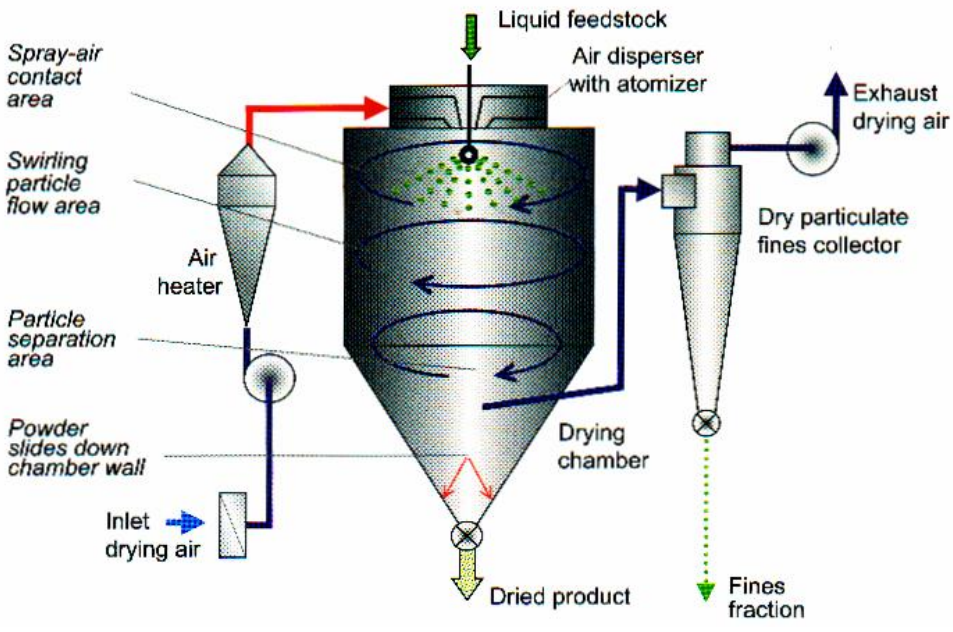

Figure 2.7: Line diagram of a spray dryer (Masters, 2002)

2.3.2. Convective drying

Convective mass transfer at an interface, for example a liquid-gas interface, occurs when the liquid and the gas move with different velocities relative to each other (Incropera et al., 2011). During spray drying, simultaneous convective heat and mass transfer takes place, because heat is convectively transferred to the droplet surface to supply the enthalpy of vaporization necessary for convective mass transfer of water vapour into the gas phase. The boundary layer theory assumes that convective mass transfer takes place in a thin boundary in the immediate vicinity of the surface, where the fluid is in laminar flow. The convective mass transfer coefficient k_c is a parameter that is used to describe the ratio between the actual mass (or molar) flux of a species into or out of a flowing fluid and the driving force that causes the flux. It depends on the relevant physical properties of the fluid, the geometry of the system, the thickness of the boundary layer and the relative velocity between fluid and gas (Adhikari et al., 2009a). Higher relative air velocities and thinner boundary layers increase the convective mass transfer.

The one-dimensional convective molar flux (mol/s) of water vapour into the flowing air stream can be described with Equation 2.2, which transforms, under consideration of the ideal gas law $c=p/(RT)$, to Equation 2.3. The latter equation is valid for systems with a low mass transfer rate and a low mass fraction of vapour (less than 0.05). For higher mass transfer rates, the coefficients are usually corrected by the log mean pressure difference (Equation 2.4) (Incropera et al., 2011).

$$\frac{dN_w}{dt} = k_c A \left(c_{w,sat} - c_{\mathrm{w},\infty}\right) \tag{2.2}$$

$$\frac{dN_w}{dt} = k_c A \frac{1}{RT} \left(p_{w,sat} - p_{w,\infty}\right) \tag{2.3}$$

$$\frac{dN_w}{dt} = k_c A \frac{p_{atm}}{RT} \, ln\left(\frac{p_{atm} - p_{w,\infty}}{p_{atm} - p_{w,sat}}\right) \tag{2.4}$$

where k_c is the convective mass transfer coefficient, which might be obtained by correlations, using dimensionless numbers or by experimental drying studies, p_{atm} is the atmospheric pressure, $c_{w,sat}$ and $p_{w,sat}$ are the partial concentration and pressure of the vapour at the droplet surface, $c_{w,\infty}$ and $p_{w,\infty}$ are the partial concentration and pressure of the vapour in the air outside the boundary layer, A is the interfacial area, R is the universal gas constant and T

is the average temperature in the boundary layer. $p_{w,sat}$ and $p_{w,\infty}$ can be calculated by the Antoine-Equation, as follows:

$$log\ p_{w,sat} = A - \frac{B}{C+T_{WB}\ [°C]} \quad (2.5)$$

$$p_{w,\infty} = \frac{RH}{100\%}\ p_{w,sat} \quad (2.6)$$

where A = 8.07131, B = 1730.63 and C = 233.426, T_{WB} = wet bulb temperature (K) and T_{air} = drying air temperature (K), RH = relative humidity of the bulk air (%).

2.3.3. Evaporation of droplets containing dissolved solids

The evaporation of a droplet containing dissolved solids varies from the evaporation of a pure liquid droplet in the following ways (Masters, 1972):

1) The presence of solutes in the drying droplet decreases the vapour pressure of the liquid (water activity falling below unity), which causes lower evaporation rates than pure liquid droplets of equal size.
2) There is a transformation of the droplet into a particle, involving:
   a) Droplet drying with mass transfer of the solutes and solvents within the drying droplet,
   b) Increase in solution viscosity due to concentration of solutes, which causes a reduction in the mutual diffusion coefficient of the water-solute system,
   c) Possible glass formation or crystallization of solutes (depending on the material) due to the increased concentration of the solutes,
   d) Shell, skin or crust formation at the droplet surface,
   e) Drying of the porous particle once solidification has occurred, including capillary flow of liquid in the shell, skin or crust.

The transformation of a droplet into a particle is illustrated in Figure 2.8. The drying rate changes from an initial constant rate (1st stage of drying) to a falling rate (2nd stage of drying) due to the formation of dried solids on the droplet surface, which creates a barrier to moisture evaporation (Figure 2.9) (Pisecky, 1997).

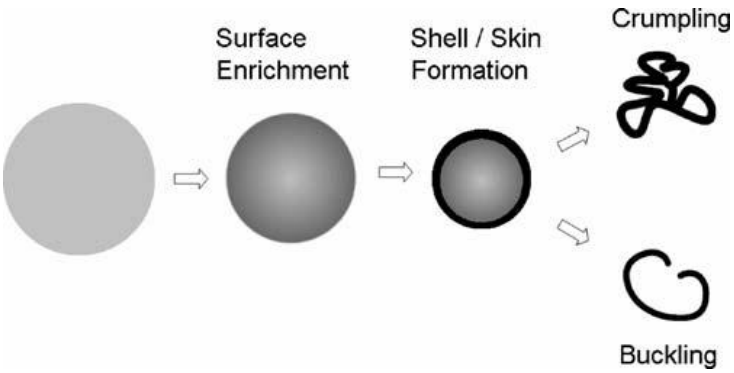

Figure 2.8: Particle formation during spray drying (Vehring, 2008; Vehring et al., 2007).

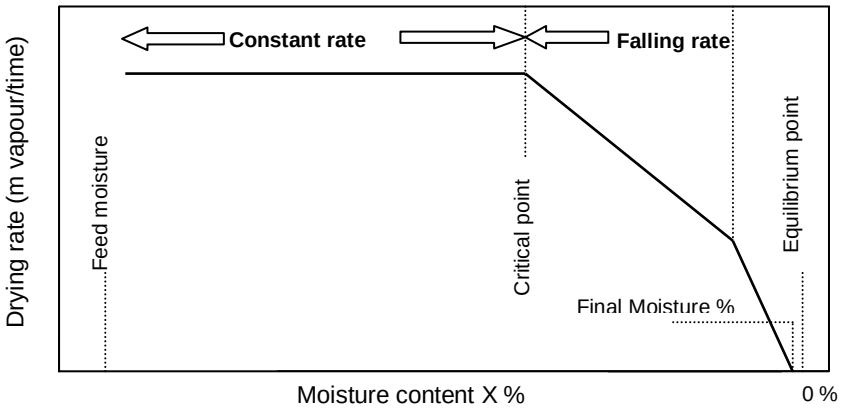

Figure 2.9: Different drying rates during drying of a droplet, containing dissolved or suspended solids, modified from Pisecky (1997).

During the constant rate period, the surface is saturated, that is, the water activity is unity (the surface vapour pressure is equal to the surface vapour pressure of pure water), and the drying of the droplet is externally controlled by the boundary layer. Moisture migrates from the droplet interior towards the droplet surface (Masters, 1979) while the temperature of the droplet stays constant. During water evaporation, the droplet shrinks, and the solutes within it become progressively more concentrated. Due to the concentration of solutes, the viscosity of the drying droplet increases progressively. Therefore the mass transfer of different solutes due to diffusion within the drying droplet reduces (Kim et al., 2009b).

The first period of drying ceases when the average droplet moisture content falls to a critical value, which is characterized by a solid phase appearing on the droplet surface. This occurs because the surface saturation can no longer be maintained in the face of evaporation from the surface caused by migration of moisture from the interior of the droplet towards the

surface, which results in a crust formation (Masters, 1979; Pisecky, 1997). The water activity a_w falls below unity, in other words, the water vapour partial pressure at the droplet surface $p_{W,sat}$ reduces, and therefore the water evaporation rate reduces. Different possible mechanisms for surface formation are described in the literature, and these will be discussed in Section 2.3.5.

After crust (or film) formation on the surface of the drying droplet, the falling rate period begins and the drying rate decreases. The crust hinders water evaporation from the droplet because it acts as a barrier to moisture transfer (Masters, 1979). As the evaporation rate decreases, the particle temperature increases above the wet-bulb temperature until it reaches the temperature of the surrounding air. The temperature profile of the drying droplet containing solids is illustrated in Figure 2.10.

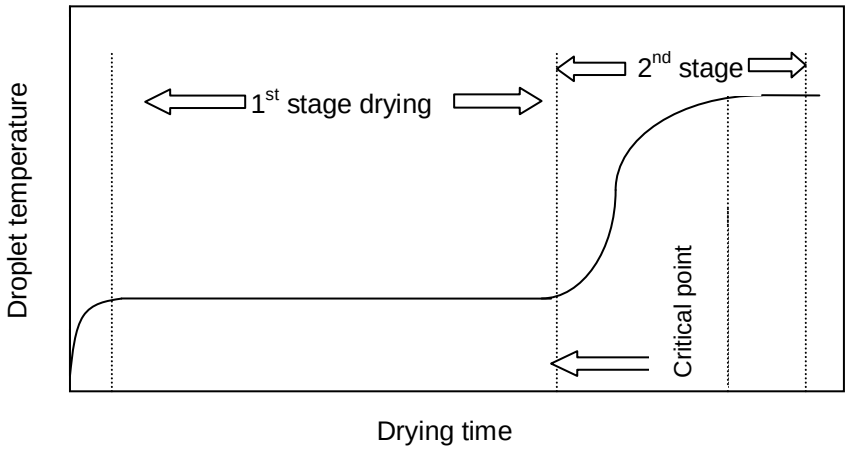

Figure 2.10: Development of droplet temperature during drying of a droplet containing dissolved or suspended solids - modified from Pisecky (1997).

2.3.4. Solute segregation during spray drying

Various mechanisms have been suggested in the literature to describe mass transfer of solutes and its effect on solute segregation within a drying droplet. These will be outlined in this section.

Solute segregation due to differential diffusion caused by moisture content gradients

Meerdink and van't Riet (1995) state that, during the drying of a droplet, the evaporation of water causes water concentration gradients within the droplet, resulting in a diffusion of water molecules towards the surface (Adhikari et al., 2007b; Kim et al., 2003; Meerdink & van't Riet, 1995). These water concentration gradients also result in increasing solute concentrations at the surface, which cause solutes to diffuse towards the core of the droplet. Kim suggests that a segregation of components during spray drying is expected, due to differences in the diffusion coefficients of these components. Due to lower diffusivities, larger molecules diffuse more slowly towards the droplet interior, and are therefore expected to enrich at the droplet surface to a greater extent than smaller molecules. Adhikari et al. (2007a) calculated, using a solute-fixed coordinate system model, that moisture gradients develop within a drying droplet, which might drive solute segregation. As observed by several researchers, this mechanism could offer a possible explanation for the surface enrichment of large high-molecular-weight molecules, such as polymers, fat globules or protein, at the expense of smaller molecules, such as lactose or sucrose, during spray drying (Elversson & Millqvist-Fureby, 2006; Fäldt & Bergenståhl, 1994; Jayasundera et al., 2009; Kim et al., 2009b; Nijdam & Langrish, 2006).

Solute segregation due to different Peclet numbers

The shrinkage of the droplet during drying results in a radially receding droplet surface (Kim et al., 2003). Vehring (2008) postulates that, when the drying rate is high enough, the evaporating surface can move faster inwards than the dissolved components can diffuse away from the surface, which results in dissolved components being captured and "dragged" inwards by the surface, with a consequential surface accumulation of these components. This only occurs when the Peclet number, *Pe*, is higher than 1. The *Pe* is a dimensionless number, which describes the ratio of advection (here the surface velocity) to diffusion (Equation 2.7).

$$Pe_i = \frac{L\,v}{D_i} = \frac{\kappa}{8\,D_i} \qquad (2.7)$$

where L is the characteristic length, v is the velocity of the solvent, D_i is the diffusion coefficient of the solute and κ is the drying rate.

Vehring (2008) explains that small molecules such as lactose have a smaller *Pe* (a higher diffusion coefficient in water) than larger molecules, such as high-molecular-weight carbohydrates or polymers, and therefore can diffuse more quickly towards the core of the droplets. Larger molecules with high *Pe* are therefore more likely to dominate the droplet surface than smaller molecules, as illustrated in Figure 2.11. However, Vehring (2008) also states that the *Pe* of a molecule can increase drastically once a critical concentration is reached and the dissolved molecule undergoes a phase transition. The diffusion coefficient of the precipitated form is drastically reduced due to the considerable increase in effective size; large precipitates or crystals therefore tend to enrich at the droplet surface more than smaller monomers, which have a higher diffusivity (smaller *Pe* numbers). Vehring (2008) postulates that the surface enrichment of a component can be controlled by the solubility of that component and its initial concentration. Components with low solubility and high initial concentrations tend to precipitate faster and, due to the strong increase in their *Pe* numbers upon precipitation, enrich on the surface.

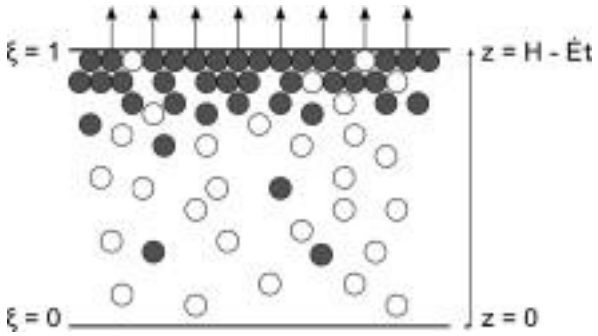

Figure 2.11: Surface segregation of solutes of various Peclet numbers: *Pe* > 1 (black), *Pe* < 1 (white) (Trueman et al., 2012).

Trueman et al. (2012) provide a mathematical model which shows that, when the size ratio of two solutes increases from 1 to 5, more segregation between these solutes occurs due to larger differences in their diffusivities. They also report that two solutes with *Pe* numbers

on either side of unity can separate at a drying solvent surface, because the solute with a *Pe* number smaller than unity is mobile enough to diffuse away from the evaporative surface, while the solute with a *Pe* number greater than unity will be captured at the surface due to its low mobility. This "stratification" effect was also shown by Nikiforow et al. (2010) for two solutes with *Pe* numbers above and below unity. According to Trueman et al. (2012), this effect only occurs for solute size ratios between 1 and 5. Above this point, the smaller molecules are capable of diffusing into the voids between the larger molecules (those with *Pe* > 1), as also shown by Luo et al. (2008) for a disperse system of monodisperse nano- and latex particles.

Solute segregation in the presence of surface active components

Several authors have shown that the surface of spray-dried particles is often dominated by surface active components, such as proteins or surfactants, irrespective of their solubility or size (Adhikari et al., 2009b; Fäldt & Bergenståhl, 1994, 1996; Jayasundera et al., 2010b; Kim et al., 2009a, 2009b; Millqvist-Fureby & Smith, 2007; Nijdam & Langrish, 2005, 2006; Wang & Langrish, 2010). Graham and Phillips (1979a) stated that the process of adsorption of surface active components at a surface involves the transport of the molecules towards the air-water interface by diffusion, followed by the adsorption of the molecules into the air-water interface, with subsequent final rearrangements of the adsorbed molecules. Because spray drying takes place within a short time-frame, Landström et al. (2003) assumed that the adsorption behaviour of proteins is controlled mainly by diffusion, but also depends on the ability of the molecule to penetrate into an existing adsorbed protein film. The latter depends on the surface activity of the protein.

Competitive adsorption

Competitive adsorption phenomena between different types of proteins and between proteins and surfactants have been well studied by a number of researchers (Brash & Horbett, 1995; Dickinson et al., 1988; Euston et al., 1995; Gaiani et al., 2011; Jayasundera et al., 2010a; Landström et al., 2000; Landström et al., 2003). Surface activity plays an important role in the competition between the different species for the air-water interface. However, this does not necessarily imply that the most surface active solute will always dominate the

interface (Dickinson, 1999). Competitive adsorption between different surface active species is complex and depends on kinetic and thermodynamic factors, such as the rate of transport towards the interface by diffusion and convection, the relative affinity of the solute for the surface (surface activity), the time available for and rate of possible rearrangements of the solute at the surface, interactions between surface active solutes (e.g. protein-surfactant or protein-protein interactions) and the possible displacement of already adsorbed molecules by another species (Dickinson, 2011). These kinetic and thermodynamic factors are influenced by many physicochemical properties of the surface active solutes, such as their size, shape, charge distribution, overall charge and hydrophobicity (Dickinson, 2011).

Competitive adsorption studies between different proteins were performed by Landström et al. (2000), using mixtures of β-casein and β-lactoglobulin in one experiment, and mixtures of bovine serum albumin (BSA) and β-lactoglobulin in another experiment. The larger and more surface active proteins, β-casein and BSA, dominated the surface at higher protein concentrations, while at lower concentrations, the adsorption of both β-casein and BSA was independent of the adsorption of β-lactoglobulin, and therefore no competitive adsorption could be observed. Millqvist-Fureby and Smith (2007) performed competitive adsorption studies between protein and lecithin, and showed that, given a sufficient concentration of lecithin, proteins were excluded by this highly surface active phospholipid.

Elversson and Millqvist-Fureby (2006) used the concept of "*in-situ coating"* to demonstrate the competitive adsorption behaviour of proteins and polymers. They found that the surface active polymer hydroxypropyl methylcellulose *(HPMC)* completely excluded the protein *BSA* from the surface, when the polymer concentration exceeded 1 wt% of total solid concentration in solution. The same exclusion of *BSA* was observed when using poloxamer as competitive polymer, although the total surface enrichment of poloxamer was lower than that of *HPMC*. Jayasundera et al. (2010a, 2010b) showed competitive adsorption between proteins (sodium caseinate *(Na-Cas)* and pea protein isolate *(PPI)*) and different non-ionic surfactants (sodium stearoyl lactylate *(SSL)*, polysorbate 80 *(Tween-80)*, sodium dodecyl sulfate *(SDS*)). They showed that the addition of just 0.5-1.0 wt% of any of these surfactants displaced a substantial amount of protein from the surface. This shows that adding a small amount of surfactant to a protein solution can result in partial or complete displacement of the proteins from the air-water interface.

Solute segregation in the presence of fat

Several published studies have reported the enrichment of large amounts of free fat on the surface of spray-dried milk powders, especially whole milk powders (Dickinson, 2001; Fäldt & Bergenståhl, 1995; Farkye, 2006; Gaiani et al., 2007; Kim et al., 2003, 2009a; Nijdam & Langrish, 2005; Pisecky, 1997; Vega & Roos, 2006; Vignolles et al., 2007). The free fat is defined as the fraction of fat which is not encapsulated by proteins, but which exists in form of "fat pools" or "patches" rather than globules on the surface of powders (Pisecky, 1997). These studies all confirmed that there is segregation and hence re-distribution of milk components in droplets during spray drying, since the composition of the particle surface was considerably different to that of the solution mixture. The surface of whole milk powder was almost completely covered with fat (Kim et al., 2009a).

Different mechanisms for the accumulation of free fat on the surface of spray-dried particles have been described in the literature, and are summarized as follows. Kim et al. (2009b) suggest that larger fat globules are preferentially present at the surface of emulsion droplets when leaving the atomization device. Those fat globules are disrupted during atomization and thus appear in high concentrations as free fat on the powder surface, after spray drying is completed. Kim suggests that there is further segregation of components during drying due to their different diffusivities. Since fat globules are larger than proteins and lactose, they have a lower diffusivity into the core of the droplet (driven by moisture content gradients) and therefore become enriched at the droplet surface.

Since the high temperatures used in the spray drying process can cause cracks and pores within the dried particle and can also induce a vacuole formation through vapour expansion within the particle (Pisecky, 1997), Nijdam and Langrish (2005) postulate that the liquid fat can be forced through those cracks and pores towards the surface when the vacuole becomes over-pressurized. Fäldt and Bergenståhl (1995) suggested that the spray drying of an oil-in-water (O/W) emulsion, such as milk (a dispersion of "encapsulated" fat globules within a continuous water phase), leads to emulsion instability due to the increased ratio of fat to water that results from water evaporation. This causes fat droplets to come closer to each other during drying, so that they aggregate to larger, more unstable droplets. Due to the increased ratio of fat droplet coalescence during progressive drying, fat migration is facilitated and free fat is present at the droplet surface.

Effect of spray drying conditions on solute segregation

A) Proteins:

Spray drying conditions seem to have a significant effect on the amount of protein adsorbed. Kim et al. (2009b), Nijdam and Langrish (2006) and Gaiani et al. (2010) found higher surface protein concentrations at lower air drying temperatures for various milk mixtures (3-component systems) and protein/lactose mixtures (2-component system). They explained that less time is available for proteins to adsorb at the surface at higher temperatures, because the droplets dry more quickly. Wang and Langrish (2010) made the same observations for a mixture of lactose/casein, while for a lactose/WPI mixture they could not find a clear trend.

Kim et al. (2009b) performed a detailed study of the effects of spray drying conditions on the surface composition of milk powders. They observed that, when spray drying a milk solution using a small-scale laboratory spray dryer, the solution's solid content affected the protein surface enrichment. Kim et al. (2003) reported higher protein concentrations on the surface of spray-dried milk powder when solutions of lower solid contents were used. They explained that, due to a lower solution viscosity at lower solid contents, the re-distribution of milk components during drying might be enhanced, since the diffusivities of the components increase with decreasing viscosity. Furthermore, Kim et al. (2009b) investigated the effect of droplet size on the surface compositions. Increasing the droplet size had no clear effect on the particle surface composition of the powder fractions containing particles between 20 and 200 µm in size.

B) Fat:

Spray drying conditions seem to have a significant effect on the amount of free fat covering the surface of spray-dried particles. Higher air inlet temperatures were often reported to decrease the amount of free fat on the particle surfaces (Kelly et al., 2002; Kim et al., 2009b; Park & Chinnan, 1995). However, there are contradictory studies in the literature, with some authors reporting that the free fat content increased with increasing outlet temperatures due to possible formation of cracks within the drying particle and subsequent release of fat towards the surface (Dickinson, 2003; Kelly et al., 2002; Pisecky, 1997). Moreover, Kim et al. (2009b) showed that smaller fat globules, caused by more frequent

homogenization passes during emulsification, resulted in a lower amount of surface free fat, due to an increased stabilization of encapsulated fat globules with decreased fat globule size.

The atomization device used can affect the amount of surface free fat (Vignolles et al., 2007). The free fat content was shown to be lower in powders that originated from a spray nozzle compared to a rotary atomizer. Increasing the atomization pressure (for spray nozzles) or rotational speed (for rotary atomizer) resulted in decreased surface free fat, possibly due to an enhanced homogenization effect (Park & Chinnan, 1995). Fäldt & Bergenståhl (1995) found that using cyclones as particle separation devices increased the amount of surface free fat due to enhanced mechanical stress on the particles, which provoked the release of fat onto the powder particle surface.

According to Pisecky (1997), the physical state of lactose is important. He states that amorphous lactose protects free fat from forming while crystalline lactose promotes free fat formation. The type of fat used also affects the extent of fat accumulation at a particle's surface. Kim et al. (2005a) showed that triglycerides with lower melting points were more highly concentrated in the free fat fraction of the particle surface, while those with higher melting points were more highly concentrated in the encapsulated fat fraction. However, after long-term storage of milk powder to allow crystallization of amorphous lactose within the particles, an increase in the free fat coverage was observed. This was caused by 1) formation of cracks and pores due to the volume reduction that occurs upon the phase transformation, and 2) damage to the walls of fat globules by sharp crystals, which caused free fat to leak out through the pores of the fat globules towards the surface of the particles (Fäldt & Bergenståhl, 1995; Kim et al., 2009c).

2.3.5. Surface and particle formation during spray drying

Mechanisms of surface formation

Charlesworth and Marshall Jr (1960) stated that, in the absence of fat and surface active components, the particle surface is formed by supersaturation of dissolved components with subsequent precipitation to form a solid phase, which is deposited at the surface as a partial crust. The composition of this crust is determined mainly by the solubility and initial concentration of the dissolved components. Vehring (2008) supports this suggestion by stating that the *Pe* number of a component can increase drastically when the component

undergoes a phase transition, which occurs once a critical concentration is reached; hence large precipitates or crystals enrich at the droplet surface to a greater degree than smaller monomers. Vehring (2008) states that precipitation of solutes can occur in the bulk phase (*bulk precipitation)* or at the droplet surface (*surface precipitation)*, with subsequent shell formation in both cases, as illustrated in Figure 2.12.

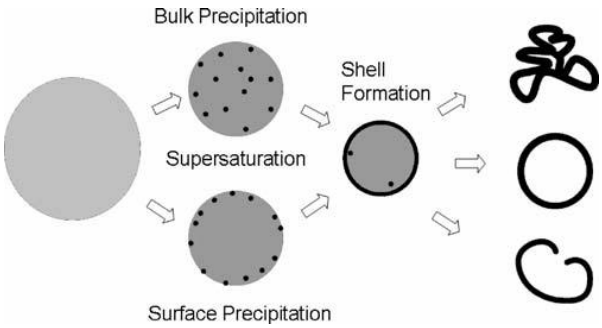

Figure 2.12: Surface formation mechanism according to Vehring (2008)

Some solutes may not have sufficient time to crystallize during the short time-frame of spray drying, which is in the order of milliseconds to seconds (Vehring, 2008). Instead, a shell is formed around the droplet due to the increase in viscosity, which freezes the solutes into a wet amorphous glass at the surface, as described by Roos (2002) for the spray drying of lactose. This increase in viscosity means that the mass transfer of other solutes within a droplet becomes gradually more limited during drying, until the individual solutes lose all mobility and become encapsulated within the continuous, amorphous matrix of the sugar. However, Vehring (2008) reported that when molecules with high initial concentration and fast crystallization kinetics are present within a spray-dried solution, they may crystallize prior to their encapsulation, and hence may dominate the particle surface.

The presence of surface active components complicates matters further. As described in Section 2.2.4, proteins adsorb at the droplet interface, which causes reorientation and rearrangement of protein residues so that the polar groups mainly point into the water, while the non-polar groups are mainly exposed to the air phase (Brash & Horbett, 1995). Structural rearrangements of protein residues can often cause complete protein denaturation (a loss of its structure and function), as occurs when the internal hydrophobic protein residues are exposed (Norde, 1992). Chen et al. (2011) suggest that the protein may lose its solubility and

precipitate on the droplet surface, causing a reduction in the concentration of dissolved protein in the vicinity of the precipitation front, which drives other proteins to diffuse from the inside of the droplet to its surface. An adsorbed protein film (monolayer) is then formed on the surface, which is compressed and dehydrated upon drying.

Formation, size and morphology of particles

The spray drying conditions can be adjusted to control particle size and morphology. The droplet size depends on the kind of atomization device and energy input, as well as the viscosity and surface tension of the spray-dried solution. Other factors, such as droplet coalescence and particle agglomeration during drying, particularly in larger, industrial spray dryers, can increase the final particle or agglomerate size. Furthermore, spray drying conditions, such as air inlet temperature, as well as the composition of the solution can have a large impact on the final particle size (Pisecky, 1997). For example, Nijdam and Langrish (2005) have shown that milk solutions spray-dried at lower temperatures (120 to 160 °C) formed powders with smaller particles which had more surface folds and wrinkles than the smoother, more spherical particles obtained by using higher spray drying temperatures (220 °C) (Figure 2.13). Nijdam and Langrish (2005) postulated that at higher air temperatures a faster solidification of the droplet surface occurs, and the crust formed is less sensitive to particle deformation caused by an internal vacuole. By performing single droplet drying experiments, Hecht and King (2000) showed droplet expansion and deflation due to vacuole formation that may be caused by entrapped air (Pisecky, 1997) or by vapour produced once the droplet interior exceeds the boiling point of the fluid (Nijdam & Langrish, 2005). Vapour bubbles formed within the droplet during drying can expand the droplet/particle (Nijdam & Langrish, 2005).

Nijdam and Langrish (2005) theorized that particle expansion occurs because the permeability of any shell formed is sufficiently low to prevent any internal overpressure being dissipated through the shell, therefore the vacuole and hence the particle expands. A subsequent deflation occurs when the particle moves into cooler regions of the dryer, causing the temperature and pressure within the vacuole to reduce. This deflation can only occur when the wall remains sufficiently moist or consists of elastic materials. Higher drying temperatures cause faster dehydration of this shell, which then cannot deflate after expansion, and this results in larger, smoother particles which are hollow and so have a lower particulate

density. Since particle expansion is also highly dependent on the material properties of the surface, particle morphology varies greatly with varying solution composition. It was shown that the spray drying of pure lactose results in smooth, spherical particles, while the addition of proteins or polymers to the lactose solution leads to the formation of larger, less dense particles with extremely folded surfaces (Elversson & Millqvist-Fureby, 2006; Vehring, 2008). This can be explained by the higher elasticity and flexibility of surface proteins or polymers, which can be more easily expanded by an overpressure of the internal vacuole; amorphous lactose, on the other hand, forms a highly viscous, rigid glass, which is more resistant to pressure differences within the particle (Dickinson, 1999, 2001).

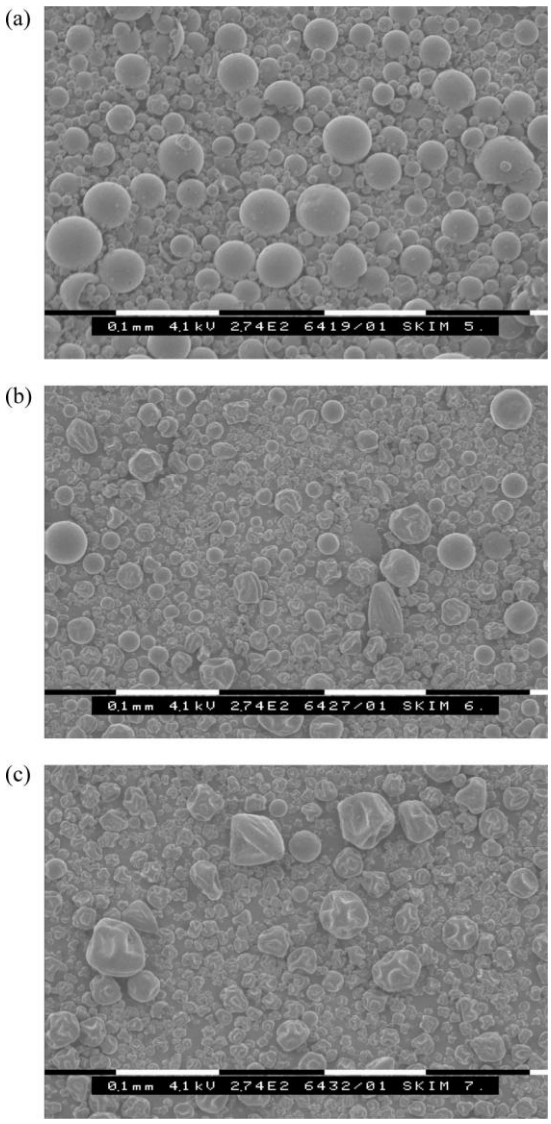

Figure 2.13: Particle morphology of spray-dried milk powder, spray-dried at different air inlet temperatures (T): a) T=220°C, b) T=160°C, c) T= 120 °C (Nijdam & Langrish, 2005).

Vehring (2008) postulated that hollow particles may be created by a mechanism different to the vacuole-formation mechanism described above. Vacuole formation upon the drying of single droplets was clearly shown by Hecht and King (2000), but those droplets were a lot larger than droplets created during spray drying. Vehring (2008) states that it is not clear whether the small time-scale of spray drying provides sufficient time for bubble nucleation and vapour expansion. He states that components with low solubility and high surface activity precipitate very quickly at the droplet surface. This results in the very early formation of a wall at the surface, which decreases the drying rate. While water diffusion out of the core of the droplet continues, a "sink-hole" is created, which causes the wall to wrinkle, depending on the wall material. Large, wrinkled, low-density particles are the result of this early shell formation. The earlier this shell formation occurs, the larger the particles and the lower their bulk density will be. This mechanism suggests that larger and more wrinkled particles can be the result of the rapid formation of a wall created by protein precipitation.

2.3.6. Additives in spray drying for microencapsulation purposes

Microencapsulation during spray drying has been used for many years to encapsulate fats, aromas, flavours or active drugs in foods or pharmaceuticals (Ré, 1998). The major reasons for microencapsulation are the protection of the product from the environment or the protection of the environment from hazardous or toxic products contained within the particulates (Elversson & Millqvist-Fureby, 2006; Gharsallaoui et al., 2007; Ré, 1998). Further reasons for encapsulating (coating) particles include improving particle flow of sticky materials, masking undesired characteristics of the active component (for example taste or odour), or controlling component release using a semi-permeable polymer membrane on the surface (Ré, 1998; Takeuchi et al., 1998; Wan et al., 1992a; Wang & Langrish, 2010).

Microencapsulation is also important in disperse systems, for example in an emulsion where fat globules are encapsulated mainly by milk proteins such as caseins and whey, and this protects them from droplet coalescence and subsequent emulsion instability (Desai & Jin Park, 2005; Gharsallaoui et al., 2007). This phenomenon enables the spray drying of milk, because the stabilized fat globules mostly retain their globular form during spray drying, although some fat may leak out of the globules towards the surface, as discussed in Section 2.3.4. When the spray-dried powder is re-dispersed into water, the fat globules in the resultant milk are still effectively dispersed and stabilized. However, fat globule size might change

during the spray drying of emulsions, such as milk, due to possible disruption by the atomization device and also droplet coalescence (Ye et al., 2007).

The materials already being successfully used as microencapsulating species in food and pharmaceutical applications are often both wall-forming and surface active, and have the ability to enrich on interfaces, such as oil/water or air-water interfaces, and form a stable wall around the encapsulated material. Thus, those materials are also useful for the *in-situ coating* of lactose. The different criteria for selecting a suitable wall material for encapsulating particles are based mainly on the physicochemical properties required of the material, such as its solubility, glass/melting transition, crystallinity, permeability to water, and film-forming and emulsifying properties (Gharsallaoui et al., 2007). For the *in-situ coating* of lactose, a suitable coating material needs to enrich on the droplet surface, cover the surface completely and form a stable coating, which should preferably act as a moisture barrier to prevent the absorption of any water that would lead to lactose crystallization.

According to Matsuno and Adachi (1993), there are 4 classes of coating materials, and these are summarized in Table 2.3 (Arvanitoyannis et al., 1998). Wall materials of type 1 are considered to be the most suitable for microencapsulation using a drying process due to their fast and dense skin formation. Type 2-4 materials are considered less efficient in the protection of encapsulated materials, because they do not form a dense skin at an early stage of drying. However, this method of classification has been criticized for its simplicity (Gharsallaoui et al., 2007). For the purpose of *in-situ coating* of lactose during spray drying, material types 1, 2 and 4 are considered equally suitable. Furthermore, lipids and polymers are two other promising materials, and were not classified in Table 4. Other suitable materials for *in-situ coating* of lactose are discussed in the following sub-sections.

Table 2.3: Overview of possible suitable wall materials, according to Gharsallaoui et al. (2007)

	Characteristics	Wall materials
Type 1	Rapid formation of a dense skin and a good protection of the core ingredient against oxygen and deterioration.	Maltodextrin Pullulan Gum arabic Gelatine
Type 2	High-molecular-weight substances with three-dimensional structure	β-lactoglobulin Albumin Other globular proteins
Type 3	Low-molecular-weight substances	Sugars Carbohydrates
Type 4	Substances that easily crystallize upon dehydration	Mannitol

Proteins

Proteins have been successfully used as microencapsulating agents in many applications due to their encapsulation efficiency and ability to bind flavours. The most commonly used proteins for encapsulating food ingredients by spray drying are milk proteins, such as whey and casein (Gharsallaoui et al., 2007). Gelatine is another water-soluble protein with good wall-forming ability (Bodvik et al., 2010), which has also shown high emulsifying activity, good stabilization properties and a tendency to form a fine, dense network upon drying (Gharsallaoui et al., 2007).

Milk proteins

Whey proteins—those proteins that can be isolated from the whey of milk—are a mixture of globular proteins, mainly β-lactoglobulins, while casein (a mixture of α_{S1}-casein, α_{S2}-casein, β-casein and κ-casein) is a flexible protein which has no distinct secondary or

tertiary structure (Dickinson, 2001). Whey proteins in solution have a more compact, ordered structure than caseins. The presence of disulfide bonds gives the whey protein a considerable degree of secondary and tertiary structure, which protects the non-polar amino acids within its core (Thompson et al., 2009). Casein proteins on the other hand have a rather flexible structure due to the lack of disulphide bonds. Their conformation is therefore much like that of a denatured protein, where the hydrophobic residues are freely exposed to the exterior water phase. β-casein molecules have 209 amino acids, and most of the first 50 of these are negatively charged at neutral pH, which makes this portion of the protein hydrophilic; however, the majority of the polypeptide chain is hydrophobic because the remaining amino acids are predominantly non-polar (Atkinson et al., 1995b). Casein proteins are thus more surface active than whey proteins due to their higher hydrophobicity and amphiphilicity.

Lipids

Kim et al. (2009b) demonstrated that it is possible to produce spray-dried milk powders with a very high surface fat content (up to 95%). A fat layer on the surface of a particle could possibly act as a good moisture barrier due to its hydrophobic, non-hygroscopic character. However, fat-coated powders are prone to extreme stickiness due to the high free fat content. According to Kim et al. (2009b), fat accumulates at the particulate surface, causing it to stick to the spray dryer wall. This results in a low product yield of milk powder. Fat-coated powders have the further disadvantage of having poor powder flow and a tendency to agglomerate, which complicates storage and handling (Fitzpatrick et al., 2004; Kim et al., 2005b). Moreover, re-dissolution into other liquid food products is made difficult by the poor wettability of these powders (Kim et al., 2002). Finally, the melting point of the chosen fat would have large impact on the stability of the coating and its ability to act as a water barrier (Kim et al., 2005a).

Polymers

Microencapsulation with polymer matrices is regularly used in the medical and pharmaceutical industries to mask unpleasant tastes or odours or to facilitate the controlled release of drugs (Peniche et al., 2003). Polymers might be useful as coating materials due to their film-forming efficiency. Chitosan, a biocompatible polymer, has been shown to be an efficient microencapsulation agent (Peniche et al., 2003), while gum arabic has shown

excellent emulsification and film-forming ability (Gharsallaoui et al., 2007). Furthermore, surface active polymers, such as hydroxypropyl methylcellulose (HPMC) or poloxamer, have been tested for *in-situ* coating of protein powders by Elversson and Millqvist-Fureby (2006), and were shown to give a high surface enrichment during spray drying. However, polymer-coated lactose powder would be likely to be hygroscopic due to the water-binding capacity of hydrophilic polymers (Gao et al., 1996; Ishikawa et al., 2000), therefore a polymer coating would not be suitable as moisture barrier.

Other materials

Carbohydrates such as starches and maltodextrin have been used as encapsulating agents (Gharsallaoui et al., 2007). However, most of the carbohydrates lack the interfacial properties required for efficient encapsulation. Moreover, a carbohydrate coating would be hydrophilic and thus would not be suitable as moisture barrier. Another possible coating material for lactose might be a component which crystallizes during spray drying, such as mannitol (Costantino et al., 1998). Small crystals might preferably enrich on the surface of those droplets due to their low diffusion coefficient (high Peclet number). According to Vehring (2008), those crystals could form a stable crystalline coating around the lactose. The advantage of a crystalline coating would be its high stability and low hygroscopicity. Flowability would be enhanced and the moisture absorption from the surrounding air would be reduced. Hence, the amorphous lactose might be effectively protected against moisture penetration and subsequent crystallization.

2.3.7. Control of powder properties

Powder functional properties play a very important role in industrial processing and in the end use of the powder. Particle size, density and morphology, which can also affect flowability, wettability and dispersibility, can be partly controlled by spray drying parameters such as atomization, air inlet temperature and solid concentration in the solution (Kim et al., 2009b; Nijdam & Langrish, 2006). Solution additives can be used to alter the surface properties, with subsequent changes in particle morphology, size and density, which results in improved powder flow (Elversson & Millqvist-Fureby, 2006; Elversson & Millqvist-Fureby, 2005; Vehring, 2008). Particle agglomeration after spray drying is a useful method for increasing the total particle size and porosity, which enhances powder flow, wettability and

dispersibility (Pisecky, 1997). Fluidized beds can also be used to apply a coating fluid to the surface of spray-dried particles in order to enhance powder properties or protect an active substance within the particle (Masters, 2002). For example, milk particles with fat on the surface have to undergo a post-treatment, including agglomeration and coating with lecithin, to enhance powder functional properties (Kim et al., 2009a).

Flowability is a very important powder property, particularly during the processing of powders, when easy powder handling during a multi-step process is required. Examples where flowability is important include flow from hoppers and silos, transportation, mixing and packaging of powders (Prescott & Barnum, 2000). Particle size is one of the most important physical properties affecting the flowability of dry powders (Buma, 1968; Fitzpatrick et al., 2004; Teunou et al., 1999). While powders with particles larger than 200 µm are considered to be free flowing, those with smaller particles tend to be more cohesive, with resultant poor powder flow (Tomas, 2004). Generally, larger particles contribute to a better powder flow due to increased ratios of gravitational to attractive forces, which reduces the cohesiveness of the powder (Tomas, 2004). Van der Waals attractions and capillary forces are examples of attractive forces.

Another important determinant of powder flow is the surface charge. Charged surfaces of the same kind increase the electrostatic repulsion between particles, which improves powder flow due to an increased ratio of repulsive to attractive forces (Amefia et al., 2006). Besides particle size and particle charge, the particle morphology (shape and surface roughness), water content and surface composition also affect powder flow considerably (Elversson & Millqvist-Fureby, 2006; Fitzpatrick et al., 2004; Kim et al., 2005b; Teunou et al., 1999). While spherical particles with smoother surfaces tend to produce better powder flows, the presence of lipids on the particle surface contributes to poorer flowability, as does increasing the water content of the powder, which enhances the attractive capillary forces between particles (Fitzpatrick et al., 2004; Kim et al., 2005b).

The glass transition temperature of the material affects powder stickiness and therefore flowability (Adhikari et al., 2001; Chen & Özkan, 2007). Small-molecular-weight components, such as sugars, have a lower glass transition temperature than high-molecular-weight components, such as proteins or polymers (Roos & Karel, 1991b). Powders containing low-molecular-weight components on their surfaces therefore have poorer powder flows due to higher particle cohesion, in particular when the powder is hygroscopic and has

already absorbed a substantial amount of moisture (Adhikari et al., 2001; Fitzpatrick et al., 2004; Teunou et al., 1999). The principle of the glass transition from a glassy to a rubbery state has been explained in Section 2.1.3.

Enhancing the effective particle (agglomerate) size by inducing the formation of larger agglomerates is a useful method for improving powder flow (Pisecky, 1997; Sarkar, 1984). The fine powder particles are fluidized, for example by a fluidized bed, to provoke multiple contacts between individual particles. The wetting of the particles by a very fine stream of water or sugar solution increases the particle cohesion and causes the formation of liquid bridges between the particles. Upon drying, these liquid bridges transform to stable solid bridges through the super-saturation and subsequent crystallization of components dissolved in the binding fluid. Agglomerate size distribution can easily be adjusted by changing process parameters and/or the residence time of the particles within the fluidized bed.

Different methods are available for measuring flowability. Direct methods include shear cell, ampoule, optical probe, centrifugal methods, cyclone and blow test, while the indirect methods include measurements of the glass transition temperature or angle of response, thermal-mechanical and rotating drum methods (Chen & Özkan, 2007; Prescott & Barnum, 2000; Teunou et al., 1999).

2.4. CONCLUSION

Despite considerable literature reporting on solute segregation phenomena during spray drying of a multi-component aqueous solution and their effects on the surface composition and morphology of the dried particle, there is still a lack of understanding about which mechanism dominates and how variations in the drying system and process parameters affect the accumulation of certain molecules during spray drying. Moreover, this principle of *in-situ coating* has been seldom exploited to tailor particle and powder functional properties through controlling the solute segregation and therefore the surface composition of spray-dried particles. This work was designed to contribute towards a deeper understanding of the mechanisms involved in solute segregation during spray drying, with the further aim of using this knowledge to design a one-step spray coating process for the coating of amorphous lactose powder. Combinations of various competing, edible coating materials were investigated under optimized spray drying conditions, and their effects on particle

morphology, size and density as well as powder yield, powder flow, wettability, crystallization delay and caking of amorphous lactose powder were explored. The overall goal was to produce a value-added, free-flowing, non-caking, coated lactose powder suitable for use as an additive in foods (dairy or non-dairy) or pharmaceuticals.

3. THE USE OF SURFACE ACTIVE MILK PROTEINS AS FUNCTIONAL COATINGS FOR SPRAY-DRIED LACTOSE POWDER

3.1. INTRODUCTION

Solute segregation between various solutes within droplets of aqueous solutions during spray drying has been observed by several authors (Adhikari et al., 2009b; Elversson & Millqvist-Fureby, 2006; Fäldt & Bergenståhl, 1994, 1995; Kim et al., 2009a; Landström et al., 2003; Nijdam & Langrish, 2006; Vehring, 2008; Wang & Langrish, 2010). This segregation can result in one of the solutes accumulating at the droplet surface in preference to other solutes, and thus dominating the final particle surface after spray drying. While the mechanisms of solute segregation, in particular during the spray drying process, are still not fully understood, a number of observations have been made and explanations suggested. Surface activity is assumed to be one of the main reasons why surface active species such as proteins accumulate on an air-water interface (Fäldt & Bergenståhl, 1996; Wang & Langrish, 2010). The development of water concentration gradients (Kim et al., 2003) and differences in Peclet numbers between solutes (Trueman et al., 2012; Vehring, 2008) are other mechanisms that can cause solute segregation during spray drying due to preferential diffusion of solutes into the droplet interior, as described in detail in Section 2.3.4 of this thesis.

The concept of solute segregation can be exploited to produce coatings and films for food and pharmaceutical industries, for example to protect sensitive materials, to encapsulate other volatile components within the drying medium (Wang & Langrish, 2010) or to change particle size, density and morphology and thus alter powder functional properties such as flowability and wettability (Fäldt & Bergenståhl, 1996). Powder properties are important because they impact on the handling of powders during transportation, mixing, compressing and packaging (Fitzpatrick et al., 2004). These powder functional properties depend on the particle size distribution, particle shape, surface morphology and bulk density of the powder, which can be influenced to a certain extent by controlling the spray drying process (Masters, 1972; Pisecky, 1997), as described in Section 2.3.7 of this thesis. Moreover, the surface composition of the spray-dried powder has a significant impact on powder functional

properties (Buma, 1968; Kim et al., 2002, 2005b; Pisecky, 1997; Teunou et al., 1999). The ability of surface active proteins to adsorb on interfaces can be exploited to form a non-sticky coating on the surface of lactose powder during spray drying to increase powder yield, as reported by Adhikari et al. (2009a). This phenomenon also has the potential to improve powder flow and minimize powder caking. Thus, coated powders with improved functionality may be produced via a one-step spray drying process (*in-situ coating).*

Goal of this investigation:

A number of papers in the literature report on the effect of feed composition and various operating conditions on protein accumulation at the surface of spray-dried particulates of sugar and protein (Fäldt & Bergenståhl, 1994; Gaiani et al., 2010; Kim et al., 2009b; Nijdam & Langrish, 2006; Wang & Langrish, 2010). These studies tend to explore the effect of only a few process parameters. In this study, a detailed examination of the effect of all the important process parameters in spray drying (from pH and sugar solubility to total solids (TS), atomisation pressure and air temperature) on protein surface concentration, particle morphology, crystallization delay and functional properties of the powder was carried out. Since there are no other such studies currently published, this investigation provides a comprehensive experimental data set to fill this gap, allowing a consistent overview of factors that affect the properties of *in-situ* coated spray-dried powders for the food and pharmaceutical industries. This broad overview also allows a clearer understanding of the physics involved in *in-situ coating* during spray drying, so that the validity of the different mechanisms proposed for solute segregation and the formation of a particle surface during spray drying can be examined.

This chapter is split into two parts. The first part aims to find methods to increase the total surface accumulation of proteins during spray drying, with the ultimate goal of excluding all lactose from the surface of the final particles. Different feed and process parameter such as total solids (TS) of the solution, air drying temperature and atomization pressure were investigated in order to change the drying time and thus the time available for the proteins to adsorb at the droplet surface during the short time-frame of spray drying (in the order of milliseconds to seconds, depending on the scale of the spray dryer (Vehring, 2008). In addition, various solution pHs were tested in order to investigate whether the

increased surface activity of proteins at a pH closer to their isoelectric points (pI) resulted in higher final protein surface loads. Most of this investigation focused on lactose as the component to be in-situ-coated during spray drying, since lactose is common in many food and pharmaceutical applications, and these industries could benefit from the availability of a lactose product less prone to particle stickiness and caking.

In order to investigate the effect of sugar solubility on the protein surface coverage of spray-dried particles, sucrose and maltose were also tested. X-ray diffraction (XRD) was used to determine whether sugar crystallization occurred during spray drying for any of the sugars tested, since there are a number of publications in the literature with different conclusions concerning crystallization of sugars during spray drying (Chiou et al., 2008; Roos, 2002), as described in Section 2.1.2. Hence, lactose, maltose and sucrose with solubilities of approximately 18%, 46% and 67% at 25°C respectively were spray-dried with Na-Cas at different ratios to determine 1) whether sugar solubility has any influence on crystallization during spray drying, and if so 2) whether crystallization has an effect on protein enrichment at the surface of the particulates.

The second part of this chapter looks at the effect of feed composition and operating conditions on the functional properties of spray-dried lactose/protein powders. Powder recovery (or yield) as well as powder flowability and wettability were analyzed, and these results were interpreted in the context of the measured surface composition, particle size, and powder bulk density. Scanning Electron Microscopy (SEM) was used to determine the effect of protein concentration on the morphology of powders analyzed directly after spray drying and after lactose was allowed to crystallize during long-term storage. The purpose of these long-term storage tests was to investigate the stabilizing effect of surface proteins on lactose crystallization and caking. The results of powder stability tests using dynamic vapour sorption (DVS) are also presented.

Na-Cas was used as the main coating additive in this study, although WPI was also used to provide supporting data and to allow comparisons to be made. Both are common milk proteins with high surface activities, and have been shown to accumulate at droplet surfaces during spray drying of aqueous solutions (Fäldt & Bergenståhl, 1994, 1995; Landström et al., 2003; Wang & Langrish, 2010).

3.2. MATERIALS AND METHODS

Materials

α-Lactose monohydrate, Na-Cas and WPI were supplied by Fonterra Research and Development Centre (FRDC) (Palmerston North, New Zealand). Sucrose and maltose were purchased from BDH (Poole, England). General properties of the different disaccharides used are listed in Table 3.1. Molecular properties of β-lactoglobulin and β-casein, the main proteins within WPI and Na-Cas, are listed in Table 3.2.

Table 3.1: Properties of spray-dried sugar species: lactose, maltose, sucrose (Haque & Roos, 2004a; Ribeiro et al., 2006; Sober, 1968; Uedaira & Uedaira, 1969)

	Lactose	**Maltose**	**Sucrose**
Formula	$C_{12}H_{22}O_{11}$	$C_{12}H_{22}O_{11}$	$C_{12}H_{22}O_{11}$
Molar mass (g/mol)	342.3	342.3	342.3
Solubility in water (25°C)	17.8 %	46.0 %	66.7 %
Glass transition temperature (totally dry)	105.4°C	~77°C	65°C
Diffusion coefficient in diluted water (25°C) (m^2 s^{-1})	5.66×10^{-10}	5.61×10^{-10}	4.23×10^{-10}

Table 3.2: Molecular properties of β-casein and β-lactoglobulin (Sober, 1968; Suttiprasit et al., 1992; Thompson et al., 2009)

	β-casein	**β-lactoglobulin**
Molecular weight (Da)	24,100	18,300
Diffusion coefficient at 20°C (m^2/s)	6.05×10^{-11}	7.34×10^{-11}
Isoelectric point (pH)	4.6	4.1

Solution preparation

Different sugar/protein solutions of 10 wt% total solids (TS) content were prepared in distilled water. Firstly, lactose solutions were prepared at 40 to 60 °C under constant agitation. In order to prevent protein aggregation, the pH of the lactose solutions was neutralized by adding aqueous NaOH solution and using a pH meter with temperature correction (CybersScan pH510, Eutech Instruments, Singapore) before proteins were added. Proteins were then dissolved by adding small amounts incrementally while constantly stirring to prevent clumping. The pH was adjusted afterwards by titration of low-molar HCl or NaOH solutions. All solutions were degassed for 30 minutes by drawing vacuum in glass flasks before spray drying. To investigate the effect of protein weight concentration, pH and TS on the protein surface enrichment of spray-dried particles, the following conditions were tested:

- Lactose/Na-Cas=99.9/0.1, 99/1, 95/5, 90/10, 80/20 wt% @ pH 6.0, 7.0, 8.5 and TS of 10wt%
- Lactose/Na-Cas=60/40, 40/60 wt% @ pH 7.0 and TS of 10wt%
- Lactose/Na-Cas=99/1 and 90/10 wt% @ pH 7.0 and TS of 5wt%, 10wt% and 20wt%
- Lactose/WPI= 90/10 wt% @ pH 5.0, 6.0, 7.0, 8.5 and TS of 10wt%

Spray drying

All solutions were spray-dried in a laboratory spray dryer (*NIRO Atomizer,* Copenhagen, Denmark) with dimensions of 175 x 92.5 cm (height x diameter) (Figure 3.1), using a single stage and open-cycle drying systems with a co-current air flow. This spray dryer was commissioned before conducting this study (see Appendix A.1). A line diagram of the spray drying system is shown in Figure 3.2. The air inlet is transported by a centrifugal exhaust fan (3-phase motor), filtered and heated up by an electric 7.5 kW air heater to the desired temperature (maximum temperature: 350°C), before entering the chamber lid, which acts as an air disperser. This ensures effective control of the air flow pattern. The hot air is then directed around the atomizer into the drying chamber.

For atomization, a two-fluid nozzle with external mixing and with an orifice diameter of 1.5 mm was used (Figure 3.3). This nozzle was compared to a rotary-atomizer and found to be more suited for the small-scale production of coated lactose powder (see Appendix A.1.2).

A cyclone was used to separate the particles. The air flow was kept constant at 100±5 m^3 h^{-1}, and a peristaltic pump was used for the feed supply to the atomizer. The base set of spray drying conditions used were inlet/outlet air temperatures of 160/76±2°C, atomization pressure of 0.6±0.05 bar and solution feed rate and temperature of 1.5±0.1 kg h^{-1} and 40±1°C, respectively. To investigate the effect of different drying rates on the protein surface enrichment of spray-dried particles, the following spray drying parameters were varied for different lactose/Na-Cas mixtures:

- Feed rate: 1.5; 2.0 kg/h (±0.1 kg/h)
- Drying temperature (inlet/outlet): 220/101[1]; 180/87[1]; 180/82[2]; 160/75[1]; 160/70[2]; 140/67[1]; 140/62[2]; 120/58[1]°C (Variation in outlet temperatures during drying: ±2°C)
- Atomization pressure: 0.2; 0.6; 1.0 bar (±0.05 bar)

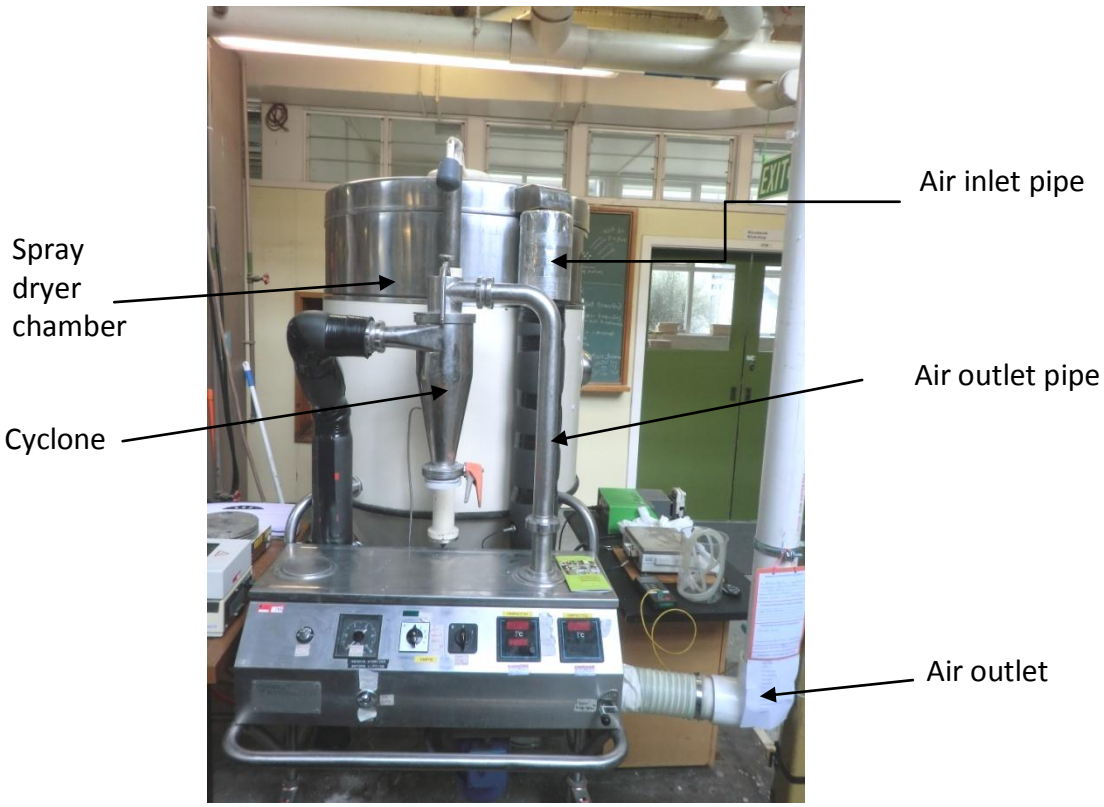

Figure 3.1: Laboratory spray dryer (Niro Atomizer, Denmark)

[1] Feed rate=1.5 kg/h
[2] Feed rate=2.0 kg/h

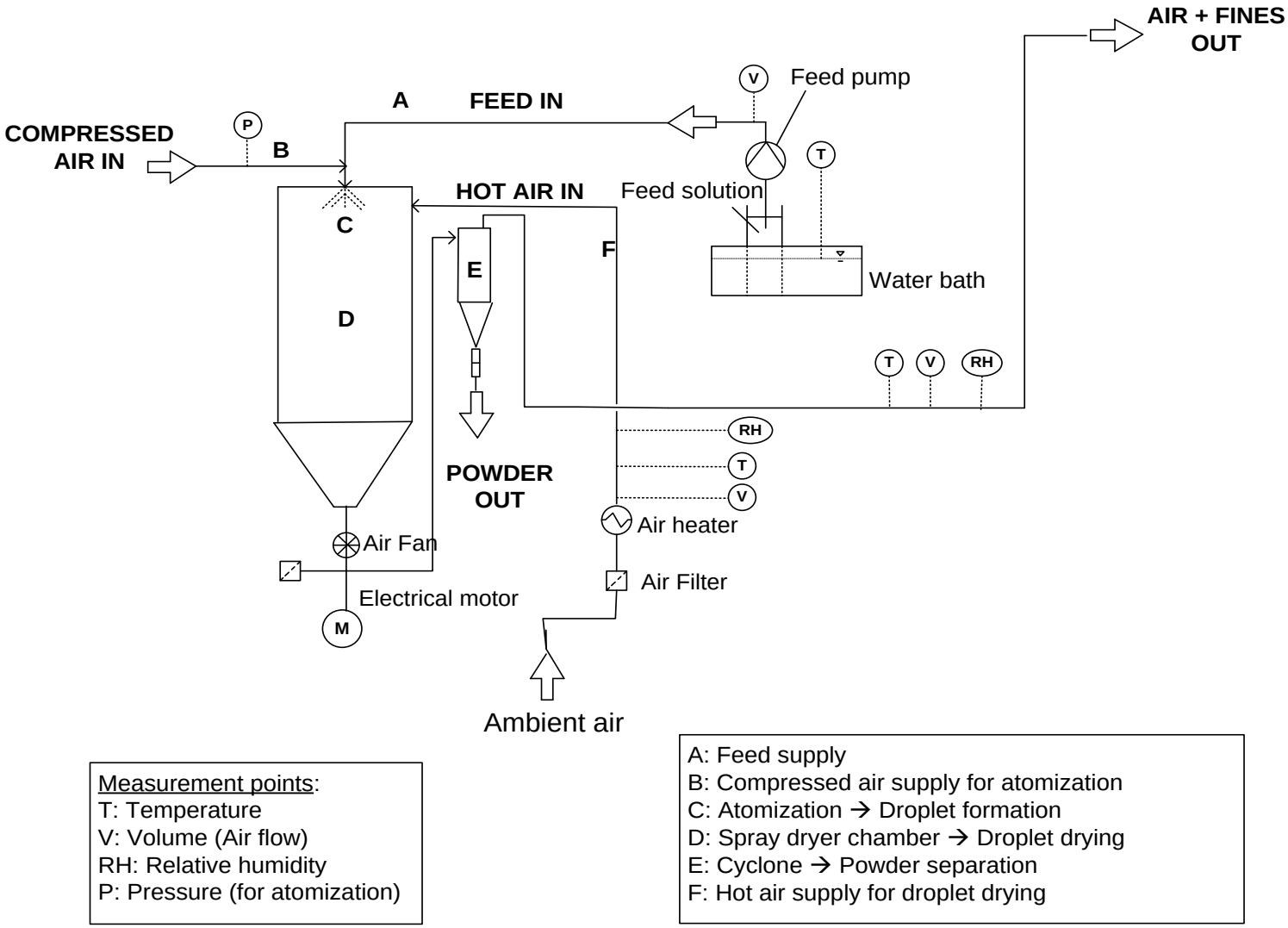

Figure 3.2. Line diagram of spray drying system

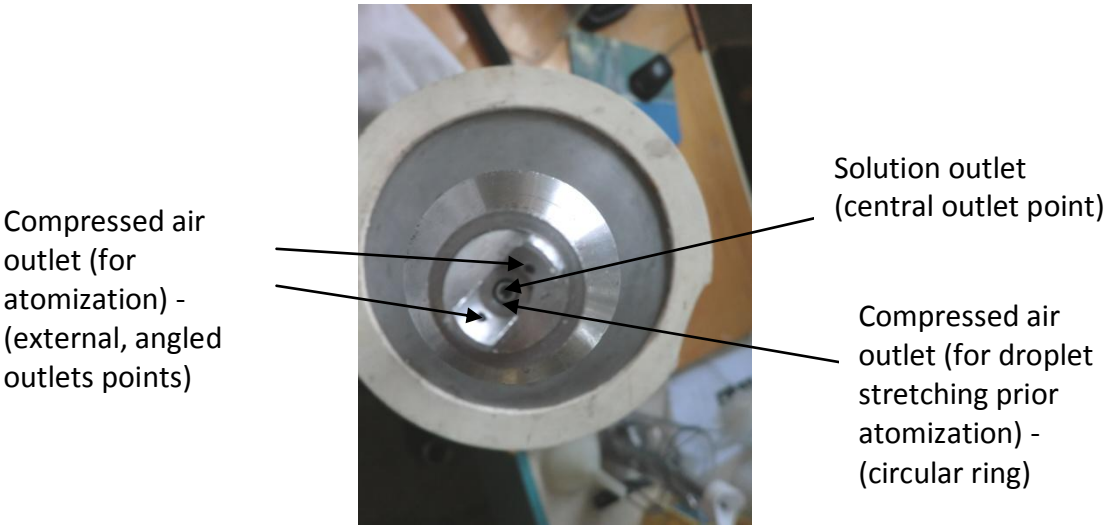

Figure 3.3: Two-fluid nozzle with external mixing, used for spray drying studies

Powder storage

One half of the spray-dried powder was stored inside a desiccator containing silica salt to keep the powder dry and prevent lactose crystallization. This powder was then used for analyzes such as Scanning Electron Microscopy (SEM), moisture sorption and measurement of functional properties. The other half of the spray-dried powder was stored unprotected at ambient air conditions to allow moisture absorption and crystallization of the lactose to occur. After several weeks of storage, SEM was used to determine the surface appearance of this crystallized powder.

X-ray Photoelectron Spectroscopy (XPS)

X-ray photoelectron spectroscopy was used to measure the surface composition of spray-dried particles. Relative atomic concentrations at the particle surface (~10 nm depth resolution (Fäldt & Bergenståhl, 1994)) of carbon, oxygen and nitrogen were recorded and used to calculate the appropriate surface concentrations of the sugar (lactose, sucrose or maltose) and proteins (Na-Cas or WPI), using the matrix calculation described by Fäldt et al. (1993) and explained in detail in Appendix A.2.1. The following elemental compositions of the pure elements were measured: lactose - carbon (57.6%) and oxygen (42.4%); sucrose - carbon (57.7%) and oxygen (42.3%); maltose - carbon (58.8%) and oxygen (41.7%); Na-Cas - carbon (71.2%), oxygen (13.8%) and nitrogen (14.8%); WPI - carbon (70.5%), oxygen (16.8%) and nitrogen (12.7%). A linear relationship between the elemental ratios of the pure

powders and the spray-dried powders is assumed to calculate the percentage component concentrations at the particulate surface.

XPS spectra were recorded on a Kratos Axis Ultra DLD (Kratos Analytical, Manchester, UK) using monochromatic Al Kα X-rays (1486.69 eV) operating at an X-ray source power of 150 W, while the charge analyzer was put on. The powdered samples were placed into a small 2 mm diameter depression in a copper sample mount and the excess powder was scraped off to leave a flat surface for analysis. Samples were exposed to the laboratory atmosphere for a maximum of 20 minutes (time taken to load 18 samples) before being admitted into the vacuum system. The chamber pressure was lower than 10^{-8} Torr during data acquisition, while the base pressure in the system was usually at 10^{-9} to 10^{-10} Torr range. The analysis area for the data collection was approximately 300 × 700 μm using the hybrid electrostatic and magnetic lens system and the slot aperture.

Peak areas for carbon, oxygen and nitrogen signals were measured and converted into the elemental concentration using CasaXPS software with Kratos supplying the relative sensitivity factors (RSF). Shirley backgrounds were used to define the quantification regions.

X-ray Diffraction (XRD)

Spectra were collected on a SuperNova Dual diffractometer (Agilent Technologies, USA), fitted with an Alpha Detector, using monochromatic K-alpha X-rays. The powdered sample, suspended in perflouronated oil and attached to a glass fibre, was exposed for a series of 300s, 360 degree phi scans. A Lorentzian correction was applied to the data.

Surface tension measurements

Surface tension measurements of all solutions were performed prior to spray drying using the pendant drop technique (CAM 2008 surface tension meter, KSV Instruments Ltd, Helsinki, Finland). Five to ten pictures were taken for each droplet, and three to five droplets were analyzed for each solution to obtain an estimate of uncertainty.

Particle Size analysis

The particle size distribution of the spray-dried powder was measured using a Microtrac particle size analyzer (Microtrac ASVR X100, Leeds & Northrup, U.K.). Small amounts of the sample were first suspended in isopropanol and sonicated for a minute in order to break up any aggregates before particle size was measured. In the particle size analyzer, the particle size distribution was monitored each minute for up to 20 minutes to allow aggregates to break up. The volume based mean diameter was recorded, once it became constant. Three to five repeat measurements were performed to obtain an estimate of measurement uncertainty.

Scanning Electron Microscopy (SEM)

Powders were sprinkled onto double sided tape on a carbon tab with surplus powder being blown off using a nitrogen duster. Samples where then coated in an EMITECH K550X sputter coater set at 1.2kV and 50 M amps, which gave a coating thickness of approximately 1 nm. The specimens were observed in a Leica S440 Scanning Electron Microscope (Leica, Wetzlar, Germany). The images were captured at 20kV, 10kV, 5kV and 1kV using random sampling in the best area. Three random samples were taken from each specimen.

(Tapped) powder bulk density

Tapped powder bulk density was measured using a 10 mL measuring cylinder filled with 1 g of previously vacuum dried powder (0.05 bar, 50 °C, ≥24h). The cylinder was tapped manually to allow the cohesive powder structure to collapse and re-arrange until no further volume reduction was observed. Three repeat measurements were performed to obtain an estimate of measurement uncertainty. Bulk densities were then calculated by dividing the mass by the measured volume.

Powder flow (powder stickiness)

Powder stickiness was indirectly determined by measuring the fraction of powder that passed through a vibrating sieve with a mesh size of approximately 0.65x0.65 mm (used as standard for all powders). The powder was vacuum-dried before measurement to remove all

moisture and then stored in a desiccator with silica salt to keep the powder dry. To compensate for the different powder bulk densities, a constant powder volume of 2.0 mL was used for the measurements. The required initial mass for each powder was calculated by multiplying its previously measured bulk density with the powder volume. Powder samples were transferred onto the sieve, which was attached to a vibrating device (Syntron magnetic feeder) and shaken at constant amplitude for 30 seconds. The remaining powder on the sieve was weighed and the percentage mass flow through the sieve was calculated. Three repeat measurements were performed to obtain an estimation of measurement uncertainty. To determine the possible effect of moisture absorption during measurement, powder flow tests were repeated with 1 and 2 minute pauses between the time the sample was loaded onto the sieve and the time that vibration was initiated. The repeated powder flows were all within the expected measurement uncertainty, which suggests that any effect of moisture absorption during the short sieving time-frame of 30 s was negligible.

Wettability

Wettability of powders was measured according to a modified form of the method described by Freudig et al. (1999). A 0.1 g sample of powder was suddenly deposited onto the surface of water heated to 50 °C in a 200 mL beaker, using a sliding container mechanism. The wetting time was the time for the last powder particle on the surface to sink below the surface. Three to five repeat measurements were performed to obtain an estimation of measurement uncertainty.

Dynamic vapour sorption (DVS)

Powder hygroscopicity and lactose crystallization were measured by using dynamic vapour sorption (Vapour Sorption Analyzer, AquaLab, Decanon, USA). A homogenous, thin layer of powder (approximately 600mg) was evenly spread onto the chamber bottom using a tea strainer to destroy agglomerates and thus minimize their effect on mass diffusion limitations of water vapour through the porous powder cake. The powders were initially dehydrated to a water activity (a_w) of 0.05 by flowing dry air from a desiccant tube across each sample; the water activity was then adjusted to 0.4, which corresponds to a relative humidity (RH) of 40%. The weight gain of the powder upon moisture absorption was

measured by an in-built high precision magnetic force balance. Water activity was determined using a chilled-mirror dew-point sensor. The water activity was adjusted by incremental steps of 0.02 (corresponding to 2% RH), each at a time limit of 6 hours, to allow the powder to equilibrate with the humid air inside the chamber and to allow lactose to crystallize once the critical water activity was exceeded. The analysis was stopped once the powder lost moisture upon lactose crystallization.

3.3. Results and Discussion

3.3.1. Part A: Investigation into surface accumulation of surface active milk proteins

Effect of Na-Cas bulk concentration

The effect of increasing protein/lactose weight ratios from 0.1/99.9 to 60/40 in aqueous solutions (10wt% TS, pH of 7.0) on the surface enrichment of Na-Cas during spray drying was investigated. Figure 3.4 shows that the spray-dried lactose/Na-Cas particles had considerably higher protein concentrations at the surface than within the bulk. Indeed, only low Na-Cas concentrations of just 0.1 wt% of the total solid content (equivalent to 0.01 wt% in solution) resulted in a Na-Cas surface concentration of approximately 38%. This agrees with the results presented by other authors that this protein accumulates at the liquid surface of droplets during spray drying, most likely due to its high surface activity (Fäldt & Bergenståhl, 1994; Wang & Langrish, 2010) and also a Peclet number effect (Vehring, 2008), as discussed in Section 2.3.4 of this thesis. It can be clearly seen that the Na-Cas surface concentration reached a plateau as the protein bulk concentration increased. This can be explained by the fact that the droplet surface became increasingly occupied by adsorbing Na-Cas proteins to the point where the surface was saturated with proteins (Graham & Phillips, 1979a), and thus no more protein could adsorb there. The saturation implies a maximum packing density is reached at the surface. Whether this maximum packing occurs due to 1) fast diffusion, adsorption and surface equilibrium of proteins or 2) possible internal moisture content gradients and/or a Peclet number effect will be investigated in Chapter 4.

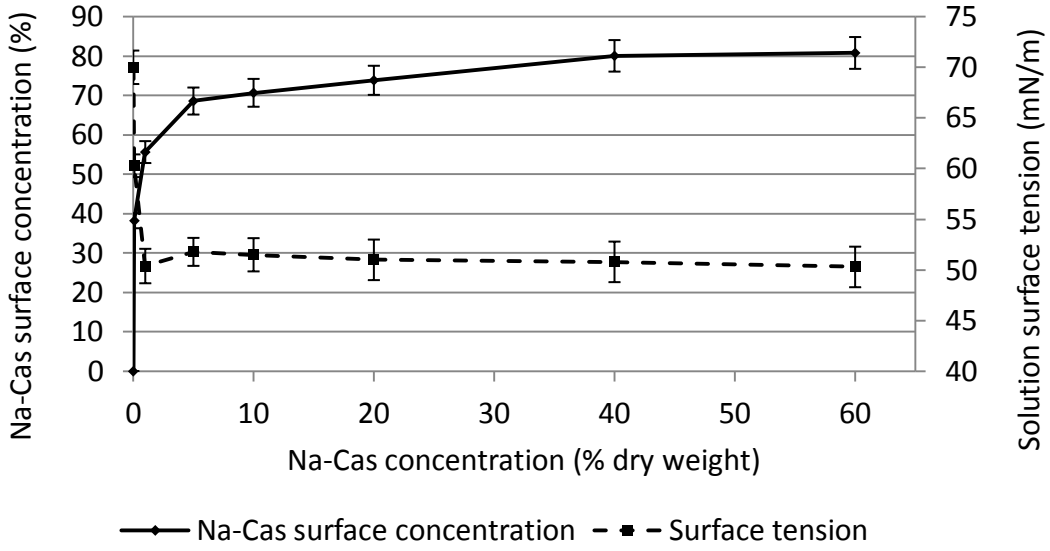

Figure 3.4: Effect of Na-Cas solid concentration on final Na-Cas surface concentration of lactose/Na-Cas particles, spray-dried at pH7 (solid line) and surface tension of aqueous lactose/Na-Cas solutions (pH7) (dashed line).

Small amounts of fat impurities within the lactose and Na-Cas powders (impurities of the powders were not known) were also likely to accumulate on the particulate surfaces during spray drying. For low protein bulk concentrations of 0.1 and 1 wt%, these impurities in the bulk solution may have been higher than the protein concentration. This would have caused a systematic error in the final calculated Na-Cas surface concentrations, due to higher measured C/O ratios (fat has significantly higher C/O ratio than proteins), when the elemental surface compositions of oxygen (O), nitrogen (N) and carbon (C) are considered for the calculation of the protein surface concentration, called Method A here. To account for any fat presence at the particle surface, nitrogen alone was considered for calculating the Na-Cas surface concentration, called Method B here. This is justified because both lactose and fat contain only oxygen and carbon, whereas the protein also contains nitrogen. Thus, the nitrogen concentration is directly related to the protein surface concentration irrespective of the presence of fat. Both methods are described in detail in the Appendix A.2.1. Protein surface concentrations, calculated by using Method B, agreed within an uncertainty of ±5% with results obtained by Method A (Figure 3.4). The only exception was the lowest Na-Cas bulk concentration of 0.1 wt%, which resulted in around 10% lower Na-Cas surface concentrations when using Method B, probably due to small amounts of fat present at the particulate surface at low protein bulk concentrations. However, due to the good agreement between both methods for protein bulk concentrations ≥ 1wt%, Method A results are shown

here and within the rest of this thesis due to the higher accuracy of the results when considering all three elements C, N and O for the calculation of the surface composition.

Surface tension measurements were performed for lactose/Na-Cas solutions of 10wt% TS, pH of 7.0 and ratios from 99.9:0.1 to 4:6 in order to demonstrate the surface active nature of Na-Cas. A clear decrease in surface tension with increasing Na-Cas solid concentrations can be seen from 70 nM/m for a pure lactose solution to around 50 nM/m for lactose/Na-Cas ratios of 99/1% (Figure 3.4). Further increase in Na-Cas bulk concentration above 1 wt% of total solids did not result in any further decrease in the surface tension. This suggests that the droplet surface during surface tension measurement became saturated at Na-Cas solid concentrations of already 1 wt% (0.1 wt% in solution). This decrease in surface tension with increasing protein concentration correlates well with the increase in protein concentration at the surface of spray-dried particles (Figure 3.4). This trend was also observed by Fäldt and Bergenståhl (Fäldt & Bergenståhl, 1994), who suggested that the composition of the dried-particle surface reflects the composition of the droplet surface during drying. As can be seen by the development of a plateau in the Na-Cas surface composition for Na-Cas bulk concentrations of around 1 to 5 wt% and higher, the process of droplet drying within the spray dryer seemed to be long enough for proteins to diffuse towards the droplet surface and adsorb there, which Adhikari et al.(2009a) and Landström et al. (2003) have also concluded. The observed slight increases in Na-Cas surface concentration at higher Na-Cas bulk concentrations were likely to be caused by lower lactose bulk concentrations, which resulted in lower amounts of dissolved lactose in the vicinity of adsorbed proteins at the surface.

Figure 3.4 and subsequent figures show that it is extremely difficult to form a complete protein coating (100% surface protein concentration) and thus completely exclude lactose from the surface of the spray-dried particles. It was discussed in Section 2.2.5 that, when sugar-protein mixtures are spray-dried, the sugar acts as a water replacer, forming a hydration coating around individual charged proteins due to hydrogen bonding of hydroxide groups on the sugar with polar groups on the protein (Arakawa & Timasheff, 1982; Belyakova et al., 2003; Fäldt & Bergenståhl, 1995; Lee & Timasheff, 1981). As a side effect, this solubilises and stabilizes proteins adsorbed at liquid interfaces, limiting structural reorientations and denaturation. Due to this hydration effect and the considerably smaller molecular size of lactose molecules compared with Na-Cas, lactose can easily penetrate through initially loosely packed adsorbed protein layers and thus also be present at the surface. This has

practical implications for the functional properties of the powders and powder stability during storage, discussed in Section 3.3.2 of this thesis.

Effect of pH

Protein surface coverage increased when the pH was lowered from 8.5 to 6.0 (Figure 3.5). This was consistent for all tested lactose/Na-Cas ratios, ranging from 99.9/0.1 wt% to 80/20 wt%. The isoelectric point (pI) is defined as the pH at which the protein net charge is zero, which for Na-Cas is around 4.6 and for a WPI mixture is between 4.5 and 4.2. As explained in Section 2.2.2 of this thesis, the surface charge of proteins in solution decreases when approaching the isoelectric point (pI). This increases the surface activity of a protein, because a lower protein surface charge reduces electrostatic repulsion between neighbouring proteins, and this decreased electrostatic barrier for protein adsorption causes higher adsorption rates at the surface (Atkinson et al., 1995b; Magdassi, 1996). We assume that, due to the reduced electrostatic repulsion between proteins at a pH closer to the pI, proteins can approach each other closer at interfaces and thus be packed into denser protein films. This is supported by studies of other researchers, who performed adsorption studies of different proteins at various solution pHs in films (Atkinson et al., 1995a; Caessens et al., 1999; Paulsson & Dejmek, 1992) as described in Section 2.2.4. This packing effect is accentuated in droplet drying since the surface area also progressively reduces as water evaporates. The tighter the packing of the protein surface layers during spray drying, the less water and therefore dissolved lactose will be available in the vicinity of the protein for hydrogen bonding.

Note that no protein precipitation (in the form of a cloudy solution or visible aggregates) was observed for any of the spray-dried aqueous lactose/Na-Cas solutions. Protein precipitation, which can occur at a pH close to the pI of the protein, would have complicated the spray drying of such a solution and could have affected the adsorption behaviour of proteins and their packing density at the interface.

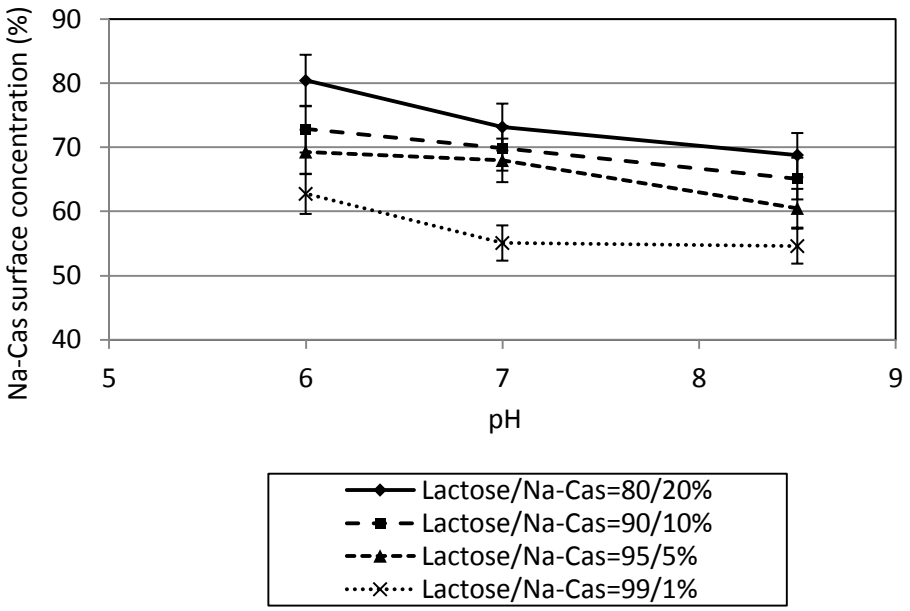

Figure 3.5: Influence of pH on Na-Cas surface concentration of spray-dried lactose/Na-Cas particles.

Surface tension of the aqueous lactose/Na-Cas solutions of various pHs was measured prior to spray drying using the pendant drop technique. Figure 3.6 shows that, within experimental uncertainty, there were no differences in the surface tensions of the aqueous solutions at various pHs, with lactose/Na-Cas (99.9/0.1, pH 8.5) as only exception, possibly due to a systematic measurement error. This implies that the equilibrium surface concentration for Na-Cas proteins at the aqueous surface was independent of the solution pH in the range tested here. This agrees with Graham and Phillips (1979a), who also showed that the surface load of adsorbed β-casein proteins at the air-water interface of a film was not affected significantly by the pH close to the isoelectric point. They found that the surface concentration of β-casein reduced only for sufficiently high pH values due to increased electrostatic repulsion between the proteins. Thus, the pH range tested here was probably too narrow to measure noticeable changes in the surface tension of aqueous lactose/Na-Cas solutions at the different pHs.

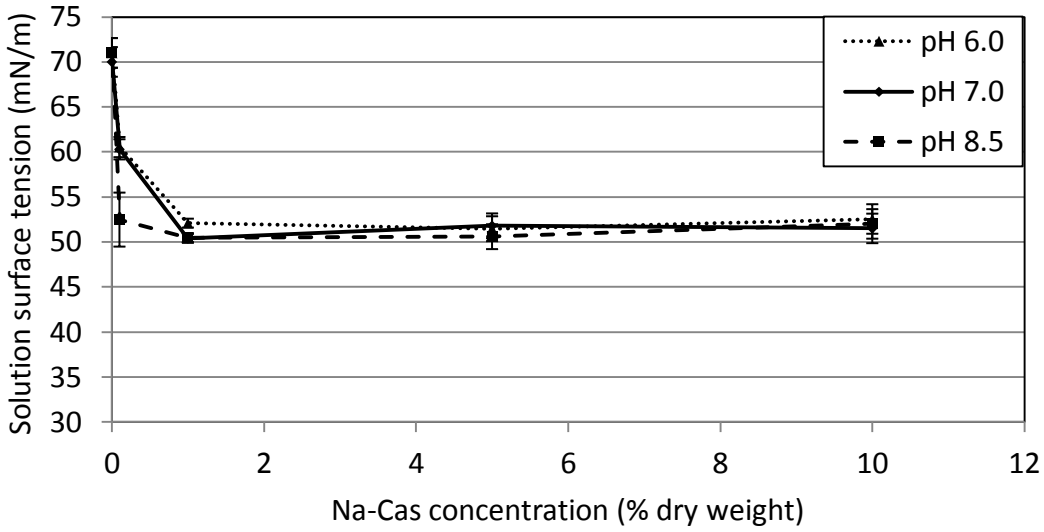

Figure 3.6: Surface tension measurements for different lactose/Na-Cas solutions (10wt% TS) at different pH.

In Figure 3.7, the surface concentration of Na-Cas is compared with that of WPI for a spray-dried lactose/protein solution of 90/10 wt% at various pHs to confirm the effect of the pH on surface enrichment for different proteins. WPI showed the same trend of increasing protein surface concentration with decreasing pH towards the pI, where intermolecular interactions between proteins become stronger. As also found by Wang and Langrish (2010), Na-Cas had a higher percent surface coverage than WPI for any given lactose/Na-Cas ratio. Surface tension measurements (γ) of lactose/Na-Cas and lactose/WPI solutions resulted in lower surface tensions for the aqueous lactose/Na-Cas (γ =51.3±0.7 mNm^{-1}) than for the aqueous lactose/WPI (γ =57.6±1.2 mNm^{-1}) solution, which indicates a higher surface activity of Na-Cas. This agrees with Mulvihill and Fox (1989), who also reported a higher surface activity of β-casein than β-lactoglobulin. Considering the higher hydrophobicity and flexibility of Na-Cas compared to WPI proteins (Thompson et al., 2009), Na-Cas proteins are likely to approach each other closer at interfaces and thus be packed into denser protein films. This is supported by Graham and Phillips (1979c) who measured higher changes in the surface pressure upon β-casein adsorption compared to more globular proteins such as BSA or lysozyme. They assumed that this arises because the casein film is more compressible due to casein being more flexible, forming loops that have higher density and that can extend into the air phase under increasing surface pressure.

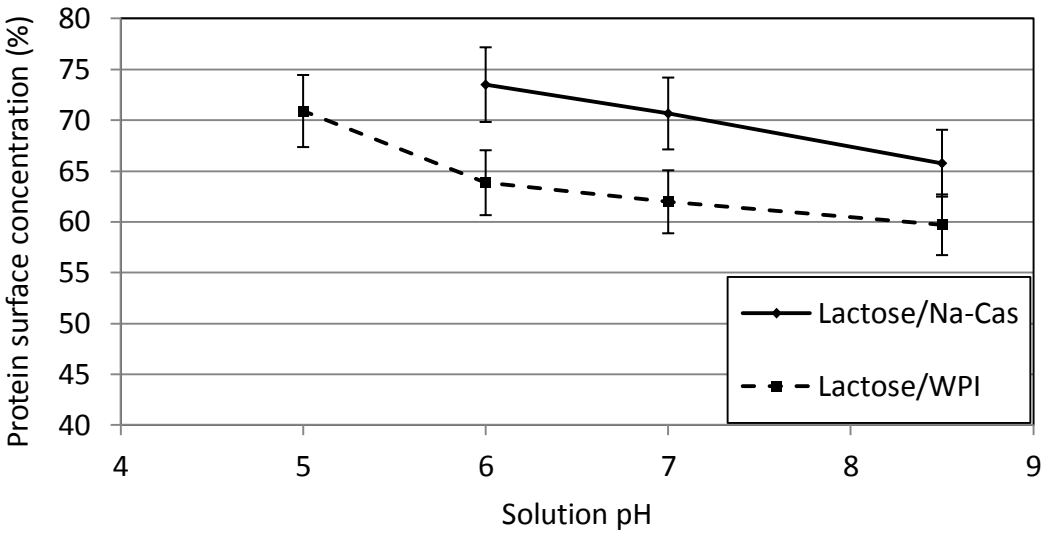

Figure 3.7: Protein surface concentration of lactose/Na-Cas (90/10 wt%) and lactose/WPI (90/10 wt%) particles spray-dried at different pH.

Differences in the Peclet numbers between both proteins due to different molecular sizes may have also contributed towards different enrichment ratios between the proteins and thus possibly different surface enrichment ratios, as suggested by Vehring (2008). The effect of the Peclet number on solute segregation phenomena during spray drying will be investigated in Chapter 4 and 5.

Effect of sugar solubility

XRD measurements of the powders were performed in order to investigate whether a partial crystallization of the lactose occurred during spray drying. Generally, α-lactose monohydrate crystals can be identified by its unique peak at a diffraction angle of 16.4°, while β-lactose can be detected by a peak at 10.5° (Rahman, 2008). As shown in Figure 3.8, no crystalline peaks can be found at diffraction angles of 10.5 and 16.4°, which indicates that no sugar crystallization occurred within the spray dryer for any of the disaccharides tested under the spray dryer operating conditions employed (XRD results of all powders are attached to the Appendix A.2.2). Moreover, Figure 3.9 shows that, within experimental uncertainty, sugar solubility did not significantly affect the protein surface concentration of dried particles at the spray drying conditions tested. This suggests that, at the spray drying conditions tested, sugar did not undergo a phase transition to a crystalline form at the

solubility limit, which would otherwise hinder or prevent protein adsorption at the surface. Rather, the sugar transformed progressively into a solid-like amorphous glass directly from the dissolved state, as stated by Roos (2002). This implies that protein mobility may be possible beyond the solubility limit, regardless of the solubility of the sugar. Even in the short timeframe of spray drying, surface active proteins such as Na-Cas seem to have sufficient time to adsorb at the air-water interface before they become encapsulated by the high-viscosity amorphous glass, irrespective of the sugar's solubility.

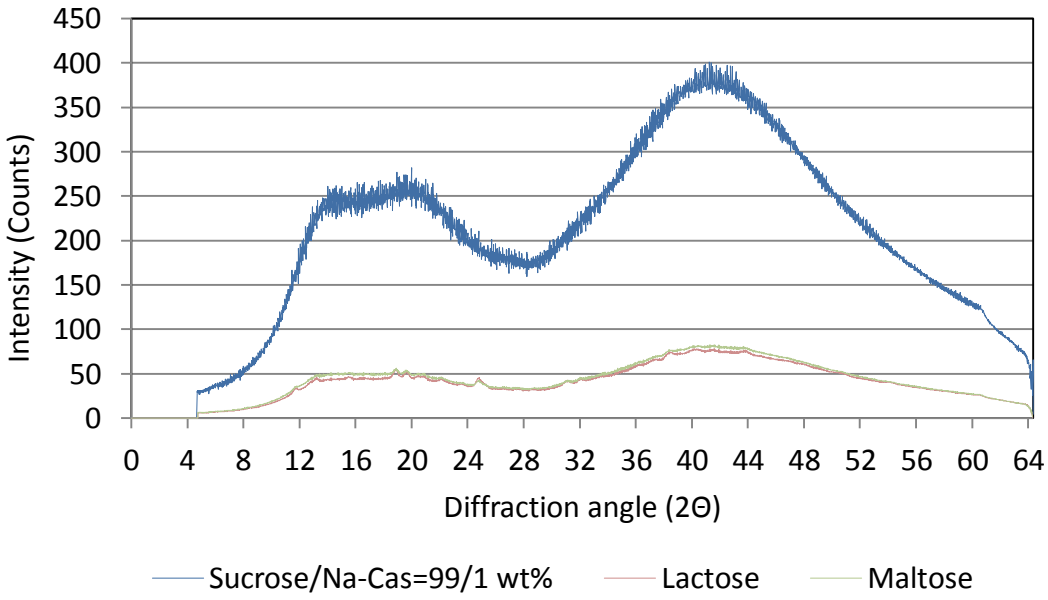

Figure 3.8: X-ray diffraction of spray-dried lactose, maltose and sucrose/protein powder.

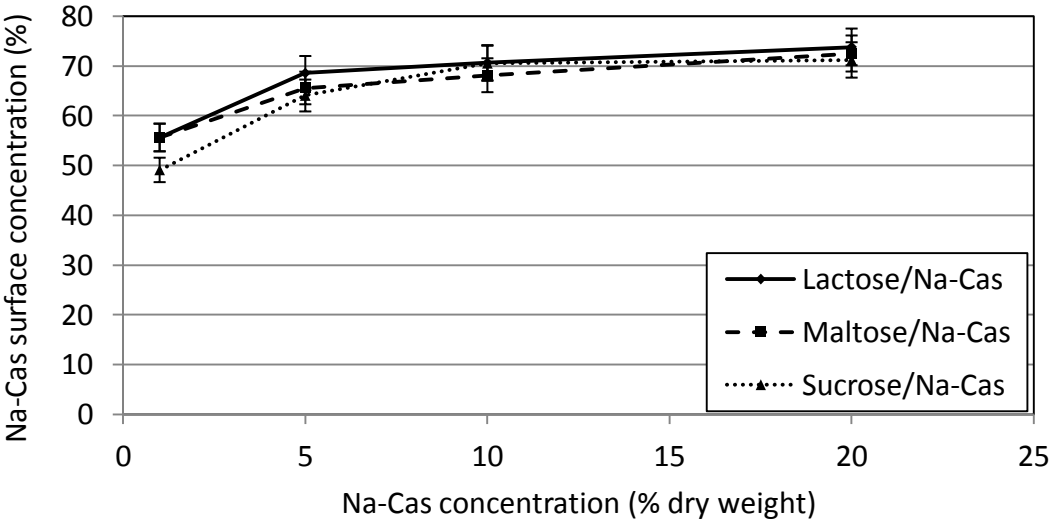

Figure 3.9: Influence of sugar solubility on Na-Cas particle surface concentration (drying temperature=160 °C, pH=7.0).

Effect of air inlet/outlet temperature and feed rate

The effect of drying time on the final protein surface enrichment of spray-dried particles was investigated for lactose/Na-Cas mixtures of 90/10 wt% by controlling the air outlet temperature through changes in the air inlet temperature and the solution feed rate. The protein surface coverage fell 2.5% (absolute) when the air inlet/outlet temperature was increased from 120/58 °C to 220/100 °C at a feed rate of 1.5 kg/h (Table 3.3). This is a small change given the significant measurement uncertainty. Increasing the feed rate from 1.5 to 2.0 kg/h for air inlet temperatures between 140 and 180 °C also had very little effect on the protein accumulation (Table 3.3).

Wang and Langrish (2010) showed a small trend of decreasing β-casein surface concentrations for higher air inlet temperatures. According to Nijdam and Langrish (2006) and Kim et al. (2009b) less time is available for proteins to adsorb at the surface at higher temperatures, since the droplets dry more quickly, which would explain the decrease in protein surface concentrations observed by these researchers However, Table 3.3 shows that this effect is very small in the experiments conducted here, which suggests that, for any of the spray drying conditions tested in this work, the protein concentration at the surface had sufficient time to reach the equilibrium concentration (or close to it) before the droplet solidified. Differences in spray drying conditions, feed composition and spray dryer designs were likely to have caused the differences in observations between this study and the studies of other researchers (Gaiani et al., 2010; Kim et al., 2009b; Nijdam & Langrish, 2006; Wang & Langrish, 2010).

Table 3.3: Influence of air outlet temperature (controlled by air inlet temperature and feed rate) on surface protein concentration of spray-dried lactose/Na-Cas particles (90/10 wt%)

Air inlet temperature (°C)	Chamber air outlet temperature (°C)	Feed rate (kg h^{-1})	Na-Cas surface concentration (%)	Error (%)
220	100	1.5	67	3
180	87	1.5	67	3
180	82	2.0	70	4
160	75	1.5	71	4
160	70	2.0	70	4
140	67	1.5	71	4
140	62	2.0	72	4
120	58	1.5	70	4

Effect of atomization air pressure

The atomization air pressure was changed at different lactose to protein ratios in order to increase the average size and hence the drying time of the droplets. For lactose to Na-Cas weight ratios of 90/10 wt%, the (volume based) mean particle size was increased from 13.3±1 to 23±3 µm when the atomization pressure was decreased from 1.0 to 0.2 bar. One might expect that more time would be available for proteins to adsorb at the droplet surface of larger droplets before the proteins become encapsulated within the continuous matrix of the lactose glass. Additionally, the total surface area of a spray with larger droplets is lower than for a spray with smaller droplets. It might be expected that a smaller surface to volume ratio would be more likely to become saturated faster by proteins for a given protein concentration. However, within experimental uncertainty, no clear differences could be observed in the final protein surface concentrations of spray-dried particles when the atomization pressure was varied, which suggests that there is no influence of the droplet size on the final protein surface concentration of spray-dried particles over the range of atomization pressures tested (Figure 3.10).

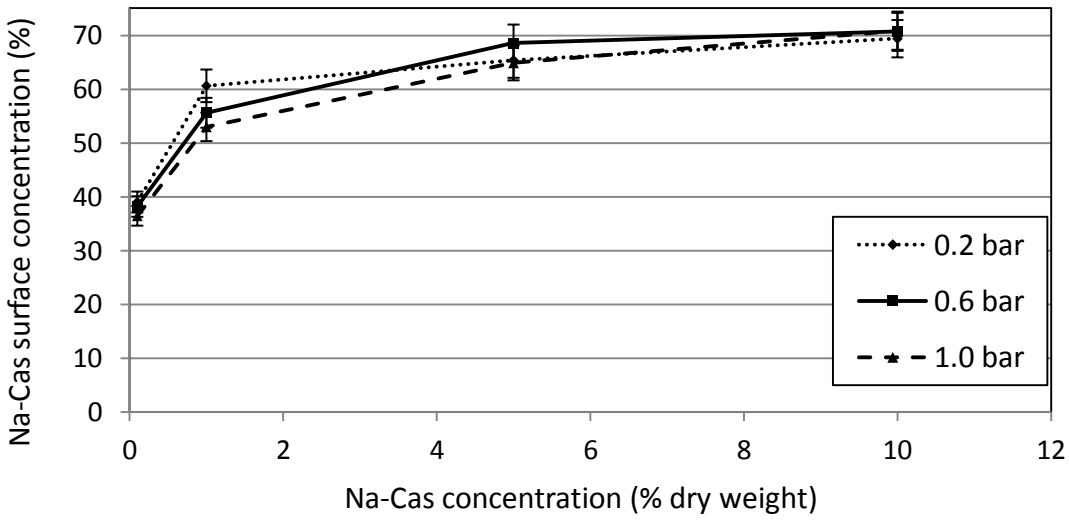

Figure 3.10: Influence of atomization pressure on Na-Cas surface concentration of spray-dried lactose/Na-Cas mixtures (pH7).

The results agree with the results of Kim et al. (2009b) who also showed no effect of surface composition of spray-dried skim milk powder for different particle sizes up to 90 µm. This implies that there is sufficient time for the Na-Cas proteins to adsorb at the droplet

surface and enrich there at the expense of lactose irrespective of droplet size and thus drying time, which further supports the previous assertion that Na-Cas proteins have sufficient time to adsorb at the surface before the droplet solidifies.

Effect of solution solid content

Figure 3.11 shows that a lower solution solids content resulted in a higher Na-Cas surface concentration for both a high protein to lactose weight ratio of 1:9 and a low protein to lactose weight ratio of 1:99. Kim et al. (2009b) attributes this to the lower viscosity of the solution at lower solid contents, which results in higher diffusion rates and hence a higher degree of segregation between dissolved components within the drying droplet before it solidifies. However, results obtained within this study and other studies such as Adhikari et al. (2009a) suggest that the surface quickly becomes saturated during spray drying. Since the saturation time is much faster than the drying time, the surface composition is unaffected by changes in temperature or droplet size, as shown in Table 3.3 and Figure 3.10. This would imply that viscosity effects are negligible. Other possible mechanisms to explain the effect of solution solids content on Na-Cas surface concentration include internal moisture content gradients and a Peclet number effect during spray drying. These effects will be explored in Chapter 4 in the light of film drying experiments.

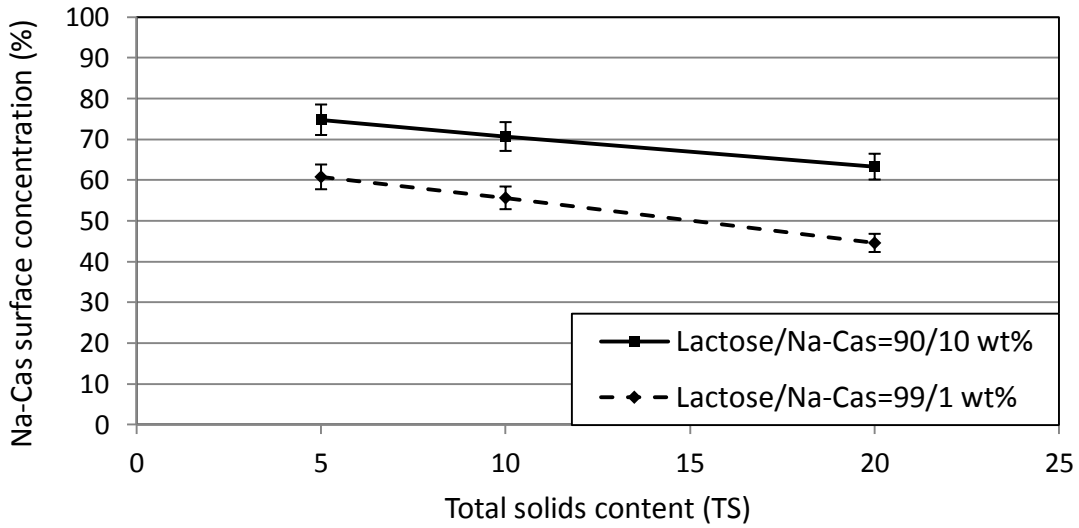

Figure 3.11: Influence of solution solid content on Na-Cas surface concentration of spray-dried lactose/Na-Cas particles (pH7).

3.3.2. Part B: Investigation into powder morphology, functional properties, lactose crystallization and caking of spray-dried lactose/protein powders

Effect of protein bulk concentration and solution pH on properties of spray-dried lactose/protein powders

Powder morphology, particle size and bulk density

Figure 3.12 shows the influence of increasing protein bulk concentrations on the morphology of spray-dried lactose/Na-Cas particles. While spray-dried pure amorphous lactose powder consisted of spherical particles with smooth surfaces, increasing protein/lactose bulk ratios resulted in an increasing appearance of wrinkles and folds. This surface roughness was also observed for spray-dried lactose/WPI powder (Figure 3.13). Surface folding and roughness or "dents" have been observed on the surface of particulates containing different flexible molecules such as proteins and polymers (Elversson & Millqvist-Fureby, 2006; Fäldt & Bergenståhl, 1994; Wang & Langrish, 2010). Dickinson (1999, 2001) explained that the adsorption of proteins causes the formation of a visco-elastic protein film at the air-water interface. Depending on the mechanical properties of the initial crust formed on the droplet surface, an internal vacuole can develop during spray drying due to entrapped air (Pisecky, 1997) or vapour formation (Nijdam & Langrish, 2005, 2006; Pisecky, 1997), causing particle deformations (expansion and subsequent deflation including surface folding), as explained in detail in Section 2.3.5 of this thesis. Those deformations are increased by the presence of flexible, elastic materials such as proteins or polymers due to an overall increase in the wall elasticity (Elversson & Millqvist-Fureby, 2006; Wang & Langrish, 2010). As a result, larger and more buckled particles of lower average particle (and hence bulk) density are produced when the protein concentration in the bulk is increased, which is confirmed by the experimental results of the present study (Figure 3.12 and Figure 3.14).

As discussed in Section 2.3.5, Sugiyama et al. (2006) and Vehring (2008) provide another mechanism of particle deformation. These authors state that, after an initial wall or crust has been formed, the particle wall becomes crumpled because the droplet can accommodate further shrinkage due to loss of moisture only by buckling of the outer wall. The crumpling of the particle wall depends only on the mechanical properties of the particle wall and how fast the particle surface is formed during drying; it is independent of the possible formation of a vacuole within the drying droplet. Both concepts would offer

possible explanations for the formation of wrinkled or buckled particles when the protein bulk concentration is increased. However, the observations made in this study (that larger particles of lower average density were produced with increasing bulk protein concentration) lend support to the theory that an expanding vacuole is the mechanism responsible for wall deformation.

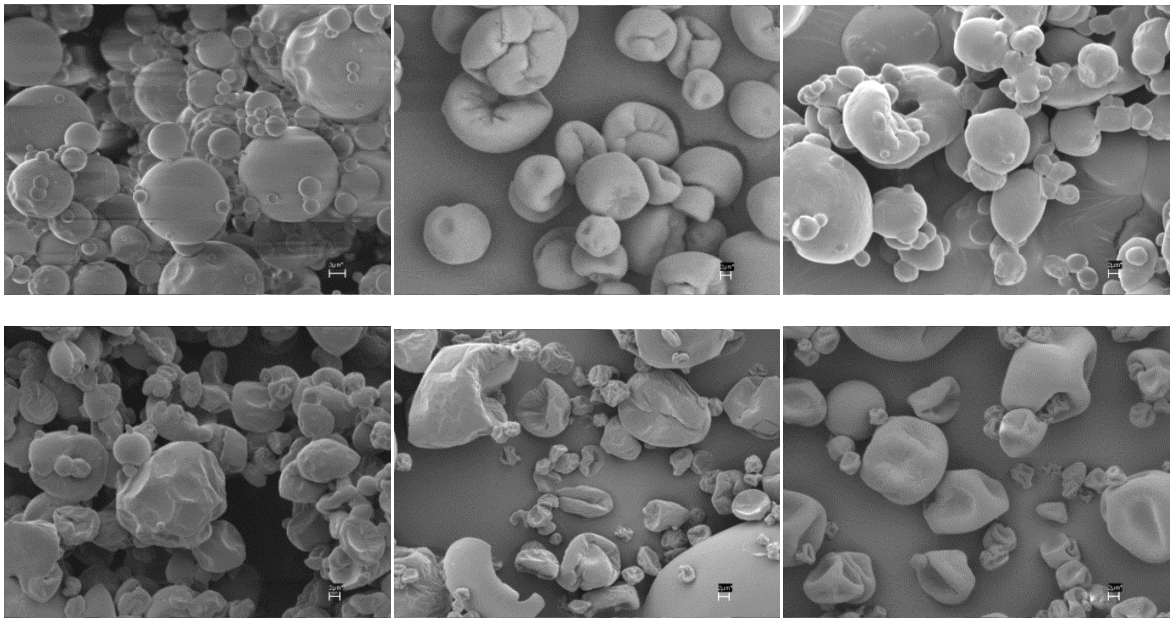

Figure 3.12: Influence of increasing protein concentration on the particle morphology of spray-dried lactose/Na-Cas particles (pH7) after spray drying (5,000 magnification). Top left: Pure lactose, top middle: Lactose/Na-Cas=99/1 wt%, top right: lactose/Na-Cas=95/5 wt%, bottom left: lactose/Na-Cas=90/10 wt%, bottom middle: lactose/Na-Cas=80/20 wt%, bottom right: lactose/Na-Cas=60/40 wt%.

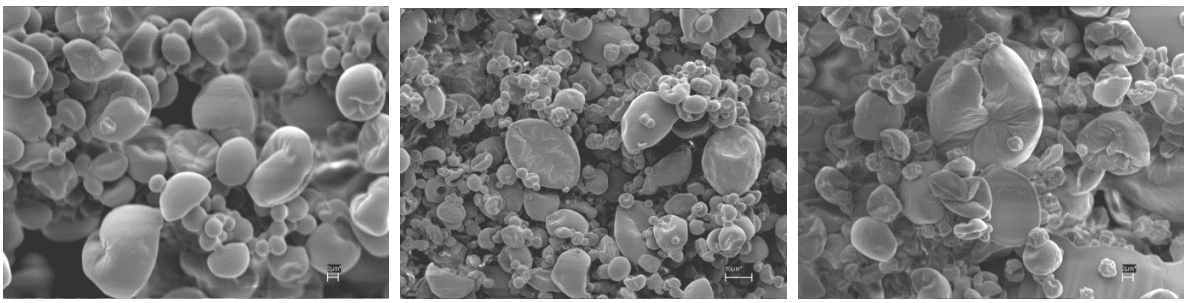

Figure 3.13**:** Powder morphology of spray-dried lactose/WPI powder after spray drying. Left: Lactose/WPI=99.9/0.1 wt%, middle: lactose/WPI=99/1 wt%, right: lactose/WPI=95/5 wt%.

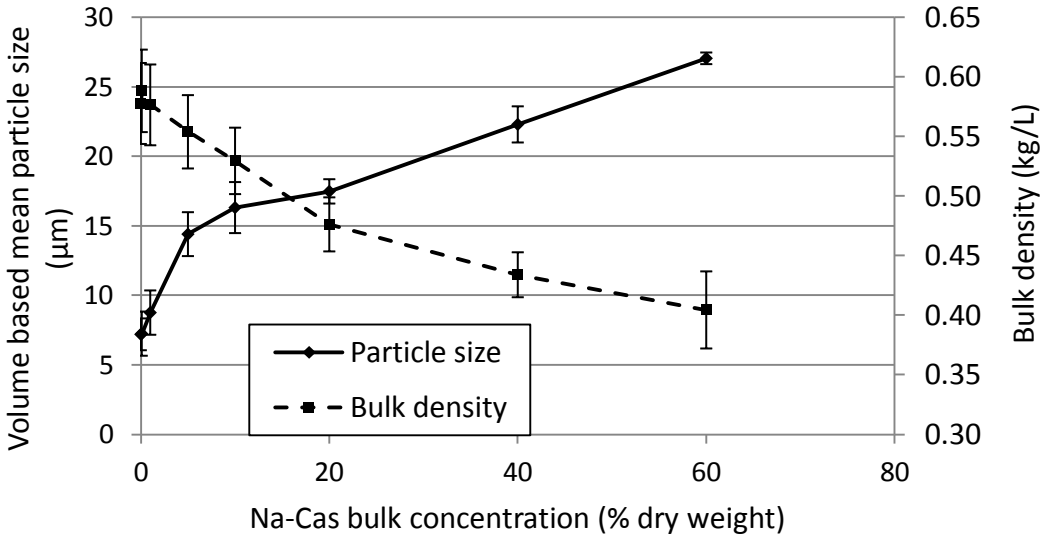

Figure 3.14**:** Effect of Na-Cas bulk concentration on particle size and bulk density of lactose/Na-Cas powder, spray-dried at pH 7.

The solution pH did not obviously affect the particle size and bulk density of spray-dried lactose/Na-Cas and lactose/WPI particles, although a pH 6 solution produced measurably higher total protein surface concentrations compared to solutions at pH values of 7 and 8.5. This was true for both lactose/protein mixtures (see Figure 3.5 and Figure 3.7). This suggests that the protein bulk concentration rather than protein surface concentration controls the visco-elasticity of the particulate wall and thus particle deformations (expansion and deflation) during spray drying. This suggestion is reasonable, because it is unlikely that a protein coat, which is only a few nanometers thick (Atkinson et al., 1995b), can affect the elasticity of the entire particle wall. This assumption is consistent with the results in Figure 3.14, which shows that the mean particle size and bulk density are correlated with the Na-Cas bulk concentration.

Particle wrinkles increased slightly for both lactose/Na-Cas and lactose/WPI particles, when the pH was lowered towards the isoelectric point (pI) of the protein (Figure 3.15). At a pH close to the pI, higher protein surface concentrations as well as stronger protein-protein interactions between lower-charged adsorbed proteins may have caused a higher protein film packing density with resulting higher film compressibility, as suggested in Part A of this study, that may have induced higher surface wrinkling.

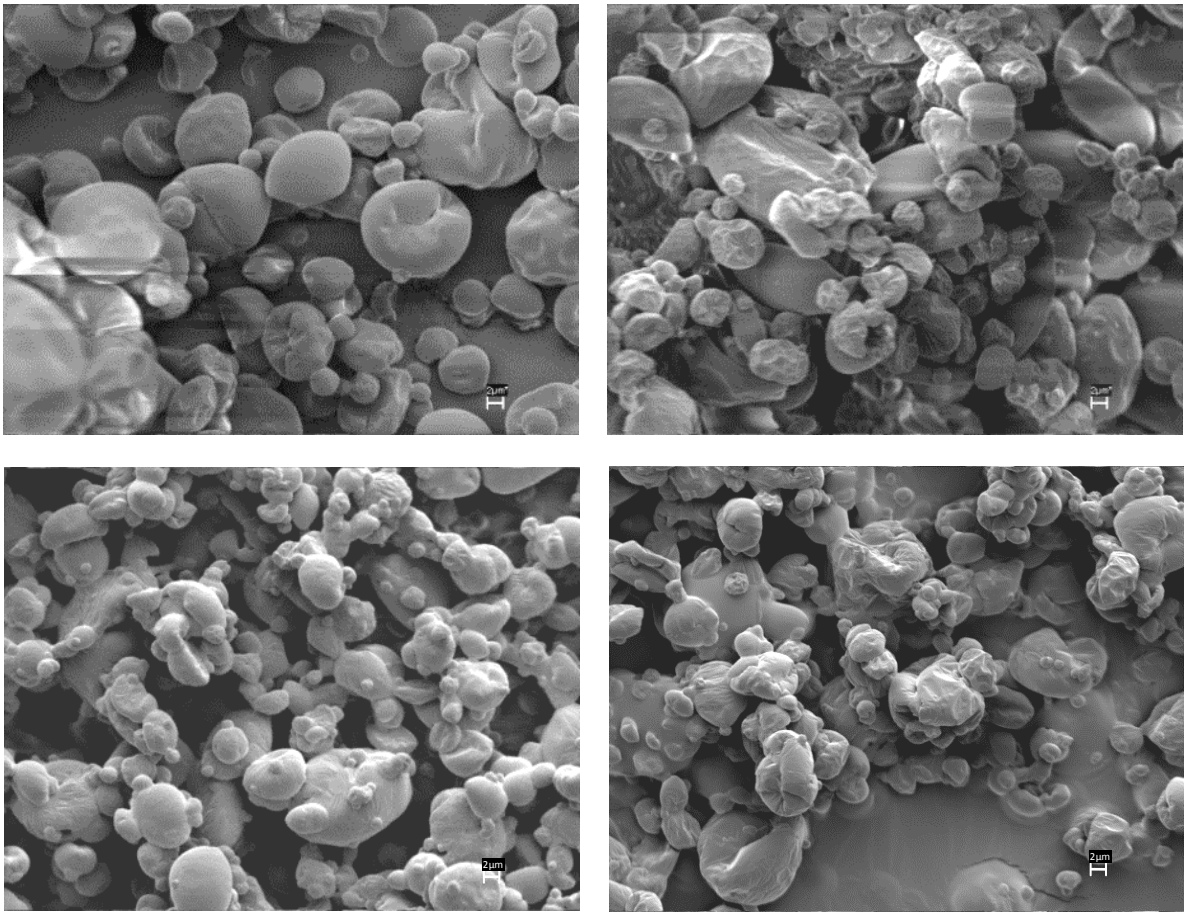

Figure 3.15**:** Particle morphology of lactose/WPI=99/1 wt% particles (top) and lactose/Na-Cas=90/10 wt% particles (bottom), spray-dried at different solution pH, pH 8.5 (left) pH 6 (right): 5,000 magnification.

Powder caking

After long-term storage of lactose/protein powders at ambient air conditions, lactose within the powder crystallized and the powder transformed into a cake whose structure was dependent on the protein bulk concentration (Figure 3.16). The addition of just 1wt% Na-Cas prevented the collapse of the particle structure (observed for the pure crystallized lactose) although separate particles were clearly joined together by crystals. An addition of 10wt% Na-Cas resulted in partly separated unique particles which had many cracks and pores throughout the particle wall due to the volume reduction and water release upon crystallization. Crystallized lactose/WPI (90/10 wt%) powder (Figure 3.17) also showed a crystalline cake structure similar to lactose/Na-Cas (90/10 wt%) powder, although particles did not seem to be separated as well as in the lactose/Na-Cas powder. Possible reasons for this might be because WPI produced a lower surface protein concentration than Na-Cas

(Figure 3.7), and because its more rigid, three-dimensional structure made it a less protective wall material than the flexible Na-Cas (Gharsallaoui et al., 2007; Thompson et al., 2009).

At Na-Cas concentrations of 20wt% and higher, no surface crystals could be observed and the particle surface did not contain the cracks and holes apparent in the crystalline particles produced at lower total Na-Cas bulk concentrations. This indicates that the protein coat prevented lactose from crystallizing at the particulate surface, although the surface consisted of around 20% lactose according to the performed XPS measurements (Figure 3.4). Due to the absence of any lactose crystals on the surface of the particles, the powder containing 20% and 40% of Na-Cas did not transform into a hard, brittle cake, as occurred for powders with lower protein bulk concentrations. Rather, a 20% protein content produced a softer, pliable cake, while at 40% protein the powder remained free-flowing.

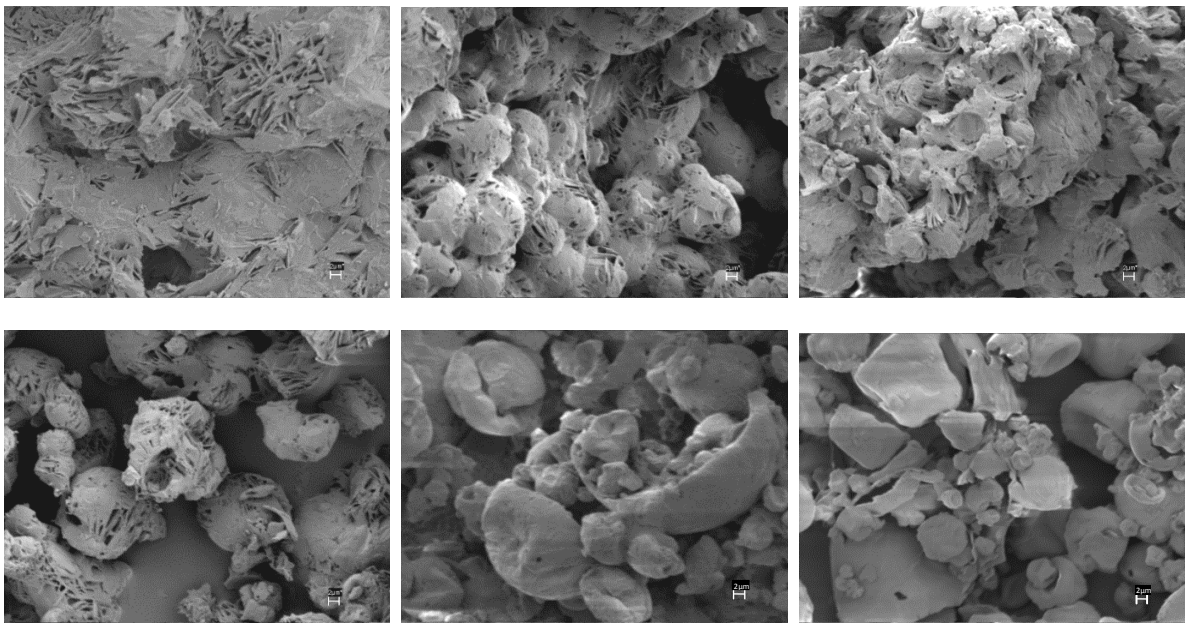

Figure 3.16**:** Crystalline particle morphology of spray-dried lactose/Na-Cas powder, spray-dried at pH 7, after several weeks of unprotected powder storage at ambient conditions (5,000 magnification). Top left: Pure lactose, top middle: lactose/Na-Cas=99/1 wt%, top right: lactose/Na-Cas=95/5 wt%, bottom left: lactose/Na-Cas=90/10 wt%, bottom middle: lactose/Na-Cas=80/20 wt%, bottom left: lactose/Na-Cas=60/40 wt%.

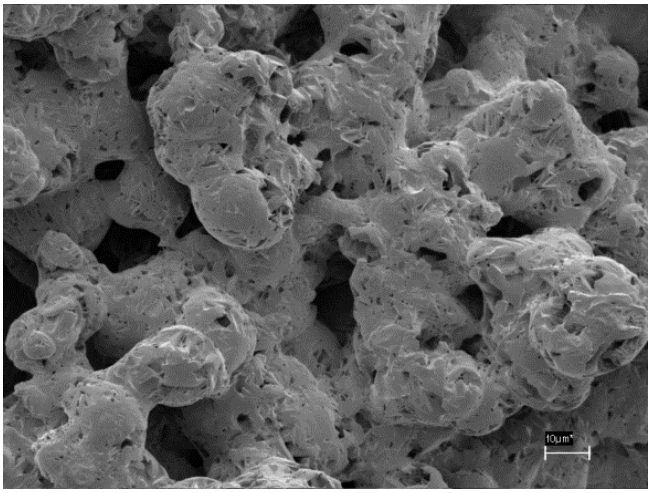

Figure 3.17**:** Crystalline particle morphology of spray-dried lactose/WPI=90/10 wt% powder (pH 7) after several weeks of unprotected storage at ambient conditions (5,000 magnification).

As discussed in Section 2.2.5 of this thesis, disaccharides such as lactose and sucrose bind to proteins to hydrate and stabilize them (Arakawa & Timasheff, 1982; Belyakova et al., 2003; Lee & Timasheff, 1981; Rodríguez Patino & Pilosof, 2011). Generally, the glass transition temperature of a bound protein/lactose complex is increased when the mass fraction of the protein is increased, because large proteins have a higher glass transition temperature than the smaller lactose (Haque & Roos, 2004a; Roos & Karel, 1991b). It seemed that Na-Cas/lactose particles with a surface composition of 80/20% and higher consists of sufficient protein to hinder crystallization of the amorphous lactose at the surface of the particles at the corresponding water activity of the powder. However, it will be shown below using DVS that some degree of crystallization occurred for the >20% protein powders (Figure 3.18). This crystallized lactose must have been located within the interior of the particle (beneath the protein coat) where the protein concentrations were lower and thus crystallization of lactose was not hindered.

Crystallization delay

Dynamic vapour sorption (DVS) measurements of pure lactose and lactose/Na-Cas powders of various ratios, spray-dried at a pH of 7, were performed in order to determine the relative humidity (RH) required to induce lactose to crystallize (Figure 3.18). Curves were plotted above one another in order to clearly separate the data for different lactose/Na-Cas ratios (water contents are thus not presented on the axis here). Crystallization of amorphous

lactose within the powder samples can be clearly seen by a loss in moisture, as also described by Jouppila and Roos (1994a). An initial moisture loss for amorphous lactose could be observed at 46% RH (Figure 3.18) where crystallization was initiated. This is consistent with data from the literature, where crystallization of pure amorphous lactose was reported at RH of ≥44% (Haque & Roos, 2004a; Haque & Roos, 2005; Jouppila & Roos, 1994a). As discussed in Section 2.1.4, lactose crystallization is a time-dependent phenomenon and its rate increases as the RH increases (Jouppila & Roos, 1994a). This increased crystallization rate can be seen in Figure 3.18, where a significantly faster and more sudden moisture loss of pure amorphous lactose powder was observed when the RH was increased from 46 to 48% RH.

Figure 3.18 shows that increasing ratios of Na-Cas within the powder samples resulted in clear delays in crystallization. Just 0.1wt% (total solids) of Na-Cas caused a delay in lactose crystallization of 2-4% RH, while lactose crystallization in lactose/Na-Cas (90/10 wt%) powder was delayed by 6% RH. When the lactose/Na-Cas powder contained 40wt% Na-Cas, lactose did not crystallize until a RH as high as 62% was reached. The crystallization delay with increasing Na-Cas bulk concentrations was additionally confirmed by DSC measurements (results attached to Appendix A.2.3). This crystallization delay can be explained by an increased lactose-protein binding at higher protein/lactose bulk ratios, resulting in higher glass transition temperatures of the lactose-protein complex within the bulk (Haque & Roos, 2004b).

As described in Section 2.2.5, interactions between proteins and polysaccharides are well studied in the literature in particular during drying where the polar lactose molecule acts as a "water-replacer" to hydrate the proteins (Belyakova et al., 2003; Fäldt & Bergenståhl, 1995). The observed crystallization delay of amorphous lactose in the presence of large proteins agrees with the findings of other authors, who used static sorption measurements at various constant relative humidity conditions (Haque & Roos, 2004a; Ibach & Kind, 2007; Wang et al., 2010). By using a dynamic vapour sorption method for this study, the RH at which lactose crystallization was initiated could be determined with good accuracy (±2%).

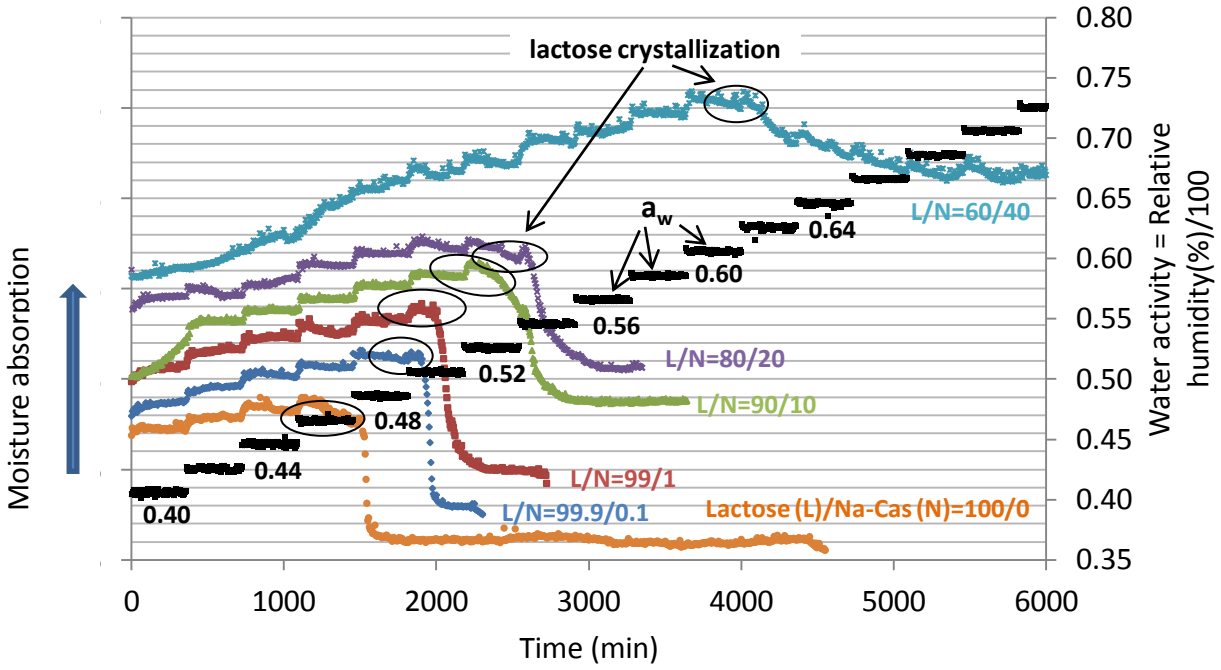

Figure 3.18**:** Dynamic vapour sorption measurements of lactose and lactose/Na-Cas ratios of 99.9/0.1; 99/1; 90/10; 80/20; 60/40, starting at an equilibrium water activity of 0.4 (40% relative humidity) with incremental water activity steps of 0.02 (2% relative humidity).

As reported by Ibach and Kind (2007), α-lactose monohydrate crystals have a bound water content of approximately 5 % within their crystalline matrix. However, in this study the final remaining water content within all crystallized powder samples was ≤3% (lactose/Na-Cas (60/40 wt%) was the only exception). Similar low moisture contents within crystallized lactose samples were observed by Ibach and Kind (2007), who crystallized amorphous lactose at an air temperature of 60 °C. This would suggest that, in the experiments shown in Figure 3.18 and Figure 3.19, not only α-lactose monohydrate was formed but also different anhydrous forms such as anhydrous α-lactose, β-lactose or a mixture of both. This is supported by Bushill et al. (1965), who reported that a compound matrix of α-lactose monohydrate and anhydrous β-lactose is formed in a ratio of approximately 5:3 when spray-dried amorphous lactose is crystallized at ambient air conditions.

Lactose/Na-Cas (90/10wt%) powders, spray-dried at various pHs, showed no difference in the moisture sorption or initiation point of lactose crystallization (Figure 3.19). Using a solution pH closer to the isoelectric point (pI) of the protein did not provide further crystallization delay, although previous experiments showed higher surface protein concentrations at this pH (Figure 3.5). This suggests that crystallization delay is independent

of any protein coat that forms on the particles, most likely because the protein coat does not provide a barrier to moisture absorption into the particle. Thus, the delay in lactose crystallization seems to rely only on lactose-protein interactions within the bulk of the particle, as also supported by Haque and Roos (2004a). This also indicates that lactose-protein interactions within the bulk of the particle are independent of the pH.

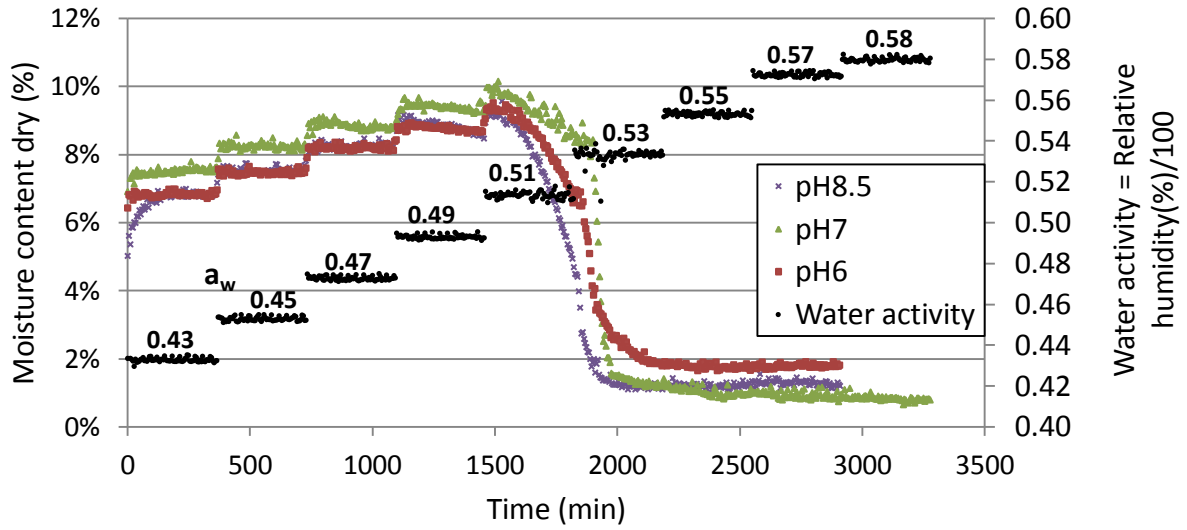

Figure 3.19: Dynamic vapour sorption measurements of lactose/Na-Cas=90/10wt% powder, spray-dried at various pHs, starting at an equilibrium water activity of 0.44 (44% relative humidity) with incremental water activity steps of 0.02 (2% relative humidity).

Powder yield

Figure 3.20 shows that the yields of all spray-dried lactose/Na-Cas powders were higher than the yield of spray-dried pure lactose. This agrees with the findings of Adhikari et al. (2009a) and Wang and Langrish (2010), who also reported an increase in the yield of a spray-dried sugar solution in the presence of a small amount of a protein. This can be explained by an increase in the glass transition temperature of the particle surface when high-molecular-weight proteins such as Na-Cas (molecular weight approximately 24 kDa) adsorb at the surface of a droplet containing a relatively small molecule such as lactose (molecular weight approximately 0.34 kDa). This trend of increasing glass transition temperature with increasing molecular weight of a food polymer has been clearly demonstrated by Roos and Karel (1991b). A higher glass transition temperature causes a lower particulate stickiness during drying and therefore less particle adhesion to the dryer walls, resulting in higher powder yield. Figure 3.20 shows that a Na-Cas bulk concentration of just 0.1 wt% was sufficient to improve the powder yield from around 55% to 65%, while a further increase in

protein bulk concentration did not cause statistically significant changes in spray dryer yield. This implies that only a small amount of Na-Cas (≤1%) is required to produce a significant improvement in spray dryer yield (10-20%). Hence, with respect to yield, there are no further benefits to be gained by increasing the Na-Cas bulk concentration beyond this. It is probable that the surface of the spray-dried droplets became saturated at protein bulk concentrations of around 1-5 % (see Figure 3.4).

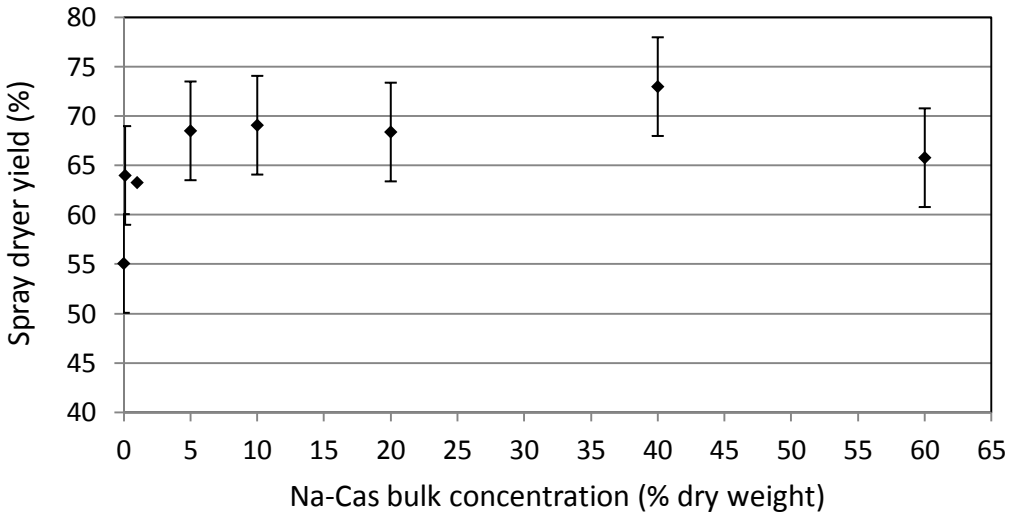

Figure 3.20**:** Effect of increasing protein concentration on the product yield of spray-dried lactose/protein mixtures (pH7).

Powder flow

Figure 3.21 shows the percentage powder flows of spray-dried lactose/Na-Cas powders through a vibrating sieve, with varying protein bulk concentrations (solid line) and protein surface concentrations (dashed line). Generally, higher flow-through is expected for less agglomerated (non-bridging) powders. In the flowability tests, particle stickiness could not directly affect powder flow, because the glass transition temperature of the particulate surfaces was well above ambient temperature due to standardization of the powders by vacuum drying. However, there was an indirect influence of particle stickiness on the flowability because of the opportunity for weak agglomeration of particles during spray drying, when the powder was collected inside a jar beneath the cyclone of the spray dryer for up to 30 minutes. Temperatures of around 75 °C (corresponding to the air outlet temperature of the spray dryer) and relatively high moisture contents (3 to 5 %) in the collection jar meant that the glass transition temperature (of lactose, at least) was exceeded by more than 10°C,

hence particle stickiness could have occurred that caused particles to agglomerate. The powder flow through the vibrating sieve was affected by the observed powder agglomeration, indicated by a coarser texture and more cohesive appearance of the powder.

Spray-dried pure lactose powder was very sticky due to its low glass transition temperature (Adhikari et al., 2009a) and it therefore agglomerated easily. This resulted in no powder flow through the vibrating sieve (Figure 3.21). Small amounts of protein significantly reduced powder stickiness during spray drying, because the presence of high-molecular-weight proteins on the particle surface enhanced the overall glass transition temperature of the particle surface (Wang & Langrish, 2010). This resulted in less agglomerated powders and therefore higher percentage flows through the sieve (Figure 3.21, solid line). The larger particles that result from increasing protein/lactose bulk ratios (Figure 3.14) would have also contributed to reduced powder agglomeration and therefore improved powder flows. Powder flow did not improve significantly for Na-Cas bulk concentrations above 20wt% (Figure 3.21, solid line), most likely because the surface was saturated with protein at this point (see Figure 3.4). A linear trend between the protein surface concentration and the powder flowability (Figure 3.21, dashed line) indicates that powder flowability was directly affected by the particle surface composition. The powder flowability measurements of lactose/WPI powders confirmed this, because they showed the same trend and had powder flowabilities similar to lactose/Na-Cas powder (results attached to the Appendix A.2.4).

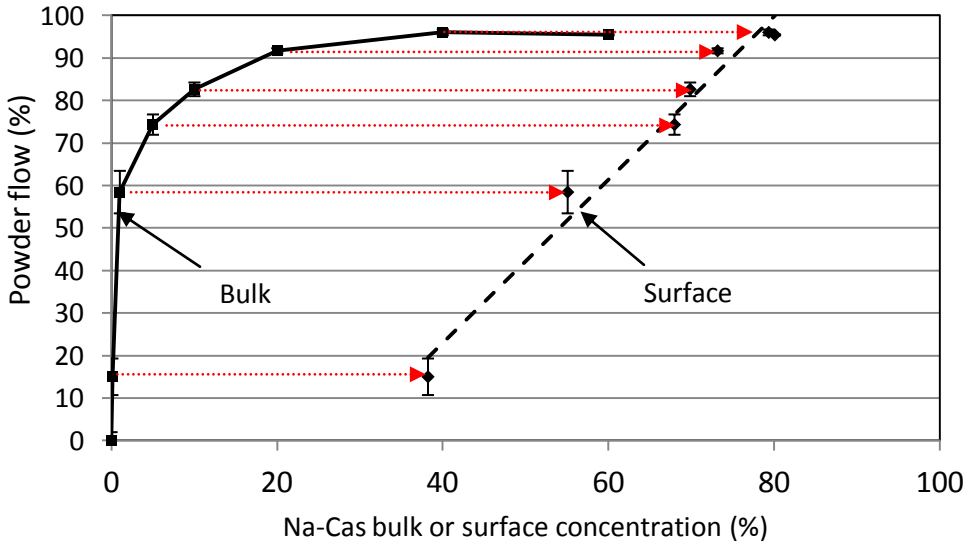

Figure 3.21**:** Effect of protein bulk concentration (solid line) and protein surface concentration (dashed line) on the percentage flow of spray-dried lactose and lactose/Na-Cas powder (pH7) through a vibrating sieve. The red arrows show the difference between bulk and surface Na-Cas concentration.

Differences in the solution pH did not cause obvious changes in the powder flows of lactose/Na-Cas (see Figure 3.23), most likely because the pH did not markedly affect particle size and particle bulk density (results not included here), and protein surface concentrations did not differ significantly amongst lactose/protein powders spray-dried at various pHs (Figure 3.5).

Powder wettability

The wetting time of lactose/Na-Cas powders in water was higher than for pure lactose powder (Figure 3.22, solid line). Lactose was instantly wetted upon exposure to the water surface due to its hydrophilic, polar nature. The presence of just 1 wt% of Na-Cas in bulk caused a delay in wetting time of approximately 1.5±0.5 minutes. As mentioned in Section 2.2.4, proteins expose their hydrophobic parts towards the surface once adsorbed at the air-water interface during spray drying (Magdassi, 1996; Norde, 1992; Thompson et al., 2009). These structural reorientations of proteins at the surface result in a less polar, more hydrophobic particle surface than for pure spray-dried lactose powder. Hence, protein-containing lactose powders have reduced wettability in a polar solvent such as water.

While the wetting time increased steadily between protein bulk concentrations of 20 and 80% (Figure 3.22, solid line), there was a sudden jump in wetting time when the protein surface concentration exceeded around 75% (Figure 3.22, dashed line). There is no reasonable physical explanation based on surface composition alone to account for this, which suggests that another factor such as particle buoyancy must be affecting the wetting time. Thus, a decrease in particle density with increasing protein/lactose bulk ratios, as observed in Figure 3.14, was likely to have contributed to longer wetting times due to higher buoyancy of lighter particles in particular at Na-Cas surface concentrations above 75%. At this point, particulate density probably became too low to allow the particles to sink below the water surface, which meant the powder could not be efficiently wetted.

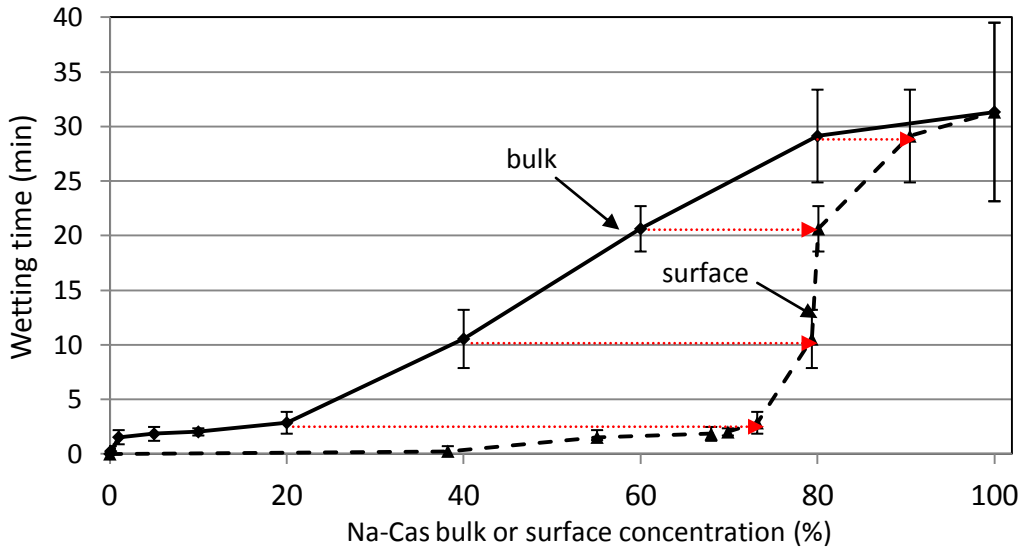

Figure 3.22**:** Effect of protein bulk concentration (solid line) and protein surface concentration (dashed line) on wetting time of spray-dried lactose/Na-Cas powder (pH7). The red arrows show the difference between bulk and surface Na-Cas concentration.

The pH of the spray-dried lactose/Na-Cas solutions had very little effect on the wetting time of the lactose/Na-Cas powders (Figure 3.23). For powders containing Na-Cas bulk concentrations of 1 and 10wt%, a small trend of increasing wetting times can be seen when the pH approaches the pI of the protein, although the differences in wetting times were within the limits of experimental uncertainty. Longer wetting times with a pH closer to the pI were likely to be caused by higher protein surface concentrations (Figure 3.5). Furthermore, proteins may have configured themselves at the droplet surface differently during spray drying at different pHs because of the effect of the pH on protein charge and hydrophobicity (Dee et al., 2004; Kato et al., 1984; Magdassi, 1996), which may affect the wetting time.

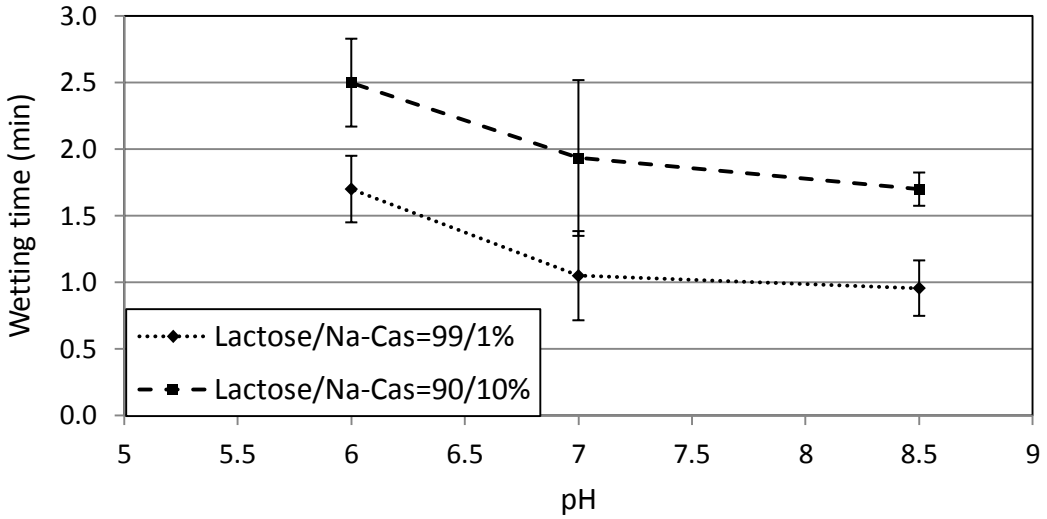

Figure 3.23**:** Effect of feed pH of spray-dried solutions on wetting time of lactose/Na-Cas powders.

The functional properties of pure protein powders, spray-dried at various solution pHs, were also examined and the results were compared with those of lactose/protein powders. In contrast to the lactose/Na-Cas powders, where changing the solution pH had little effect on powder functional properties, a decreasing solution pH resulted in reduced powder flow and longer wetting times for pure Na-Cas powders, and this effect was particularly marked when the solution pH approached the pI of the protein (Figure 3.24). Proteins have a lower surface charge at a solution pH closer to their pI, thus higher amounts of non-charged and non-polar protein residues were likely to be extended towards the air-phase during spray drying. Since the pH had no effect on particle size, morphology and bulk density of Na-Cas particles (results given in Appendix A.2.5), it can be assumed that, in the absence of a stabilizing agent such as lactose, different pH-induced structural orientations of Na-Cas proteins at the droplet surface caused the differences in powder flow and wetting times of pure Na-Cas powders.

As discussed in Section 2.2.5, a sugar such as lactose was shown to stabilize the protein structure and thus protect proteins from partial unfolding (Arakawa & Timasheff, 1982; Belyakova et al., 2003; Dickinson, 2008; Lee & Timasheff, 1981). Hence, for spray-dried lactose/Na-Cas particles, adsorbed Na-Cas proteins may have been stabilized against extensive rearrangements at the surface by lactose-protein binding (which is presumably independent of pH), since no clear differences in powder flow and wetting times were observed as the pH was decreased (Figure 3.24).

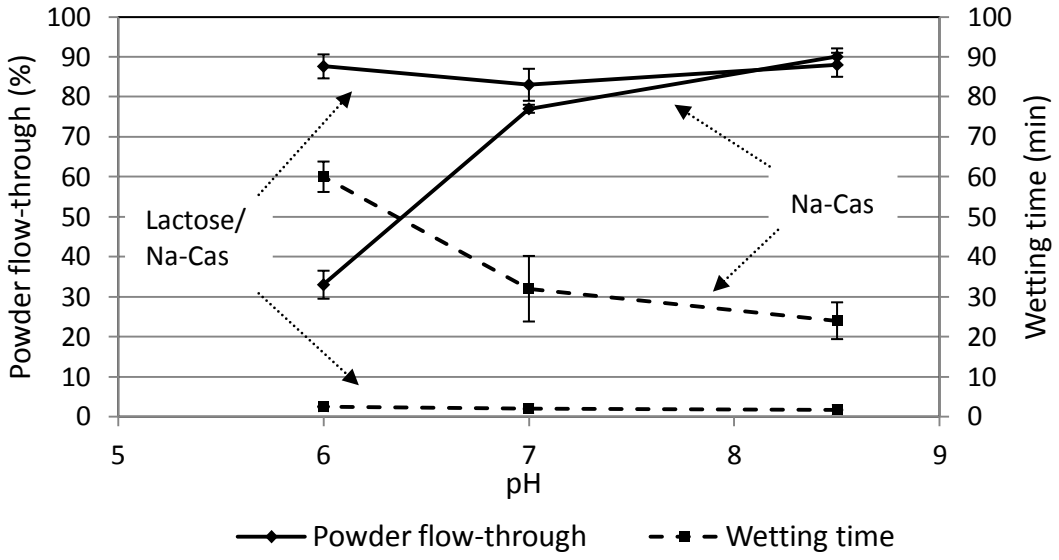

Figure 3.24**:** Effect of solution pH on powder functional properties of spray-dried Na-Cas and lactose/Na-Cas=9/1 wt% powder: powder flow (solid line), wetting time (dashed line).

Effect of feed solution and spray drying parameter on properties of spray-dried lactose/Na-Cas powders

Total solid content

Higher total solid contents (TS) within the spray-dried lactose/Na-Cas solutions resulted in larger particles due to the higher mass of solids per particle and the higher feed solution viscosities, which resulted in larger droplets upon feed solution atomization (Table 3.4). For lactose/Na-Cas ratios of both 99/1% and 90/10%, an increase in powder bulk density was measured with increasing TS. It is likely that with higher TS, a thicker wall with lower moisture content developed on the surface of a droplet during spray drying. If an internal vacuole had formed and expanded, this thicker wall would not have "stretched" as much as a thinner wall, resulting in particles of higher average density.

The flowability of spray-dried lactose/Na-Cas powder was improved with increasing TS (Table 3.4), which may be the result of the larger particles produced at higher TS. Wetting time decreased slightly with increasing TS, although there is a wide margin of error in these measurements. The higher particulate density and lower protein surface concentrations both contributed towards the faster wetting of powders spray-dried at higher TS.

Table 3.4: Effect of total solids (TS) on particle and powder functional properties of spray-dried lactose/Na-Cas (99/1% and 90/10%) powders

Latose/Na-Cas = 99/1				
Total solids (%)	**Vol. based particle size (µm)**	**Powder bulk density (kg/L)**	**Flowability (%)**	**Wetting time (min)**
5	10 ± 1	0.53 ± 0.05	52 ± 4	1.8 ±0.3
10	17 ± 2	0.59 ± 0.06	63 ± 5	1.7 ± 0.4
20	18 ± 1	0.67 ± 0.07	92 ± 1	1.6 ± 0.4
Latose/Na-Cas = 90/10				
Total solids (%)	**Vol. based particle size (µm)**	**Powder bulk density (kg/L)**	**Flowability (%)**	**Wetting time (min)**
5	11 ± 1	0.42 ± 0.04	55 ± 3	2.3 ±0.5
10	17 ± 2	0.5 ± 0.05	77 ± 2	2.0 ± 0.3
20	19 ± 2	0.53 ± 0.05	93 ± 1	1.7 ± 0.2

Figure 3.25 shows the particle morphology of lactose/Na-Cas powder spray-dried at 5 and 20 wt% TS. Both powders consisted of particles with high numbers of surface wrinkles and folds. Wu et al. (2014) also observed a highly wrinkled particle structure for skim milk powders spray-dried at TS of 32.6 wt% and lower, while TS of 41.5wt% and higher caused larger, smoother and more hollow particles. They assumed a faster crust formation for droplets spray-dried at higher TS due to a faster surface saturation, and postulated that this early crust formation increased the mechanical integrity of the crust that resisted the drying stress. Thus, further shrinkage upon drying was prevented, resulting in larger, more hollow and smoother particles with less surface wrinkling. Such particles would have a lower density and thus the powder would have a lower bulk density. Interestingly, the current experiments show a small trend towards increasing bulk density with increasing TS (Table 3.4). However, for total solids contents of 20wt% and lower, the particle wall in the present experiment seemed to be flexible and hydrated enough at given spray drying conditions to cause a particle wall deformation, as was also observed in the study of Wu et al. (2014).

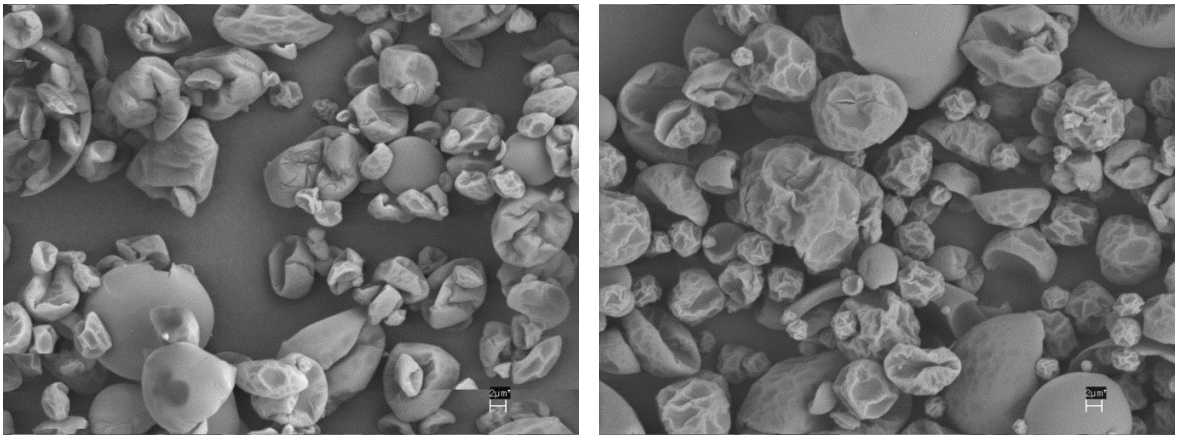

Figure 3.25**:** Effect of total solids (TS) in feed on particle morphology of lactose/Na-Cas=90/10 wt% particles, spray-dried at 160/75 °C air inlet/outlet temperature and 0.6 bar atomization pressure. Left: 5 wt% TS, right: 20 wt% TS

Atomization pressure

Higher atomization pressures resulted in smaller particles due to the higher energy input upon atomization (Table 3.5). Powder bulk density decreased slightly with increasing atomization pressures for lactose/Na-Cas ratios of both 99/1% and 90/10% (Table 3.5). It is possible that the rapid formation of smaller particles caused the observed lower powder bulk density. This is supported by Vehring (2008), who assumes that lower density particles are produced when particle surface formation is fast. In that case, particle deflation would have been hindered due to a higher mechanical rigidity of an earlier-formed and less-hydrated particle wall, as also suggested by Wu et al. (2014). No obvious effect of the atomization pressure on the particle morphology was observed in this study (Figure 3.26). Lactose/Na-Cas powders, spray-dried at 0.2 bar and 1.0 bar, both had extensive surface wrinkles and folds. Thus, it seems that, due to the low air inlet/outlet temperatures during spray drying (160/75 °C), there was sufficient time for smaller droplets, spray-dried at higher atomization pressure, to expand and deflate (mechanism described in Section 2.3.5) during spray drying. This would have been supported by a longer hydration of the particle wall, which would explain the high level of wall deformation seen in Figure 3.26.

Table 3.5: Effect of atomization pressure on particle and powder functional properties of spray-dried lactose/Na-Cas (99/1% and 90/10%) powders at 10wt% total solid content and pH7

Latose/Na-Cas = 99/1				
Atomization pressure (bar)	**Vol. based particle size (µm)**	**Powder bulk density (kg/L)**	**Flowability (%)**	**Wetting time (min)**
0.2	22 ± 1	0.62 ± 0.06	92 ± 1	2.1 ± 0.5
0.6	17 ± 2	0.59 ± 0.05	63 ± 5	1.7 ± 0.4
1.0	13 ± 1	0.53 ± 0.05	52 ± 4	1.4 ± 0.3
Latose/Na-Cas = 90/10				
Atomization pressure (bar)	**Vol. based particle size (µm)**	**Powder bulk density (kg/L)**	**Flowability (%)**	**Wetting time (min)**
0.2	23 ± 3	0.56 ± 0.06	92 ± 1	2.5 ± 0.5
0.6	17 ± 2	0.5 ± 0.05	77 ± 2	2.0 ± 0.3
1.0	13 ± 1	0.43 ± 0.04	71 ± 2	1.6 ± 0.3

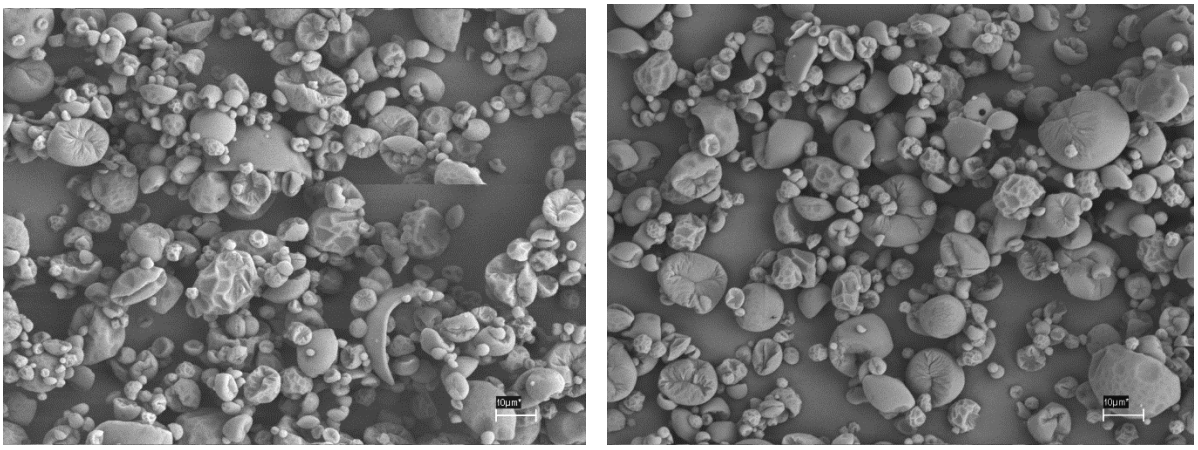

Figure 3.26**:** Effect of atomization pressure on particle morphology of lactose/Na-Cas=90/10 wt% powder, spray-dried at 160/75 °C air inlet/outlet temperature, total solids of 10 wt% and different atomization pressures. Left: 0.2 bar, right: 1.0 bar.

Powder flowability decreased with increasing atomization pressures on account of smaller droplets being produced upon atomization. As discussed Part A of this study, the atomization pressure was found to have no clear effect on the surface composition of spray-dried lactose/Na-Cas particles (Figure 3.10). Thus, the surface composition of the powders cannot account for the different flows produced at various atomization pressures in this study. There was a small trend towards decreasing wetting times of lactose/Na-Cas powders spray-dried at higher atomization pressures. Faster wetting of smaller particles was likely to occur due to the increased total specific surface area of smaller particles. The lower particle density

measured for smaller particles did not seem to have an overwhelming negative effect on the powder wetting.

Air inlet and outlet temperatures

No clear effect of the air drying temperature on particle size, powder bulk density and powder morphology of spray-dried lactose/Na-Cas powders could be found in this study (Table 3.6 and Figure 3.27). This is not in line with the observations of Nijdam and Langrish (2005), who measured larger particles of lower bulk density for milk powders spray-dried at higher air inlet temperatures. They explained that, while particles at low air inlet temperatures could be expanded by an internal vapour vacuole and also deflated when the particle moved into cooler region of the dryer, deflation of the particles was hindered at higher air inlet temperatures by a faster solidification of the droplet. This then caused larger, smoother particles of lower average density for higher drying temperatures. However, in this study SEM micrographs did not show any increased particle surface folding at lower air inlet temperatures due to possible particle deflation (Figure 3.27). This indicates that, for the spray drying studies presented here, the particles had enough time to expand and deflate, both at the lower and the higher air inlet temperatures.

Differences in the morphology of spray-dried lactose/protein particulates between this study and the one performed by Nijdam and Langrish (2006) were likely to be caused by differences in the drying rate and thus time available for the particles to expand and deflate during spray drying. This study used a low TS (10wt%) whereas a TS of 41.2% was used in the study of Nijdam and Langrish (2005). Moreover, Nijdam and Langrish (2005) used a Buchi MINI scale spray dryer, with resulting lower feed rates and therefore higher air outlet temperatures, both of which clearly affect the drying time of a droplet. Their higher air inlet and outlet temperatures (220/125 °C) and higher TS would have caused a considerably faster droplet drying time than for the present study, where the highest air inlet/outlet temperature was 220/100 °C. Thus, it seems that for the study described in this chapter there was enough time during the drying process for the particles to expand and deflate before becoming solidified.

Powder flowability and powder yield were also unaffected within a wide range of air outlet temperatures (Table 3.6). Only at the extremes of air inlet/out temperatures (220/101 °C, 120/58 °C and 140/62 °C), slower powder flow and slightly lower powder yields were

observed, which may have been caused by a lowering of the glass transition temperature. The high particle surface temperature of particles spray-dried at the high air inlet temperature of 220 °C would have contributed towards a higher particle wall stickiness during spray drying, as would have the high moisture content of particles spray-dried at low air inlet temperatures. This higher particle surface stickiness would have caused a lower spray dryer yield and stronger particle agglomeration during drying, resulting in a worse powder flow. A similar observation was made by Wang and Langrish (2010), who also measured lower powder yields of spray-dried lactose/casein powders at high and low air inlet temperatures of 210 and 134 °C, while a drying temperature of 170 °C resulted in increased powder yield probably due to a higher glass transition temperature and thus lower particulate stickiness.

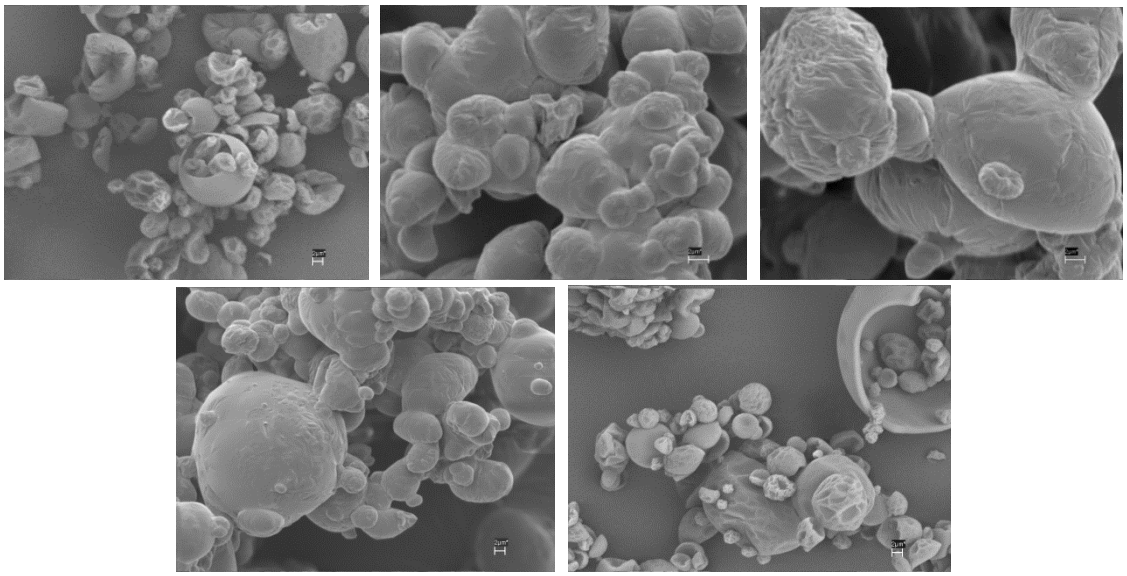

Figure 3.27**:** SEM micrographs of lactose/Na-Cas=90/10% powders, spray-dried at 10wt% TS, 0.6bar atomization pressure at different air inlet/outlet temperatures (T,in/T,out). Top left: 220/101±2 °C, top centre: 180/87±2 °C, top right: 160/75±2 °C, bottom left: 140/67±2 °C, bottom right: 120/58 ±2 °C.

Table 3.6: Effect of air outlet temperature on particle and powder functional properties of lactose/Na-Cas=90/10% particles, spray-dried at pH7 and TS of 10wt%

Air outlet temperature (°C)	Vol. based particle size (µm)	Powder bulk density (kg/L)	Flowability (%)	Powder yield (%)
101	16 ± 2	0.5 ± 0.05	54 ± 1	71 ± 3
87	14 ± 2	0.5 ± 0.05	88 ± 2	69 ± 3
82	16 ± 2	0.5 ± 0.05	87 ± 2	74 ± 3
75	13 ± 2	0.5 ± 0.05	86 ± 1	75 ± 3
70	14 ± 2	0.5 ± 0.05	79 ± 1	80 ± 3
67	16 ± 2	0.5 ± 0.05	85 ± 3	74 ± 3
62	14 ± 4	0.5 ± 0.05	53 ± 9	72 ± 3
58	15 ± 3	0.5 ± 0.05	39 ± 3	71 ± 3

3.4. CONCLUSION

PART A:

The pH of the lactose/Na-Cas solution influenced the surface enrichment of the proteins on the spray-dried particles. As the pH of the solution approached the pI of the protein, the protein surface concentration increased, most likely due to higher protein surface activity and denser protein packing at and near the droplet surface. Sugar solubility had no influence on the surface enrichment of Na-Cas, and no crystallization was observed in any of the powders tested, irrespective of the sugar tested, which shows that the sugars did not undergo a phase transition to form crystals above the saturation limit under the operating conditions tested. Rather, the viscosity of the aqueous sugar solution increased progressively as water evaporated until a glass formed. This potentially allowed protein mobility well above the solubility limit of the sugar.

Lower solution solid contents resulted in higher protein surface enrichment. The reason for this will be explored in detail in Chapter 4. A lower drying rate, controlled by reducing the air temperature and increasing the solution feed rate, did not result in a clear increase in protein surface enrichment over the range of operating conditions tested. The droplet size, as controlled by the atomisation pressure, also had no clear effect on the protein surface enrichment. Hence, over the range of operating conditions tested, the time-scale of spray drying appeared to be sufficient for Na-Cas to adsorb at the droplet surface and reach a maximum packing there before the surface solidified, irrespective of the droplet drying time.

PART B:

The surface composition affected powder functional properties of lactose/Na-Cas powders significantly. A higher protein concentration on the surface of spray-dried lactose/Na-Cas particles resulted in enhanced product recoveries and powder flows, presumably due to higher glass transition temperatures and the resulting larger particles. Wetting time was increased with increasing protein to lactose ratio, most likely due to the higher hydrophobicity of the final particle surfaces and the formation of particles of lower average density. An increase in surface folds and dents was observed with increasing protein bulk concentration, which was attributed to the increased wall elasticity with higher total protein concentrations. Furthermore, a crystallization delay was observed for lactose powder containing increasing bulk concentrations of Na-Cas, which indicates enhanced protein-sugar binding that increased the total glass transition temperature of the lactose/protein complex.

While the solution pH had a negligible effect on the powder functional properties of lactose/Na-Cas and lactose/WPI powders, the pH showed a clear influence on pure spray-dried Na-Cas powder. A pH closer to the pI of the protein resulted in poorer powder flow and a longer wetting time, probably due to a higher number of hydrophobic, non-charged protein residues exposed towards the droplet surface of an aqueous Na-Cas solution. Since during the spray drying of an aqueous sugar/protein solution, the sugar stabilizes the adsorbed proteins via hydrogen bonding, lactose possibly prevented Na-Cas from different molecular rearrangements at the air-water interface at various pHs, resulting in similar powder properties.

Increasing the solution solid content (TS) resulted in larger particles of higher bulk density, and powder with better flow and a shorter wetting time, thus powder functional properties were improved. The same trend was observed when decreasing the atomization pressure, which produced larger droplets and thus larger final particles with improved functional properties. In the range of 70 to 90 °C, the air outlet temperature did not affect functional properties of lactose/Na-Cas (90/10%) powders spray-dried at 10wt% TS and an atomization pressure of 0.6 bar, probably due to similar protein surface concentrations, particle size distributions, bulk densities and powder morphologies. However, lower and higher air outlet temperatures (< 60 °C and > 90 °C) caused poorer powder flows, presumably due to lower glass transition temperatures resulting in higher particle agglomeration during drying. The latter could have been caused by A) particle temperatures

being too high, as a result of high drying air temperatures and B) moisture contents being too high within the dried particles, as a result of low drying air temperatures.

4. INVESTIGATION OF SOLUTE SEGREGATION BETWEEN LACTOSE AND NA-CASEINATE FOR DIFFERENT DRYING SYSTEMS

4.1. INTRODUCTION

The phenomenon of solute segregation has been observed for various aqueous solutions during spray drying (Elversson & Millqvist-Fureby, 2006; Fäldt & Bergenståhl, 1994, 1996; Jayasundera et al., 2009; Landström et al., 2003; Millqvist-Fureby & Smith, 2007; Nijdam & Langrish, 2005; Vehring, 2008; Wang & Langrish, 2010) and during film drying (Graham & Phillips, 1979b; Trueman et al., 2012) due to the presence of surface active molecules such as proteins, which are driven to accumulate at the air-water interface. As explained in Section 2.3.4, moisture concentration gradients that can develop during rapid drying may also cause solute segregation because solutes preferentially diffuse towards the droplet interior, depending on their diffusion coefficients (Kim et al., 2003, 2009a). Due to this mechanism, large slow diffusing proteins accumulate on spray-dried milk droplets, while the smaller, faster diffusing lactose molecules mainly appear within the interior of the particles (Kim et al., 2003). Besides the mechanisms of moisture gradients and surface activity, Vehring (2008) postulates that, for high drying rates, as occur during spray drying, large components with a low mobility (i.e. large molecules, aggregates or insoluble crystals with high Peclet numbers *(Pe)*) can be captured at the droplet surface by the rapidly receding evaporative surface. This can only happen when the surface moves faster inwards than the dissolved solute can diffuse away ($Pe > 1$), as explained in Section 2.3.4.

In the work described in Chapter 3 (Part A), Na-Cas was added to lactose solutions before spray drying in order to investigate the effect of increasing protein/lactose ratio, pH, totals solid of the feed (TS), droplet size and drying temperature on the accumulation of the protein on the particle surface. Although important conclusions could be drawn about the concepts of protein enrichment at the droplet surface during spray drying, the effects of moisture content gradients and differences in lactose and protein Peclet numbers (*Pe*) on solute segregation were still not clear. Moreover, little is known about the importance of the *Pe* number on segregation phenomena within droplets dried at different spray dryer scales, or about how particle and powder functional properties change upon process scale-up. In order

to produce a novel, valuable and commercially viable product, a successful scale-up from laboratory scale to pilot and industrial scale is necessary. Thus, it has to be shown that the one-step spray drying process for producing coated lactose powders can be successfully transferred to large-scale production, without negative impacts on the coating, powder functional properties and powder stability (for example, lactose crystallization and caking). The purpose of this chapter was to address these issues.

Goal of this investigation:

The goal of Part A of this study was to explore the factors that influence solute segregation within drying aqueous lactose/protein films and droplets by comparing the surface composition of the slowly dried films with that of the spray-dried particles. Different parameters, such as lactose/Na-Cas ratio, drying temperature, total solid content (TS) and solution pH, were varied for both drying systems in order to investigate the possible effects of time limitation, moisture content gradients and *Pe* number on solute segregation between lactose and protein. The drying time is important, because it may limit the time available for the proteins to adsorb, re-orientate and stretch at the air-water interface during spray drying, as proposed by Landström et al. (2000). Because moisture content gradients are expected to be significantly higher during droplet drying than during film drying, an increased solute segregation between lactose and protein during spray drying might be expected in the droplets. The larger *Pe* numbers of solutes may result in a further enrichment of larger proteins at and beneath the droplet surface for $Pe > 1$. Moreover, the rapidly receding droplet surface that occurs during spray drying may cause a further "packing" of adsorbed proteins, which would exclude water and therefore dissolved lactose from the surface. In contrast, during film-drying (when $Pe < 1$) the effect of the *Pe* number on the surface enrichment of the proteins is negligible, and surface area reduction is negligible.

In order to investigate whether moisture content gradients exist during drying that might drive solute segregation, a fixed-solute coordinate system, similar to that proposed by Crank (1979), was used to simulate moisture content gradients within the drying films at different drying temperatures and TS. For that purpose, films of a constant thickness of around 125 micron were produced and dried in a drying tunnel under controlled conditions. The mass

transfer coefficients were experimentally determined and fitted to the model to allow calculation of the film shrinkage and moisture content gradients within the drying films.

In Part B of this study, laboratory- and pilot-scale spray dryers were used to spray dry lactose/Na-Cas solutions with a solid ratio of 9/1 and total solids contents of 10 and 20 wt%. The goal of this study was to investigate the effect of process scale-up on solute segregation phenomena during spray drying and to determine how particle and powder functional properties change as a result. Air inlet/outlet temperature and feed temperature were the same between the laboratory-scale and pilot-scale spray dryer to minimize possible effects of different drying conditions on Na-Cas surface enrichment as well as powder functional properties.

4.2. MATERIALS AND METHODS

4.2.1. Part A: Film drying versus spray drying study

Solution preparation and spray drying

α-Lactose monohydrate and Na-Cas powders were supplied by Fonterra Research and Development Centre (FRDC) (Palmerston North, New Zealand). Aqueous lactose/Na-Cas solutions were prepared in deionised water, according to the method described in Section 3.2. Lactose/Na-Cas solutions with 10wt% total solids (TS) and pH 7.0 were prepared at solid weight ratios of 99.9/0.1, 99/1, 95/5 and 90/10. In addition, lactose/Na-Cas solutions with 90/10 solid weight ratios were prepared at pH 7.0 and TS of 5 wt% and 20 wt%, and at pH 8.5 and pH 6 with TS 10 wt%. The pH was adjusted after protein addition, according to the procedure described in Section 3.2.

Spray drying experiments were performed as described in Chapter 3. This chapter uses the results from Chapter 3 to allow comparison between the surface compositions of films and particles.

Film drying

Films were dried in a tray dryer (Figure 4.1) equipped with a highly-sensitive balance (dryer outlet) to measure the weight loss of the films during drying (Figure 4.2). The thin

films were produced on completely clean glass plates with a 101x106x1 mm glass area, purchased from Zitt-Thoma GmbH (Freiburg, Germany). This involved placing a droplet of 1 mL volume on the glass plate and using a coating knife, made of stainless steel with a 150 deep micron channel, to distribute the droplet into a homogenous film with an area of approximately 90x90 mm. The thicknesses of the films were estimated by the initial mass, solution density and area of the produced film to be 125±5 micron thick. Due to the lowering of the surface tension by the proteins, an even film could be produced that was constant in thickness and did not de-wet on the glass plate during drying to form irregular patches. Prior to film formation, glass plates were heated to the drying temperature in the tray dryer.

To ensure the film temperature was as close as possible to the wet bulb temperature during drying, solutions used for producing the films were pre-warmed to the appropriate wet bulb temperatures (for the various drying temperatures). The air flow in the drying tunnel was adjusted to a low speed of 1.1±0.1 m/s immediately after films were produced. The drying air was dehumidified in a water-contact tower before it re-entered the drying tunnel (closed-cycle air system). A line diagram of the tray dryer is shown in Figure 4.3. Films were dried at 40±1 °C and a relative humidity (RH) of 28±1 %, which corresponds to a wet-bulb temperature of 24 °C. Other lactose/Na-Cas (90/10 wt%, 10wt% TS, pH 7.0) films were dried at 30±1 °C and RH 47±2%, 60±2 °C and RH 13±1%, and 80±2 °C and RH 5±1%, which correspond to wet-bulb temperatures of 22, 31 and 35 °C, respectively. The film weight during drying was automatically monitored in-line and exported into MS Excel to plot the drying curves.

After successful film drying, dried films were immediately vacuum-packed and stored in the fridge to prevent moisture absorption, which would have caused lactose to crystallize. Film drying produced a transparent film with no evidence of lactose crystallization. If lactose crystallization had occurred, the transparent film would have been transformed into a white, opaque film, such as was observed when an initially transparent film was stored unprotected overnight. Prior to XPS analysis, films were cut into approximately 5x5 mm squares with a glass diamond cutter.

X-ray Photoelectron Spectroscopy

X-ray photoelectron spectroscopy (XPS) was used according to the method described in Chapter 3.

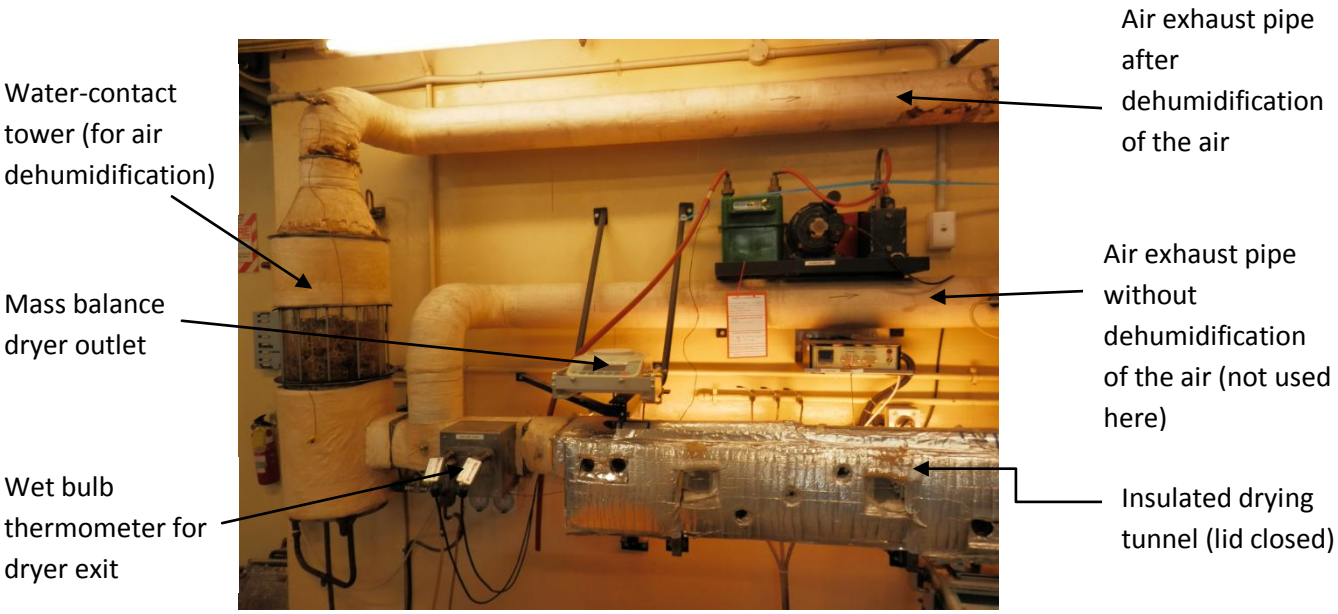

Figure 4.1. Tray dryer with water-contact tower for air dehumidification.

Figure 4.2. Tray dryer exit with open chamber lid and mass balance where glass plates were put for film drying.

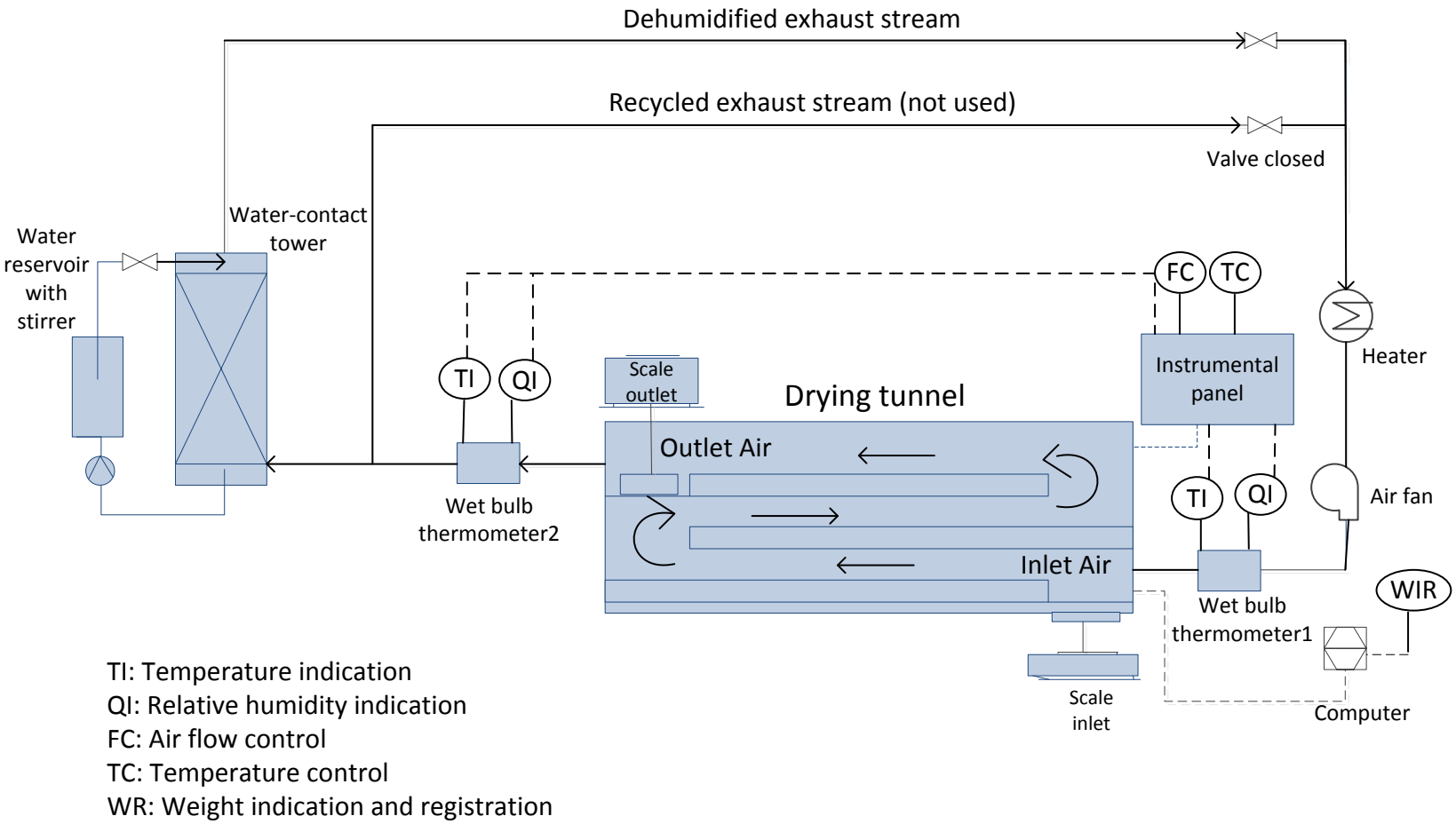

Figure 4.3. Line diagram of tray drying system, used for film drying.

4.2.2. Part B: Scale-up study

Solution preparation

Lactose α-monohydrate and Na-Cas were supplied by Fonterra Research and Development Centre (FRDC) (Palmerston North, New Zealand). 100 kg of a 10 wt% lactose/Na-Cas (90/10 wt%) solution and 50 kg of a 20wt% lactose/Na-Cas (90/10 wt%) solution, both containing deionized water, were prepared at FRDC in a stirred 200L stainless steel vessel using a Cowles mixer with variable speed agitator (Palmerston North, New Zealand) (Figure 4.4). The water was first heated up to temperatures of about 60 °C, before adding the Na-Cas stepwise. Na-Cas was added prior to lactose in order to prevent the pH of the solution reducing to an acidic pH, which may have caused protein aggregation should it have approached the isoelectric point of Na-Cas (pH=4.6). After the addition of the solutes, the lactose/Na-Cas solution was stirred for another hour at a temperature of approximately 60 °C to ensure complete dissolution of proteins and lactose, before being fed into the pilot-scale spray dryer. 1L aliquots of the feed solutions were taken and cooled before being sent to Christchurch for laboratory-scale spray drying, which took place the following day.

Figure 4.4: Solution preparation inside a 200L volume stainless steel vessel with mixer attached (right) + heat exchange column (left) to heat the solution to desired feed temperatures for spray drying.

Spray Drying

Pilot-scale:

The pilot spray dryer with an integrated fluidized bed (IFB) dryer had a diameter of 290, height of 559 cm (above IFB) and a chamber volume of 19.28 m^3, located at FRDC (Palmerston North, New Zealand) (Figure 4.5). Air was filtered by a EU3 pre-filter and EU5 main filter to prevent entry of foreign matter into the dryer. Spray drying was performed at co-current inlet air flows of 2700±5 m^3/h, feed flow rates of 60±3 L/h, feed inlet temperatures of 46-47 °C and air inlet/outlet temperatures of 175/90±2 °C. A pressure nozzle (nozzle orifice number 63=orifice size 0.93mm) with a nozzle swirl core (number 21) was used. Powder build-up at the dryer wall was prevented by pneumatic hammers. Powder fines that were too light to be separated at the exterior of the dryer wall entered the outlet pipe located at the bottom centre of the dryer chamber, where they were collected in a cyclone connected to the dryer chamber and returned to the dryer chamber by using ambient compressed air. The integrated fluidized bed was not used here for further powder drying, thus a single-stage drying system was used.

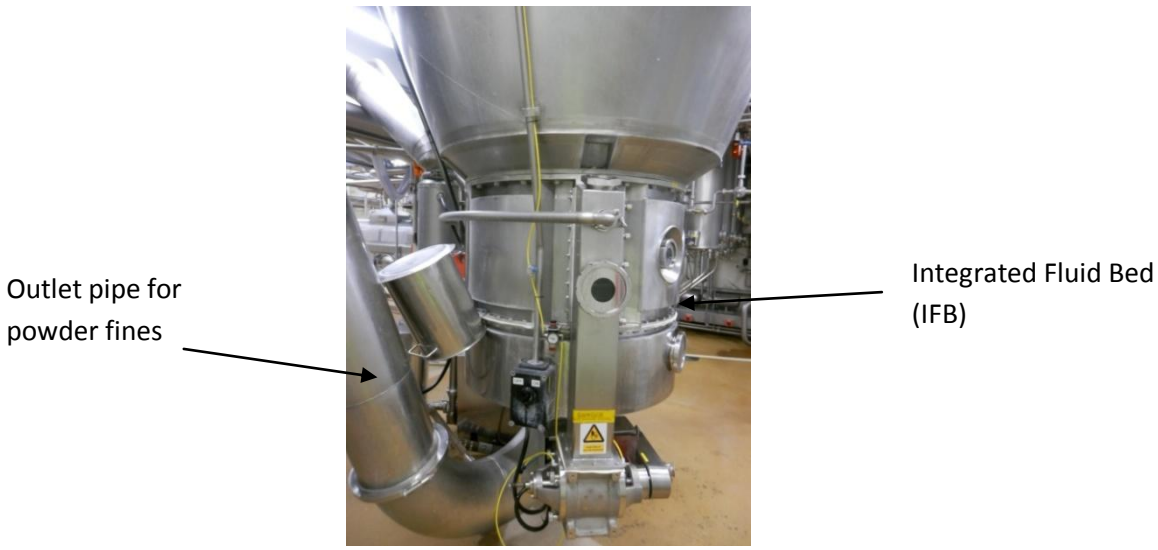

Figure 4.5: Bottom of pilot spray dryer, showing the IFB (integrated fluid bed) and outlet pipe where fines are transported pneumatically and returned towards the spray drying chamber.

Laboratory-scale:

Laboratory-scale spray drying used a *NIRO Atomizer*, Copenhagen, Denmark, with dimensions of 175 x 92.5 cm (height x diameter). For atomization, a two-fluid nozzle with an orifice diameter of 1.5 mm was used. The co-current air flow was kept constant at 100±5 m^3 h^{-1} and a peristaltic pump was used for the feed supply to the atomizer. The air inlet/outlet air temperatures were 175/85±2°C, the atomization air pressure was 0.2±0.05 bar, the solution feed rate was 1.5±0.1 kg h^{-1} and the solution temperature was 60±1°C.

Powder Analysis

X-ray photoelectron spectroscopy (XPS), powder flowability, wettability, particle size distribution, powder bulk density and powder morphology were measured according to the procedures described in Chapter 3.

4.3. MATHEMATICAL MODEL

4.3.1. Model for evaporation of aqueous films

The area specific evaporation rate of water vapour from the film surface [kg/(m^2 s)] for a constant-rate drying period is derived from the following differential equation from Section 2.3.2, assuming a one-dimensional diffusion in a binary system (Adhikari et al., 2007a).

$$\dot{m}_w = k_c \frac{p_{atm} M_W}{R\,T} ln\left(\frac{p_{atm}-p_{W,\infty}}{p_{atm}-p_{W,sat}}\right) \quad (4.1)$$

where k_c is the convective mass transfer coefficient (m/s), p_{atm} is the atmospheric pressure (Pa), $p_{W,\infty}$ is the water vapour partial pressure in the bulk flow of the drying chamber, $p_{W,sat}$ is the water water vapour partial pressure (Pa) at the surface of the film, R is the universal gas constant [kg m^2/(s^2 kg mol K)], T is the interfacial film temperature (K) and M_W is the molar mass of water (kg/kmol).

Temperature gradients within the drying films were assumed to be negligible. This assumption is valid, because the Biot number (*Bi*) was much less than 1. *Bi* describes the ratio of external heat transfer between film and air and the internal heat transfer inside the film. *Bi* can be expressed by following equation (Incropera et al., 2011):

$$Bi = \frac{R_{cond}}{R_{conv}} = \frac{h\,L}{k_W} \tag{4.2}$$

where h is the heat transfer coefficient [W/(m^2 K)], L is the characteristic length of the film (m) and k_W is the thermal conductivity of water [W/(m K)]. When Bi<<1, the resistance to heat conduction within the film (R_{cond}) is much less than the resistance to heat convection in the boundary layer (R_{conv}) (Incropera et al., 2011), and therefore a uniform temperature can be assumed in the film. In this film drying study, Bi was around 0.1 for the different drying temperatures, hence the assumption of uniform film temperatures in the model was valid.

Solutions were heated up to the appropriate wet-bulb temperature before films were produced, therefore the initial heating period of the film was assumed to be negligible. It was assumed that the film temperature remained constant at the wet-bulb temperature during the constant drying-rate period (before a crust has formed on the surface). Possible heat transfer from the air to the exposed glass plate through convection, as well as from the glass plate to the bottom of the film through conduction, were not considered. These assumptions were justified, because the convective mass transfer coefficient k_c was determined by fitting Equation 4.1 to the experimental drying rate in the constant-rate drying period. This mass transfer coefficient was used directly in the simulations to guarantee that the external mass transfer rate was predicted accurately. The appropriate water vapour partial pressures in the bulk of the air fluid and the film surface ($p_{W,\infty}$ and $p_{W,sat}$, respectively) were calculated by the Antoine Equation (Equation 2.5 and 2.6, Chapter 2).

4.3.2. Solute-fixed coordinate model

For the evaporation of an aqueous film containing solids, the solute-fixed coordinate model was used to simulate moisture gradients within the drying films. This model is explained in detail by Crank (1979). Adhikari et al. (2007a) used this model for the drying of aqueous fructose and lactose solutions. The model uses a stationary reference frame for the solute ("fixed coordinate"), based on the concept that the volume of the solute during drying does not change. This simplifies the governing equations. Moisture content profiles are solved on a grid placed in this stationary reference frame. A simple transformation allows a switch between the stationary reference frame to the observer's reference frame ("shrinking coordinate") to allow the shrinkage of the film due to solvent evaporation to be predicted. It

was assumed that no solute segregation between lactose and protein occurred during film drying. This assumption is supported by Nijdam et al. (2014), who showed that solute segregation did not occur in their study of film-dried aqueous lactose/BSA solutions, except in the immediate vicinity of the surface, where proteins formed a saturated monolayer. Thus a binary system was used, with water ("W") as the solvent and lactose and Na-Cas as a single homogenous solute ("S"). Based on these assumptions, the governing equation, derived from Fick's second law of diffusion becomes

$$\frac{\partial X_W}{\partial t} = \frac{\partial}{\partial z}\left(D_W^S \frac{\partial X_W}{\partial z}\right) \tag{4.3}$$

where X_W is the water content (kg water/kg solute) and D_W^S is the Fickian diffusion coefficient in the solute-fixed coordinate system. This differential equation was solved numerically by using the finite differences method. A spatial variable *z* (m) was defined here to describe the distance across the dry film in the solute-fixed coordinate system, while a variable *y* (m) was defined to describe the distance across the wet film in an observer's ("shrinking") coordinate system. Equation 4.4 was used to allow the transformation between the shrinking and fixed coordinate systems.

$$\frac{\partial z}{\partial y} = \varphi_s \tag{4.4}$$

where φ_s is the volume fraction of the solute (m^3 solute/ m^3 total). Equation 4.4 assumes a one-dimensional film shrinkage in the vertical dimension only. In that case, the relationship between the Fickian diffusion coefficient in the solute-fixed coordinate system D_W^S and the Fickian diffusion coefficient in the observer coordinate system D_W is given by following equation:

$$D_W^S = \varphi_S^2 \, D_W \tag{4.5}$$

Equation 4.5 is only valid for binary diffusion of water and solute, as assumed for this model. Because a mutual diffusion coefficient for a water-lactose-Na-Cas system is not available in the literature, a sensitivity analysis of the diffusion coefficient had to be performed, as described in detail in Section 4.3.5. The volume fraction of the solute φ_s was determined using following equation, assuming negligible excess volume of the mixture, as follows:

$$\varphi_s = \frac{\rho_W}{\rho_s X_W + \rho_W} \tag{4.6}$$

where ρ_s and ρ_W are the densities of the dry solute (kg solid/m^3 solid) and pure water, respectively (kg water/m^3 water). The density of the dry solute ρ_s was calculated by following equation:

$$\rho_s = \frac{1}{\left(\frac{x_{Lact}}{\rho_{Lact}} + \frac{x_{Na-Cas}}{\rho_{Na-Cas}}\right)} \tag{4.7}$$

where ρ_{Lact} and $\rho_{Na\text{-}Cas}$ (kg/m^3) are the densities of dry lactose and Na-Cas and x_{Lact} (kg lactose/kg total solids) and $x_{Na\text{-}Cas}$ (kg Na-Cas/kg total solids) are the mass fractions of lactose and Na-Cas in the dried solids.

When Equations 4.4, 4.6 and 4.7 are considered, the relationship between solute-fixed and observer's coordinate system can be expressed by following equation:

$$\frac{\partial z}{\partial y} = \varphi_s = \frac{\rho_W}{\frac{x_W}{\left(\frac{x_{Lact}}{\rho_{Lact}} + \frac{x_{Na-Cas}}{\rho_{Na-Cas}}\right)} + \rho_W} \tag{4.8}$$

Equations 4.4, 4.6 and 4.7 enable the calculation of the actual film thickness y during film drying. The thickness of the dried film z_{max} was calculated from the initial wet film thickness y^0_{max} by integration of Equation 4.4, as follows:

$$z_{max} = (\varphi_s y_{\max})^0 \tag{4.9}$$

The initial wet film thickness y^0_{max} was calculated by the initial film volume $V_{film}{}^0$ and film area A_{film}, assuming a constant film thickness, as follows:

$$y^0_{max} = \frac{V^0_{film}}{A_{film}} = \frac{m^0_{film}}{\rho^0_{sol}\, A_{film}} \tag{4.10}$$

where $m^0{}_{film}$ is the initial film mass and $\rho^0{}_{sol}$ is the initial solution density (kg total/m^3 total).

Assuming that the initial wet film is uniform in composition, the initial condition can be stated as:

$$X_W = X^0_W \qquad \text{t=0 and } 0 \le z \le z_{max} \tag{4.11}$$

The water flux j_W^S at the boundary between glass and film was assumed to be zero, while the water flux at the boundary between film and air was controlled by the evaporation rate of water vapour, assuming thermodynamic equilibrium at the surface (Equation 4.1).

$$j_W^S = \frac{\partial X_W}{\partial z} = 0 \qquad t \geq 0 \text{ and } z = 0 \qquad (4.12)$$

$$j_W^S = -\rho_s D_W^S \frac{\partial X_W}{\partial z} = \dot{m}_W \qquad t \geq 0 \text{ and } z = z_{max} \qquad (4.13)$$

4.3.3. Simplified drying model

A simplified drying model was also adopted in this study. This model assumes that the drying rate is externally controlled by the boundary layer and is constant. For this constant rate drying period, the water activity of the film surface remains at unity ($a_W = 1$) and no crust or film capable of acting as barrier for moisture evaporation forms at the film surface, as discussed in Section 2.3.3. For this model, uniform water contents were assumed over the thickness of the drying films, and shrinkage only occurred in the vertical direction (thickness dimension). The average water contents of the films $\overline{X}_W(t)$ were calculated from a mass balance over the film, as follows:

$$(z_{max}\,\rho_s)\frac{\partial \overline{X}_W}{\partial t} = -\dot{m}_W \qquad (4.14)$$

which has the analytical solution

$$\left(\overline{X}_W - \overline{X}_W^0\right) = -\frac{\dot{m}_W}{z_{max}\,\rho_s}\,t \qquad (4.15)$$

The initial volume fraction of the solute $(\varphi_s)_0$ (m^3 solute/m^3 total) can also be expressed by following equation:

$$(\varphi_s)_0 = \frac{(x_s \rho_{sol})_0}{\rho_s} \qquad (4.16)$$

where x_s is the mass fraction of the solute (kg solute/kg total), ρ_{sol} and ρ_s are the densities of the aqueous solution (kg total/m^3 total) and dry solute (kg solute/ m^3 solute), respectively.

Using Equation 4.9 and 4.16, Equation 4.15 can also be expressed as:

$$\left(\overline{X}_W - \overline{X}_W^0\right) = -\frac{\dot{m}_W}{(x_s\rho_{sol})_0 y_{max}} t \qquad (4.17)$$

Equation 4.17 forms the constant drying-rate model, which was used to calculate the average water content $\overline{X}_W$ of the aqueous solute-containing films at given drying time (t). The modelled drying curves using Equation 4.17 were fitted to the experimental drying curves by adjusting the external mass transfer coefficient. This ensured that the drying rate was correctly predicted and therefore the accuracy of the solute-fixed drying model for simulating the internal transport of moisture (and therefore moisture concentration gradients) within the drying films could be properly assessed.

4.3.4. Numerical solution

Equation 4.3 was solved numerically in MATLAB, using the finite differencing method (Crank, 1979). The MATLAB code is attached to the Appendix A.3.1. The moisture profiles within the drying film were discretized. The length of the film was divided into i=10 equally sized cells with $\Delta z = z_{max}/i$ and boundary nodes m=1 for the bottom of the film (z=0) and m=11 for the film surface (z_{max}). Backwards differencing was used for the time dimension. Incremental small time steps Δt were chosen in order to ensure numerical stability in accordance with the numerical stability criterion for this discretization scheme: $\Delta t < \Delta z^2/(2D_W^S)$. A grid and time-step sensitivity analysis was performed, where the number of spaces was doubled and time-steps were halved (see Appendix A.3.2). This resulted in differences in the water contents of <0.1% for any the water contents calculated throughout the film thickness.

Figure 4.6 shows the solute-fixed coordinate system with the grids m (distance of Δz amongst grids) and the time-steps n with Δt. Shrinkage of the film during drying was determined by the increase in the solute volume fraction φ_s with each successive time step. This allowed the transformation from Δz to Δy for known φ_s for each node. The water contents for each time (n) and film depth (m) for m=1→11 were determined for each node m and n. For n = 1 (t=0s), the initial water contents of the film were known and used to calculate the initial solute volume fractions $\varphi_s(m,1)$, mutual diffusion coefficients $D_W^S(m,1)$ and cell widths $\Delta y(m,1)$ for $1 \leq m \leq 11$.

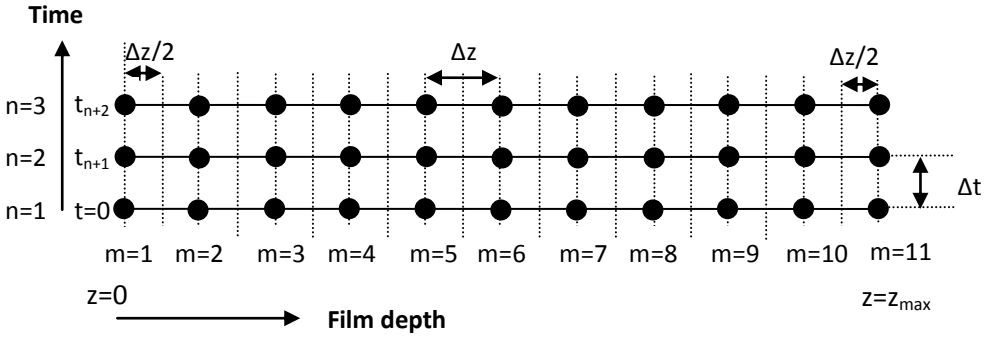

Figure 4.6. Time (n) and distance grids (m) along the film depths for solute-fixed coordinate system.

For $n \geq 1$ (n=n+*1*), the water contents for each node were discretized by using Equation 4.3 and considering the boundary conditions (Equations 4.12 and 4.13) for the external nodes m=1 and m=11, as follows:

For m=1:

$$X_W(1,n+1) \approx 2\frac{D^S_{W(1,n)}+D^S_{W(2,n)}}{2}\frac{\Delta t}{\Delta z^2}[X(2,n)-X(1,n)]+X(1,n) \quad (4.18)$$

For $2 \leq m \leq 10$:

$$X_W(m,n+1) \approx \frac{\Delta t}{\Delta z^2}\left[\frac{D^S_{W(m,n)}+D^S_{W(m+1,n)}}{2}[X(m+1,n)-X(m,n)]-\frac{D^S_{W(m,n)}+D^S_{W(m-1,n)}}{2}[X(m,n)-X(m-1,n)]\right]+X(m,n) \quad (4.19)$$

For m=11:

$$X_W(11,n+1) \approx \left[\frac{-\dot{m}_W M}{\rho_s}-\left[\frac{D^S_{W(11,n)}+D^S_{W(10,n)}}{2}\frac{[X(11,n)-X(10,n)]}{\Delta z}\right]\right]\frac{2\Delta t}{\Delta x}+X(11,n) \quad (4.20)$$

These calculated water contents can then be illustrated in the form of a matrix, as follows:

$$X_W(m,n) = \begin{bmatrix} X_W(1,1) & \cdots & X_W(11,1) \\ \vdots & \ddots & \vdots \\ X_W(1,n) & \cdots & X_W(11,n) \end{bmatrix} \quad (4.21)$$

The mutual diffusion coefficients $D_W^S(m,n,)$ in the fixed-solute coordinate system, which were required to calculate $X_W(m,n+1)$, were calculated for each time and grid-step individually using Equation 4.5, as follows (illustrated in form of a matrix):

$$D_W^S(m,n) = \begin{bmatrix} D_W\ \varphi_s^2(1,1) & \cdots & D_W\ \varphi_s^2(11,1) \\ \vdots & \ddots & \vdots \\ D_W\ \varphi_s^2(1,n) & \cdots & D_W\ \varphi_s^2(11,n) \end{bmatrix} \quad (4.22)$$

The solute volume fractions $\varphi_s(m,n)$, which were required to calculate $D_W^S(m,n,)$, were calculated by Equation 4.6, as follows (illustrated in form of a matrix):

$$\varphi_s(m,n) = \begin{bmatrix} \frac{\rho_s}{\rho_s X_W(1,1)+\rho_W} & \cdots & \frac{\rho_s}{\rho_s X_W(11,1)+\rho_W} \\ \vdots & \ddots & \vdots \\ \frac{\rho_s}{\rho_s X_W(1,n)+\rho_W} & \cdots & \frac{\rho_s}{\rho_s X_W(11,n)+\rho_W} \end{bmatrix} \quad (4.23)$$

The last step involved transformation from the solute-fixed coordinate to the observer's coordinate system. The cell width Δz was transformed to Δy, taking account of the solute volume fraction, by using Equation 4.4 ($\Delta y=\Delta z/\varphi_s$), as follows (illustrated in form of a matrix):

$$\Delta y(m,n) = \begin{bmatrix} \frac{\Delta z}{\varphi_s(1,1)} & \cdots & \frac{\Delta z}{\varphi_s(11,1)} \\ \vdots & \ddots & \vdots \\ \frac{\Delta z}{\varphi_s(1,n)} & \cdots & \frac{\Delta z}{\varphi_s(11,n)} \end{bmatrix} \quad (4.24)$$

4.3.5. Diffusion Coefficient

A binary mutual (Fickian) diffusion coefficient D_W exists for aqueous solutions containing a solvent (in this case water) and a solute (in this case lactose and Na-Cas). The mutual diffusion coefficient is a strong function of the water content. At infinite dilution, mutual diffusion and self-diffusion of individual components become identical (Vrentas & Vrentas, 1993). Because the water content decreases during drying of an aqueous solution, the mutual diffusion coefficient falls to lower levels accordingly, although between water fractions of 1 and 0.5, it does not reduce significantly (Nijdam et al., 2014). In this model, the calculation of water content gradients within the drying film was performed only for the constant drying–rate period, when a_w=1 (the water vapour pressure at the film surface $p_{w,sat}$ equals the vapour pressure of pure water at temperature *T)*. For aqueous solutions containing a TS of 10wt%, the calculations were performed until water fractions dropped to 0.8 (equivalent to water contents of 4 kg/kg), while for aqueous solutions containing TS of 5 and 20wt%, the calculations were performed until water fractions dropped to 0.9 and 0.7 (equivalent to water contents of around 10 and 2 kg/kg) respectively. This ensured that changes in the diffusion coefficient during this initial drying period were small. To summarize, in the simulation performed here, constant values for the diffusion coefficient as well as a_w =1 were applied for this initial drying period.

Since a mutual diffusion coefficient for aqueous lactose/Na-Cas solutions is not known, a sensitivity analysis of the diffusion coefficient was performed here using a range of diffusion coefficients. Sober (1968) provides a mutual diffusion coefficient for aqueous β-casein of 6.05×10^{-11} m^2/s at infinite dilution at 20°C, while Ribeiro et al. (2006) provides a mutual diffusion coefficient for aqueous lactose of 5.66×10^{-10} m^2/s at infinite dilution at 25°C. To represent the likely range of mutual diffusion coefficients, the mutual diffusion coefficient for aqueous β-casein solutions was chosen as lower limit, while the mutual diffusion coefficient for aqueous lactose solutions was chosen as upper limit. In addition, a central diffusion coefficient, lying between the upper and lower limit, was chosen for aqueous lactose/Na-Cas solutions.

The Stokes-Einstein equation was used to scale the diffusion coefficients (given above for 20 and 25 °C) according to the different film temperatures. A constant hydrodynamic radius was assumed for lactose and β-casein at infinite dilution, irrespective of the temperature, thus the Stokes-Einstein equation can be written as $D_W \eta/T = constant$, where η

is the kinematic viscosity of the solvent and T is the absolute temperature. Wet bulb temperatures T_{WB} of 21.7, 24.3, 30.5 and 35.0 °C, measured during drying at drying air temperatures T_{air} of 30, 40, 60 and 80 °C, respectively, were chosen as film temperatures. In Table 4.1, the range of calculated diffusion coefficients for the different aqueous lactose/Na-Cas solutions at various temperatures are shown. These were used for the simulations.

Table 4.1: Scaled diffusion coefficients for different film (wet bulb) temperatures for lactose (upper D_W) and Na-Cas (lower D_W) and a lactose/Na-Cas system (central D_W)

T_{air} (°C)	30	40	60	80
T_{WB} (°C)	21.7	24.3	30.5	35
$D_{W,upper}$ (m^2/s)	5.3E-10	5.7E-10	6.4E-10	7.2E-10
$D_{W,middle}$ (m^2/s)	1.1E-10	1.4E-10	1.6E-10	2.0E-10
$D_{W,lower}$ (m^2/s)	6.6E-11	7.0E-11	8.3E-11	9.4E-11

4.4. RESULTS AND DISCUSSION

4.4.1. Part A: Film drying versus spray drying study

Drying experiments and simplified model

Table 4.2 shows the film drying conditions, together with the experimental mass transfer coefficients. The convective mass transfer coefficient stayed constant at 0.0215±0.001 m/s for all drying films**,** irrespective of protein to lactose ratio, air drying temperature, pH and total solid content (TS). This was confirmed by several repeat measurements that all showed identical drying curves with a constant mass transfer coefficient within an experimental uncertainty of ±0.001 m/s. These data suggested that initial film area, thickness and drying conditions for the various films were fairly uniform.

Table 4.2: Summary of drying conditions including experimentally determined mass transfer coefficient for various air drying temperatures (top) and various TS (bottom)

Na-Cas/lactose (% dry basis)	Temperature (°C)	Air velocity (m/s)	Air relative humidity (%)	Mass transfer coefficient, k_c (m/s)
1/9	30	1.1±0.2	49±2	0.0215±0.001
1/9	40	1.1±0.2	28±2	0.0215±0.001
1/9	60	1.1±0.2	13±1	0.0215±0.001
1/9	80	1.1±0.2	6±1	0.0220±0.001

Total solids (%)	Temperature (°C)	Air velocity (m/s)	Air relative humidity (%)	Mass transfer coefficient, k_c (m/s)
5	40	1.1±0.2	28±2	0.0215±0.001
10	40	1.1±0.2	28±2	0.0215±0.001
20	40	1.1±0.2	28±2	0.0210±0.001

Figure 4.7 shows the drying curves of aqueous lactose/Na-Cas films (10 wt% TS) dried at different air temperatures. Irrespective of the drying temperature, a constant-rate drying period was observed for the initial drying stage, in which water contents reduced from 9 kg/kg down to approximately 4 kg/kg, equivalent to water fractions of between 0.9 and 0.8, while a falling-rate drying period was observed at lower water contents. Aqueous lactose/Na-Cas films of various TS, dried at constant air temperature of 40 °C, showed similar drying curves, although the falling-rate drying periods started at water contents of around 10 kg/kg for the 5wt% lactose/Na-Cas films and 2 kg/kg for the 20wt% lactose/Na-Cas films, respectively (Figure 4.8).

Other authors have reported that the water activities of lactose and a common milk protein (BSA) fell from 1 to 0.93 (for lactose) and remained at unity (for BSA), when the water mass fraction of both materials was reduced from 1 to 0.5 (Bhandari & Burel, 2007; Kachel et al., 2013). A water activity below unity marks the point where the falling-rate drying period starts. Thus, an almost constant rate period should have been observed down to a water content of 1 kg/kg for all the lactose/protein films investigated in this study. The fact that this did not occur suggests that the onset of the falling rate period, in this study at least, was a result of another phenomenon.

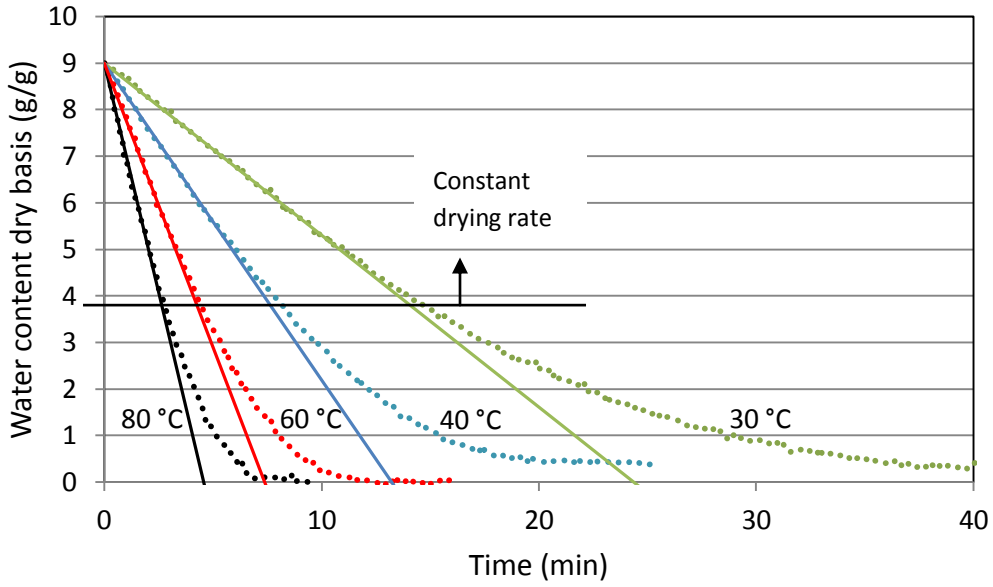

Figure 4.7. Drying curves for thin films of aqueous solutions of lactose/Na-Cas (9/1 dry basis, 10wt% TS), dried at various air temperatures. Points are experimental data, lines are predictions of the simplified model.

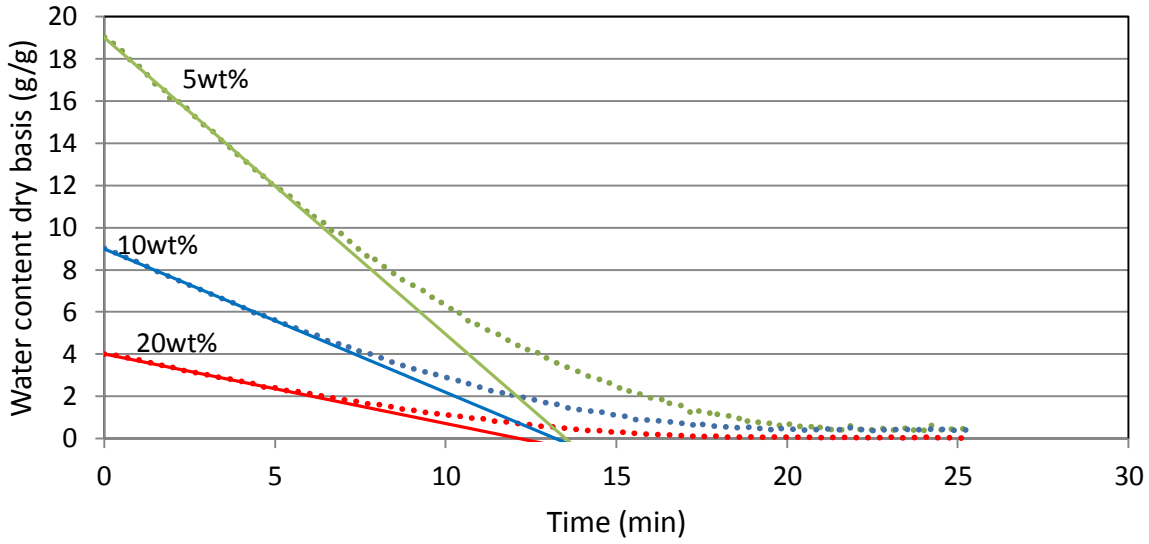

Figure 4.8. Drying curves for thin films of aqueous solutions of lactose/Na-Cas (9/1 dry basis, various total solids), dried at 40 °C. Points are experimental data, lines are predictions of the simplified model.

One possible explanation for the earlier start of the falling-rate drying periods could be that at water contents above 1 kg/kg a protein film formed at the air-water interface, and this acted as a moisture barrier to reduce a_w and hence reduce water evaporation, due to strong hydrogen bonding with water molecules. However, drying of a pure lactose film resulted in

the same depression in the evaporation rate as was observed for lactose/Na-Cas (9/1 wt%) films (Figure 4.9), which suggests that the sudden start of the falling-rate period was not caused by the existence of a protein film. Another possibility could be that the leading edge of the films dried more quickly than the trailing edge due to an enhanced mass transfer coefficient there. At the leading edge of the film, the mass transfer boundary layer formed and gradually thickened in the airflow direction towards the trailing edge of the film. The mass transfer coefficient was relatively high at the leading edge where the boundary layer was thinner, and decreased towards the trailing edge where the boundary layer was thicker. Thus, the leading edge of the film dried more quickly than the trailing edge, and entered the falling rate period earlier. The falling rate period at the leading edge of the film could have begun well before the average moisture content of the film (as determined using the mass balance on the tray dryer) reduced below 1 kg/kg. In addition, small imbalances in the level of the film plate in addition to drag by the air flow could have caused a flow of the film during drying, and hence films of non-uniform thickness. Thinner sections of a film would enter the falling rate period earlier than thicker regions of the film. The non-uniformities were confirmed by visually examining the films after drying was completed, and they showed small gradients in the film thickness across the film. The mass transfer coefficients for use in the solute-fixed coordinate system model were extracted from the experimental drying curves during the constant-rate period, when it could be assumed that a_w was unity everywhere across the film surface.

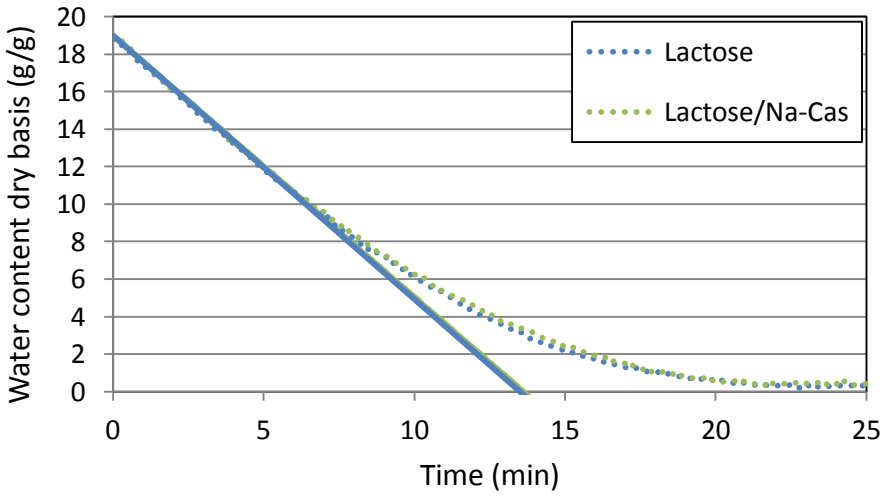

Figure 4.9. Drying curves for thin films of aqueous solutions of lactose and lactose/Na-Cas (9/1 dry basis, 5wt% TS), dried at 40 °C. Points are experimental data, lines are predictions of the simplified model.

Solute-fixed coordinate system model

Figure 4.10 (a-d) shows the predicted moisture content gradients within the films at various drying temperatures, together with the shrinkage of the films. While moisture content gradients were very small at 30 °C, an increase in air temperature caused an increase in moisture content gradient, which was expected due to the faster drying rate and therefore faster removal of moisture from the air-water interface (Kim et al., 2003), as discussed in Section 2.3.4. As can be seen in Figure 4.10, there were significant differences between the calculated water contents for the upper and lower diffusion coefficients. The moisture content profiles representing the upper limit of the mutual diffusion coefficient (corresponding to aqueous lactose) show small water content gradients (Figure 4.10, solid line), while the moisture content profiles representing the lower limit of the mutual diffusion coefficient (corresponding to aqueous β-casein) show significantly larger moisture concentration gradients (Figure 4.10, dotted line). For the lactose/Na-Cas films used in this study, it was assumed that the real water content gradients lie somewhere between the upper and the lower calculated gradients. However, considering that the solid mass fraction of lactose/Na-Cas was 9:1, it is reasonable to assume that the moisture content gradients lie closer to the upper limit of pure aqueous lactose solutions, where moisture content gradients were small and almost not visible at lower drying temperatures (30 and 40 °C).

The low moisture content gradients at 30 and 40 °C suggest that, at these temperatures, solute segregation between lactose and Na-Cas due to moisture content gradients is small, but is expected to be larger at the higher drying temperatures, where moisture content gradients are significantly larger. Higher moisture contents gradients are predicted to cause a higher surface accumulation of the larger Na-Cas proteins, at the expense of the smaller lactose. This was investigated in the following study, where the surface compositions of films dried at different drying temperatures were analyzed by XPS.

a) 30 °C

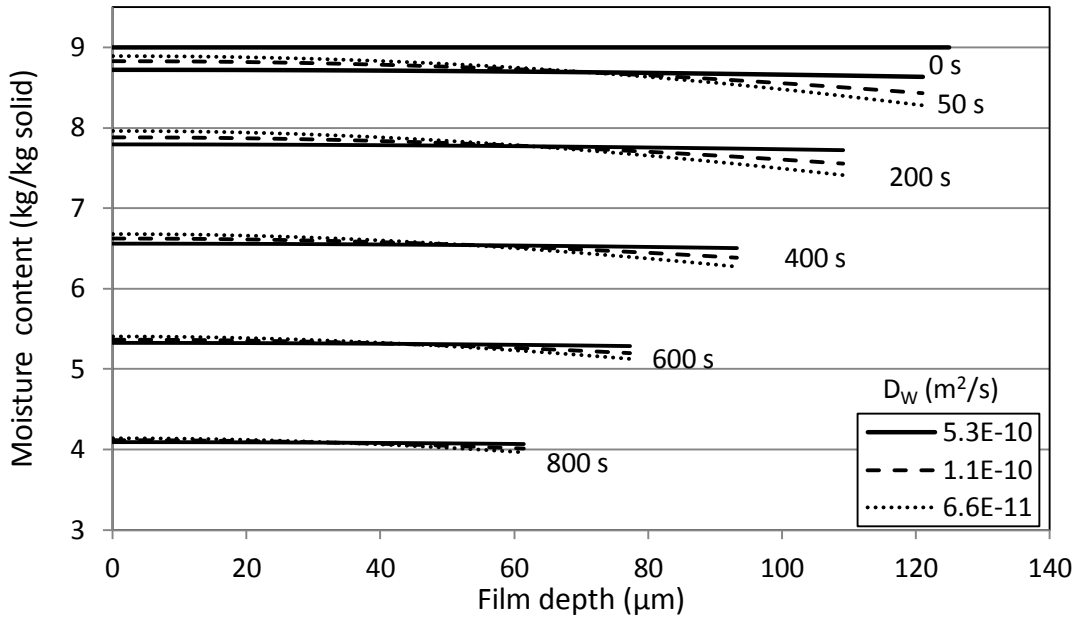
Moisture content (kg/kg solid)
Film depth (µm)
0 s
50 s
200 s
400 s
600 s
800 s
D_W (m²/s)
5.3E-10
1.1E-10
6.6E-11

b) 40 °C

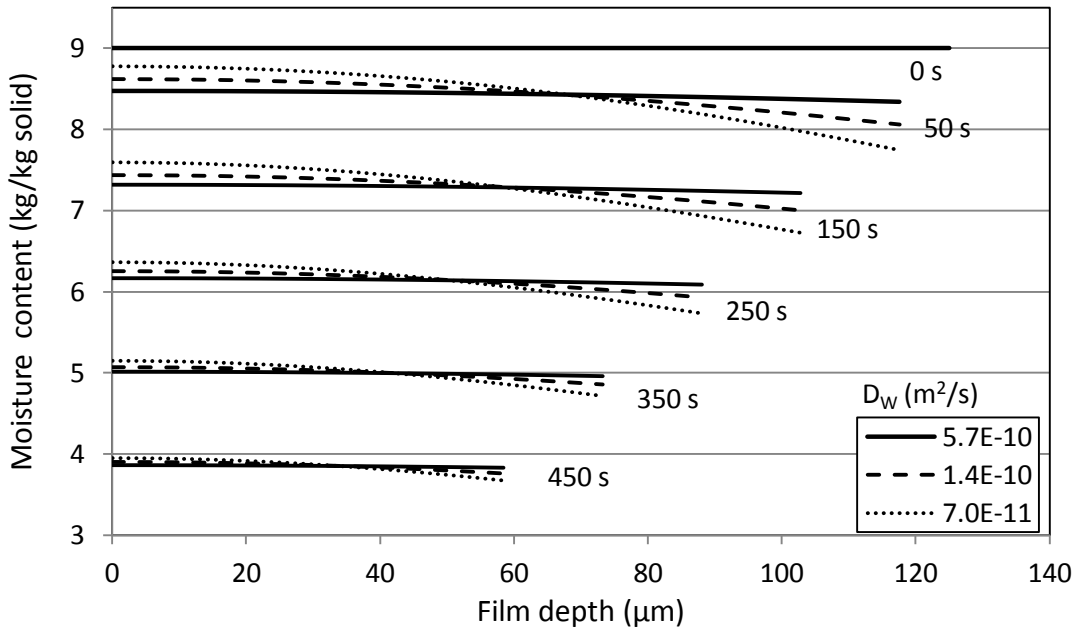
Moisture content (kg/kg solid)
Film depth (µm)
0 s
50 s
150 s
250 s
350 s
450 s
D_W (m²/s)
5.7E-10
1.4E-10
7.0E-11

c) 60 °C

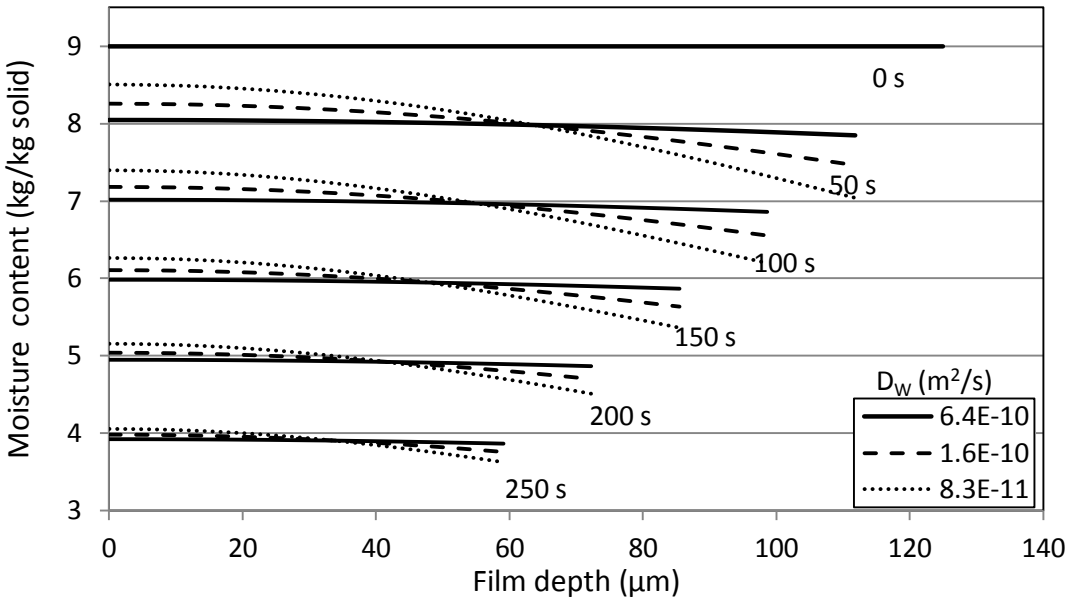

d) 80 °C

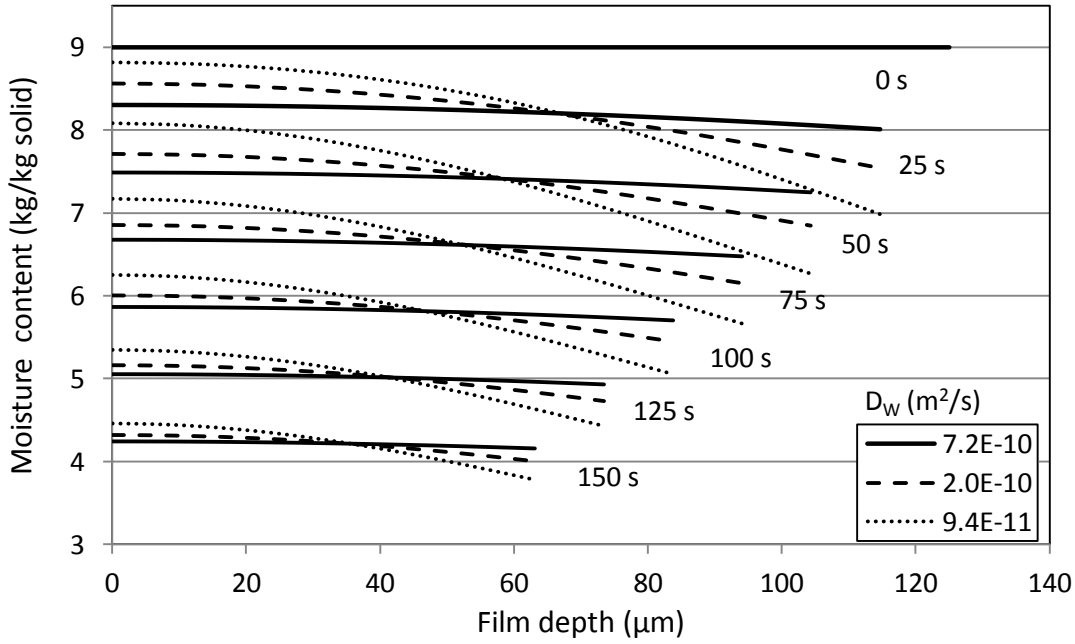

Figure 4.10. Simulated water contents (X_W) within a drying aqueous lactose/Na-Cas film (9/1 dry basis, 10wt% TS) during proceeding drying: sensitivity analysis of the diffusion coefficient (D_W). Drying air temperatures ±1°C: a) 30 °C, b) 40 °C, c) 60 °C, d) 80 °C.

Surface composition of films versus spray-dried powders

Effect of lactose/Na-Cas bulk ratio

Figure 4.11 compares the experimental Na-Cas surface concentrations of dried films and spray-dried powders at various protein bulk concentrations. Both films and powders were prepared from solutions containing 10wt % TS, and the drying temperatures were 40 °C and 160°C (at the air inlet), respectively. The protein surface composition of the dried films increased to approximately 60% when the protein bulk concentration was raised to 5wt%, but did not increase further when the protein bulk concentration was raised beyond this. Further experiments with drying films, in which the protein bulk concentration was constant (lactose/Na-Cas=9/1 wt%) but the drying temperature and TS content was varied (Figure 4.12 and Figure 4.13) revealed little variation in protein surface composition (60±2% protein for all films). This suggests that 1) the surface became saturated at similar surface concentrations for all these conditions and 2) drying times for all drying films were sufficient (Figure 4.7) for proteins to adsorb to the film surface due to their surface activity and form a saturated mono-layer there.

While the Na-Cas surface concentrations of both powders and films were similarly for low protein/lactose solid ratios of 0.1/99.9 and 1/99, further increasing the protein/lactose ratios had a greater effect on the surface concentrations of protein in spray-dried powders than it did on the slower-dried films (Figure 4.11). During spray drying, the fast receding droplet surface may cause proteins to pack above the saturation limit within the adsorbed protein film (due to the surface area being reduced upon droplet shrinkage). These more dense, closely packed protein films formed during spray drying would have excluded water, and therefore dissolved lactose molecules from the droplet surface, thereby restricting them to deeper regions of the droplet. This might offer one explanation why spray-dried powders have higher Na-Cas surface concentrations than dried films.

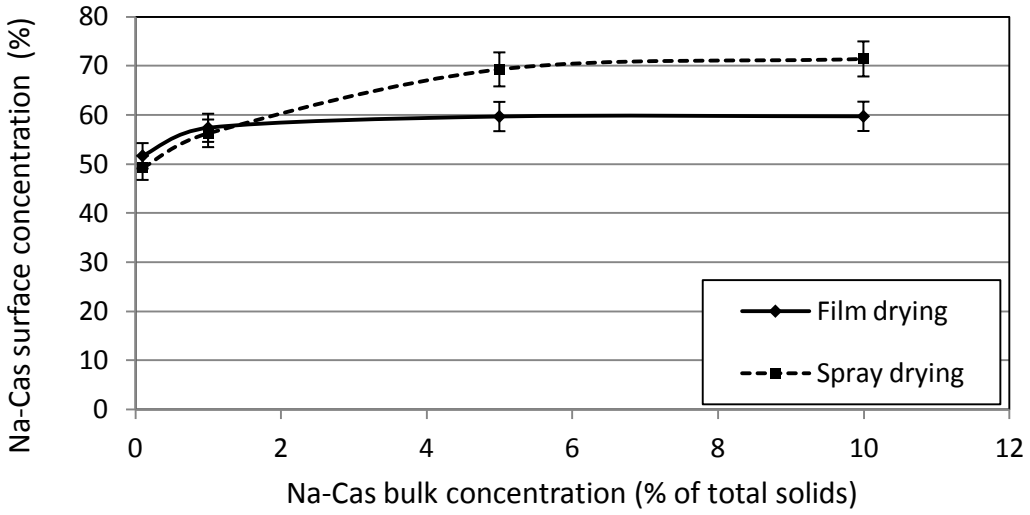

Figure 4.11: Effect of Na-Cas bulk concentration of aqueous lactose/Na-Cas solutions with 10 wt% TS on Na-Cas surface concentration of A) films, dried at 40 °C (solid line) and B) particles, spray-dried at 160/75 °C air inlet/outlet temperature (dashed line).

A Peclet number larger than unity during spray drying may have further contributed towards higher solute segregation between lactose and protein in this drying system (Vehring, 2008). Using Equation 2.7 (Section 2.3.4), *Pe* numbers of 6.07 and 0.75 were estimated for Na-Cas and lactose, respectively, during the spray drying performed in this study (see Appendix A.3.3). In a film drying system (lactose/Na-Cas of 90/10 wt%, 10 wt% TS, 80 °C drying air temperature), *Pe* numbers of 0.2 and 0.02 were calculated for Na-Cas and lactose, respectively (see Appendix A.3.3), using the following equation (Trueman et al., 2012).

$$Pe = \frac{6\pi\eta R_i \dot{E} H}{kT} \qquad (4.25)$$

where R_i is the hydrodynamic radius of the molecule i, η is the kinematic viscosity of the solvent, $\dot{E}$is the evaporation velocity, H is the initial film thickness and kT is the thermal energy. Thus, the *Pe* number of Na-Cas is only above unity during spray drying, which indicates that only during spray drying could Na-Cas proteins have accumulated at and beneath the particle surface as a result of being collected by the fast receding droplet surface. This theory is supported by the data of Vehring (2008) and Trueman et al. (2012).

The observed differences between the total protein surface concentrations of spray-dried powders and those of films were consistent with the findings of Nijdam et al. (2014) and

Fäldt and Bergenståhl (1994) for aqueous lactose/BSA solutions. In the former study, the surface concentration of BSA in the films was constant at approximately 50% for protein bulk concentrations between 10 and 40 wt%, which suggested that equilibrium surface concentrations had been reached. Nijdam et al. (2014) also calculated a *Pe* number of less than unity for BSA and lactose, thus solute segregation due to a *Pe* number effect did not occur in their study. In contrast, Fäldt and Bergenståhl (1994) spray-dried an aqueous lactose/BSA solution (*Pe* of BSA estimated to be >> 1) and measured BSA concentrations of approximately 70% for protein bulk concentrations between 10 and 40%. Thus, with the spray-dried powder the BSA surface concentrations were found to be around 20% higher compared with the films. This further suggests that, in slow film drying, the surface activity and hence surface equilibrium concentration of the protein alone determine the final protein concentration on the film surface, while in spray drying, the protein surface concentration is further enhanced by other effects such as a *Pe* number and surface area-reduction. Once a closely-packed protein monolayer was formed, the *Pe* number effect may have caused more proteins to accumulate beneath the surface to form protein multi-layers.

Note that, because the penetration depth of XPS analysis is only about 10 nm (Fäldt & Bergenståhl, 1994), only protein sub-layers packed within a depth of 10 nm would have been detected. Due to a Peclet number effect during spray drying, further protein sub-layers could have formed beneath a depth of 10nm that would have been outside of the detectable range of XPS analysis.

Effect of drying air temperature

Figure 4.12 shows the effect of the film drying temperature on the Na-Cas surface concentration of dried films. These measurements showed that air temperature had no significant effect on protein surface enrichment. Although lower drying temperatures would have given the proteins more time to saturate the surface, the results of the spray drying studies (Chapter 3) indicated that enough time was given for proteins to adsorb and saturate the surface, even during the short time-frame of spray drying. Significant moisture content gradients existing within films dried at higher temperatures (see Figure 4.10) did not seem to have an effect on the surface composition, measured by XPS, because if this were the case the surface concentration of the protein would be expected to increase with increasing drying temperature.

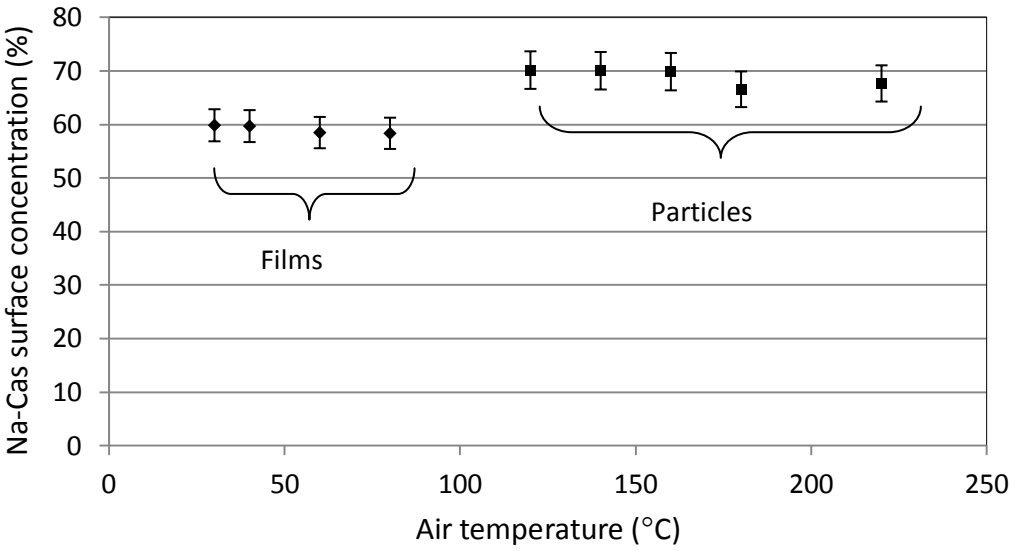

Figure 4.12: Effect of drying air temperature of aqueous lactose/Na-Cas solutions (9/1 wt%, 10wt% TS) on Na-Cas surface concentration of A) films and B) spray-dried particles.

Lactose/Na-Cas particles produced by spray drying at various air inlet temperatures also did not show higher Na-Cas surface concentrations at higher drying temperatures (Figure 4.12), although *Pe* numbers increased with increasing drying rate (see Equation 2.7). This suggests that the maximum packing density at the surface of dried droplets, at a given droplet size and TS, was already achieved even at the lowest drying air temperature of 120 °C (inlet). Thus, any further increase in *Pe* numbers and moisture content gradients at higher drying temperatures had no effect on the surface composition, at least within the detectable range of XPS analysis (~ 10 nm deep surface layer (Fäldt & Bergenståhl, 1994)). However, it is possible that Na-Cas continued to accumulate below this point due to Peclet number and moisture-content gradient effects, causing a thickening of the protein layer beyond 10 nm that could not be detected by XPS.

Since the surface composition of drying films was not affected by the Peclet number (because $Pe < 1$) or moisture content gradients (because higher moisture content gradients at higher drying temperature (Figure 4.10) did not result in higher Na-Cas surface concentrations, see Figure 4.12), the surface saturation level of the films (60±2%) (Figure 4.11 and 4.12) must have been determined by surface activity alone. Surface activity also explains a portion of the observed solute composition on the particle surface, perhaps up to 60%. The observed additional 10% (essentially the difference in Na-Cas surface concentration between the film and the particle) or more of the protein surface composition at

protein bulk concentrations ≥ 5 wt% must have been due to the combined effect of 1) tighter packing as the surface area of the evaporating droplet reduced, and 2) the *Pe* number effect.

Effect of total solids (TS)

Figure 4.13 shows the effect of the total solids (TS) on protein surface concentrations of films and powders. Decreasing total solids resulted in higher final protein concentrations for spray-dried powders, as pointed out in Chapter 3 (Part A). The opposite (i.e. lower final protein concentrations with decreasing total solids) was observed for dried films, although the effect was slight. The reason for the increase in protein surface concentration with decreasing TS for spray-dried powders is not completely clear. One possible explanation could be that more water was available to evaporate from droplets with lower TS, which therefore underwent more shrinkage than occurred in droplets containing higher TS. Due to this increased shrinkage, the droplets with lower TS could have packed more proteins at and beneath their surfaces in sub-layers, so that the total protein surface concentration (existing within a detectable XPS range of around 10nm thickness) became higher.

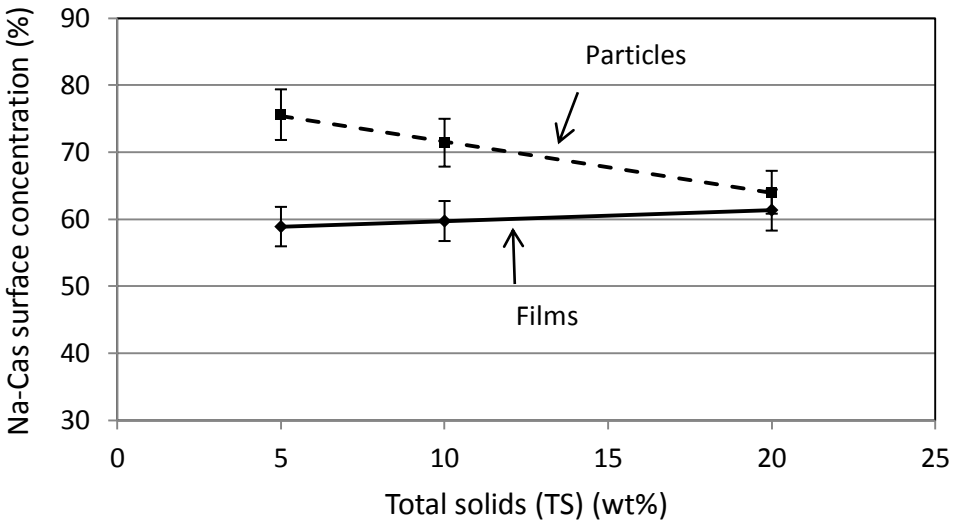

Figure 4.13: Effect of total solids content of aqueous lactose/Na-Cas=9/1 wt% solutions on Na-Cas surface concentration A) films, dried at 40 °C (solid line) and B) particles, spray-dried at 160/75 °C air inlet/outlet temperature (dashed line).

Effect of solution pH

Figure 4.14 compares the effect of the pH on the Na-Cas surface concentration of slow-dried films with that of fast-dried particles. Both particles and films showed an increase in Na-Cas surface concentration as the pH was lowered. This is consistent with the findings of other researchers who performed adsorption studies of proteins at flat surfaces at various pHs (Atkinson et al., 1995b; Caessens et al., 1999; Paulsson & Dejmek, 1992). As also pointed out by Atkinson et al. (1995), the increase in the surface concentration of Na-Cas proteins for solutions spray-dried at a pH closer to the iso-electric point (*pI*) of the protein is caused by a higher packing of adsorbed proteins due to lower electrostatic repulsion, as also mentioned in Chapter 3 (Part A). The effect of the pH on the packing density of adsorbed proteins was clear for both dried films and particles, but may have been accentuated during droplet drying due to the progressive reduction of the droplet surface area.

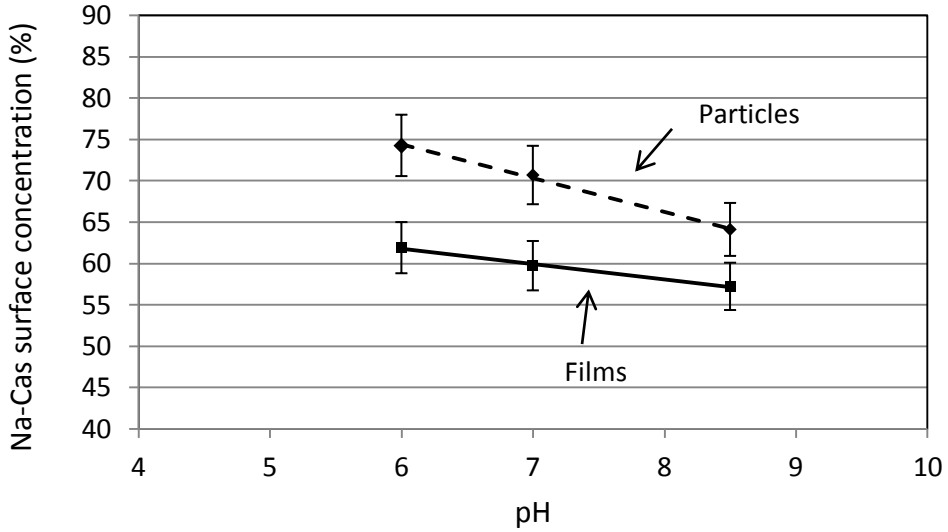

Figure 4.14: Effect of solution pH of aqueous lactose/Na-Cas solutions with 10 wt% TS on Na-Cas surface concentration of A) films, dried at 40 °C (solid line) and B) particles, spray-dried at 160/75 °C air inlet/outlet temperature (dashed line).

4.4.2. Part B: Process scale-up study

Particle size, powder bulk density and powder morphology

Figure 4.15 shows the effect of the scale of the spray drying method on the volume-based mean particle size. Due to the larger nozzle and significantly increased feed rates used, the particles produced by the pilot-scale spray dryer were considerably larger than those produced by laboratory-scale spray drying. Raising the TS of the solution further contributed to a larger particle size due to the higher solution viscosity and the reduction in the amount of water which had to be evaporated. The powders produced in the pilot-scale spray dryer not only had larger particles, but also a significantly higher bulk density (Figure 4.16). This confirms the results given in Chapter 3 (Table 3.5), that lower atomization pressure (as is the case in the pilot-scale spray dryer) produces larger particles and powders with higher powder bulk densities. In Chapter 3, it was pointed out that lower powder bulk densities for smaller particles (as produced in the lab-scale spray dryer) were likely to be the result of a faster solid-wall formation that hindered particle deflation, and this theory is also supported by the studies of Vehring (2008) and Wu et al. (2014). Another possible reason for the lower total bulk densities measured for the smaller particles might be their increased stickiness, as indicated by their more agglomerated powder structure (Figure 4.17, A). Those agglomerates may have been difficult to destroy during (tapped) powder bulk density measurement, and therefore could have contributed to a lowering of the bulk density.

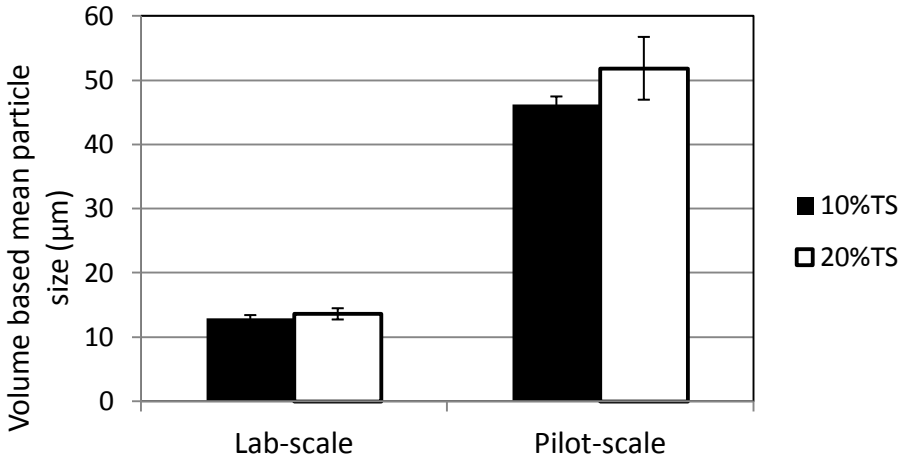

Figure 4.15: Effect of different spray drying scales and total solids on particle size of spray-dried lactose/Na-Cas=90/10 wt% powder.

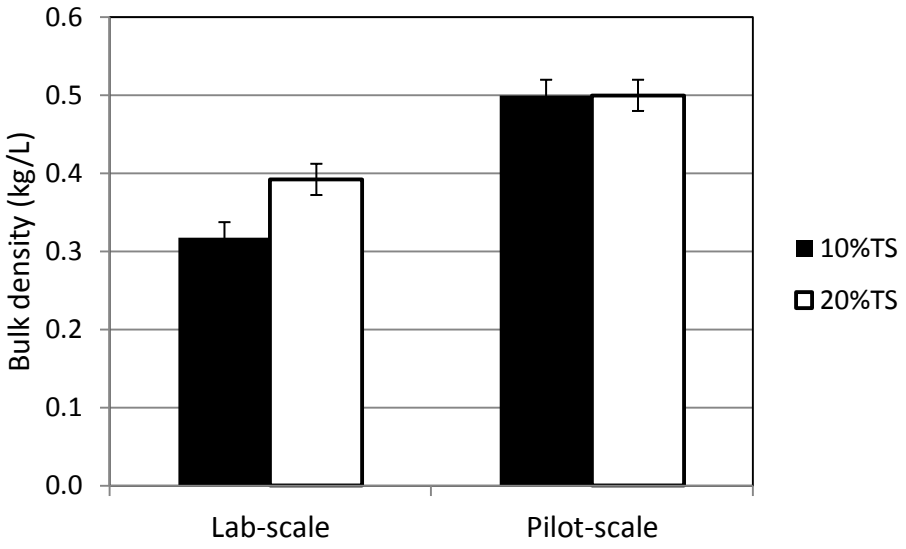

Figure 4.16: Effect of different spray drying scales and total solids on bulk density of spray-dried lactose/Na-Cas=90/10 wt% powder.

Figure 4.17 shows that both laboratory- and pilot-scale spray drying produced hollow particles with folded surfaces, most likely because of the presence of inner vacuoles. It is clear that the laboratory-scale spray-dried powder displayed a higher degree of surface folding. This was likely to be caused by a stronger initial particle inflation, resulting in a higher degree of subsequent crumpling of the particle wall when the particles moved into cooler regions of the spray dryer. This is consistent with its lower measured powder bulk density (Figure 4.16). Although fines were returned to the spray drying chamber during the pilot-scale run, no obvious powder agglomeration could be observed (Figure 4.17, B), probably because the droplets dried very fast, and therefore particle stickiness was not sufficient to allow the fines to adhere to the larger particles to form agglomerates.

A)

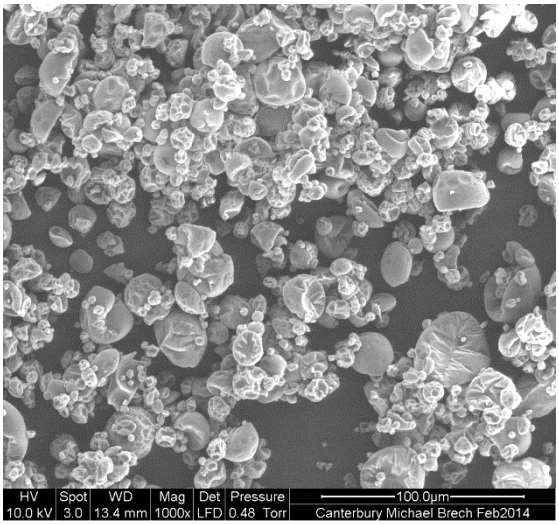

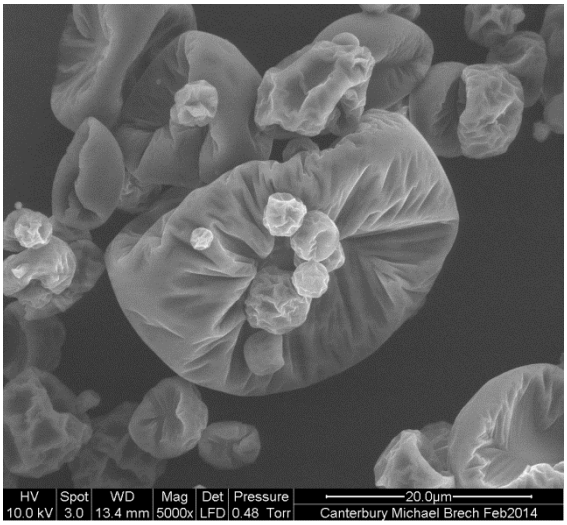

B)

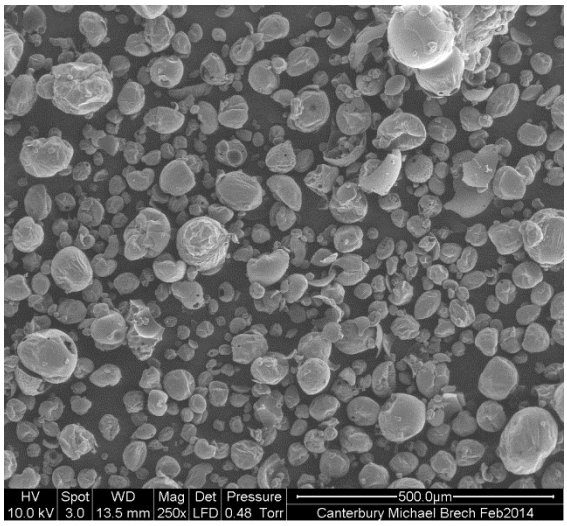

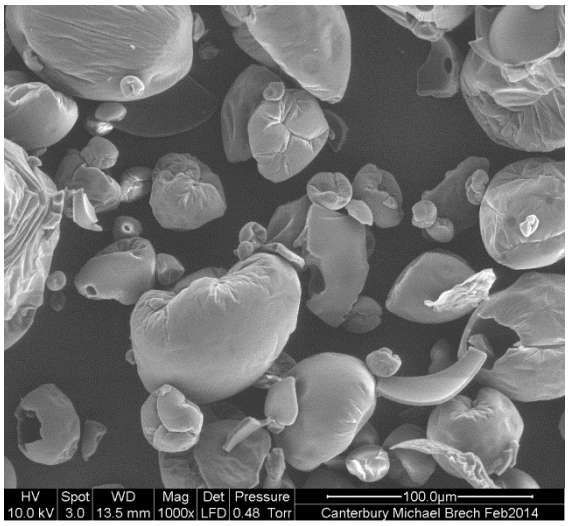

Figure 4.17: Effect of different spray drying on morphology of spray-dried lactose/Na-Cas powder (9/1% of total solids, 20wt% TS), prior to lactose crystallization (free-flowing powder). A) laboratory-scale spray-dried powder, magnification 1,000x (left), 5,000x (right). B) Pilot-scale spray-dried powder, magnification 250x (left), 1,000x (right).

Surface composition of spray-dried powders

Figure 4.18 shows the Na-Cas surface concentration of laboratory- and pilot-scale spray-dried lactose/Na-Cas (90/10%) powders at 10wt% and 20wt% total solids (TS). For both laboratory- and pilot-scale spray-dried powders, the protein surface concentration decreased with increasing TS. This agrees with the data given in Chapter 3 (Figure 3.11), which shows that lower protein surface concentrations were also found for lactose/Na-Cas (99/1 and 90/10 wt%) powders when the TS was increased from 5wt% to 20wt%. Compared to the particles produced by the laboratory-scale spray dryer, those produced by the pilot-scale dryer had lower protein surface concentrations (Figure 4.18). This occurred even though drying times

were longer for the larger droplets in the pilot-scale spray dryer, which means there was more time available for proteins to saturate their surfaces. This suggests that drying time is not the limiting factor affecting the surface concentration of proteins on the dried particulates, which agrees with the conclusion drawn in Chapter 3. In previous experiments (described in Chapter 3), it was found that altering the atomization pressure of the (laboratory) spray dryer did not produce any measurable difference in the final Na-Cas surface concentration, probably because the effect on particle size was too small. It is not clear why higher protein surface concentrations were found for the laboratory spray-dried powder than for the pilot-scale powder. Possibly the differences in droplet sizes and their relative degree of shrinkage may have affected solute segregation during drying. This requires further investigation.

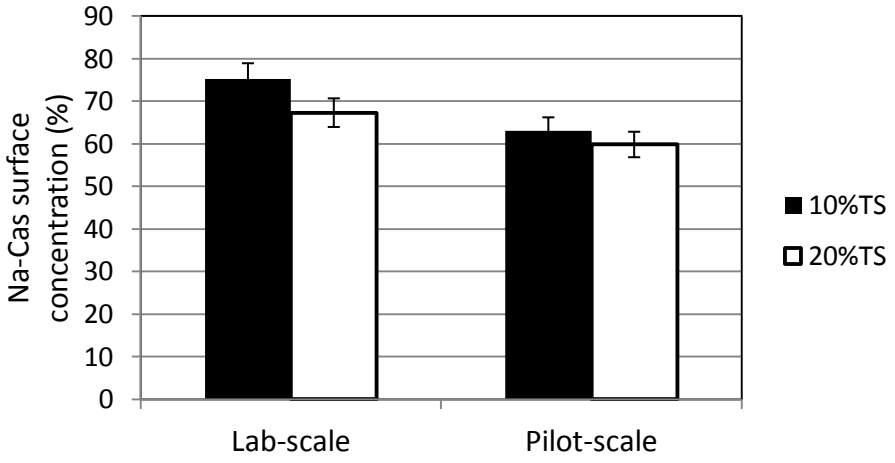

Figure 4.18: Effect of different spray drying scales and total solids on protein surface enrichment of spray-dried lactose/Na-Cas (90/10 wt%) powder.

Powder flowability

Powder flowability was significantly improved for pilot-scale powders compared with laboratory powders (Figure 4.19), most likely due to the larger particle sizes, which decreased particle stickiness by increasing the ratio of gravitational forces to attractive van-der-waals (vdw) forces (Tomas, 2004). This is supported by Figure 4.17 (B), which shows significantly larger and less agglomerated particles for pilot-scale spray-dried powders. Increasing the TS of aqueous lactose/Na-Cas solutions spray-dried in a laboratory spray dryer resulted in an improvement in powder flowability, perhaps because the particles were slightly larger and had a higher average density (Figure 4.15 and 4.16). Powder flows for the pilot-scale spray-

dried powders (with 10 or 20 wt% TS) appeared to be the same at 100%; the limitations of the measuring device meant that any difference was unable to be detected.

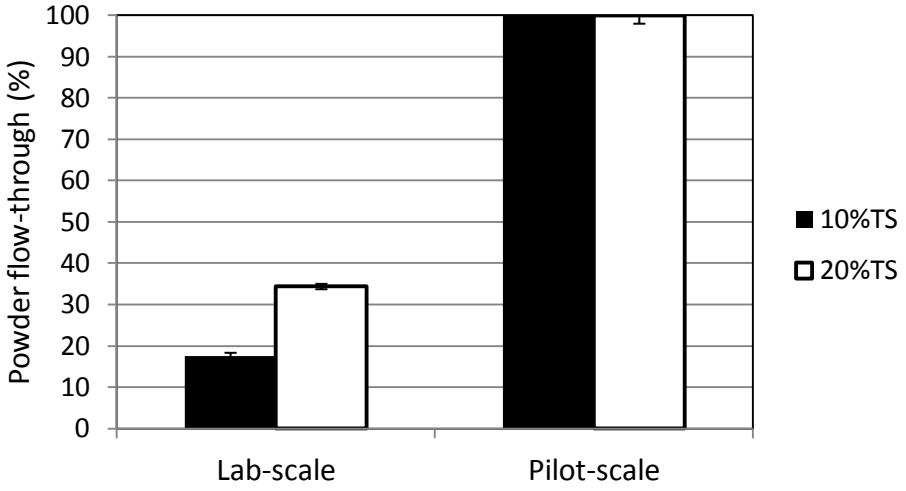

Figure 4.19: Effect of different spray drying scales and total solids on powder flowability of spray-dried lactose/Na-Cas (90/10 wt%) powder.

Powder wettability

Figure 4.20 shows the wetting times of spray-dried powders. While laboratory spray-dried powders needed approximately 3.4 minutes for 10 wt% TS and 3.1 minutes for 20 wt% TS solutions to be completely wetted, the wetting of pilot-scale powders occurred instantly (< 1s). Although the lower protein surface concentrations of pilot-scale spray-dried powders could have caused them to wet faster (due to the higher amount of the more polar lactose on the surface of the particles), this alone is unlikely to have been responsible for the extremely fast wetting of the powders. More likely, the higher bulk density of pilot-scale powders (Figure 4.16) caused their particles to sink beneath the water surface faster compared with the smaller, less-dense laboratory-scale powders. Higher TS contents decreased the wetting time of laboratory-scale powders, although the difference is slight when experimental uncertainty is considered. Decreased wetting times for increasing TS were also measured for laboratory spray-dried lactose/Na-Cas (99/1 and 90/10%) powders (see Chapter 3, Table 3.5). Powders with higher TS have higher powder bulk densities (Figure 4.16) and/or lower protein concentrations on the particle surface (Figure 4.18), which aids wetting .

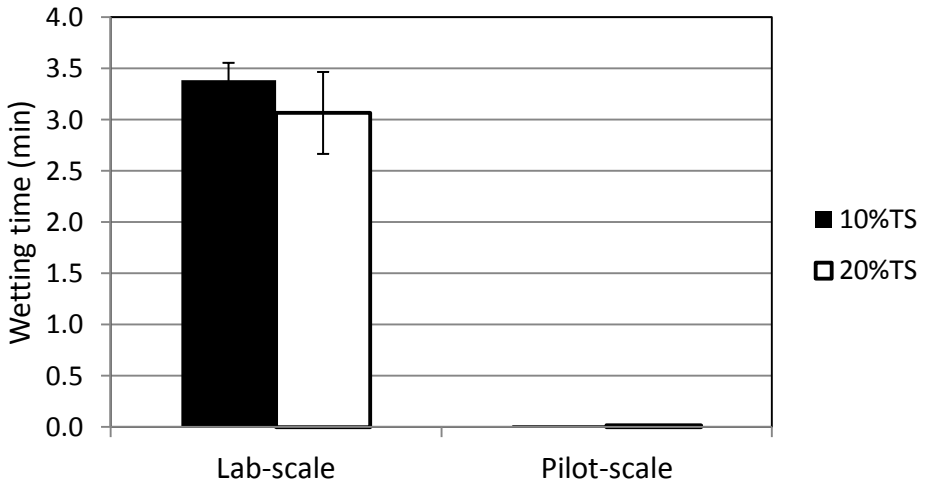

Figure 4.20: Effect of different spray drying scales and total solids on wetting time of spray-dried lactose/Na-Cas=90/10 wt% powder.

Lactose crystallization and powder caking

Figure 4.21 and Figure 4.22 show the crystalline powder structures of the laboratory-scale and pilot-scale spray-dried powders. The SEM pictures were taken after the powders were left unprotected for a week to allow moisture absorption from the environment and subsequent lactose crystallization. In both laboratory- and pilot-scale powders, neighbouring particles were joined by solid bridges, which were responsible for the transformation from an initially flowable powder into a hard, brittle cake. However, the crystalline structures differed, depending on whether the powder was obtained from the small-scale or large-scale process. While the laboratory-scale crystallized powder showed larger crystals and an overall coarser texture, crystals on the surfaces of the pilot-scale powders were significantly smaller and finer, and seemed to have sharper edges. Those differences become obvious when comparing the crystalline structure at the same magnifications.

The reasons for the powders having different crystalline lactose structures are not completely clear. Higher protein/lactose ratios on the surface of laboratory spray-dried powders might have delayed lactose crystallization due to a higher overall glass transition temperature at the particulate surface. On the other hand, moisture sorption was probably accelerated for the laboratory-scale powder due to its smaller particles and therefore higher total surface area. Crystals might thus have grown at different crystallization rates for the two different powders, which would account for their different sizes and shapes. This is supported

by Listiohadi et al. (2005), who showed the effect of crystal growth velocity on α-lactose monohydrate crystals, which took a variety of shapes, ranging from prism form for very high velocity growth to diamond-shaped, pyramid and tomahawk forms for slower crystal growth.

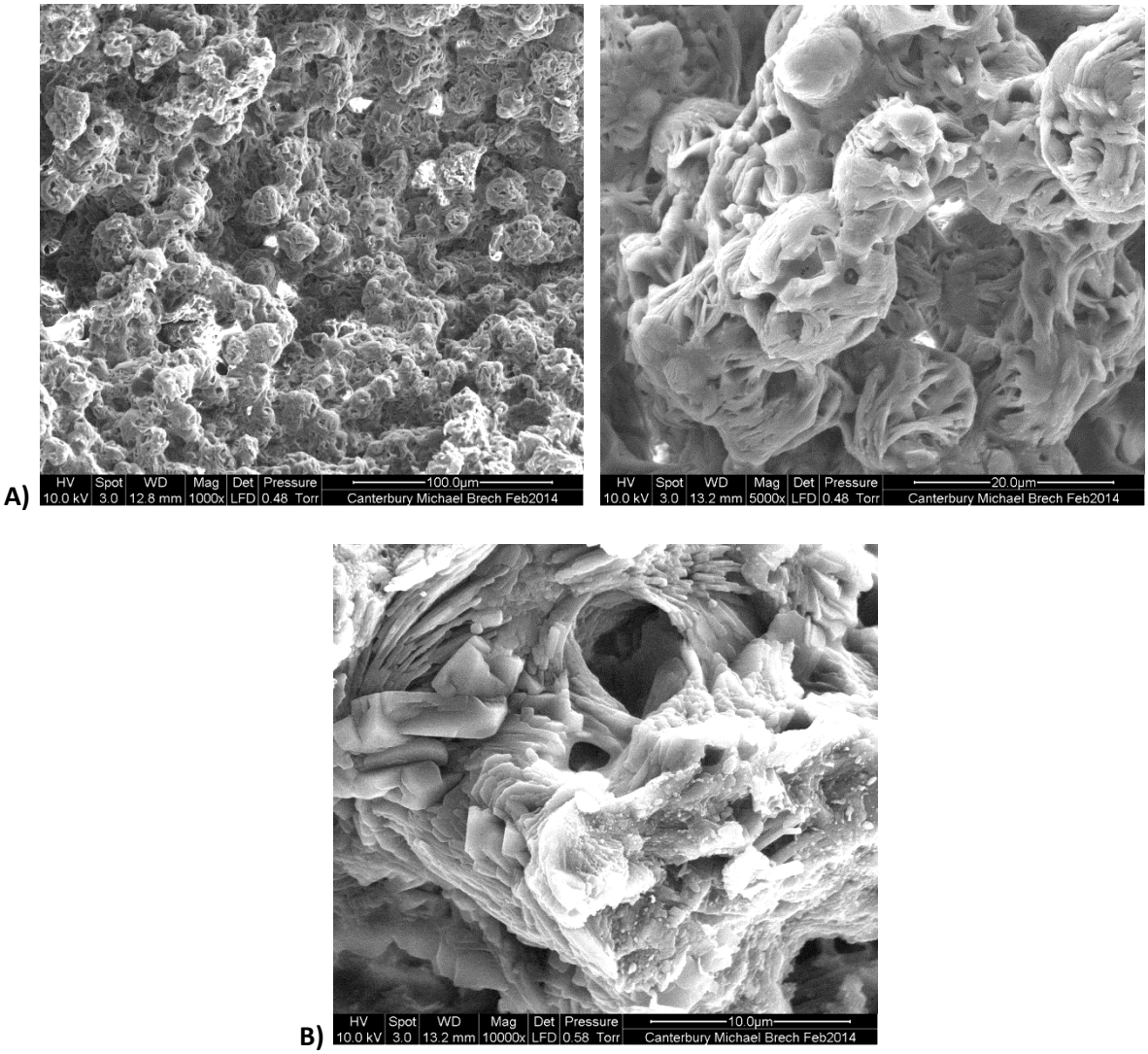

Figure 4.21: Effect of different spray drying on morphology of laboratory spray-dried lactose/Na-Cas powder (9/1% of total solids, 20wt% TS), after lactose crystallization (powder cake). Magnifications: A, left: 1,000x, A, right: 5,000x, B: 10,000x.

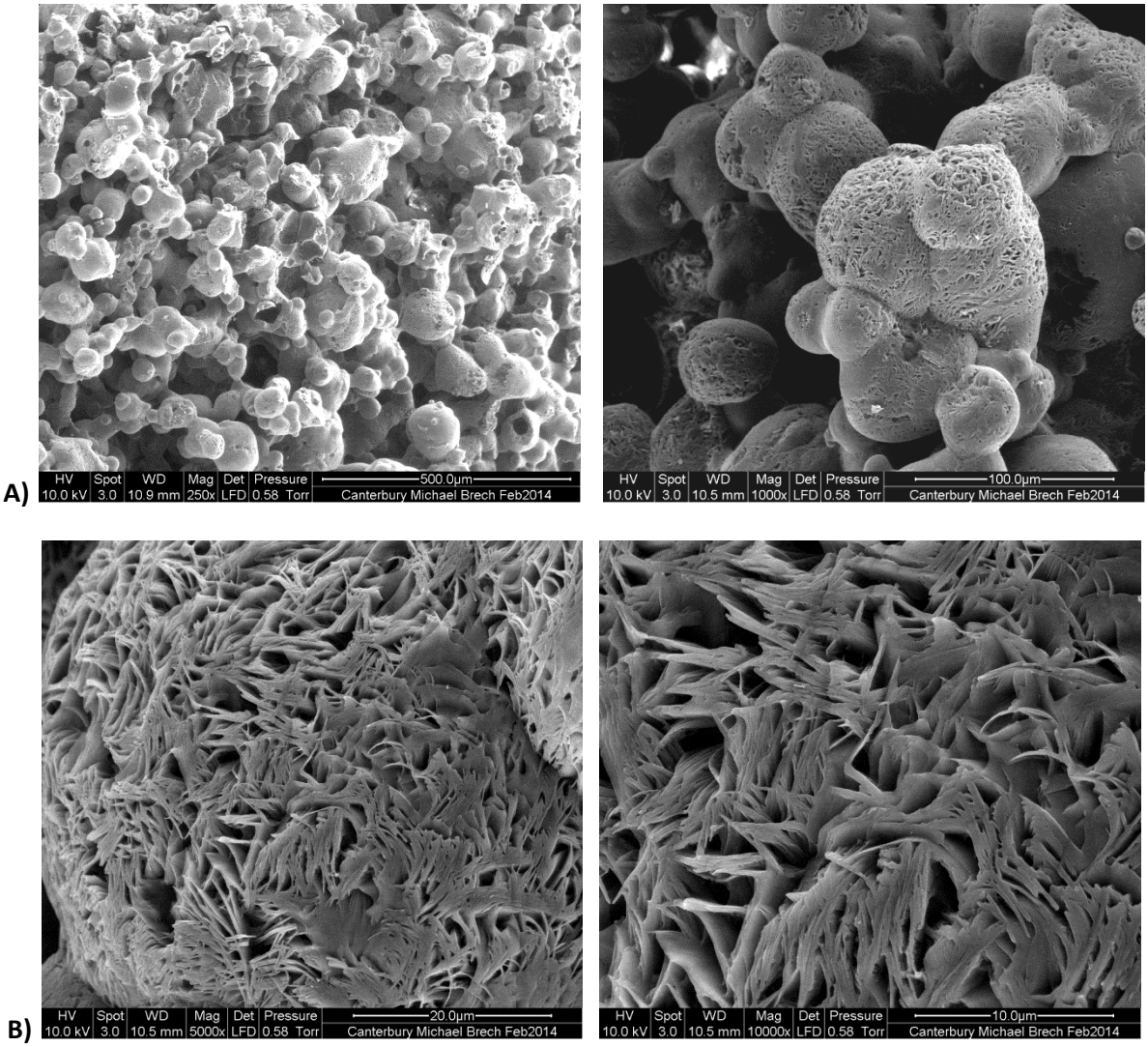

Figure 4.22: Effect of different spray drying on morphology of pilot-scale spray-dried lactose/Na-Cas powder (9/1% of total solids, 20wt% TS), after lactose crystallization (powder cake). Magnifications: A, left: 250x, A, right: 1,000x, B, left: 5,000x, B, right: 10,000x.

Summary of scale-up applicability

Aqueous solutions of higher TS are favoured for spray drying because the feed volume, the spray drying time and the energy required for water removal are reduced. This preliminary investigation used lactose/Na-Cas solutions of very low TS (10 and 20wt%), but TS ideally needs to be increased to 30 to 50 wt% in order to make the spray coating process more cost-efficient and to further improve powder functional properties such as powder flow and wettabilty. However, since protein accumulation at the droplet surface during drying was reduced with higher TS, achieving an efficient coating of the particles during spray drying

(*in-situ* coating) would be limited if solutions with higher TS were used. To compensate for this, either the concentration of protein (or another additive) needs to be raised, or droplet sizes have to be reduced. The latter can have a negative impact on powder flowability due to smaller particles being produced. Thus, process parameters have to be chosen very carefully when a product with a high surface concentration of coating material as well as superior powder functional properties is desired. Production on a smaller-scale is generally recommended for high-value, coated powders, while a large-scale operation is recommended for the production of powders with improved functional properties.

In Chapter 5, other promising additives were explored, which may produce increased surface concentrations of the coating material for the pilot-scale spray-dried powder than Na-Cas could produce here.

4.5. CONCLUSION

PART A:

Moisture content gradients within drying thin aqueous lactose/Na-Cas films were calculated using the solute-fixed coordinate system model (Crank, 1979) and solving the resulting differential equation numerically using the finite difference method. Moisture content gradients in drying films were found to be higher at higher air drying temperatures due to a faster removal of water from the air-water surface. Surface analysis of films dried at various temperatures revealed that higher drying temperatures did not result in higher Na-Cas surface concentrations. This suggests either that moisture-content gradients have no effect on solute segregation, or that moisture-content gradients were insufficient to cause solute segregation during slow film-drying.

The surface compositions of the dried films were compared with those of spray-dried particles at various protein/lactose ratios, drying temperatures, TS contents and pH values. Compared to slow-dried films, spray-dried powders clearly had higher Na-Cas concentrations on their surfaces for protein bulk concentrations ≥5 wt%. This suggests the reduction of surface area that occurs during droplet drying (but not during film drying) was likely to cause an increase in the density of adsorbed protein films and sub-layers, which acted to exclude dissolved lactose from the surface. Moreover, the *Pe* number, which is larger than unity for Na-Cas during spray drying, has an effect on protein-lactose segregation which can also

contribute to higher total protein concentrations measured at the surface of spray-dried particles.

The drying air temperature did not significantly affect surface compositions of either films or spray-dried powders, while a lower TS content resulted in higher Na-Cas surface concentrations for spray-dried powders but not for dried films. A higher total shrinkage of droplets produced at lower TS might have caused more proteins to be packed at and beneath the droplet surface. A pH closer to the pI of the protein caused an increase in Na-Cas surface concentration for both spray-dried powder and dried films, although this trend was more pronounced for spray-dried powders. This indicates that proteins were likely to pack together more closely at a pH closer to the pI of the protein —at which point electrostatic repulsion between proteins is lowest—and thus excluded lactose from the surface.

PART B:

The protein surface concentrations of laboratory-scale spray-dried lactose/Na-Cas powders were compared with those of pilot-scale spray-dried powders. Laboratory-scale spray-dried powders showed clearly higher Na-Cas concentrations on their particulate surfaces, possibly due to differences in the initial droplet sizes, degree of shrinkage or drying times. The lower particle coating efficiency found with the larger-scale spray drying complicates the scale-up of the production of coated particles via a one-step spray drying process. However, powder functional properties were significantly improved for powders produced on a larger scale, because they have larger particles of higher average density. The total solid content did not noticeably affect the final powder properties of pilot-scale powders, while the powder functional properties of laboratory-scale spray-dried powders could be further improved by increasing TS.

5. INVESTIGATION OF VARIOUS (SURFACE-COMPETING) ADDITIVES AS COATING MATERIALS FOR SPRAY-DRIED LACTOSE

5.1. INTRODUCTION

Solute segregation during spray drying in the presence of fat or surface active materials such as proteins, surfactants and polymers can be exploited to encapsulate and thus protect aromas or active drugs in a process known as microencapsulation (Gibbs et al., 1999), as discussed in Section 2.3.6. A coating additive needs to enrich at the hydrophobic interface, so surface activity is important, but the additive also needs to form a stable protective film around the encapsulated material, or at the air-liquid interface, if it is to be suitable as a wall material. Thus, the binding properties of the adsorbed species at the interface play an important role in the formation of a stable protective barrier. In spray-dried sugar solutions such as lactose, this stable protective barrier can be essential in preventing a particulate structural collapse upon crystallization and preventing powder caking, as shown in Chapter 3 (Figure 3.16).

A number of researchers (Brash & Horbett, 1995; Dickinson et al., 1988; Euston et al., 1995; Gaiani et al., 2011; Jayasundera et al., 2010a; Landström et al., 2000; Landström et al., 2003) have studied competitive adsorption systems with different combinations of proteins and different combinations of proteins and surfactants, as discussed in detail in Section 2.3.4. During the spray drying of an aqueous solution containing more than one surface active solute, these solutes will compete for the freshly-formed droplet surface directly after atomization. This competitive adsorption may further improve powder properties because it may mean that two additives with different complementing and beneficial properties are present at the particulate surface.

Chapter 3 described how solute segregation was exploited during spray drying of aqueous lactose/Na-Cas and lactose/WPI solutions. The one-step spray drying process presented in that chapter aimed to coat the particle surface with surface active milk proteins in order to decrease particulate stickiness and thus increase powder yield, improve powder flow and delay lactose crystallization. Although powder yield and powder flow could be

improved by the addition of only small amounts of protein (1 wt% of total solids), significantly higher protein bulk concentrations (≥ 20 wt% of total solids) were required to form a protective coating at the particle surface that prevented powder caking. In practice, such high bulk concentrations of an additive within a food powder are often undesirable and expensive and should be therefore kept as low as possible. The investigation in the present chapter explores alternative edible coating materials not investigated in Chapter 3 to determine their ability to enrich on the droplet surface during spray drying and affect powder functional properties and powder caking. The aim is to find an additive that is effective as a coating at much lower bulk concentrations than required for the proteins tested in Chapter 3. A secondary aim of the present study is to determine how the surface competition between different surface actives species affects the final surface composition and functional properties of spray-dried powders.

Goal of this investigation:

Various coating additives were tested for their ability to 1) enrich on the droplet surface during drying and change particle properties, 2) delay or prevent lactose crystallization and caking, and 3) increase product yield and improve powder functional properties such as powder flow and wettability. These results are presented in Part A of the present chapter. The tested additives were gelatine, lecithin, anhydrous milk fat (AMF) and hydroxylpropyl methylcellulose (HPMC), and these additives were compared with Na-Cas (results taken from Chapter 3). Dynamic vapour sorption (DVS) analysis was performed on spray-dried coated powders to investigate whether the coating material acts as a possible moisture barrier, and to assess the degree to which lactose crystallization can be delayed. Scanning Electron Microscopy (SEM) was used to analyze the particulate structure before and after lactose crystallization in order to investigate the protective wall material properties of different additives. Caking tests were also performed in order to investigate whether the wall materials were capable of preventing the powder from caking.

In a further investigation, various combinations of surface active food molecules (Na-Cas, WPI, lecithin and HPMC) were added to aqueous lactose solutions before (fast) spray drying or slow film drying in order to investigate how they competed for the air-water interface in these two different drying systems. Through a comparison of the surface

composition of the spray-dried powders and slow-dried films, conclusions could be drawn about the importance of the Peclet number effect, proposed by Vehring (2008), and surface competition occurring within different drying systems. In addition, the effect of surface composition of spray-dried powders on particle size, powder bulk density, powder morphology, functional properties and powder caking could be determined. This knowledge may enable technologists to predict, control and adjust particle and thus powder properties. This may allow the tailoring of powder properties (for example to produce improved powder flow and/or wettability) in a way that cannot be realized with a single coating additive. The design (or "engineering") of particles with various unique properties may have useful applications in the food and pharmaceutical industries. These results are presented in Part B of the present chapter.

5.2. MATERIALS AND METHODS

Materials

Na-Cas (M_w ~ 24 kDa), WPI (M_w ~ 18 kDa), lecithin (M_w ~ 0.75 kDa) and AMF were supplied by Fonterra Research and Development Centre (Palmerston North, New Zealand). HPMC (M_w ~ 22 kDa), gelatine (M_w ~ 20-22 kDa) and α-Lactose monohydrate (M_w ~ 0.34 kDa) were supplied by Sigma Aldrich (Germany).

Solution preparation and spray drying

Solutions of aqueous lactose and an additive with dry weight ratio of 9:1 and total solids content of 10 wt% were prepared in distilled water. Firstly, lactose solutions were prepared at around 60°C under constant agitation. In order to prevent possible aggregation of additives, the pH of the lactose solutions was neutralized by adding aqueous NaOH solution and using a pH meter with temperature correction (CybersScan pH510, Eutech Instruments, Singapore) before the additives were added. The coating substance was dissolved by adding small amounts incrementally while constantly stirring to prevent clumping. Solutions were stirred during cooling down for up to 2 hours to enable complete dissolution and hydration of the coating materials. AMF was added to the lactose solutions in the form of an emulsion of 20 wt% solid content (95 wt% AMF, 5 wt% Na-caseinate) with a fat globule size distribution of 0.2 to 2 micron and a mean volume based globule size of 1.0 micron, previously prepared by

a pilot plant homogenizer (2-step: 3000 over 1000 psi, T=60 °C at Riddet Institute, Massey University, Palmerston North, NZ).

For the competitive adsorption study (Part B), solutions of lactose and the two additives with dry weight ratios of 99:0.5:0.5, 95:2.5:2.5 and 90:5:5 and total solids of 10 wt% were prepared, according to the same method, described above. All solutions were spray-dried in a laboratory spray dryer (*NIRO Atomizer,* Copenhagen, Denmark), described in Chapter 3 (Figure 3.1), at an air flow of 105±5 m^3 h^{-1}, inlet/outlet temperatures of 160/75±1 °C, atomization pressure of 0.6 bar, and solution feed rate and temperature of 1.6±0.2 kg h^{-1} and 40±1 °C, respectively. Three repeats were performed for each type of powder to obtain an estimate of uncertainty for the different powder analyzes.

Analysis

Surface tension measurements and X-ray photoelectron spectroscopy (XPS) were used according to the method described in Chapter 3. The following elemental compositions of the pure powders were measured by XPS: lactose - carbon (57.6%) and oxygen (42.4%); Na-Cas - carbon (71.2%), nitrogen (13.8%) and oxygen (14.8%); WPI - carbon (70.5%), nitrogen (12.6%) and oxygen (16.8%); lecithin - carbon (81.5%), nitrogen (1.2%) and oxygen (16.3%); AMF - carbon (90.8%) and oxygen (9.2%); HPMC - carbon (67.3%) and oxygen (32.7%); gelatine - carbon (74.3%), nitrogen (10.9%) and oxygen (14.7%).

Powder flowability, powder bulk density, wettability and particle size distribution were measured according to the methodology described in Chapter 3. Three repeat runs were performed to obtain an estimate of uncertainty. Powder hygroscopicity and lactose crystallization were measured by using dynamic vapour sorption (Vapour Sorption Analyzer, AquaLab, Decanon), also described in Chapter 3. Film drying was performed according to the method described in Chapter 4. Viscosity measurements of all solutions were performed prior to spray drying using a Brookfield DV-E viscometer (Middleboro, USA) at 100 rpm (spindle 61) at a constant temperature of 21±1 °C.

A Scanning Electron Microscope (SEM) was used (XL30S FEG, Philips, Netherlands) to capture images of the different powders before and after they were stored at ambient conditions for one week to allow lactose to crystallize. Powders were sprinkled onto double

sided tape on a carbon tab with surplus powder being blown off using a nitrogen duster. Samples were then coated in a Q150RS sputter coater with platinum as target at 1.2kV and 20 mA, which gave a coating thickness of approximately 5-20 nm. The images were captured at magnifications of 10,000, 5,000, 1,000 and 250, using random sampling in the best area. Three to five random samples were taken from each specimen.

5.3. Results and Discussion

5.3.1. Part A: Surface enrichment of various coating materials during spray drying

Surface accumulation of spray-dried coating additives

Figure 5.1 shows that all tested additives dominated the surface of spray-dried lactose/additive particles, despite the additive concentration only being 10% of the dry weight. For comparison, the surface concentrations of AMF, Na-Cas, gelatine, lecithin, and HPMC were 64%, 70%, 72%, 73%, and 90%, respectively (Brech et al., 2013). This demonstrates the ability of these materials to accumulate and adsorb on the droplet surface at the expense of lactose during the short time-frame of spray drying, as also found in other studies (Elversson & Millqvist-Fureby, 2006; Fäldt & Bergenståhl, 1994, 1995; Kim et al., 2009a; Millqvist-Fureby & Smith, 2007; Nijdam & Langrish, 2006; Wang & Langrish, 2010). With the exception of AMF, a significant driving force for this accumulation and adsorption is likely to be the surface activity of the tested additives (Elversson & Millqvist-Fureby, 2006; Fäldt & Bergenståhl, 1994; Millqvist-Fureby & Smith, 2007; Nijdam & Langrish, 2006; Wang & Langrish, 2010). The maximum packing densities of the adsorbed species depends on the charge, structure, flexibility and rearrangement of the molecule at the surface (Graham & Phillips, 1979b, 1979c; Norde, 1992). Other authors reported that effects such as moisture content gradients and a Peclet number effect can also contribute to solute segregation phenomena during spray drying (Kim et al., 2009b; Vehring, 2008). Thus, solute diffusion within the drying droplet can also have an effect on the preferential surface accumulation of solutes, with the diffusion rate dependant on the molecular size of the solute and the solution viscosity (Kim et al., 2009a). There is currently no conclusive evidence in the literature regarding which of these physical mechanisms dominates surface enrichment.

Various mechanisms of fat enrichment on the droplet surface during drying have been proposed, as discussed in Section 2.3.4. Fäldt and Bergenståhl (1995) state that fat may leak

out of the fat globules due to increasing emulsion instability when fat globules within a droplet approach each other as the drying droplet shrinks. Kim et al. (2009b) suggest that larger fat globules are preferentially present at the surface of emulsion droplets when leaving the atomization device and are disrupted during atomization, thus appear in high concentrations as free fat on the surface of emulsion droplets.

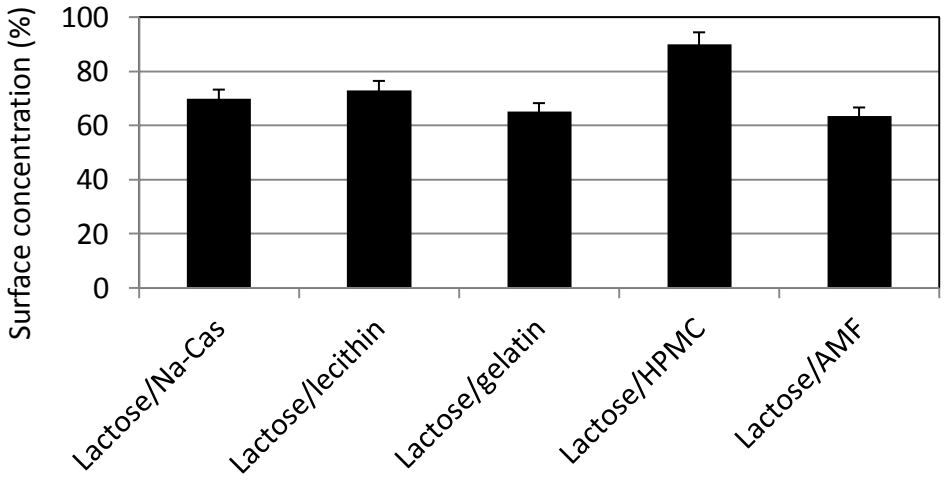

Figure 5.1: Surface composition of different spray-dried lactose/additive powders (90/10 dry wt%).

The viscosity of all solutions was measured prior to spray drying at 100 rpm shear rate and 21 ±1°C air temperature, and the results were as follows: 3.9cp for lactose/Na-Cas, 4.5cp for lactose/lecithin, 5.5cp for lactose/gelatine, 3.3cp for lactose/AMF and 20.7cp for lactose/HPMC. Lactose/HPMC had a significantly higher solution viscosity than the other solutions due to the water holding and viscosity enhancing properties of HPMC (Arboleya & Wilde, 2005). Thus, the rate of diffusion of HPMC molecules towards the air-water interface would have been slower than that of the other additives. However, the high surface concentration measured for HPMC molecules (Figure 5.1) indicates there was still sufficient time for HPMC to diffuse to the droplet surface and adsorb there. This suggests that, in a system with lactose and one other solute, diffusion is not a limiting factor on the final surface composition of the spray-dried particles.

The following surface tensions of the aqueous solutions (1 wt% additive in solution) prior to spray drying were measured (Brech et al., 2013): 63.2±0.9 mNm^{-1} for lactose/gelatine, 56.2±0.9 mNm^{-1} for lactose/lecithin, 53±3 mNm^{-1} for lactose/AMF and 51.3±0.7 mNm^{-1} for lactose/Na-Cas and 49.2±0.8 mNm^{-1} for lactose/HPMC. The surface tension of pure water was 72.5±0.4 mNm^{-1}, which shows that the additives reduced surface

tension and were therefore present at the air-water surface during drying (Fäldt & Bergenståhl, 1994; Graham & Phillips, 1979a). HPMC reduced surface tension more than the other additives due to its higher surface activity. The surface tension data for HPMC and Na-Cas are consistent with the data from other authors, who measured surface tensions of between 46 and 48 mN m^{-1} for 1 wt% HPMC solutions (Arboleya & Wilde, 2005; Elversson & Millqvist-Fureby, 2006) and 50 to 52 mN m^{-1} for 1 wt% β-casein solutions (Arboleya & Wilde, 2005). This correlates well with the relatively high surface concentration of HPMC compared with the surface concentrations of the other additives (Figure 5.1). The higher surface enrichment of this highly flexible polymer may have also been caused by its higher compressibility, resulting in a higher packing density at the droplet surface. Muñoz et al. (2000) reported that the long flexible polymer chains can straighten up to form a "brush formation" upon increasing surface pressure, with most of the long polymer chains pointing into the solvent phase; this may have increased the film thickness and allowed more polymers to occupy the surface at a higher density.

Spray dryer yield, particle size distribution and powder bulk density

The spray dryer yield increased considerably when using the additives Na-Cas, lecithin, or gelatine, while AMF resulted in poor yields compared with pure lactose (Figure 5.2). Due to lactose having a relatively small molecular size (molecular weight approximately 0.34 kDa), its glass transition temperature is lower than those of the additives Na-Cas, lecithin and gelatine, which have molecular weights ranging from 0.75 kDa to 24 kDa. Roos and Karel (1991b) showed a trend of increasing glass transition temperature with increasing molecular weight of a food polymer, as pointed out in Chapter 3. Hence, the enrichment of longer-chain molecules on the surface of a droplet containing a relatively small molecule such as lactose increases the overall glass transition temperature there and thus reduces particle stickiness, as shown previously for Na-Cas in Chapter 3 (Part B). This results in higher spray dryer yields compared with pure lactose, as also found by Wang and Langrish (2010) and Adhikari et al. (2009a).

AMF was an exception due to its low fat melting temperatures (ranging from -40 to +40 °C (Kim et al., 2005a)) and hence sticky nature, thus fat on the surface of spray-dried lactose particles reduced the yield considerably. Lactose powder with HPMC had lower spray dryer yields than lactose powders with Na-Cas, gelatine and lecithin. HPMC (~22 kDa) has a

similar molecular weight to Na-Cas (~24 kDa) and gelatine (~20-22 kDa), which implies it has similar glass transition temperature to those additives and should therefore reduce surface stickiness with equal effectiveness. However, due to the lower measured bulk density of lactose/HPMC powder compared with the other powders (Figure 5.3), the particles may have been too light to be efficiently separated by the cyclone of the spray dryer, which would account for its product yields being lower than those of the denser lactose/lecithin, lactose/Na-Cas and lactose/ gelatine powders. This demonstrates that spray dryer yield in this work is affected not only by the stickiness of the particles, but also by the effect of particulate density on the efficiency of the spray dryer cyclone.

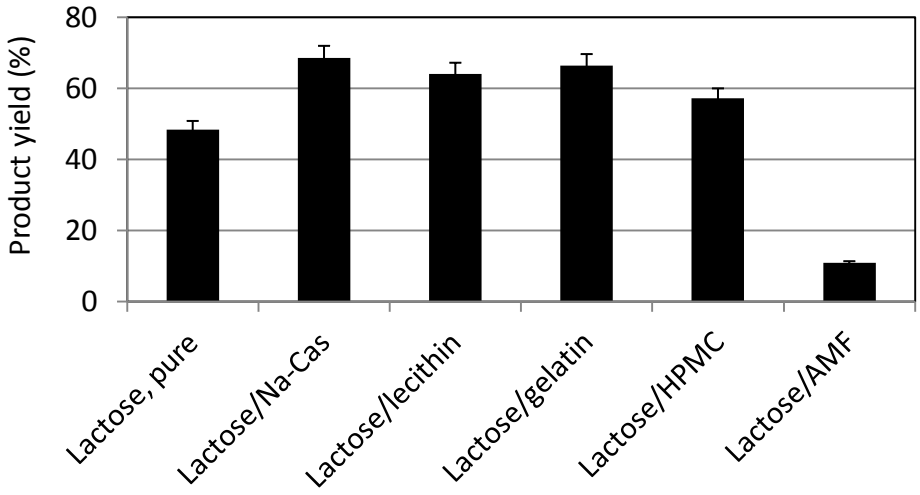

Figure 5.2: Effect of different coating additives (10 wt% of total solid content) on the spray dryer yield.

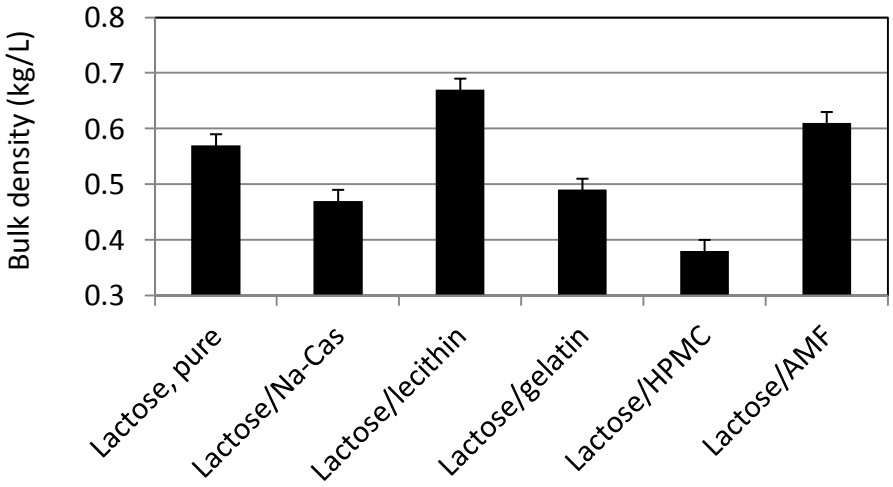

Figure 5.3: Effect of different coating additives (10 wt% of total solid content) on bulk density.

The variation in bulk density with the addition of different additives can be explained by the flexibility of adsorbed molecules at the particle surface, which changes the visco-elasticity of the particle wall (Dickinson, 1999). As discussed in Chapter 3 (Part B), Dickinson (1999, 2001, 2003) showed that the presence of flexible proteins such as caseins, and polymers such as HPMC, cause the formation of an elastic film on the air-water interface. HPMC in particular provides significant film elasticity due to its long, highly flexible molecular structure (Elversson & Millqvist-Fureby, 2006), and therefore HPMC-coated lactose powder has significantly larger particles with lower bulk density than do other powders (Figure 5.3 and Figure 5.4). This increased elasticity allows more expansion of particulates when vapour vacuoles form inside the particles during drying, as also shown in Chapter 3 (Part B). The same conclusions can be drawn for Na-Cas and gelatine, and explains the differences in particle size and bulk density of lactose powders that contain these additives compared with powders that contain non-flexible molecules such as lecithin or fatty acids (in AMF) on their particle surfaces (Figure 5.3 and Figure 5.4). Millqvist-Fureby and Smith (2007) measured a reduction in particle size (compared with pure lactose) when lecithin was used as an additive, whereas our study showed an increase in particle size (see Figure 5.4), despite an increase in bulk density (see Figure 5.3). However, this anomalous result may have been due to the lecithin/lactose particles forming strong agglomerates, which may have impeded accurate measurement of particle size. These agglomerates can be seen in SEM photographs (Figure 5.5 C).

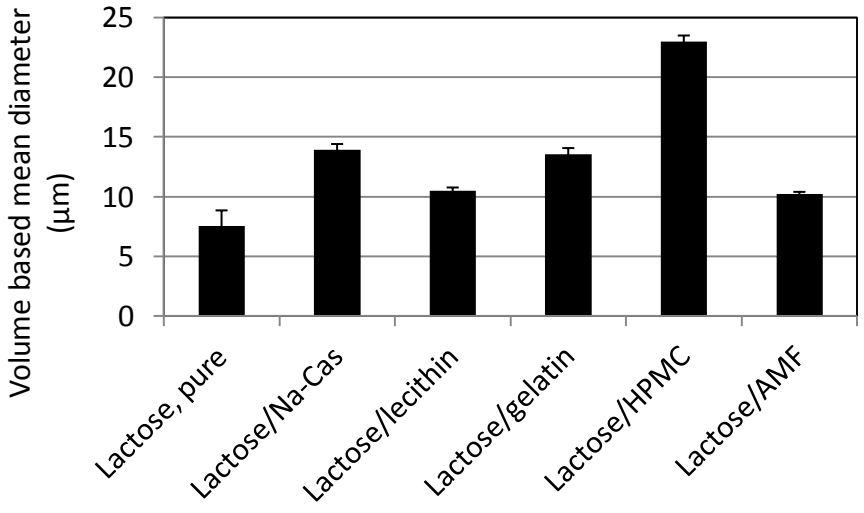

Figure 5.4: Effect of different coating additives (10 wt% of total solid content) on volume based mean diameter.

Powder morphology

Figure 5.5 shows the effect of the additives on the particle morphology. Pure spray-dried lactose formed smooth spherical particles (Figure 5.5 A), while the addition of Na-Cas, gelatine and HPMC resulted in folded particle surfaces (Figure 5.5 B, D, E). These results are consistent with previous research on the morphology of lactose particles that contain long flexible molecules, such as caseins or HPMC, which increase the elasticity of the particle wall (Elversson & Millqvist-Fureby, 2006; Nijdam & Langrish, 2006; Wang & Langrish, 2010). As discussed in Chapter 3 (Part B), particle-wall elasticity allows more expansion of internal-vacuole-containing particulates in the hotter regions of the spray dryer and deflation of these particulates and folding of their surfaces in cooler regions of the dryer (Nijdam & Langrish, 2006).

The folding of the particle surface was most clearly seen with HPMC and gelatine. The higher elasticities of HPMC- and gelatine-containing films may account for this finding, as both molecules are known for their ability to cross-link and form gel networks (Bigi et al., 2001; Bodvik et al., 2010; Dickinson, 2003). However, the bulk densities of lactose/gelatine and lactose/Na-Cas powders were the same within uncertainties (Figure 5.3), while lactose/HPMC powder had a significantly lower bulk density (Figure 5.3) and larger particles (Figure 5.4), which suggests that HPMC-containing films caused the highest wall elasticity of the additives tested, most likely due to the more flexible structure of this polymer. AMF caused significant agglomeration of the spray-dried particles due to the high degree of stickiness of fat (Figure 5.5 F). Using lecithin as additive resulted in spherical particles similar in appearance to the pure lactose particles (compare Figure 5.5 A+C), although for reasons that are not clear, the lactose/lecithin powder appeared to agglomerate more. Nevertheless, the lack of folding on the particulate surfaces of both the lactose/lecithin and pure lactose powders indicates that lecithin did not increase the elasticity of the particle wall in the way that HPMC, gelatine and Na-Cas did, most likely due to its smaller molecular size and lack of flexibility. This agrees well with the findings of Millqvist-Fureby and Smith (2007) as well as Elversson and Millqvist-Fureby (2006), who report a "less cohesive" film was produced when low-molecular-weight surfactants occupy the particulate surface, which results in smooth, spherical particles.

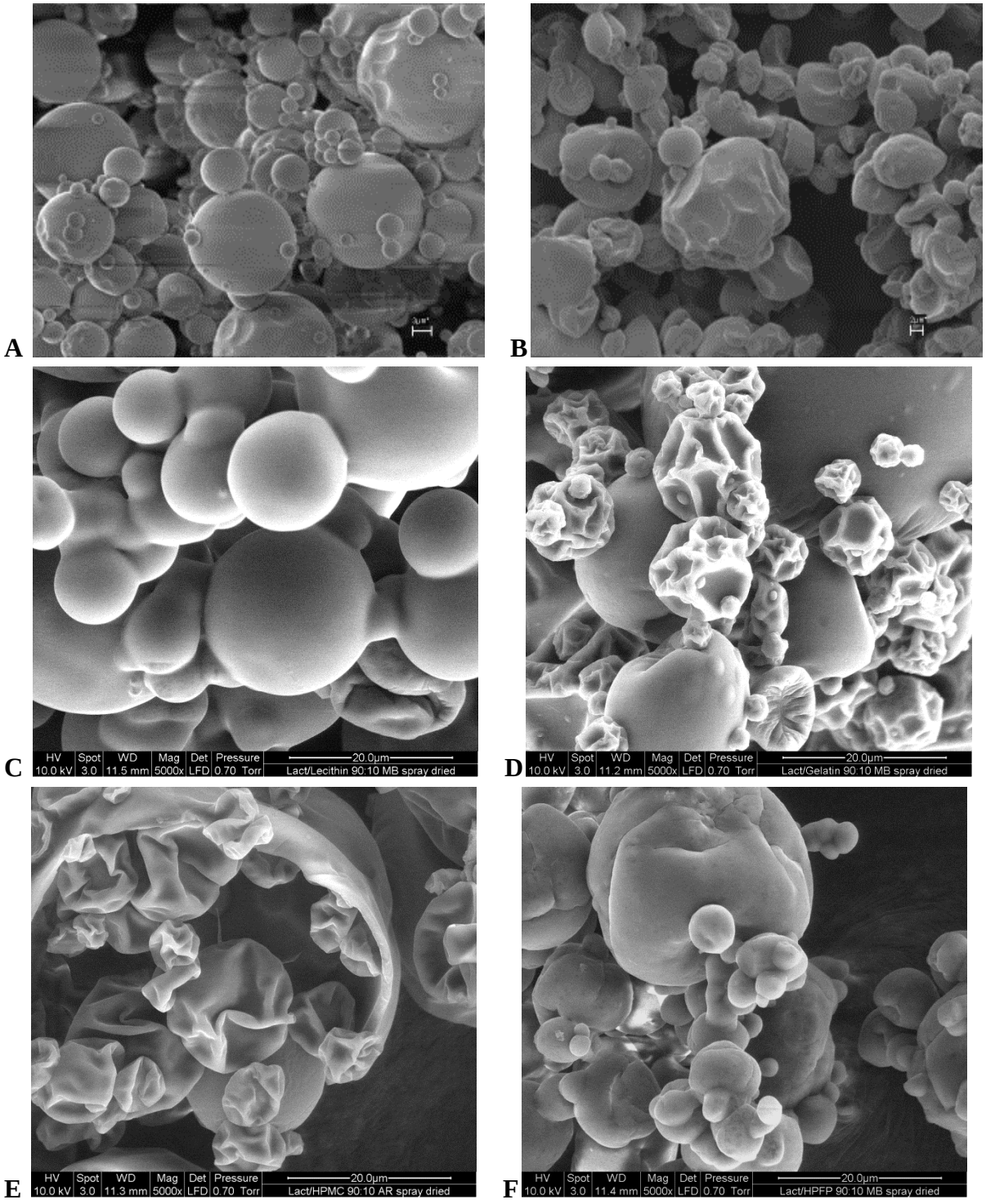

Figure 5.5: SEM photographs (5,000 magnification). Effect of different coating additives (10 wt% of total solid content) on the particle morphology: A) Pure lactose; B) lactose/Na-Cas; C) lactose/lecithin; D) lactose/gelatine; E) lactose/HPMC; F) lactose/AMF.

Powder flowability / stickiness

Figure 5.6 shows the powder flows of the different spray-dried powders. Using Na-Cas, HPMC and gelatine as additives increased the powder flow significantly compared with pure lactose, due to the increase in glass transition temperature of the particulate surface and a resultant reduction in agglomeration of particulates. This agrees with the findings of the study reported in Chapter 3 (Figure 3.21), where a linear relation between the protein surface concentration and the powder flow was seen. The larger size of individual particles in these powders compared with pure lactose powder, as seen in Figure 5.4, may have further aided the reduction of powder agglomeration and consequent improvement in powder flow. The best powder flows were measured for lactose/HPMC and lactose/Na-Cas powders. Why their flowability was higher than that of lactose/gelatine powder is not completely clear, given the similar molecular sizes and thus glass transition temperatures of these additives (Na-Cas M_w ~ 24 kDa; HPMC M_w ~ 22 kDa; gelatine M_w ~ 20-22 kDa). One explanation could be the larger measured size of lactose/HPMC particulates compared with lactose/gelatine particulates (Figure 5.6). In addition, the surface of the lactose/gelatine particulates was much more crumpled than the lactose/Na-Cas particulates (Figure 5.5). The increased surface folding may have increased friction between the particles and reduced the powder flowability for lactose/gelatine powder compared with lactose/Na-Cas powder, which had a comparable particle size.

Unlike gelatine, Na-Cas and HPMC, lecithin did not significantly improve powder flow, perhaps due to its relatively low glass transition temperature, which might explain the more agglomerated state observed for the lactose/lecithin powder (Figure 5.5 C). The smaller particulate size of lactose/lecithin powder compared with lactose/Na-Cas, lactose/HPMC and lactose/gelatine powders would also contribute to its stronger agglomeration and therefore its lower powder flow. An AMF coating did not result in any improvement in the powder flowability due to the stickiness of fat and hence highly agglomerated nature of the powder. This finding agrees well with the low product yield measured for AMF-coated powder (Figure 5.2).

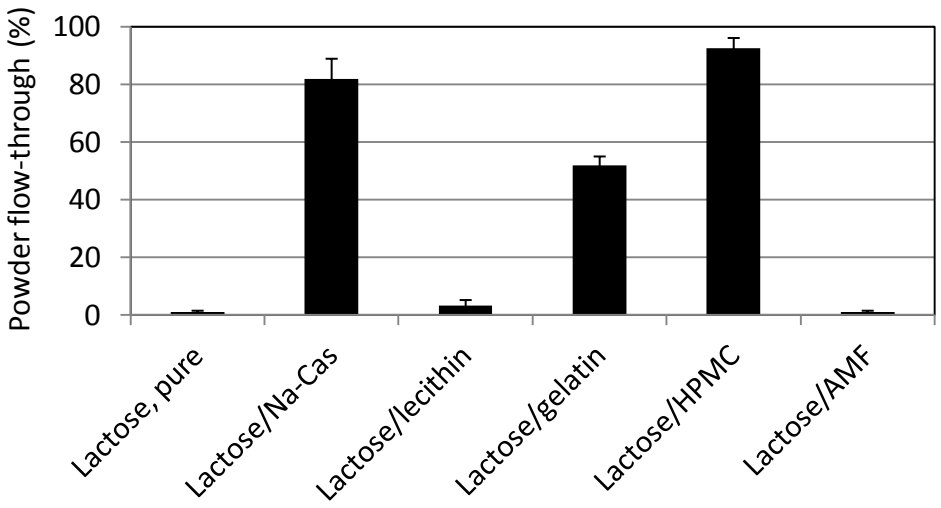

Figure 5.6: Effect of different coating additives (10 wt% of total solid content) on powder flow through a vibrating sieve.

Wetting time

Figure 5.7 shows the wetting times of the different powders at a water temperature of 50°C. Since amorphous lactose is a very hygroscopic, polar molecule, it wetted instantly upon exposure to the water surface. A similar observation was made when using lecithin as an additive. Lecithin is also used as coating additive for milk powders to improve their wettability (Millqvist-Fureby & Smith, 2007). All other additives caused an increase in wetting time. As also discussed in Chapter 3 (Part B), possible reasons for this could be the relatively high buoyancy of the larger particles of lower density; this may particularly be the case for the lactose/HPMC powder, which showed a wetting time significantly longer than that of the other powders. In addition, the adsorbed species would be expected to change the hydrophilic surface of the amorphous lactose to a more hydrophobic surface, considering that proteins, surfactants and surface active polymers such as HPMC tend to orientate their hydrophobic parts towards the air-phase upon adsorption, depending on their flexibility and the distribution of hydrophilic and hydrophobic residues along their chain length (Arboleya & Wilde, 2005; Graham & Phillips, 1979a).

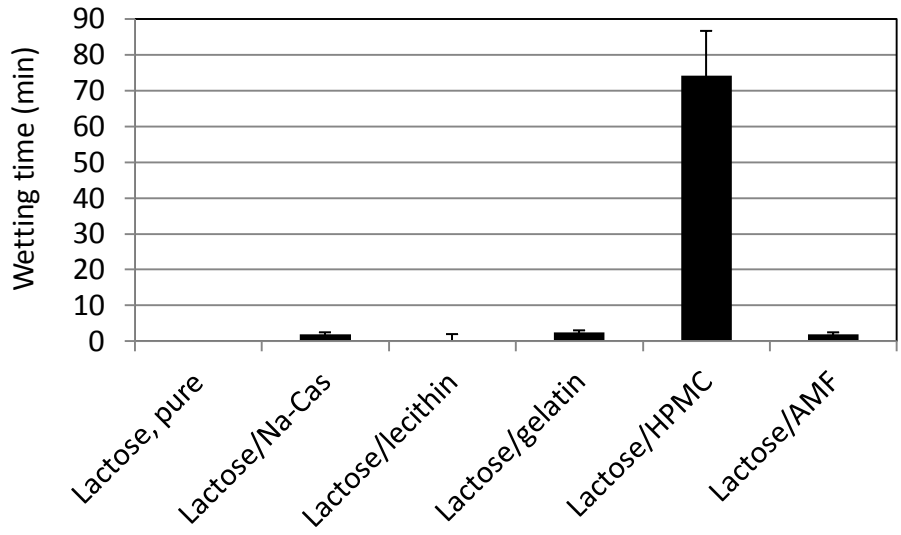

Figure 5.7: Effect of different coating additives (10 wt% of total solid content) on the wetting time of the powder.

Moisture sorption and lactose crystallization

Dynamic vapour sorption measurements were performed in order to investigate the ability of the coating additives to act as a moisture barrier and to delay lactose crystallization (Figure 5.8). Pure amorphous lactose powder started to crystallize at a relative humidity (RH) of between 44 and 46% and a dry water content of approximately 8.5 to 9 % of dry weight. The very small moisture loss observed at 44% RH indicates that lactose crystallization may have been already initiated at the 44% RH, although moisture loss was more pronounced at 46% RH. Increasing the RH to 48±2% resulted in a sudden complete loss of the moisture due to an increase in the lactose crystallization rate. This is consistent with the results of Haque and Roos (2004a), who also measured lactose crystallization of a pure amorphous lactose powder at RH ≥ 44% and water contents of between 9 and 10% dry weight.

A) Lactose

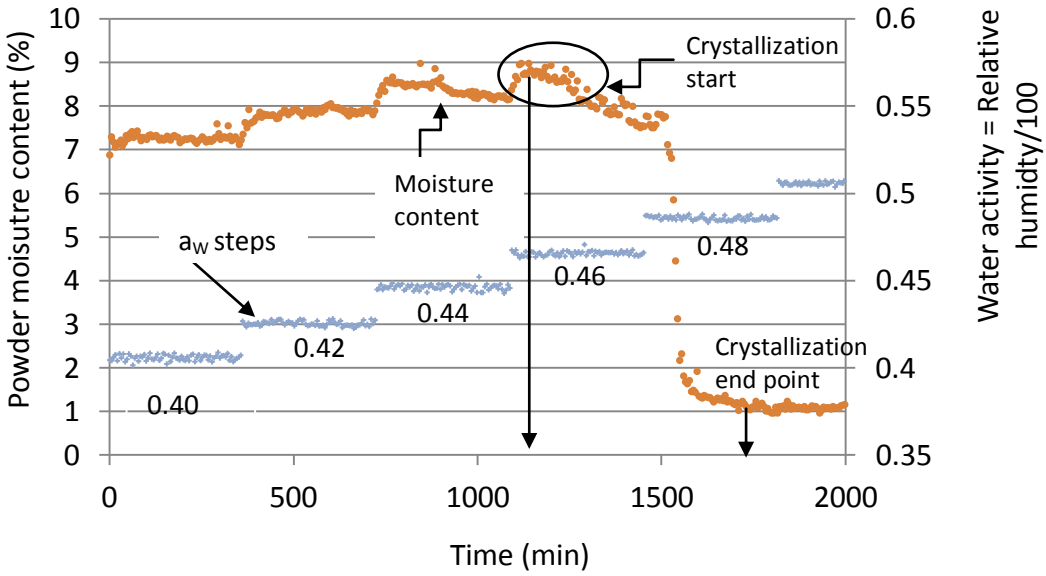

B) lecithin/lactose (10/90)

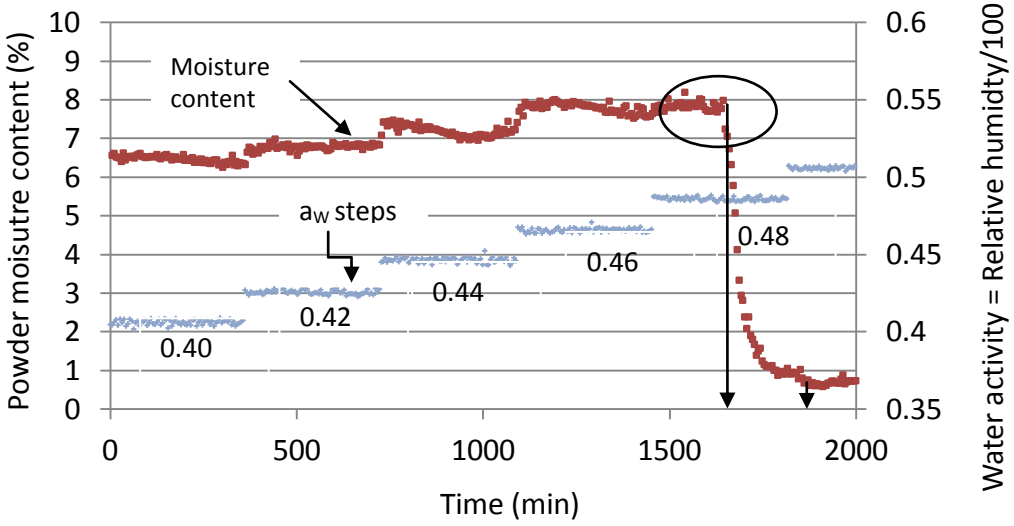

C) AMF/lactose (10/90)

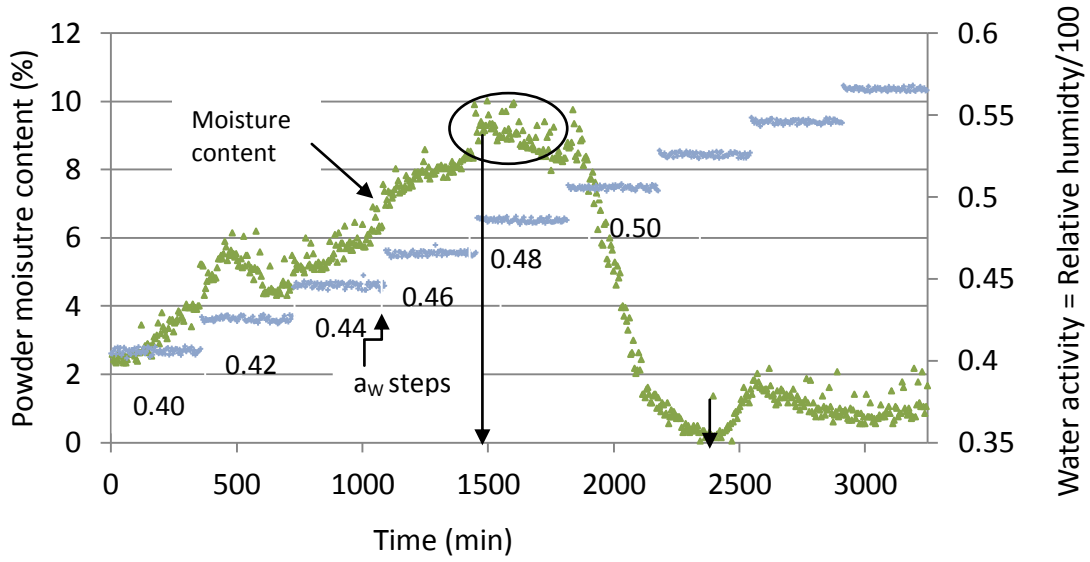

D) Na-Cas/lactose (10/90)

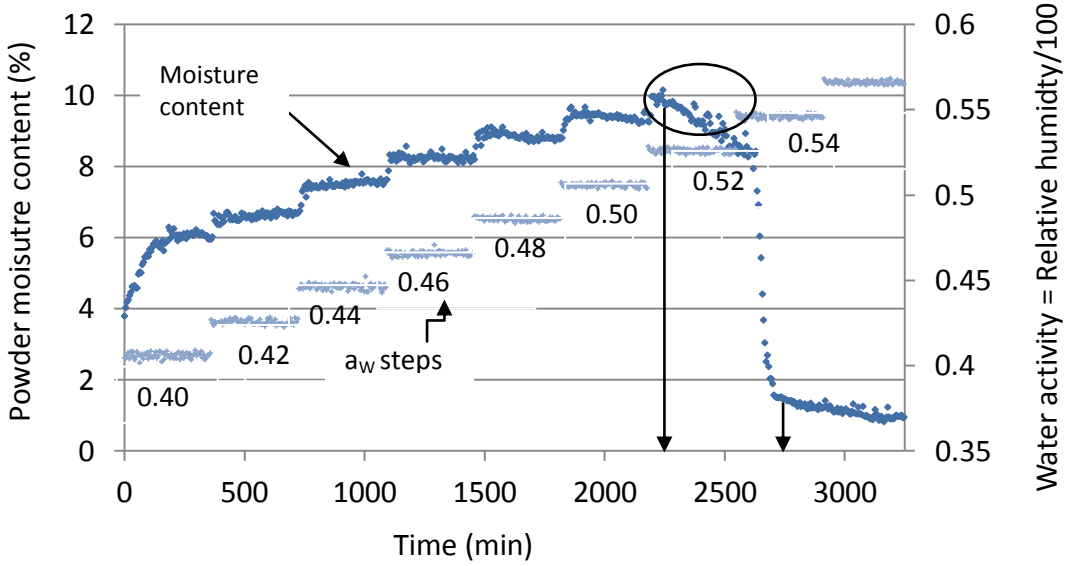

E) HPMC/lactose (10/90)

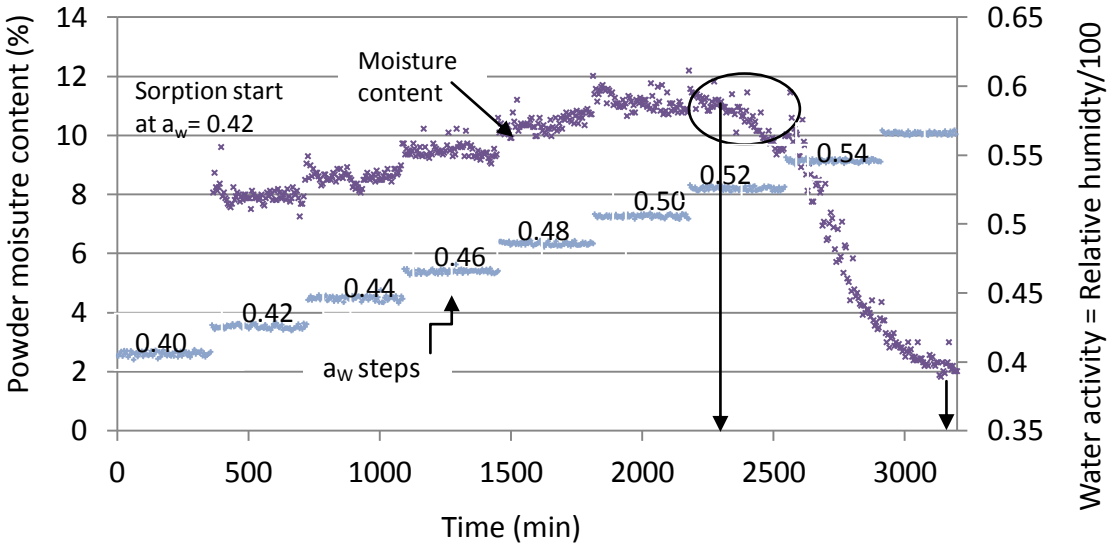

F) Gelatine/lactose (10/90)

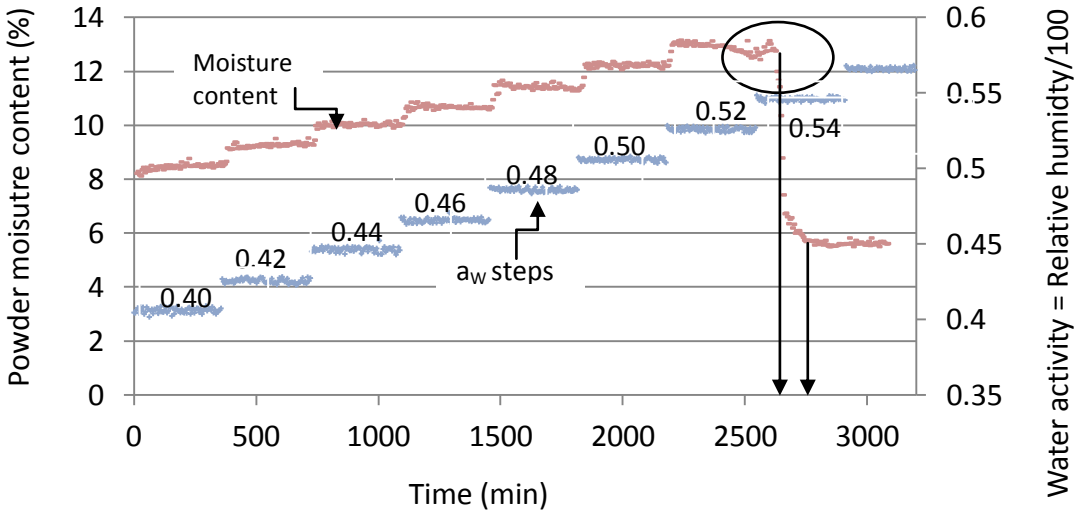

Figure 5.8: Dynamic vapour sorption measurements of amorphous lactose and lactose/additive =90/10 wt% powders: A) Pure amorphous lactose, B) lactose/lecithin, C) lactose/AMF, D) lactose/Na-Cas, E) lactose/HPMC (sorption start at a_W=0.42), F) lactose/gelatine.

All additives tested in this study delayed lactose crystallization, as evidenced by the higher RH required to induce lactose crystallization. Lecithin-coated lactose powder showed a sudden moisture loss at RH of 48%. Fat-coated lactose powder also absorbed moisture until a RH of 48%, where moisture was lost upon lactose crystallization; the sudden moisture loss occurred at 50% RH. The coating additives Na-Cas and HPMC delayed lactose crystallization more than did lecithin and milk fat. With both lactose/Na-Cas and lactose/HPMC powders, lactose crystallization was initiated at RH of 52%. In lactose/gelatine powder lactose crystallization was delayed until 54% RH, which is more than in any other compound powder tested. This is consistent with the results of Haque and Roos (2004a), who measured higher crystallization temperatures for lactose/gelatine powders (at RH of 44%), compared with lactose/Na-Cas, lactose/WPI and lactose/BSA powder. Generally, the delays in lactose crystallization observed in this study in the presence of various additives were caused by lactose-additive interactions, resulting in higher lactose glass transition temperatures of the compound powder, as pointed out in Chapter 3 (Part B). High-molecular-weight additives such as gelatine, Na-Cas and HPMC tend to form larger complexes with lactose (with resulting higher glass transition temperatures and therefore higher lactose crystallization delays) than smaller molecules such as lecithin or fatty acids do.

None of the additives were useful for providing a moisture barrier for amorphous lactose within the particulates, since the powders with additives absorbed similar amounts of moisture as the pure amorphous lactose powder. Gelatine was the only additive that increased the moisture sorption capacity of the lactose powder at a point just before crystallization occurred: 13% water content for gelatine compared with 9% water content for lactose. This means that the gelatine-lactose powder could be exposed to more humid conditions before crystallization occurs. The moisture sorption capacity of Na-Cas, HPMC and lecithin-coated lactose powder just before crystallization occurred did not change significantly compared to that of the pure amorphous lactose powder. Haque & Roos (2004a) also measured higher moisture sorption for lactose/gelatine powder compared with pure lactose and lactose/protein powders. They assumed that gelatine consists of a higher number of polar groups capable of forming more hydrogen bonds with water molecules. These polar groups possibly also formed a greater number of bonds with lactose molecules, resulting in a greater crystallization delay for lactose/gelatine powder (Figure 5.8) compared with Na-Cas and HPMC, which have similar molecular weights but fewer polar groups.

Powder caking

The spray-dried powders were stored at ambient room conditions for one week to absorb moisture from the environment, and thus to allow lactose crystallization and powder caking. No additive tested in this section of the study prevented lactose crystallization and caking of the powder. Therefore, although the additives enriched at the particle surface, as can be seen in Figure 5.1, they could not form an adequate physical barrier that prevented moisture diffusion into the particles and hence crystallization of lactose. Figure 5.8 showed, however, that the presence of high-molecular-weight additives such as Na-Cas, HPMC and gelatine can at least delay crystallization and reduce crystallization rates by increasing glass transition temperatures due to hydrogen bonding with lactose.

The crystalline cake structure can be seen in Figure 5.9. Only the presence of HPMC (E) and, to a lesser extent, Na-Cas (B) within the particle wall provided sufficient structural support to prevent a collapse of the particulates upon lactose crystallization, as was observed for pure lactose and the other lactose/additive powders. In addition, lactose/HPMC powder was the only powder that did not transform into a hard brittle powder cake, but rather formed a softer pliable cake. It appeared that HMPC formed a physical barrier on the particle surface that reduced caking by preventing lactose crystals in neighbouring particles from growing into each other. HPMC is a flexible polymer that may have formed a dense, protective network (film) on the particle surface (Bodvik et al., 2010). Due to its ability to cross-link and form networks (Bodvik et al., 2010), the presence of HPMC throughout the interior of the particle was likely to have provided structural support, which may have strengthened the whole particle and therefore prevented its collapse upon crystallization. Assuming that HPMC not only formed a thin mono-layer upon adsorption but also accumulated into several multi-layers beneath the droplet surface (due to *Pe* number > 1), a thicker, stable HPMC wall may have been formed, capable of further providing some degree of structural integrity to the particle during lactose plasticization and subsequent crystallization.

Lactose/Na-Cas powder transformed into a hard, brittle cake upon crystallization, which is similar to what was seen with the other powders, although distinct particulates were preserved (Figure 5.5). Na-Cas is a flexible polymer-like protein (Dickinson, 2001; Fäldt & Bergenståhl, 1995), which may have similar, although clearly not as effective, networking and film-forming properties to HPMC. Gelatine (Figure 5.9, D) was also expected to provide a certain degree of structural support due its film-forming capability at the surface

(Arvanitoyannis et al., 1998; Bigi et al., 2001; Gharsallaoui et al., 2007), but this work showed that HPMC and Na-Cas were significantly more effective in this respect.

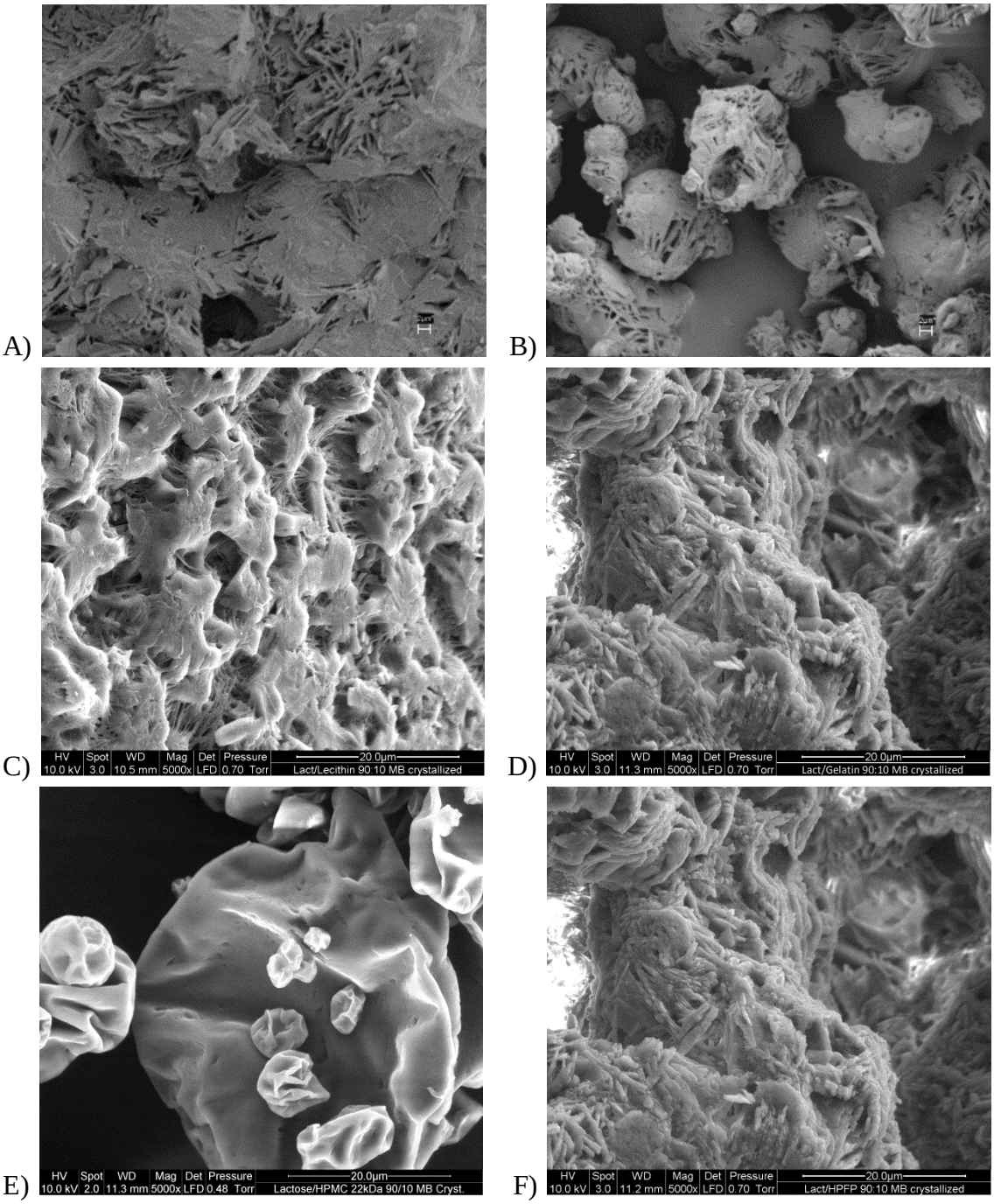

Figure 5.9. SEM photographs (5,000 magnification). Effect of different coating additives (10 wt% of total solid content) on the particle morphology after lactose crystallization: A) Pure lactose; B) lactose/Na-Cas; C) lactose/lecithin; D) lactose/gelatine; E) lactose/HPMC; F) lactose/AMF.

5.3.2. Part B: Competitive adsorption between different surface active species

Surface composition of spray-dried powders

HPMC versus 1) Na-Cas, 2) WPI, 3) lecithin

Figure 5.10 to 5.12 show the surface compositions of spray-dried lactose/HPMC/Na-Cas (Figure 5.10), lactose/HPMC/WPI (Figure 5.11) and lactose/HPMC/lecithin (Figure 5.12) powders for decreasing lactose/additive bulk ratios from 99/0.5/0.5% to 90/5/5%. Na-Cas, WPI and lecithin tended to be excluded from the droplet surface in favour of HPMC during spray drying. At the lowest additive bulk concentration used (0.5 wt% of both HPMC and protein), small amounts of Na-Cas protein (approximately 8%) were detected on the particulate surface, but when the additive concentration increased to 5% wt (2.5wt% of both HPMC and protein) both Na-Cas and WPI were completely excluded from the surface. For the spray-dried lactose/HPMC/WPI powders, WPI was almost completely excluded from the surface with just 0.5wt% of each additive (HPMC and WPI). For the spray-dried lactose/HPMC/lecithin powders, no lecithin could be detected at the particulate surface at lactose/additive bulk ratios of 99/0.5/0.5%, while small fractions were detected at higher additive bulk concentrations .

Because proteins and lecithin were the only species within the spray-dried aqueous lactose/HPMC/protein and lactose/HPMC/lecithin solutions that contain nitrogen within their molecular structure, the absence (or the presence of only small fractions) of nitrogen on the particulate surface during XPS measurement clearly confirmed that proteins and lecithin were indeed completely (or almost completely) excluded from the droplet surface. Those results agree with the findings of Elversson and Millqvist-Fureby (2006), who reported a complete encapsulation of another surface active molecule (BSA proteins) by HPMC, following a spray drying process for polymer concentrations as low as 1 wt% of total solids. Elversson and Millqvist-Fureby (2006) assumed the adsorbed polymers produced a steric effect, because they pointed their long tails inwards towards the solution and therefore prevented other larger molecules such as proteins from adsorbing. This is further supported by the work of Muñoz et al. (2000) and Blomqvist et al. (2005) who report a "brush" formation of various polymers upon surface saturation, where the long, flexible polymer chains stretch away from the surface towards the interior, while a remaining anchoring end remains attached to the surface. A "brush" formation could have excluded the larger proteins and lecithin from the air-water interface, whereas the small low-molecular-weight lactose molecules would not

have been subject to any steric effect. Thus, lactose molecules could have easily diffused through the adsorbed polymer matrix to reach the droplet surface, in a mechanism similar to that described in Section 3.3.1 for an adsorbed protein monolayer.

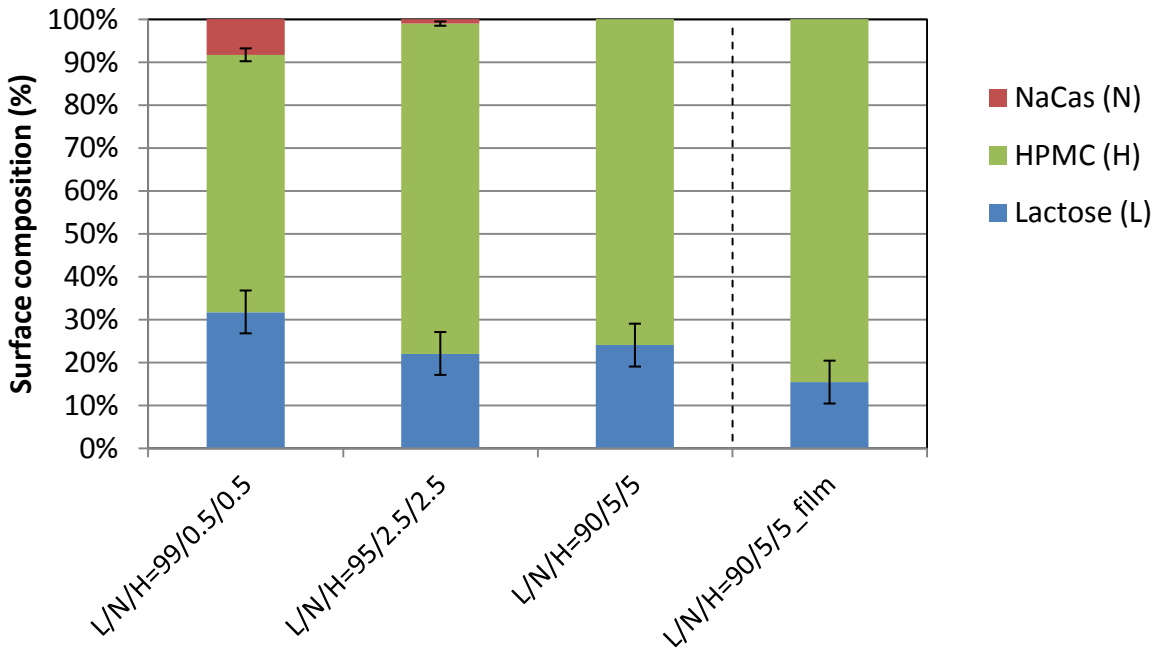

Figure 5.10: Surface composition of spray-dried lactose/HPMC/Na-Cas powders at increasing additive ratios and dried lactose/HPMC/Na-Cas=90/5/5 films (right).

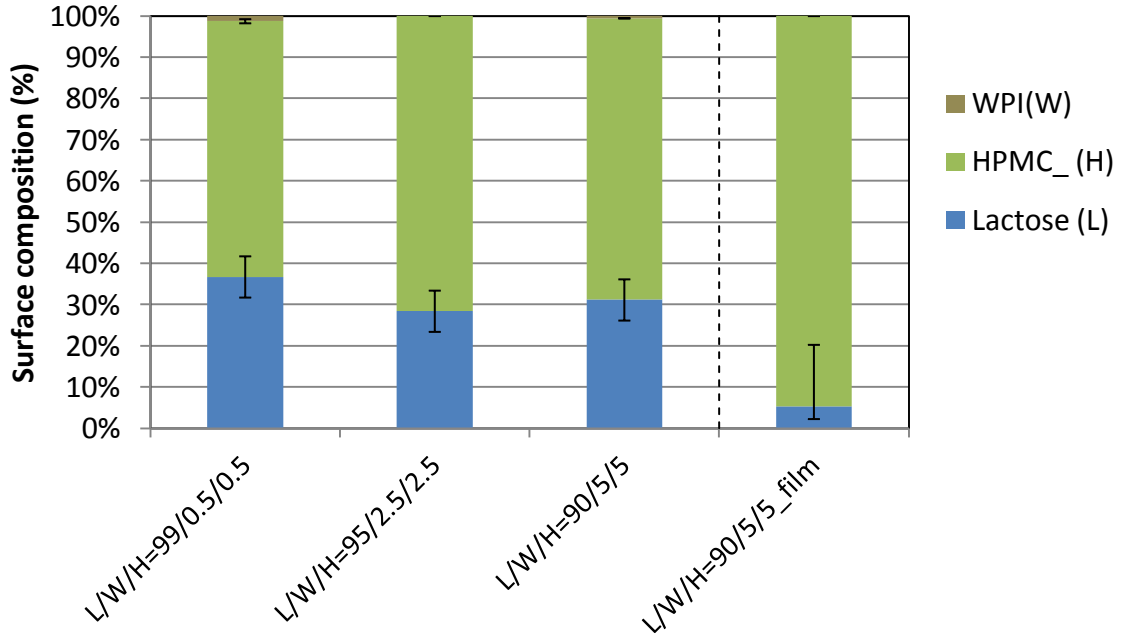

Figure 5.11: Surface composition of spray-dried lactose/HPMC/WPI powders at increasing additive ratios and dried lactose/HPMC/WPI=90/5/5 films (right).

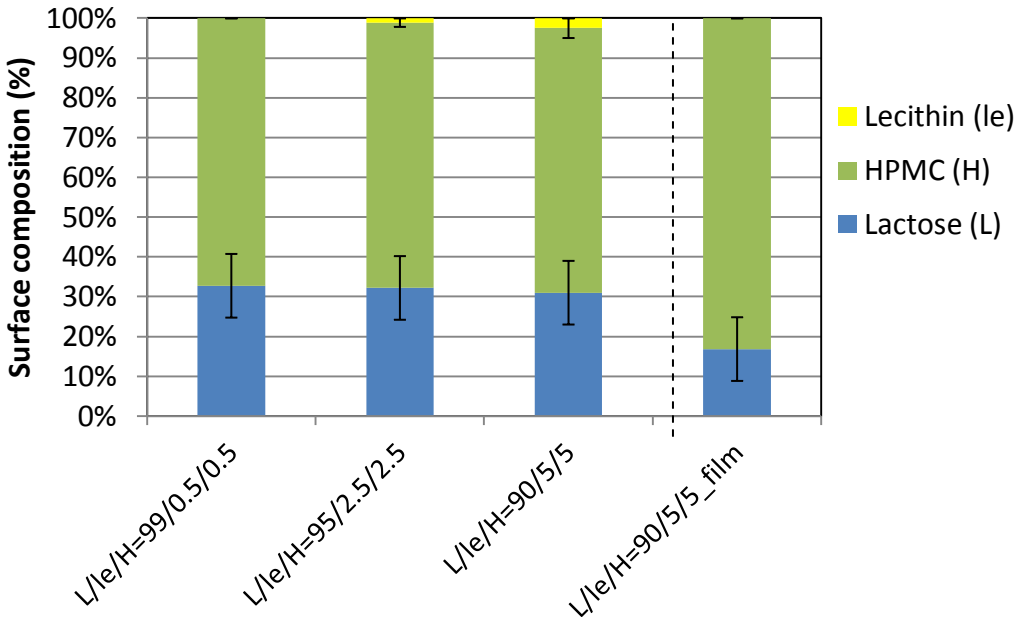

Figure 5.12: Surface composition of spray-dried lactose/HPMC/lecithin powders at increasing additive ratios and dried lactose/HPMC/lecithin=90/5/5 films (right).

The surface of the slow-dried films of lactose/HPMC/Na-Cas, lactose/HPMC/WPI and lactose/HPMC/lecithin (bulk ratio of 90/5/5wt%) consisted of mainly HPMC, with a small amount of lactose, while the Na-Cas and the WPI proteins as well as the lecithin molecules were completely excluded, as was also observed for the spray-dried powders (Figure 5.10 to 5.12). Furthermore, the surface compositions of the dried films showed slightly higher HPMC surface concentrations for all films compared with spray-dried particles of the same solid bulk compositions. During slow film drying, more time was given for HPMC molecules to exclude the other additive from the surface and re-arrange their conformational structure to a more compact, thermodynamically favourable state than during spray drying, where time was limited. This was likely to have been the cause of the higher HPMC surface concentration for slow drying films, as well as the reason for the complete exclusion of lecithin and the proteins from the film surface (Figure 5.10 to 5.12). A lower surface tension was measured for 1 wt% HPMC solutions (49.2±0.8 mNm^{-1}), than for 1wt% WPI solutions (57.6±1.2 mNm^{-1}), 1wt% Na-Cas solutions (51.3±0.7 mNm^{-1}) and 1wt% lecithin solutions (53±3 mNm^{-1}), which shows that HPMC had the highest surface activity of all the tested additives. Thus, the higher surface activity, as well as a steric effect of HPMC molecules, seems to be the dominant mechanisms in the exclusion the other additives (Na-Cas, WPI or lecithin) from the surface of films and droplets. The importance of the surface activity on surface accumulation

during drying is supported by Landström et al. (2003), who performed a competitive adsorption study between β-casein and β-lactoglobulin (the main protein component of WPI) during spray drying, and discovered that the more surface active monomeric β-casein could out-compete β-lactoglobulin (as evidenced by higher surface loads), while the significantly larger (and less surface active) β-casein in associated form could not.

Besides the surface activity, the molecular size has a big impact on how fast a surface active molecule diffuses towards the air-water interface and adsorbs there (Landström et al., 2000; Landström et al., 2003). HPMC (~22kDa), Na-Cas (~24 kDa) and WPI (~18kDa) vary only slightly in their molecular weights. Since no data on the molecular size or diffusion coefficient of HPMC (with an average molecular weight of 22 kDa) is available in the literature, it is assumed here that the molecular sizes and therefore diffusion coefficients do not differ significantly between these molecules, resulting in similar *Pe* numbers. Compared with the proteins, lecithin has a significantly lower molecular weight than the HPMC tested (0.75 kDa versus around 22 kDa for HPMC). Thus, it can be assumed that lecithin molecules are significantly smaller than the long, flexible HPMC polymers, and probably have larger diffusion coefficients, which means they ought to diffuse towards the air-water interface faster. Lecithin would therefore be expected to adsorb first.

The absence of lecithin (or the presence of only small amounts of it) at the surface of dried particles and films indicates that the competitive adsorption process is more dependent on the adsorption of the molecule from the subsurface to the air-water interface, as controlled by surface activity, than on diffusion rate, as influenced by molecular size. An energy barrier exists when the interface is already partly occupied by a surface active species (Graham & Phillips, 1979a; Landström et al., 2003). In that case, the more surface active molecule preferentially adsorbs from this subsurface to the interface. Thus, although lecithin may have occupied the air-water interface first due to its faster diffusion, sufficient time was given, even during spray drying, for the HPMC molecules to adsorb into the air-water interface and exclude most of the adsorbed lecithin molecules from the surface due to their higher surface activity. Surface activity is mainly determined by molecular flexibility, hydrophobicity and the strength of solute-surface interactions (Landström et al., 2003; Magdassi, 1996). Thus, thermodynamic factors seem to dominate kinetic factors in systems that allow sufficient time for the competitive adsorption process. In a competitive adsorption process, surface activity

seems to dominate over a possible Peclet number effect, because the measured HPMC surface concentrations of the spray-dried particles were lower than those of films.

Lecithin versus Na-Cas

Unlike HPMC, neither lecithin nor Na-Cas could exclude the other species completely from the surface. Lecithin dominated the surface of spray-dried lactose/lecithin/Na-Cas particles for all various solid compositions (Figure 5.13). This was clearest for higher additive bulk concentrations (95/2.5/2.5 wt% and 90/5/5 wt%), where lecithin displaced a substantial amount of the larger Na-Cas protein from the droplet surface (Figure 5.13). A preferential displacement of surface active proteins from the air-water and oil/water interface by lecithin is supported by the studies of other authors (Adler et al., 2000; Euston et al., 1995; Jayasundera et al., 2010b; Millqvist-Fureby & Smith, 2007).

The dried lactose/Na-Cas/lecithin (90/5/5 wt%) films showed a clear domination of Na-Cas proteins at their surfaces, which is in contrast to spray-dried particles where lecithin dominated the particulate surface. This suggests that the more surface active Na-Cas protein partly displaced the lecithin from the air-water interface during film drying, most likely because more time was given for the flexible Na-Cas proteins to re-orientate and stretch at the film surface, via the mechanism described by Graham and Phillips (1979c). Those reorientations would allow a higher number of hydrophobic protein residues to make contact with the air-water interface, with a resulting stronger attachment of the protein (Landström et al., 2003) leading to the exclusion of previously adsorbed lecithin molecules from the surface. Dickinson (2011) states that those time-dependant rearrangements of proteins can cause a complete protein unfolding, which would consequentially result in irreversibly attached proteins. During spray drying, the available time may have been limited for Na-Cas proteins to fully re-orientate upon adsorption and thus exclude lecithin from the surface. This is supported by Landström et al. (2003), who also reported that the time-scale of spray drying is probably too short to allow extensive rearrangements of proteins upon adsorption. In contrast, rearrangements of the significantly more flexible HPMC polymers appears to have been fast enough to exclude most of the lecithin from the droplet surface during spray drying, as observed in Figure 5.12.

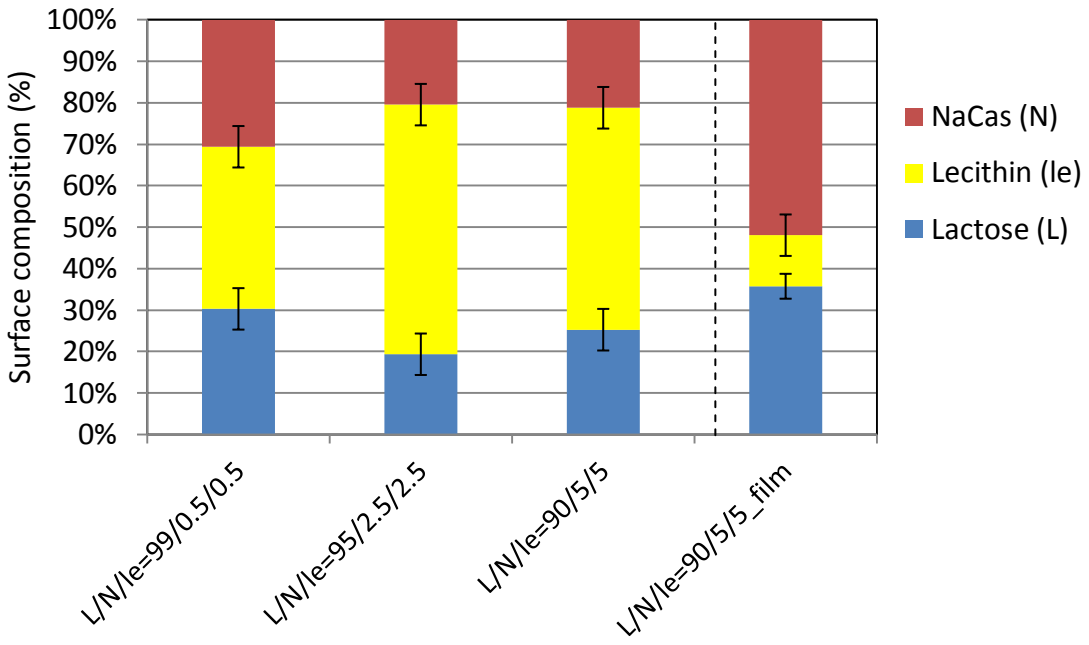

Figure 5.13: Surface composition of spray-dried lactose/Na-Cas/lecithin powders at increasing additive ratios and dried lactose/Na-Cas/lecithin=90/5/5 films (right).

Effects of *Pe* number or moisture content gradients on solute segregation during spray drying could not be clearly shown here. Both Na-Cas and lecithin had *Pe* numbers above unity during spray drying (for given spray drying conditions) and might therefore have further enriched the surface in sub-layers during spray drying. This might explain why the total additive surface concentration (Na-Cas and lecithin) is slightly higher (~10%) for spray-dried particles than for films for the same bulk composition. Due to the drying rate being higher during spray drying, higher moisture content gradients would be expected for drying droplets, and these should have caused further solute segregation between Na-Cas and lecithin, which would have contributed to higher Na-Cas/lecithin ratios at the surface of spray-dried particles, compared with dried films. However, since the difference was only slight, the surface activity and drying time must have been the dominant mechanisms in controlling the final surface composition of these films and particles.

Lecithin versus WPI

The surface composition of slowly dried films of an aqueous solution of lactose/lecithin/WPI with solid weight ratios of 90/5/5 wt% showed a clear domination of

lecithin in preference to WPI on the film surface (Figure 5.14). This was expected, since lecithin has a higher surface activity than WPI, indicated by a lower measured surface tension for aqueous lecithin solutions. Furthermore, due to its lower molecular weight, lecithin is expected to diffuse faster towards the film surface and thus occupy the air-water interface at an earlier stage than the larger WPI. It seems that, during slow film-drying, sufficient time was available for surface active species to compete for the air-water interface, thus the surface activity of the molecule seems to be the main determinant of the final surface composition of dried films, as also suggested before. This would explain why, for all the different dried films within this competitive adsorption study, the more surface active species dominated the film surface, irrespective of the molecular size and thus differences in the diffusion rates of the different surface active molecules.

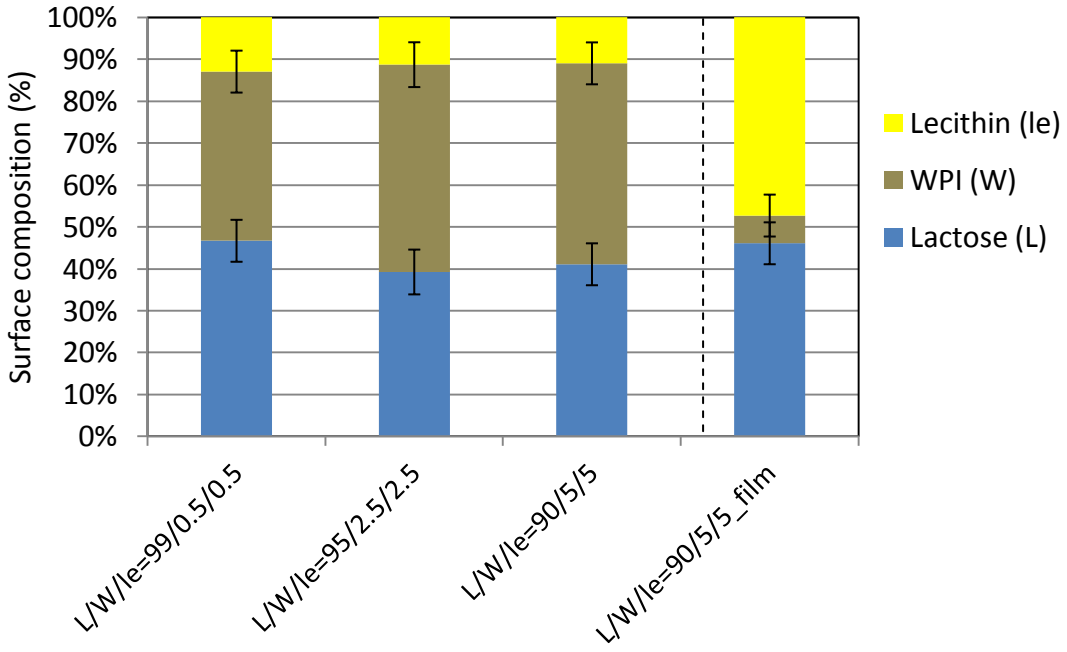

Figure 5.14: Surface composition of spray-dried lactose/WPI/lecithin powders at increasing additive ratios.

The surface composition of spray-dried lactose/lecithin/WPI particles showed a clear domination of WPI proteins on the particulate surface (Figure 5.14), which was an unexpected result, particularly given that lecithin dominated the surface of spray-dried lactose/Na-Cas/lecithin particles (Figure 5.13). As mentioned before, Landström et al. (2003) performed a competitive adsorption study between β-lactoglobulin (the main protein within WPI) and monomeric β-casein during spray drying and found out that β-casein was clearly more competitive, most likely due to its higher surface activity. Thus, lecithin would have

been expected to also dominate the particulate surface of spray-dried lactose/lecithin/WPI particles, in the same way it dominated the film surfaces after film drying. This would seem to suggest that factors besides surface activity, such as differences in drying time, drying rates, moisture gradients or interactions between adsorbed proteins or protein/lecithin were likely to have affected the competitive adsorption behaviour during spray drying. The results of this study demonstrate the high complexity of competitive adsorption phenomena for different surface active species of various molecular weight and surface activity, in particular for different drying systems.

Particle and powder functional properties

Morphology of spray-dried powders

Figure 5.15 shows the particle morphology of spray-dried lactose powders containing two additives, each present at bulk concentrations of 5wt%. All particles had a highly wrinkled and folded surface structure (Figure 5.15, A-C). As shown in Figure 3.12 and 3.13 (Chapter 3, Part B), the particulate surfaces of lactose/Na-Cas and lactose/WPI (9/1 wt%) contained significantly smaller folds, while the particulate surfaces of lactose/lecithin (9/1 wt%) powders were smooth (Figure 5.5, C). In contrast, the particle morphology of lactose/HPMC (9/1 wt%) powder (Figure 5.5, F) was similar to that of the lactose/HPMC/protein and lactose/HPMC/lecithin powders (Figure 5.15, A-C). Thus, it is clear that HPMC was responsible for the highly folded particle structure, because its high flexibility resulted in a high particle wall elasticity during particle formation, as pointed out in Part A of this chapter.

The particle morphologies of lactose/lecithin/protein powders of 90/5/5 wt% total solid ratio (Figure 5.15, D+E) were significantly smoother than those of the HPMC-containing powders, irrespective of the type of protein used (WPI or Na-Cas). This was due to the proteins being less flexible than the highly flexible HPMC. When comparing the particle morphologies of the lactose/lecithin/protein powders (Figure 5.15, D+E) with those of the lactose/lecithin and lactose/protein powders (Figure 5.5, B and C), it can be seen that the lactose/protein powders had a wrinkled surface structure (although not as pronounced as seen in HPMC-coated particles), while lactose/lecithin powder consisted of very smooth particles without obvious particle wrinkles, and lactose/lecithin/protein powders had an even particle surface with a small amount of folding. The smoothness of the lactose/lecithin particles is due

to the absence of any molecular flexibility, as pointed out in Part A of this chapter. The addition of protein to the mixture (lactose/lecithin/protein powders) produced a slightly folded particle structure, most likely due to the presence of proteins within the particle wall, which increased the wall elasticity more compared with pure lactose or lactose/lecithin.

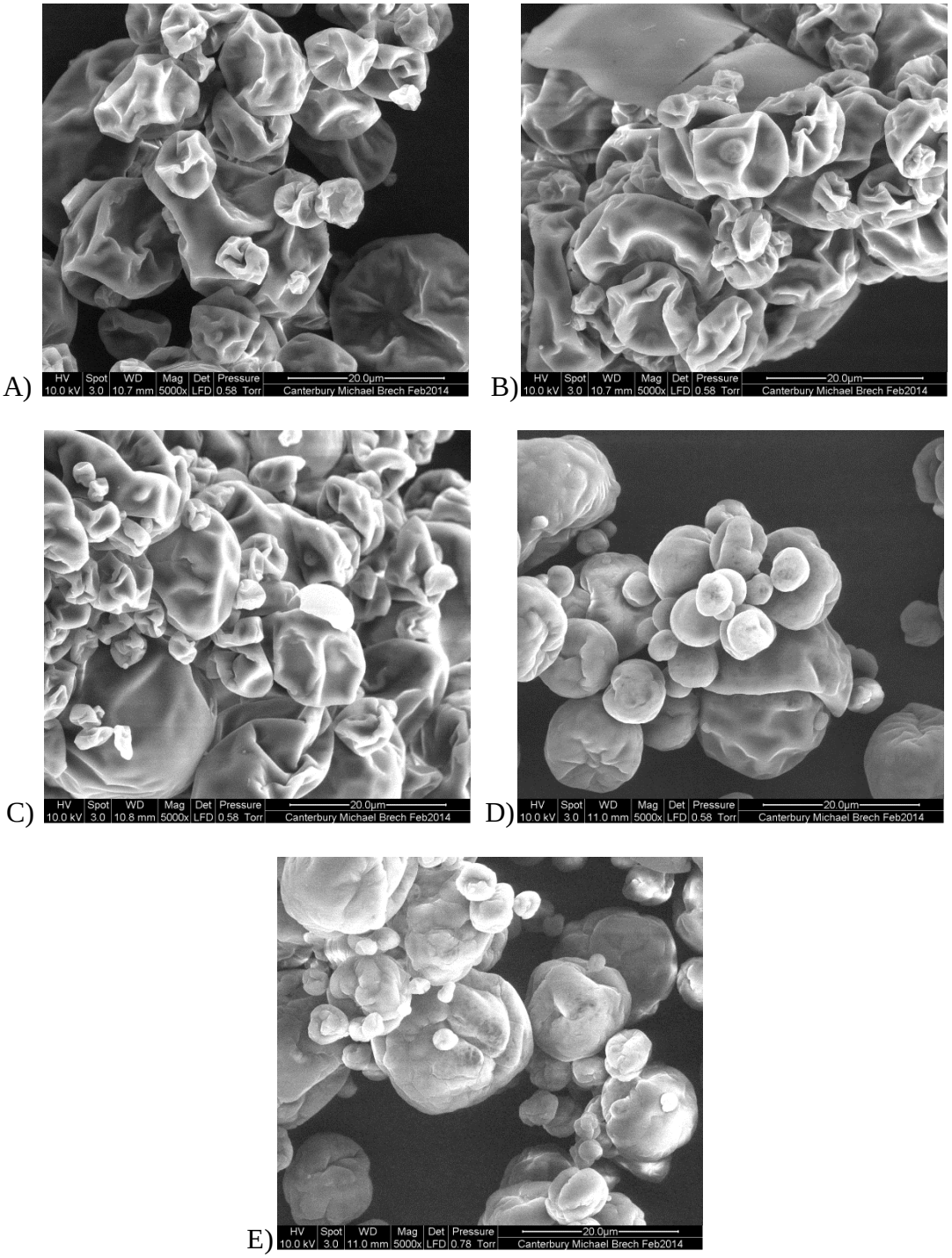

Figure 5.15: Particle morphology of spray-dried powders, analyzed by SEM(5,000x magnification), prior to lactose crystallization. A) Lactose/HPMC/Na-Cas=90/5/5, B) lactose/HPMC/WPI=90/5/5, C) lactose/HPMC/lecithin=90/5/5, D) lactose/Na-Cas/lecithin =90/5/5, E) lactose/lecithin/WPI=90/5/5.

Particle size and powder bulk density

Particle size, powder bulk density and powder functional properties of different spray-dried lactose/additive powders were analyzed. A general trend of increasing particle size was observed with an increase in total additive concentration from 1wt% to 10wt% of total solids (Figure 5.16). This increase in particle size was likely to be caused by 1) a higher solution viscosity when increasing the solid concentration and 2) the higher total percentage of flexible molecules within the lactose matrix, resulting in increased wall elasticity and thus increased particle inflation via the expansion of the internal vacuole, as described in Chapter 3 (Part B). This particle expansion caused the powder bulk density to decrease due to lower particulate densities (Figure 5.17). It can be seen very clearly that significantly larger and less-dense particles were produced when HPMC was present. This is due to the ability of the long, highly flexible HPMC polymers to increase the wall elasticity, compared to less flexible proteins such as Na-Cas and WPI or non-flexible, small molecules such as lecithin. This is supported by the highly folded particle surface of HPMC-containing powders (Figure 5.15, A-C).

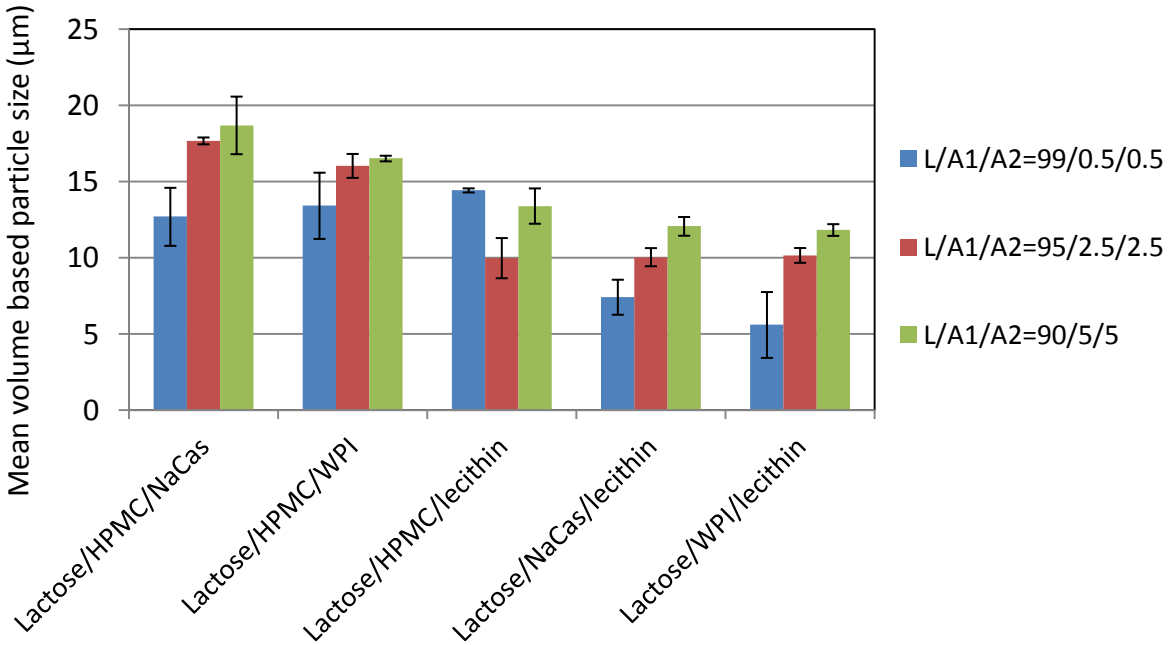

Figure 5.16: Effect of different spray-dried lactose-additive powders on the volume based mean particle size.

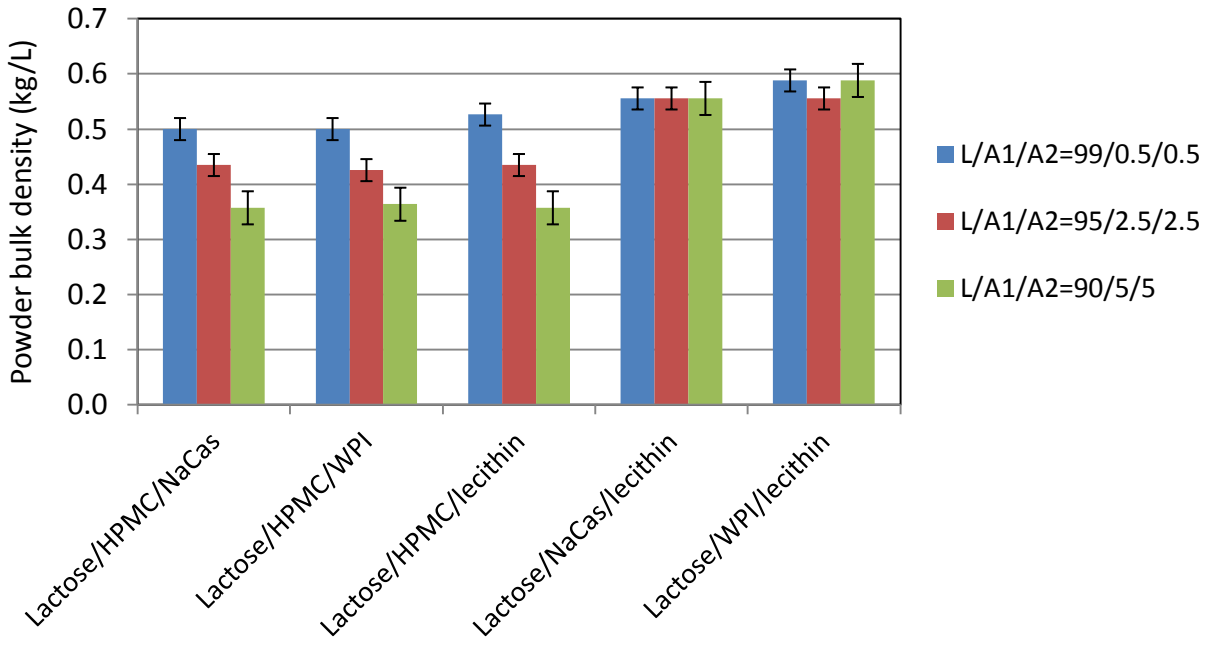

Figure 5.17: Effect of different spray-dried lactose-additive powders on the powder bulk density.

Compared to proteins, lecithin could not make a significant contribution to wall elasticity, as shown in Part A of this chapter, thus lecithin/HPMC-containing lactose particles were smaller than those containing flexible molecules such as HPMC and proteins as additives. When the total additive bulk concentration of HPMC-containing powders was increased from 1wt% to 10wt%, particle sizes increased and powder bulk densities decreased (Figure 5.16 and Figure 5.17), despite fairly constant particle surface compositions (Figure 5.10 to Figure 5.12). This supports the assumption made in Chapter 3 (Part B), that the wall elasticity is controlled by the total amount of additive in the bulk rather than just the surface film.

For reasons not clear, no differences in the powder bulk densities between lactose/HPMC/protein and lactose/HPMC/lecithin powders were observed (Figure 5.17). Lower powder bulk densities would have been expected for the larger lactose/HPMC/protein particles. While the powder bulk densities of all HPMC-containing powders decreased with increasing total additive concentrations in the bulk, the powder bulk density of lactose/lecithin/protein powders remained fairly unchanged, although the particle sizes increased. Once again, powder bulk densities would have been expected to decrease with increasing protein concentrations in the bulk due to lower particle densities. It is possible that

powder bulk density measurements were affected by powder agglomeration and extensive surface folding.

Powder flow

In Figure 5.18, the powder flows through a vibrating sieve are illustrated. Lactose powders containing HPMC and proteins (Na-Cas or WPI) as additives gave the best powder flows, and the effect was clear even at very low total additive bulk concentrations (0.5wt% of each additive). This further supports the findings described in Part A of this chapter, that the presence of large molecules such as HPMC, Na-Cas or WPI causes an increase in the glass transition temperature at the particle surface which reduces particulate stickiness and thus particle agglomeration within the spray dryer. Although the lecithin-containing lactose/HPMC powders produced inconsistent data, powder flow was not as good as lactose/HPMC/protein powders, in particular for higher additive concentrations. Since the particle surface compositions of all three HPMC-containing powders were fairly even (Figure 5.10 to Figure 5.12), with little or no protein or lecithin present at the surface, the powder surface composition cannot account for the differences in the powder flows. Thus, the smaller particles for lecithin-containing lactose/HPMC powders (Figure 5.16) were responsible for the reduced powder flow seen with these powders.

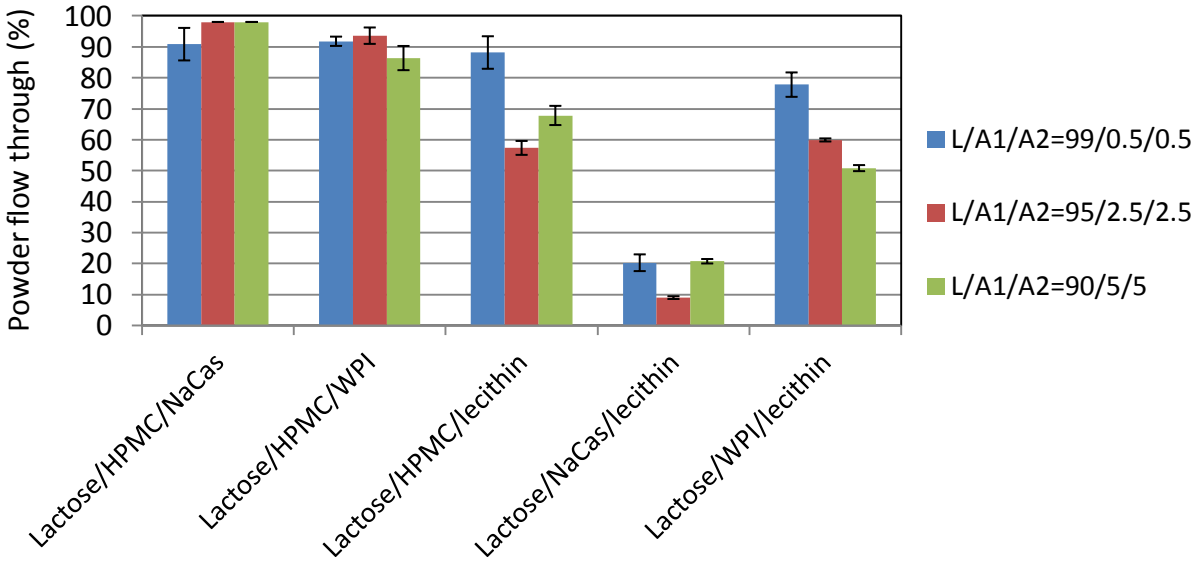

Figure 5.18: Effect of different spray-dried lactose-additive powders on the powder stickiness.

Powder flows of lactose/lecithin/Na-Cas powders were poor compared with the other powders, probably due to the high amount of lecithin at the particle surface (Figure 5.13). Lecithin-coated lactose powder showed very poor powder flow, as reported in Part A of this chapter (Figure 5.6), due to the small molecular size of lecithin and thus its inability to significantly increase the glass transition temperature at the droplet surface. This is probably also the reason why powder flows of lactose/lecithin/Na-Cas powders were poorer than those of lactose/lecithin/WPI powders. The latter powder showed significantly lower lecithin surface concentrations and higher surface protein concentrations than did lactose/lecithin/Na-Cas powders (Figure 5.13 and 5.14). Furthermore, the similar particle sizes and powder bulk densities of both protein-containing lactose/lecithin powders (Figure 5.16 and Figure 5.17) indicate that their different surface compositions, and hence different surface glass transition temperatures, were the most likely reason for the variations in the powder flow. It is not clear why the powder flow of lactose/lecithin/WPI powders was reduced with increasing total additive concentrations, considering that there was little variation in surface composition over the range of additive concentrations used (Figure 5.14). The opposite effect would have been expected due to the increases in particle sizes with higher total additive concentrations (Figure 5.16).

Wettability

Figure 5.19 shows the wetting times of the various powders. Lactose powders containing HPMC and either Na-Cas or WPI displayed significantly longer wetting times when the total additive concentrations were increased. This behaviour is very different to that of the other powders, where wetting times remained almost unchanged with increasing additive concentrations. As discussed in Part A of this chapter, the presence of HPMC on the particle surface is expected to cause a strong delay in wetting time due to the low powder bulk density that hinders particles from sinking beneath the water surface. Furthermore, a gel layer forms at the surface of HPMC-coated lactose powders due to the swelling of polymers upon hydration (Gao et al., 1996; Ishikawa et al., 2000). Here, the low bulk density is assumed to be the main reason for the very long wetting times seen with lactose/HPMC/protein powders, considering that their particle surface compositions did not change when the total additive concentrations exceeded 1 wt% (Figure 5.10 and Figure 5.11), while powder bulk density decreased (Figure 5.17). Besides the lowering of the bulk density, another effect of increasing

HPMC bulk concentrations might have been the formation of a thicker polymer coating, on account of a greater accumulation of polymers beneath the air-water interface. This would have additionally contributed to longer wetting times, because a thicker gel layer would have formed around the particles, which would have hindered dissolution (Ishikawa et al., 2000).

The presence of lecithin considerably decreased the wetting times of all lecithin containing powders, despite the fact that, for lactose/HPMC/lecithin powders, the particle surface was covered mainly by HPMC molecules (Figure 5.12), which should have delayed wetting to a similar extent as occurred with the lactose/HPMC/protein powders. Moreover, the powder bulk density of lactose/HPMC/lecithin powders is low, similar to that of the protein-containing lactose/HPMC powders (Figure 5.17), hence it was expected that this would have further delayed the wetting time, as it appeared to do in the protein-containing lactose/HPMC powders. However, it seems that the presence of even small amounts of lecithin at the particulate surface accelerated the wetting of the powder (Kim et al., 2009a; Millqvist-Fureby & Smith, 2007).

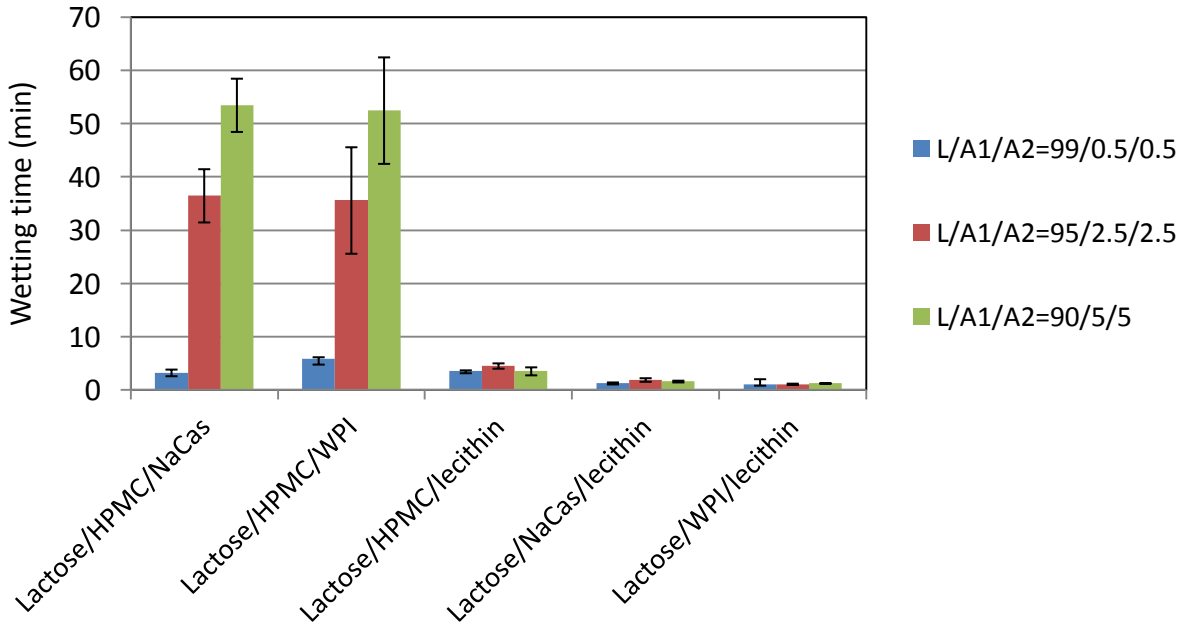

Figure 5.19: Effect of different spray-dried lactose-additive powders on the wetting time.

Out of all powders, wetting times of lactose/lecithin powders containing protein were the lowest. No clear differences were seen in wetting times for the different lactose/lecithin/protein mixtures, although lecithin surface concentrations were considerably

higher for lactose/lecithin/Na-Cas particles (Figure 5.13) than for lactose/lecithin/WPI powders (Figure 5.14). This again supports the assumption that the presence of only a minimum amount of lecithin at the particulate surface seems to be sufficient to produce a fast powder wetting.

Lactose crystallization and powder caking

Figure 5.20 shows the crystalline particle structures of coated lactose powders containing two coating additives, each present at bulk concentrations of 5 wt%. Only HPMC-containing powders retained a degree of particulate structure, probably due its unique ability to form networks (Bodvik et al., 2010), which may have formed throughout the particle wall. Lactose/HPMC (90/10 wt%) powders showed a similar crystalline particle structure (Figure 5.9). Neither of the protein-containing lactose/HPMC powders had significant amounts of crystals at the surfaces of the particles, which indicates that lactose crystals were mainly located beneath the protective polymer coating. Compared to the protein-containing lactose/HPMC powders (Figure 5.20 A and B), lecithin-containing lactose/HPMC powders (Figure 5.20 C) showed a different crystalline powder structure. They displayed surface crystals where sharp edges can be very clearly seen, and the particulate structure seems to become partly lost, despite the particle surface being largely covered with HPMC molecules, as is the case for the protein-containing lactose/HPMC powders (see surface composition graphs Figure 5.10 to Figure 5.12). Thus, for reasons not clear, it seems that the additional presence of lecithin within the particle wall destabilized the polymer coat and allowed lactose to crystallize at the surface, although only a very small amount of lecithin was detected at the particle surface of lactose/lecithin/HPMC (90/5/5 wt%) powders (Figure 5.12).

The crystalline particulate structure of lactose/lecithin/Na-Cas and lactose/lecithin/WPI powders (Figure 20 D+E) was completely lost upon lactose crystallization, and this was similar to what was seen with crystallized lactose/lecithin (90/10 wt%) powder (Figure 5.9, C). In contrast, the crystalline powder structures of lactose/Na-Cas and lactose/WPI powders (both 90/10 wt% solid fraction) (Figure 3.17 and 3.18, Chapter 3, Part B) clearly showed an intact particulate structure, where particles were partly separated and partly joined by solid crystal bridges. Thus, it seems that the additional presence of lecithin within a spray-dried lactose/protein matrix affects the powder structure and lactose crystallization at the particulate. It can be assumed that the additional presence of low molecular weight lecithin

decreases the overall glass transition temperature of the powder mixture, whereas large, high molecular weight proteins contribute to a higher glass transition temperature, resulting in the powder having higher stability against crystallization and caking. This would also explain why the protein-containing lactose/HPMC powders were the only ones that did not transform into a hard brittle cakes upon lactose crystallization, but instead formed soft, pliable cakes.

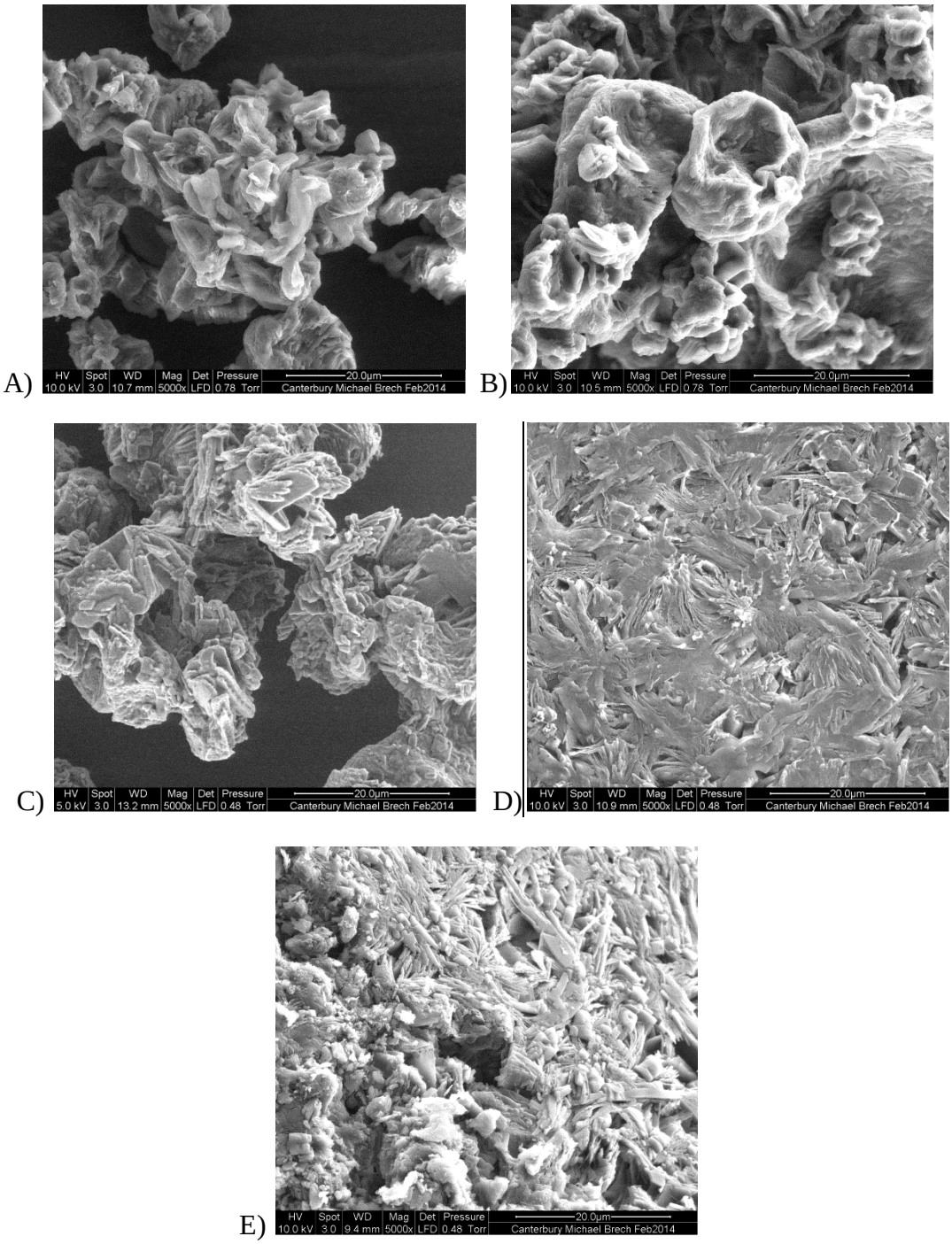

Figure 5.20: Particle morphology of spray-dried powders, analyzed by SEM(5,000x magnification), after lactose crystallization. A: Lactose/HPMC/Na-Cas=90/5/5, B: lactose/HPMC/WPI=90/5/5, C: lactose/HPMC/lecithin=90/5/5, D: lactose/Na-Cas/lecithin= 90/5/5, E) lactose/lecithin/WPI=90/5/5.

5.4. CONCLUSION

Part A:

Adding small quantities of surface active additives to a lactose solution prior to spray drying increased the powder yield and flowability of lactose powders. High-molecular-weight surface-active molecules, such as proteins and polymers, accumulated on the droplet surface during drying at the expense of the smaller-molecular weight lactose, and reduced particle stickiness by providing a coating material with a relatively high glass transition temperature. Na-Cas was the most promising additive for improving both spray dryer yield and powder flow. HPMC resulted in the best powder flow, however it caused low powder bulk densities, relatively low product yields and long wetting times. AMF offered no improvement in product yield or powder flow due to its sticky nature, caused by the low melting-point of fat. Lecithin and gelatine both increased product yield, although, of these two additives, only gelatine resulted in a significant improvement in powder flow. None of the additives tested improved wettability above that of the pure lactose powder.

Only HPMC prevented lactose from forming a hard brittle cake upon crystallization during storage at ambient room conditions. Gelatine caused the greatest delay in lactose crystallization; gelatine-containing lactose powder required a higher humidity and absorbed more moisture than any other powder tested, before crystallization occurred. Besides gelatine, HPMC and Na-Cas were also very efficient in delaying lactose crystallization. Crystallization of fat-coated lactose powder occurred earlier and at lower relative humidities compared with Na-Cas-, HPMC- and gelatine-containing lactose powders. Lecithin as coating additive resulted in only slight crystallization delays, probably due to its low molecular weight, which caused only a minor increase in glass transition temperature via hydrogen bonding with lactose. Generally, larger molecules such as proteins, which have a high affinity for lactose molecules, are better at increasing glass transition temperatures and delaying lactose crystallization.

Part B:

Surface competition between various surface active molecules was investigated, as was the effect of binary combinations of additives on the final particle surface composition, the powder functional properties, and the powder stability upon lactose crystallization. HPMC

was the only additive which was able to completely exclude other competing species, such as milk proteins and lecithin, from the droplet surface during spray drying and film drying. The most likely reason for this exclusion is its higher surface activity and highly flexible structure, which allows it to re-arrange very quickly upon adsorption and exclude other additives due to steric effects. Solute segregation and competitive adsorption of differently sized surface active species during spray drying did not appear to be influenced by a possible Peclet number effect or by moisture content gradients. When lecithin and Na-Cas competed for the droplet surface during spray drying, lecithin dominated at combined additive concentrations of 5wt% (2.5wt% lecithin, 2.5wt% Na-Cas) and higher. For slow drying films, the opposite occurred and Na-Cas dominated the film surface, probably because in a film drying system Na-Cas had more time available to re-arrange, stretch and therefore exclude the smaller lecithin from the air-water interface. For reasons not clear, WPI dominated the particle surface when competing with lecithin, despite its lower surface activity. Thus other factors, such as protein-protein, protein-surfactant and protein-surface interactions, also seem to play an important role in surface competition. This shows that competitive adsorption phenomena between different surface active species is very complex and depends on various different factors that require further investigation.

The presence of different additives within spray-dried lactose had a large impact on powder morphology, particle size, powder bulk density, powder functional properties and powder stability upon lactose crystallization. It was found that the presence of HPMC resulted in the largest particles with the lowest average density, with increasing particle size and decreasing bulk density being measured for higher HPMC bulk concentrations. HPMC-coated powders had the best powder flows of all powders tested here; however wetting times were very long, probably due to the low-density particles and the polymer coat that transformed into a highly viscous gel upon powder dissolution, making particle wetting difficult. The HPMC coat provided the best protection against powder caking, most likely due to the high total surface concentrations and strong cross-linking at its surface. The presence of lecithin within a spray-dried lactose solution had negative impacts on powder flowability and powder stability (caking), while wetting times were significantly improved.

In summary, HPMC is the best choice as a coating additive when powder stability and powder flowability need to be improved and a delayed powder dissolution is desired. When significantly improved powder flow as well as fast powder dissolution is desirable, this can

be achieved by using a combination of HPMC and lecithin as additives. The presence of both lecithin and protein as coating additives results in a powder that wets more easily than HPMC-containing powders, but has reduced flowabilty and stability, therefore it is not recommended to use lecithin in addition to a protein. The presence of both protein and HPMC as coating additives within spray-dried lactose does not cause any further improvement in powder properties and powder stability, compared with a pure HPMC or pure protein coating. However, the HPMC bulk concentration can be decreased from 10 to 5wt% when using a protein such as Na-Cas as additional coating additive (5 wt%), resulting in similar positive outcomes with regards to powder flow and powder stability and therefore reducing costs, since HPMC is more expensive than Na-Cas. This study shows that it can be useful to use two different coating additives, with similar or different properties, during spray drying to tailor powder properties in a way that cannot be realized with a single coating additive.

6. THE USE OF HYDROXYPROPYL-METHYLCELLULOSE AS A FUNCTIONAL COATING FOR SPRAY-DRIED PHARMACEUTICAL LACTOSE

6.1. INTRODUCTION

Surface active polymers such as hydroxypropyl-methylcellulose (HPMC) or methyl-cellulose (MC) are used as additives in the food and pharmaceutical industries, where they have microencapsulation and coating applications (Section 2.3.6). They are widely used to prepare sustained release matrix tablets because they are nontoxic, easy to handle and are effective in delaying the dissolution rate (Gao et al., 1996; Ishikawa et al., 2000; Tahara et al., 1995). Drug delivery systems for oral dosing that affect a delayed release of the drug are highly desirable, and the therapeutic results are superior to those achieved with drugs that dissolve rapidly (Tahara et al., 1995). An effective drug delivery system is one that will ensure a controlled, sustained drug release over a longer period, thereby reducing the risk of overdose or negative side effects, and removing the requirement to ingest several drug doses throughout the day.

In the work described in Chapter 5, it was found that HPMC was a promising coating material because it accumulated in high levels on the surface of lactose particles during spray drying, forming a stable protective coating that prevented excessive powder caking upon lactose crystallization. Moreover, HPMC was able to exclude other surface active species such as proteins or lecithin from the droplet surface. Powder flowability was significantly improved, while HPMC-coated particles were considerably inflated during spray drying and therefore had a low average particulate density. Compared to other suitable coating additives such as proteins, lecithin or gelatine, HPMC resulted in considerably longer wetting times and thus slower dissolution rates of lactose powders. These properties make HPMC useful in pharmaceutical powders, where it may protect proteins from surface denaturation and thus loss of functionality during spray drying (Elversson & Millqvist-Fureby, 2006), enable the delayed release of drugs from composite tablets (Takeuchi et al., 1998), and enhance its compressibility (Tahara et al., 1995).

As discussed in Section 2.1, lactose is widely used as pharmaceutical excipient for direct compression into a tablet because it improves the compressibility and final hardness of the tablet (Sollohub & Cal, 2010). The traditional way of preparing lactose for direct pelletizing is to disperse crystalline lactose in solution and then spray dry it to produce a good flowing powder containing both crystalline and amorphous fractions of lactose within the particles, as described in Section 2.1.2. For a conventional preparation of matrix tablets containing HPMC as coating, the active pharmaceutical ingredient (API) is usually in powder form, and is blended with lactose, mannitol or other additives and fillers to form a granulate, which is then pressed into a tablet before being coated by an appropriate coating material such as HPMC (Gohel & Jogani, 2005; Gonnissen et al., 2007), as shown in Figure 6.1 (4-step process).

Takeuchi et al. (2000) reported increased compatibility and glass transition temperature for composite particles of lactose with hydroxylpropylcellulose (HPC). Thus, if a polymer such as HMPC was added to the lactose solution before spray drying, a coated lactose powder would be produced that could offer a possible alternative to the commercial lactose powder used for direct pelletizing. Such a powder would enable tablets to be made via a 3-step process (Figure 6.1). Moreover, the excellent encapsulation efficiency of HPMC molecules, described in Chapter 5 (Part B) of this thesis, may allow certain APIs, such as proteins, to be spray-dried together with lactose and small amounts of HPMC to prepare coated composite powders in a novel "spray coating" process. Those composite particles would already contain the lactose necessary to improve the compressibility of the powder when producing the tablet (2-step process), and they would contain HPMC to delay dissolution of the tablet and hence delay the release of the API. Such a process would eliminate another production step, the blending of API with the coated lactose powder prior to pelletizing, and thus would further reduce costs (see Figure 6.1).

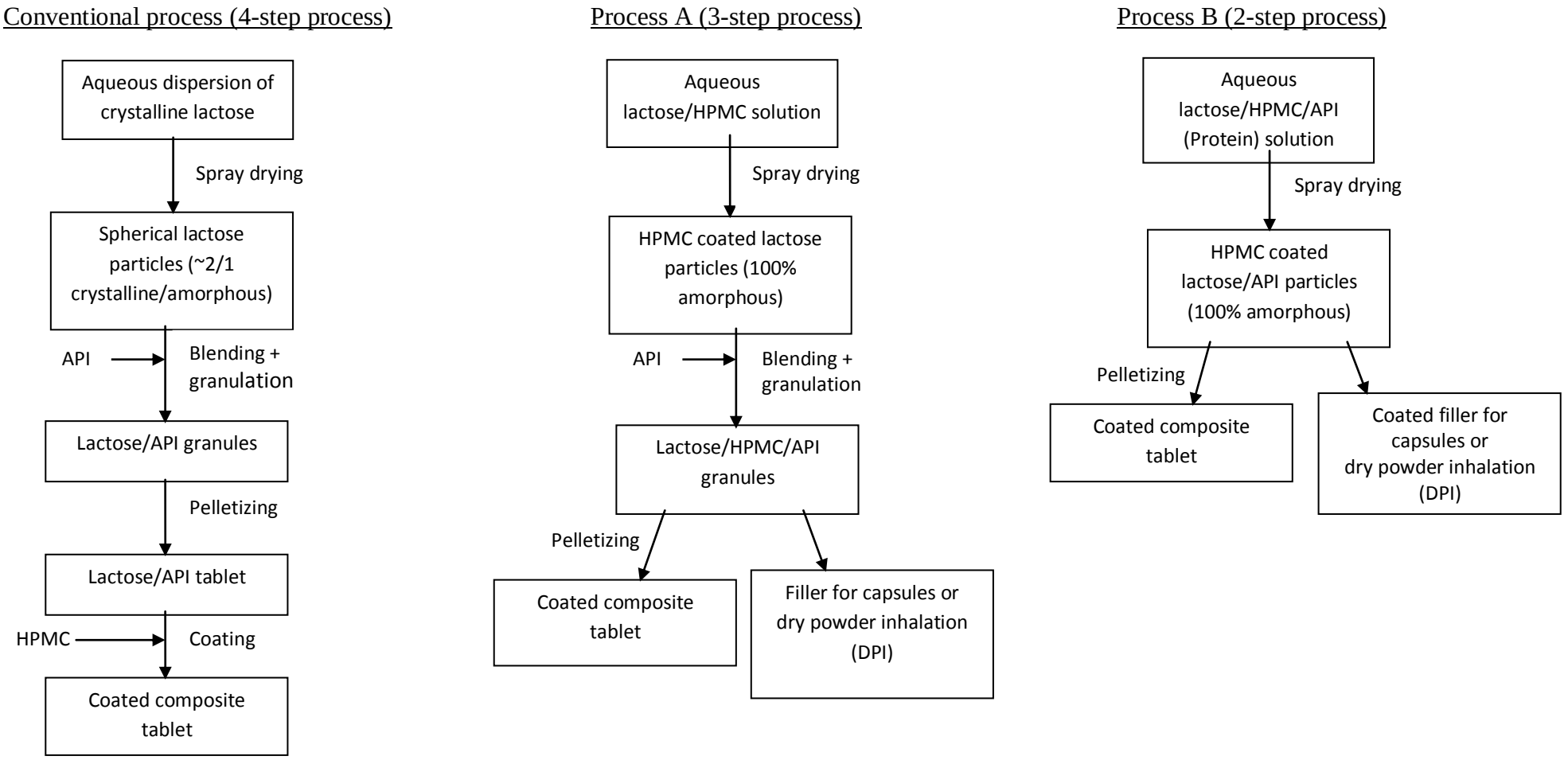

Figure 6.1: Comparison of a conventional (facilitated) production process of coated tablets via direct pelletizing with alternative processes (Gohel & Jogani, 2005; Gonnissen et al., 2007).

Goal of this investigation:

Part A of this chapter presents a novel way to prepare amorphous lactose particulates that are coated with the HPMC polymer. This part of the study looks at HPMC polymers of various molecular weight with regards to A) their surface activity and B) their ability to enrich at the droplet surface during spray drying. The ability of these polymers to act as protective coating for spray-dried lactose particles was explored, as was the impact of polymer molecular weight on particle morphology, powder density, and powder functional properties. As discussed in Chapter 5 (Part A), the powder yield was found to be affected by the glass transition temperature of the particle surface as well as the particulate density. Further to that, this chapter includes the results of investigations into whether particle stickiness and particulate density were affected by the molecular weight of HPMC molecules and what effect this had on the powder yield and powder flow.

Within Part B of this study, a novel one-step spray drying process was used to produce a coated composite powder which contained the API (here modelled by Na-Cas), the excipient (lactose) and the coating additive (HPMC) in various ratios. HPMC was investigated with regards to its ability to A) encapsulate Na-Cas during spray drying and thus provide a stable coating, B) improve powder functional properties and C) delay the release of the drug into an aqueous environment upon dissolution of the powder in a stirred vessel. The study also looks at the effect of the molecular weight of the HPMC polymer on the dissolution rate of the drug. As an additional test, the drug (Na-Cas) and the additive (HPMC) were spray-dried at various ratios in the absence of lactose in order to investigate the percentage of HPMC required to fully exclude the protein from the surface and thus completely coat it.

6.2. MATERIALS AND METHODS

Materials

α-Lactose monohydrate, Na-Cas and 3 different HPMC powders (Mw of approximately 10 kDa, 22 kDa and 86 kDa) were supplied by Sigma Aldrich (Germany). All HPMC powders had methoxyl content of 28-30% and hydroxypropyl content 7-12%. HPMC with M_W of approximately 10, 22 and 86 kDa had following properties: viscosities of 6 cp, 40-60 cp and 2,600-5,600 cp, respectively, for increasing molecular weights for 2% aqueous solutions at 20 °C.

Solution preparation

Part A:

Solutions of aqueous lactose and HPMC with various M_W , dry weight ratios of 99:1 and 9:1, and total solids content of 10 wt% were prepared in distilled water. Firstly, lactose solutions were prepared under constant agitation. The pH of the lactose solution was neutralized by adding aqueous NaOH solution and using a pH meter with temperature correction (CybersScan pH510, Eutech Instruments, Singapore) before the HPMC was carefully added under constant agitation at solution temperatures of around 80 °C, which caused the HPMC to be wetted instantly and disperse into small particles. The lactose/HPMC solution was then continuously agitated for 2 to 3 hours, during which time it cooled to temperatures of below 30 °C. This caused a complete hydration and swelling of the polymers.

Part B:

In order to evaluate the effect of varying HPMC bulk concentration, HPMC molecular weight, and pH conditions on the dissolution rate of Na-Cas, powders with different ratios of HPMC (Sigma Aldrich, USA), lactose (α-lactose monohydrate, Sigma Aldrich, Germany) and Na-Cas (casein sodium salt from bovine milk, Sigma Aldrich, New Zealand) were prepared using a one-step spray drying method. Six powders were produced with varying total solid ratios, using HPMC with a molecular weight of 22 kDa as the coating additive. Additionally, two further powders were produced using HPMC with molecular weights of 10 kDa and 86 kDa. Solids compositions of the powders are presented in Table 6.1.

Table 6.1: Solids compositions of powders produced.

Powder	Composition (lactose/HPMC/Na-Cas)
1	95/0/5
2	94/1/5
3	93/2/5
4	92/3/5
5	91/4/5
6	90/5/5
4A	92/3/5 (10kDa HPMC)
4B	92/3/5 (86kDa HPMC)

Spray drying

All solutions were spray-dried in a laboratory spray dryer (*NIRO Atomizer,* Copenhagen, Denmark), as described in Chapter 3 (Figure 3.1), at an air flow of 105±5 m^3 h^{-1}, inlet/outlet temperatures of 160/75±1 °C, atomization pressure of 0.6 bar, and solution feed rate and temperature of 1.6±0.2 kg h^{-1} and 40±1 °C, respectively. Three repeats were performed for each type of powder to obtain an estimate of uncertainty for the different powder analyzes.

Analysis

Surface tension measurements, X-ray photoelectron spectroscopy (XPS), particle size distribution, powder bulk density, powder flowability and wettability measurements were performed according to the methods described in Chapter 3. Scanning Electron Microscopy (SEM) was used according to the method described in Chapter 5.

Powder dissolution tests

Powder (1g) was added to 300 mL of deionised water heated to 36±1 °C and stirred at constant low agitation (350 rpm) using a magnetic stirrer/hot plate set. No pH correction was necessary, because the pH of the aqueous solution remained constant after the powders were dissolved. After time intervals of 1, 2, 4, 6, 10 and 20 minutes, approximately 15mL of the solution was drawn out of the beaker, using a Terumo 20mL syringe with a Millex 0.45µm syringe filter unit attached, and analyzed with a UV/VIS spectrophotometer (Shimadzu 1500 UV/Vis, Kyoto, Japan) according to its protein absorption intensity at 280 nm. Extracting the samples from a point near the edge of the beaker reduced the quantity of undissolved powder particles removed from the solution. Three repeats were performed for all spray-dried powders to obtain an estimation of measurement uncertainty. For data analysis purposes, various assumptions were made:

- The solution was assumed to be well mixed throughout the dissolution tests. Hence, the samples removed at each time period were representative of the entire solution at the time of sample extraction.
- The UV/Vis absorption at 280nm was assumed to be influenced only by the presence of Na-Cas in the solution. Hence, it was assumed the presence of lactose and HPMC

did not affect the measured absorbance. This was confirmed by producing spectra for pure aqueous lactose, pure aqueous HPMC and pure aqueous Na-Cas solutions at UV absorption of 280nm and showing a distinct peak at 280 nm for Na-Cas, and no significant peak at this wavelength for HPMC and lactose (Appendix A.4.1).

- The quantity of undissolved molecules removed from the solution via use of the filter was assumed to be negligible.
- The measured absorbance and concentration of protein in solution were assumed to be linearly related at the low protein concentrations investigated (confirmed by calibration curve, see Appendix A.4.1).
- The measured mass loss due to evaporation was < 1%. Thus, water evaporation during the time period of powder dissolution was assumed to be negligible.

6.3. RESULTS AND DISCUSSION

6.3.1. Part A: Effect of molecular weight of HPMC on surface accumulation, powder functional properties and powder caking of lactose/HPMC powders

Surface activity and surface composition of spray-dried composite particles

Figure 6.2 shows the measured surface tensions for the different lactose/HPMC solutions (10 wt% solids) with HPMC molecules of varying molecular weights (M_W). The presence of HPMC, which has a high surface activity, caused a reduction in the surface tension from that of pure water (~72 mN/m) to values between 46 and 51 mN/m. There was very little effect of the M_W of the HPMC molecules on the surface tension. The surface tension of lactose/HPMC (99/1 and 90/10 wt%) solutions was slightly lower for 10 kDa HPMC, compared with 22 and 86 kDa HPMC. Sarkar (1984) also measured higher interfacial tensions for solutions containing HPMC molecules of higher molecular weight. He proposed that the relative density of adsorbed polymers at the interface is lower when the Mw is higher, as these polymers have a tendency to form loops that extend into the bulk phase, resulting in lower attractive interactions between adsorbed molecules and solvent molecules.

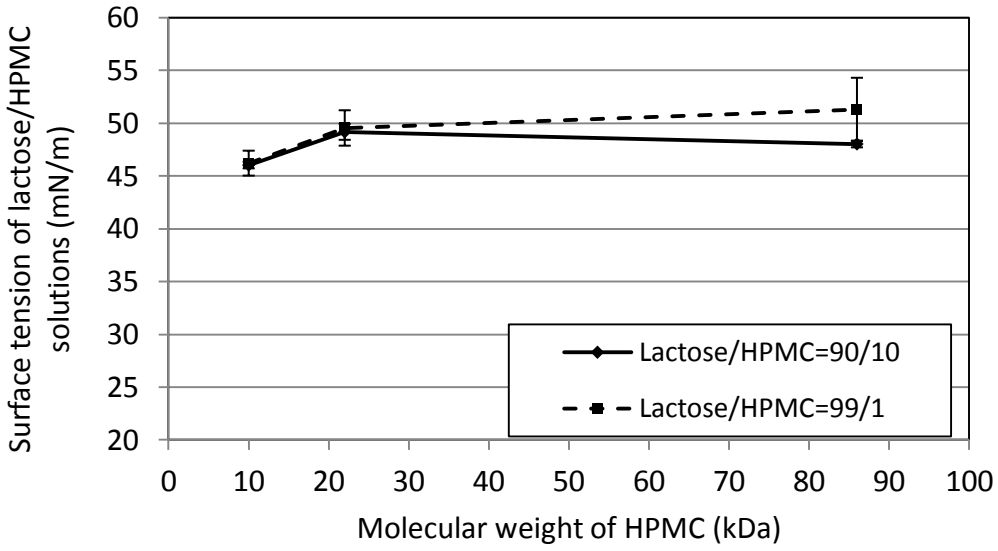

Figure 6.2: Surface tension measurements of 10wt% aqueous lactose/HPMC solutions with various M_W of the polymer.

The measurements did not reveal any significant difference in the surface tensions of aqueous lactose/HPMC solutions of 90/10 and 99/1 wt%. This indicates that only 0.1 wt% of the HPMC in solution was required to saturate the droplet surface with HPMC during the surface tension measurements. The measured surface tensions for the lactose/HPMC solutions in this study correlate well with the surface tension data obtained for 1 wt% lactose/HPMC solutions (~46 mN/m) measured by Arboleya and Wilde (2005), who used HPMC molecules with a M_W of 42 kDa.

Figure 6.3 shows that the M_W of the HPMC did not have a clear effect on its surface enrichment during spray drying, which suggests that polymer M_W does not significantly affect the surface activity, at least over the range of M_W used in this study. It can be expected that the largest HPMC (86 kDa) requires a longer time to diffuse towards the droplet surface due not just to its considerably higher M_W but also the higher solution viscosity. The short drying time could therefore have limited the diffusion of HPMC molecules to the droplet surface. However, although Figure 6.3 shows slightly lower HPMC surface concentrations for the high-molecular-weight HPMC (86 kDa) compared with the low-molecular-weight HPMC (10 and 22 kDa), differences are very small and there is not a clear, consistent trend. Chapter 5 (Part A) shows that, for additive bulk concentrations of 10 wt%, the surface enrichment of the 86 kDa HPMC polymer (~80%) was still higher than that of other smaller surface active molecules, such as lecithin (~0.75kDa) or Na-Cas (~24 kDa) (both ~70%

surface concentration), which suggests that also the large 86 kDa HPMC molecules had sufficient time to diffuse to the droplet surface during the short time period of spray drying. This indicates that the surface activity of molecules and their ability to be packed into a dense visco-elastic surface film, rather than their molecular sizes and thus diffusion rates within the drying droplet, are the dominant effects determining surface accumulation of a solute during spray drying. This supports the findings given in Chapter 5 (Part B).

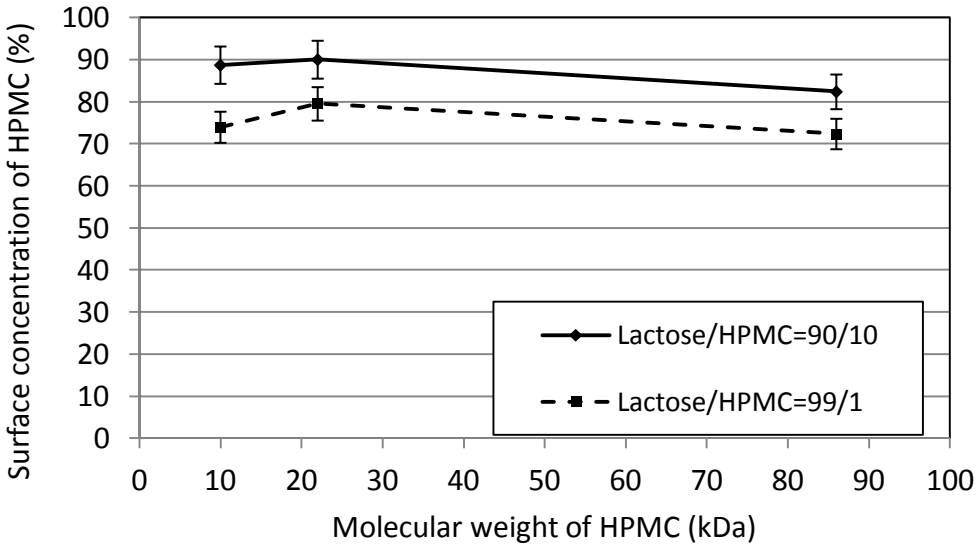

Figure 6.3: Effect of the M_W of the polymer on HPMC surface concentration of spray-dried lactose/HPMC powders.

Particle size and powder bulk density

Figure 6.4 and Figure 6.5 show the effect of the M_W of the HPMC polymers on the measured mean volumetric particle sizes and bulk densities of the spray-dried lactose/HPMC powders. Particle sizes clearly increased with increasing M_W of the HPMC molecule for both 99/1 wt% and 9/1 wt% lactose/HPMC powders (Figure 6.4). The M_W of HPMC had no clear effect on the measured bulk densities of the lactose/HPMC (99/1 wt%) powders, while, for the lactose/HPMC (90/10 wt%) powders, a significantly lower powder bulk density was observed for particles containing the 86 kDa HPMC compared with those containing the smaller 10 and 22 kDa HPMC molecules (Figure 6.5). The increased particle size and decreased bulk density of lactose/HPMC powders containing HPMC molecules of higher M_W can be explained by the higher flexibility of these molecules. This would have led to a higher particle wall elasticity and thus increased expansion of spray-dried particulates during spray

drying. This is supported by the data of Park and Chinnan (1995), who measured a greater degree of elongation in cellulose-based films when the M_W of the polymer methyl cellulose (MC) was increased. The higher solution viscosities produced by higher molecular-weight polymers would have also contributed, since larger droplets were formed upon atomization leading to the production of larger particles. A higher total number of HPMC molecules within the particle wall of lactose/HPMC (90/10 wt%) particles, compared with lactose/HPMC (99/1 wt%), increased the elasticity of the entire particle wall, causing larger particles of lower density.

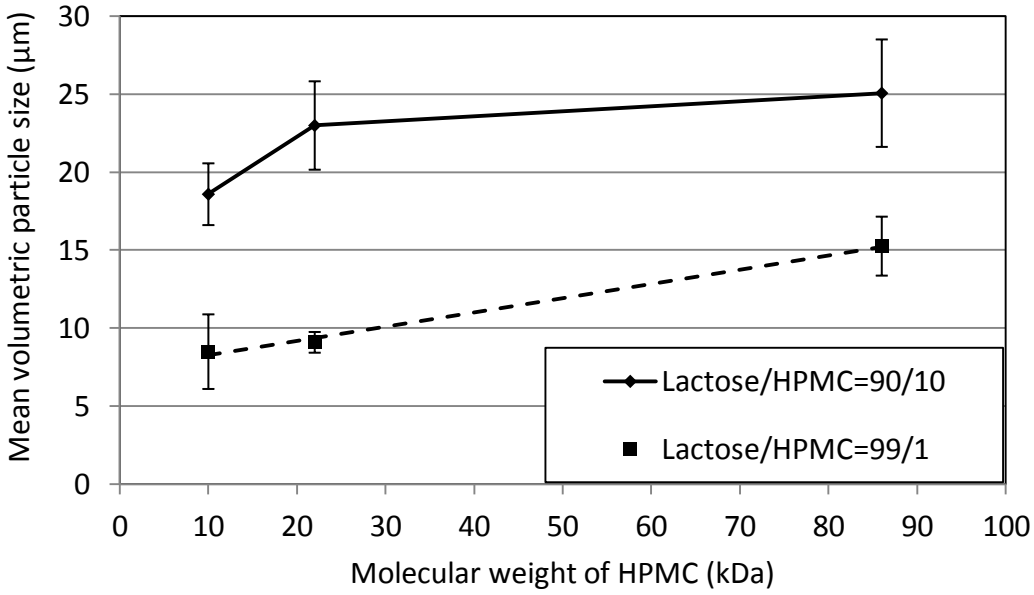

Figure 6.4: Effect of the M_W of the polymer on the mean volumetric particle size of spray-dried lactose/HPMC powders.

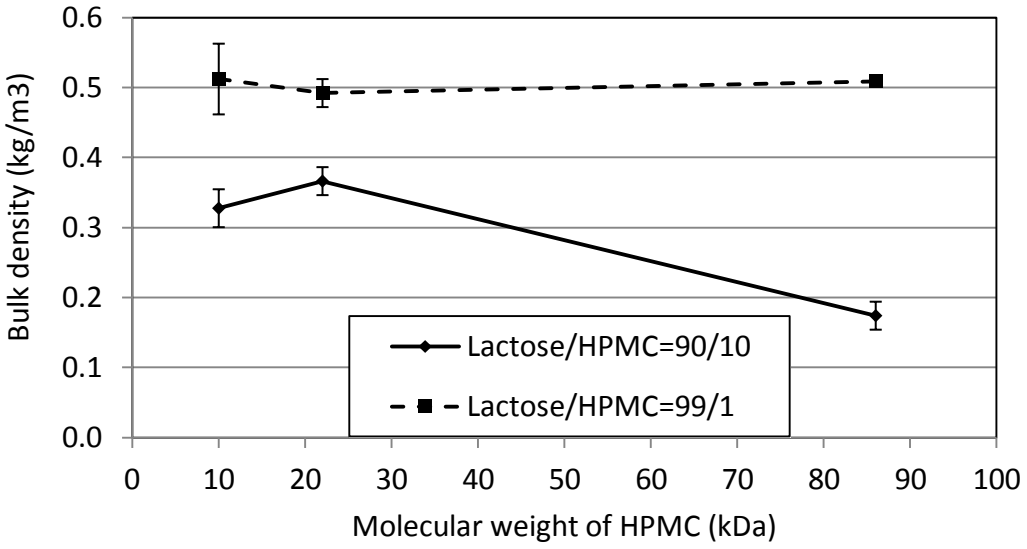

Figure 6.5: Effect of the M_W of the polymer on the powder bulk density of spray-dried lactose/HPMC powders.

Powder morphology

The extensive folding of HPMC/lactose particles, caused by the deflation of the particle wall during drying, can be seen in Figure 6.6. No clear differences in the surface morphologies of the different particles were observed. In other words, neither the lactose/HPMC solid ratio nor the M_W of the HPMC polymer affected surface texture of the spray-dried particles. This suggests that even relatively small HPMC polymers of 10 kDa can induce a sufficiently high particle wall elasticity to allow the particles to inflate and deform during spray drying, resulting in a highly wrinkled, folded particle surface structure. It also suggests that this inflation and deformation of particles occurs with HPMC concentrations as low as 1 wt%.

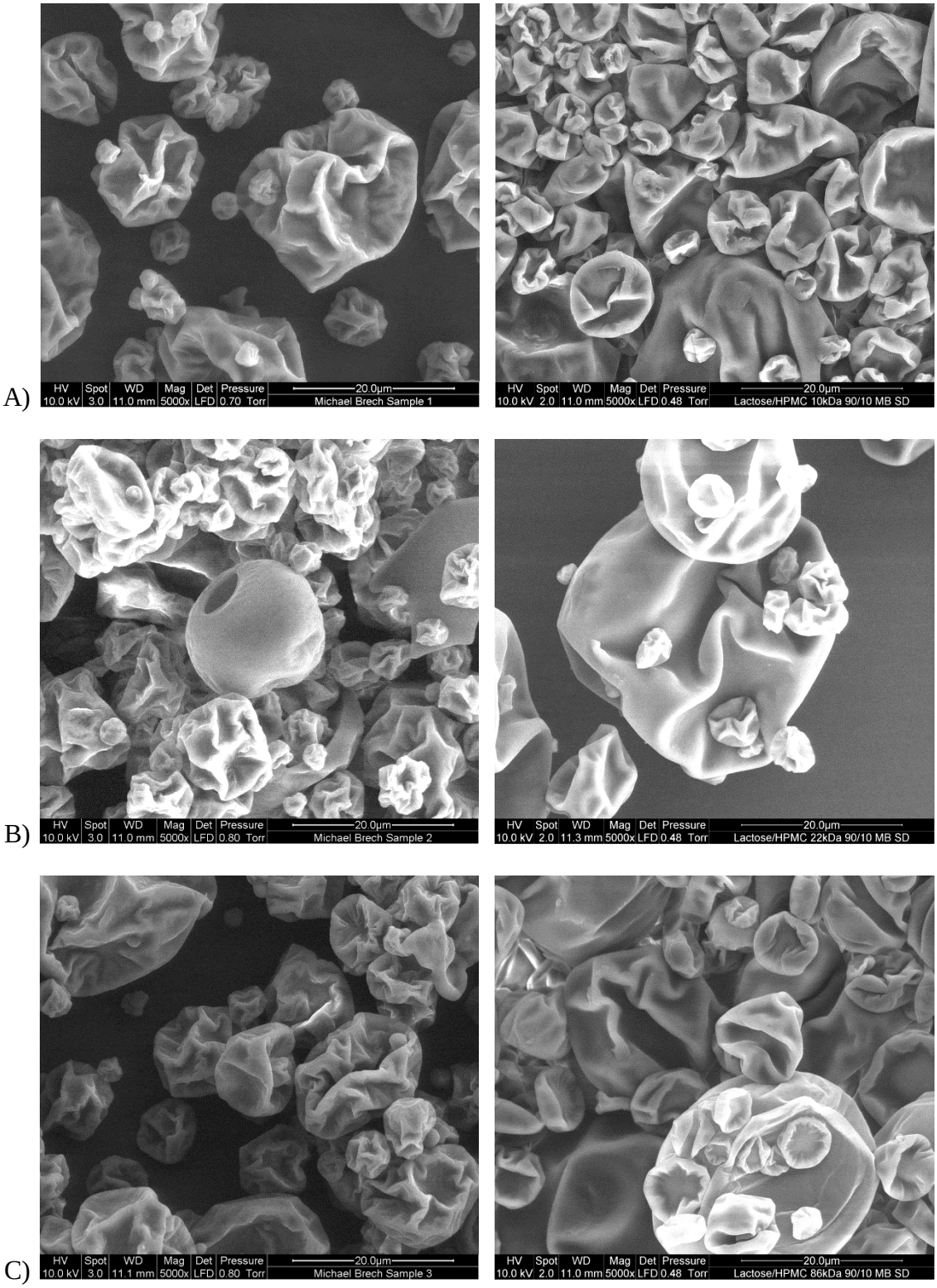

Figure 6.6: Effect of the M_W of the polymer on the particle morphology of spray-dried lactose/HPMC powders (5,000 magnification): A) M_w=10 kDa, B) M_w=22 kDa, C) M_w=86 kDa. Left: Lactose/HPMC=99/1 wt%, right: Lactose/HPMC=90/10 wt%.

Powder yield

Powder yields decreased with increasing HPMC and with increasing M_W of the polymer (Figure 6.7). It might be expected that the higher HPMC surface concentration (Figure 6.3) of the lactose/HPMC (90/10 wt%) particles and/or higher molecular-weight HPMC would have resulted in a higher glass transition temperature at the particulate surface and therefore lower surface stickiness and consequently higher product yields. However, it seems that the lower product yield obtained with higher HPMC bulk concentration and/or higher-grade HPMC (Figure 6.5) was the result, albeit indirectly, of its decreased particulate density and thus the lower separation efficiency of the cyclone.

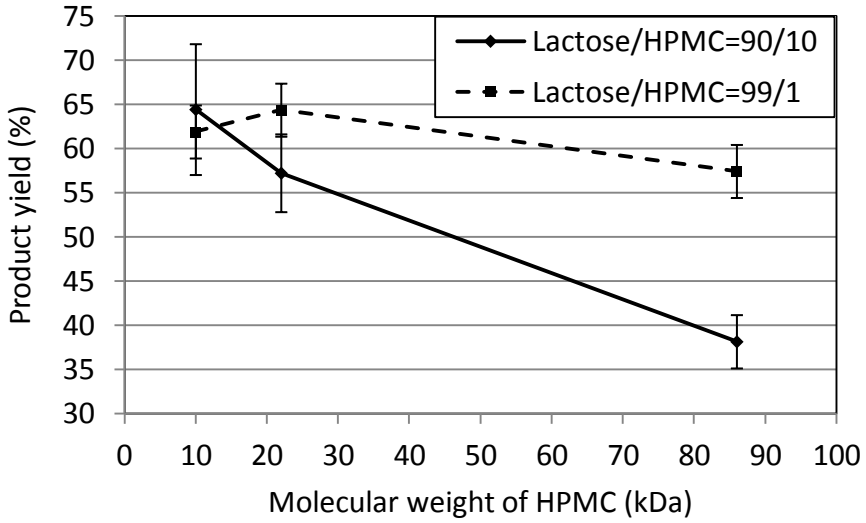

Figure 6.7: Effect of the M_W of the polymer on the powder yield of spray-dried lactose/HPMC powders.

Flowability

Figure 6.8 shows the powder flow through a vibrating sieve attached to a shaking apparatus. As reported in Chapter 3 (Part B), the flowability of pure lactose powder through this sieve is very low due to the highly agglomeration nature of this powder, caused by the low glass transition temperature of the particulates as well as the small particle sizes. The addition of 1 and 10 dry wt% HPMC to the lactose solution caused a significant improvement in powder flow. As described previously, the adsorption of larger molecules such as HPMC causes the glass transition temperature of lactose to increase, which decreases droplet and particulate stickiness during spray drying (Adhikari et al., 2009a; Wang & Langrish, 2010).

This lower particle stickiness would have resulted in a less agglomerated powder with improved powder flows. All lactose/HPMC powders showed a similarly good powder flow, which suggests even the smallest (M_W 10 kDa) were of sufficient size to increase glass transition temperature and thus decrease the stickiness and agglomeration of spray-dried particles.

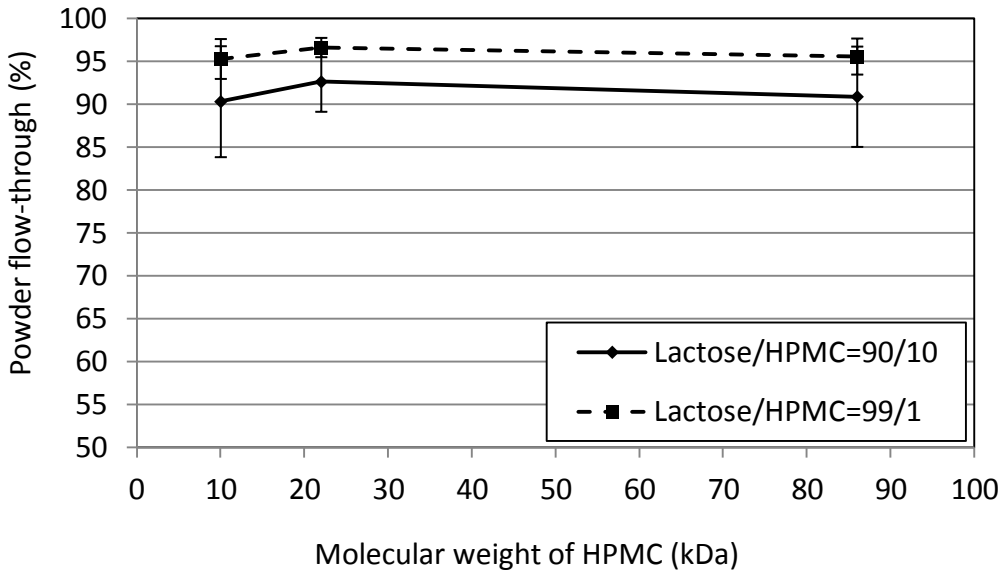

Figure 6.8: Effect of the M_W of the polymer on the powder flow of spray-dried lactose/HPMC powders.

The increase in particle sizes of HPMC-containing lactose powders compared with pure lactose powders (see Chapter 5) further contributes to decreased agglomeration and hence improved powder flow. Although higher surface concentrations of HPMC were found for lactose/HPMC (90/10 wt%) particles, this increase in surface concentration did not result in a measurable improvement in powder flow compared with the lactose/HPMC (99/1 wt%) powder. These experiments demonstrate that the presence of just 1 wt% of HPMC in the bulk is sufficient to decrease particle stickiness and powder agglomeration significantly. This finding can therefore be exploited to produce coated lactose powder with a considerably improved powder flow.

Wetting time

Figure 6.9 shows the effect of the molecular-weight of the HPMC molecule on the wetting time of the powder. Generally, the presence of HPMC on the surface of amorphous lactose powder significantly increases the wetting time compared with pure amorphous lactose powder, which is wetted instantly upon exposure to the water surface, as reported in Chapter 5. As discussed before, the increase in wetting times for HPMC-containing lactose powder is most likely caused by the higher buoyancy of the larger particles of lower density. Another factor is the masking of the hygroscopic surface of the polar lactose particles by the long polymer molecules, which form a rather hydrophobic film due to their tendency to orientate their hydrophobic groups (methoxy- and propylhydroxy-) towards the air phase upon adsorption (Sarkar, 1984). Furthermore, it was noticed that a gel layer was formed at the water-powder interface when the HPMC-coated lactose powders were dissolved in water, due to the swelling of the polymers, as also reported by Ishikawa et al. (2000). This may have further delayed the wetting of these powders due to the resistance of water to penetrate through this gel barrier.

Increasing the M_W of the HPMC resulted in an increase in wetting time for both lactose/HPMC powders (99/1 wt% and 90/10 wt%). This increased wetting time is most likely to be caused by a reduction in the particulate density and hence an increase in particle buoyancy. Moreover, in this study the gel layer formed on the water/powder interface upon dissolution of the powder appeared to be thicker and more distinct for powders containing the higher molecular weight HPMC. This would have resulted in a slower release and dissolution of lactose within the particles, as also reported by Ishikawa et al. (2000), who measured longer dissolution times for HPMC-coated tablets with increasing M_W of the polymer. Thus, high-molecular-weight polymers are useful coating agents, especially where the delayed release of a drug is desired.

Lactose/HPMC (90/10 wt%) powder showed significantly longer wetting times than lactose/HPMC (99/1 wt%) powder due to the higher concentration of HPMC in the bulk, which produced particles of lower bulk density (Figure 6.5). Higher concentrations of HPMC at the particle surface would have furthermore resulted in a thicker polymer film and thus the formation of a thicker, more viscous gel layer upon powder dissolution, as also suggested by Ishikawa et al. (2000).

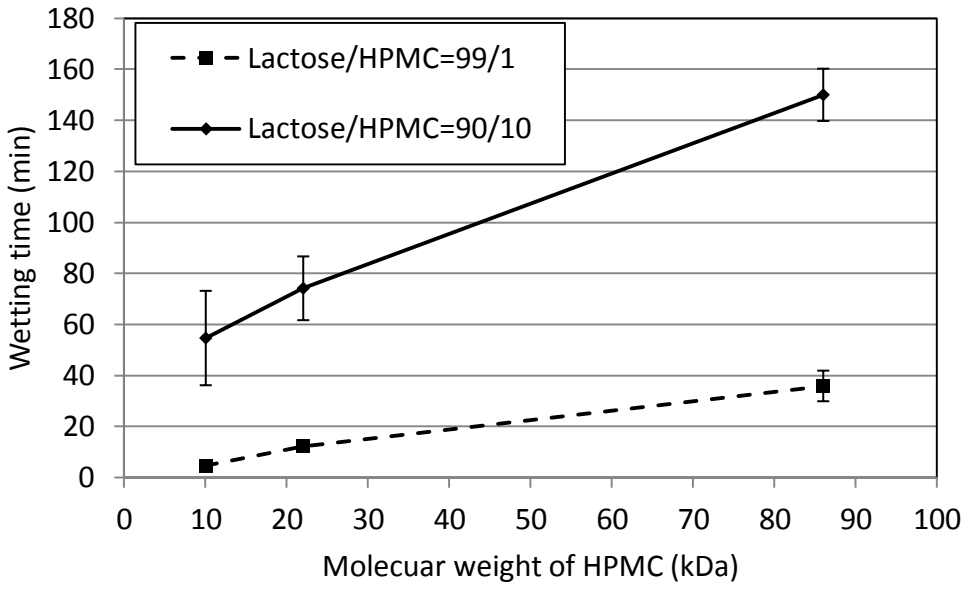

Figure 6.9: Effect of the M_W of the polymer on the wetting time of spray-dried lactose/HPMC powders.

Lactose crystallization and caking

Figure 6.10 shows SEM pictures of particulates of the various lactose/HPMC powders, after they had been stored at ambient conditions for several weeks to allow lactose crystallization. The molecular weight of the HPMC did not have an observable effect on the crystalline particulate structure for both lactose/HPMC powders (99/1 wt% and 90/10 wt%). For lactose/HPMC (99/1 wt%) particles (Figure 6.10, left), the particulate structure partially collapsed and surface crystals were clearly present, while no clear crystals could be observed on the particle surface of lactose/HPMC (90/10 wt%) powders (Figure 6.10, right). This suggests that, irrespective of the M_W of the polymer, a concentration of 10 wt% of HPMC within the bulk is sufficient to provide structural support to the particle upon lactose crystallization, while the presence of only 1 wt% of HPMC is not.

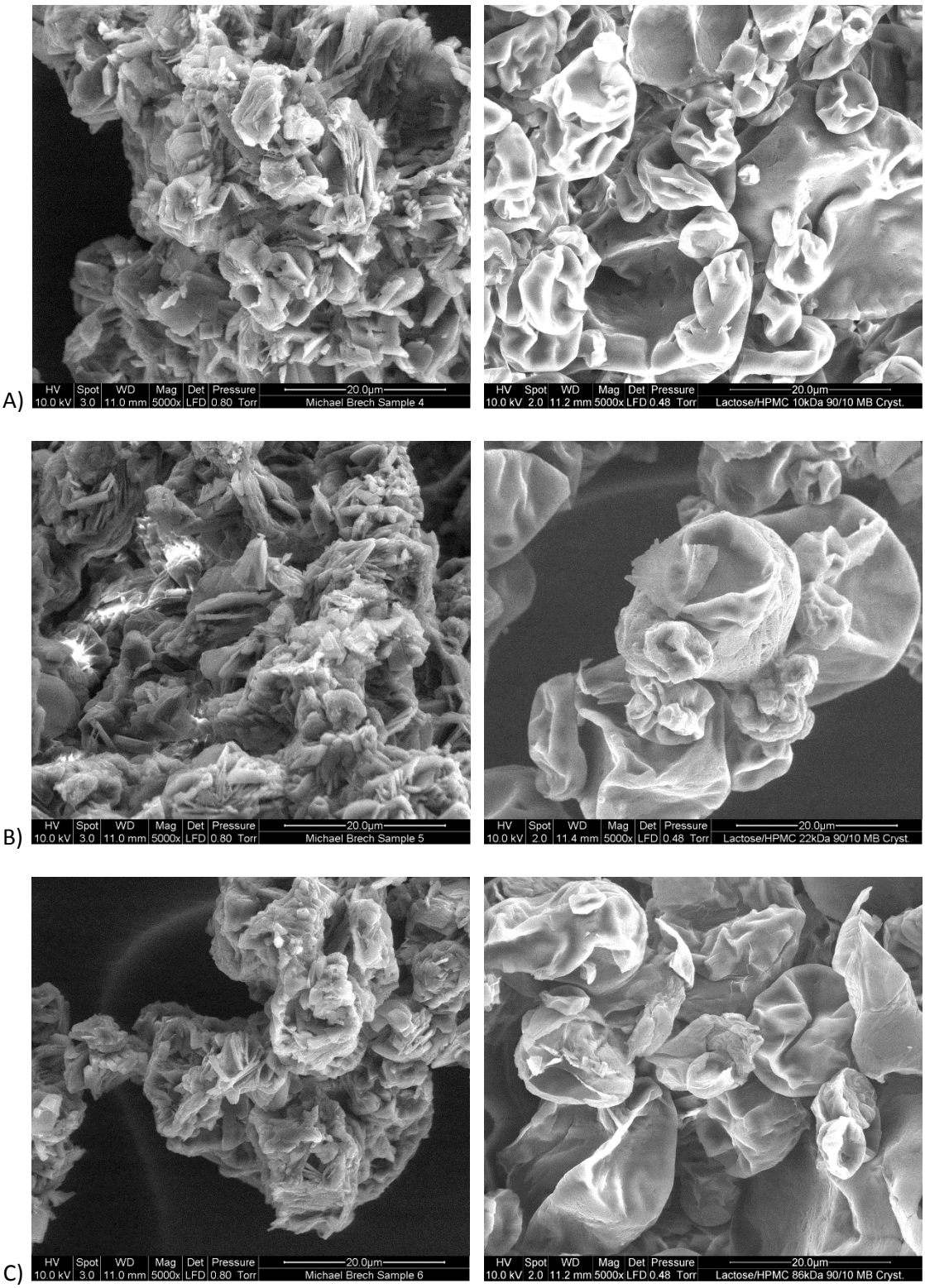

Figure 6.10: Effect of the M_W of the polymer on the crystalline powder structure of spray-dried lactose/HPMC powders (5,000 magnification): A) M_w=10 kDa, B) M_w=22 kDa, C) M_w=86 kDa. Left: Lactose/HPMC=99/1 wt%, right: Lactose/HPMC=90/10 wt%.

This was further confirmed by caking assessments of the crystalline powders. The lactose/HPMC (99/1 wt%) powders transformed into hard brittle cakes, but the

lactose/HPMC (90/10 wt%) powders did not. As already mentioned in Chapter 5, 10 wt% of HPMC was sufficient to prevent the powder from transforming into a hard cake. While the lactose/HPMC (90/10 wt%) powder that contained 10 and 22 kDa HPMC transformed into a soft, pliable cake, the presence of large 86 kDa HPMC polymers completely prevented the powder from caking and it thus remained free flowing. Larger HPMC polymers are therefore the preferred choice to stabilize amorphous lactose powder against powder caking upon lactose crystallization.

6.3.2. Part B: Investigation of HPMC as functional coating for pharmaceutical lactose powder with delayed drug-release

Surface composition

Figure 6.11 shows the surface compositions of spray-dried Lactose/Na-Cas/HPMC composite particles with increasing HPMC/Na-Cas solid ratios from 0 to 1. The particle surface composition of spray-dried lactose/Na-Cas particles, in the absence of HPMC, showed a clear accumulation of the Na-Cas protein at the particle surface, due to the high surface activity of Na-Cas proteins. The addition of only 1 wt% (of total solids) of HPMC resulted in a high degree of exclusion of Na-Cas proteins, despite the bulk concentration of Na-Cas being five times higher than that of HPMC. HPMC bulk concentrations of 2 wt% were sufficient to fully exclude Na-Cas from the droplet surface. This is consistent with the findings in Chapter 5 (Part B), where Na-Cas was also excluded from the droplet surface at HPMC/protein bulk ratios of 1:1 when the combined bulk concentration of additives was 5% (2.5 wt% HPMC, 2.5 wt% protein) (see Figure 5.10). In the present study, HPMC bulk concentrations above 2 wt% did not cause further changes in the powder surface composition, which suggests that the maximum packing density of HPMC polymers at the droplet surface had already been reached.

Figure 6.12 shows the surface composition of spray-dried HPMC/Na-Cas powders in the absence of lactose. A HPMC/protein ratio of 1:99 resulted in a HPMC surface concentration of 35%. At a bulk ratio of 20:80, the protein was complety excluded from the particle surface. This shows that HPMC only needs to be present at 20wt% of the solid concentration of Na-Cas in order to fully exclude Na-Cas from the surface. This is consistent with the results in Figure 6.11 for particles of HPMC, Na-Cas and lactose, and demonstrates the high degree of efficiency with which HPMC can encapsulate surface active proteins. Hence, a one-step

spray drying process is a successful method for the preparation of solid oral formulations of coated particles (with HPMC as coating material) that contain an API (protein) and an excipient (lactose).

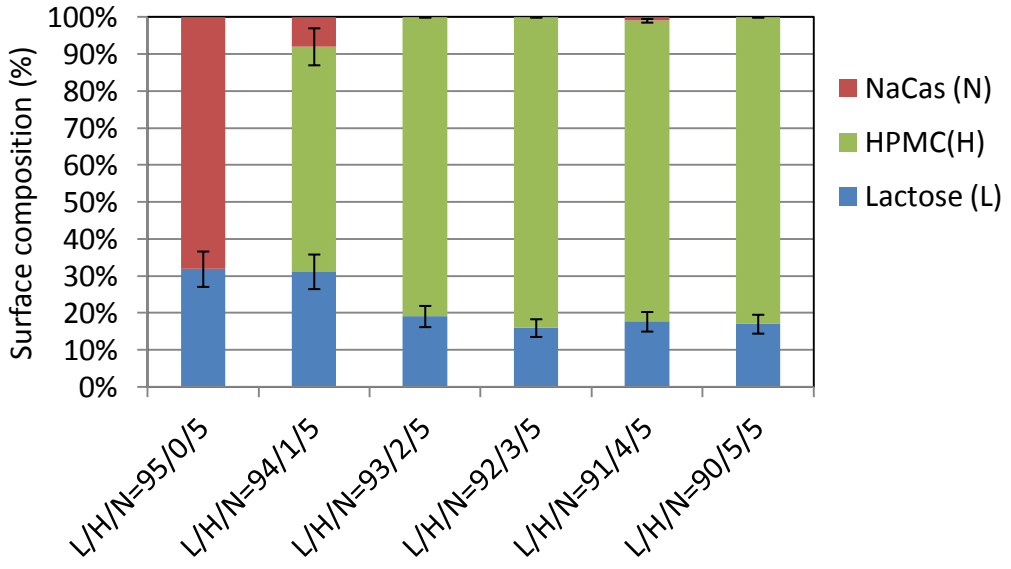

Figure 6.11: Surface composition of spray-dried lactose/Na-Cas/HPMC particles.

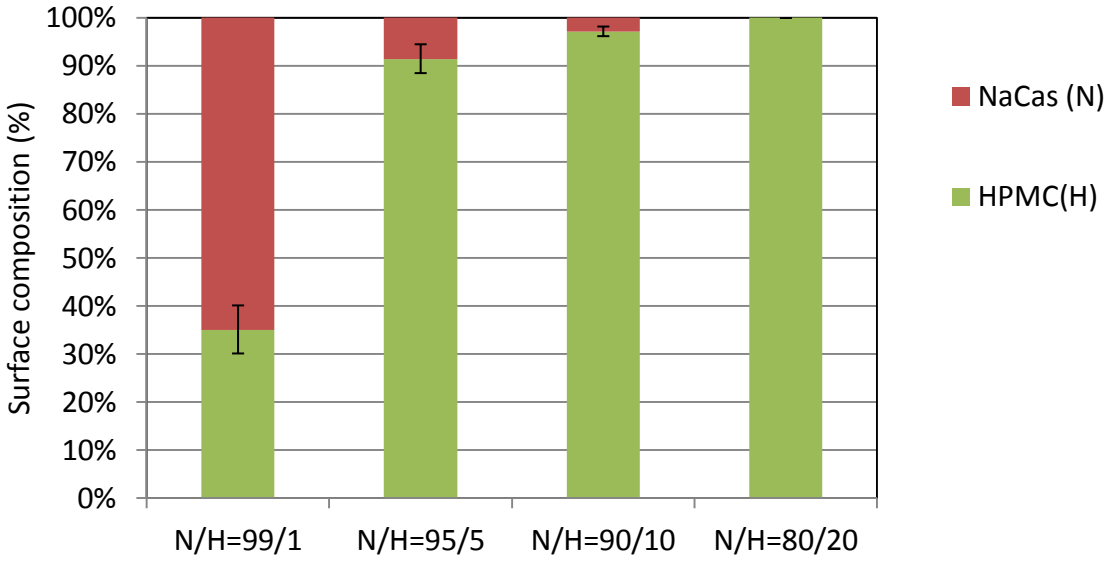

Figure 6.12: Surface composition of spray-dried Na-Cas/HPMC particles.

Figure 6.13 shows the surface composition of lactose/HPMC/Na-Cas (92/3/5 wt%) powders prepared with HPMC of various molecular weights (M_W): 10, 22 and 86kDa. The lactose/HPMC/Na-Cas powder containing the 22kDa HPMC had no Na-Cas on the particle surface, whereas lactose/HPMC/Na-Cas powders that contained the 10 kDa and 86 kDa HPMC were observed to have a small amount of Na-Cas present at the particulate surface. This anomaly was most likely caused by a margin of error in the XPS analysis or small impurities in the product from a previous spray drying run. Part A of this chapter also showed no clear effect of the M_W of HPMC on the surface composition of spray-dried lactose/HPMC powders.

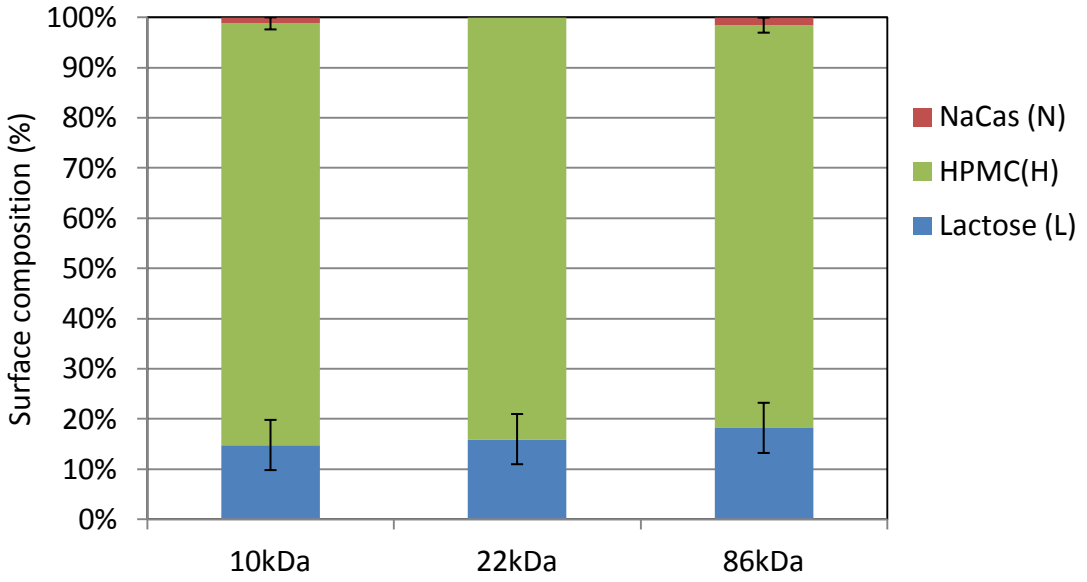

Figure 6.13: Surface concentration of spray-dried lactose/Na-Cas/HPMC=92/3/5wt% particles.

Particle size and powder bulk density

The particle sizes and bulk densities for lactose/HPMC/Na-Cas powders with constant Na-Cas bulk concentrations (5 wt%) and increasing HPMC bulk concentration are shown in Figure 6.14. The presence of HPMC caused an increase in particle size and a decrease in powder bulk density. This trends is consistent with previous results (Figure 6.3), which showed larger particles of lower density to be produced when the polymer bulk concentrations was increased from 1 to 10 wt%, caused by a higher wall elasticity. The effect of HPMC on the particle size and density was decreased for HPMC solids concentration

above 2%, probably because the wall elasticity was not significantly increased with higher HPMC bulk concentrations.

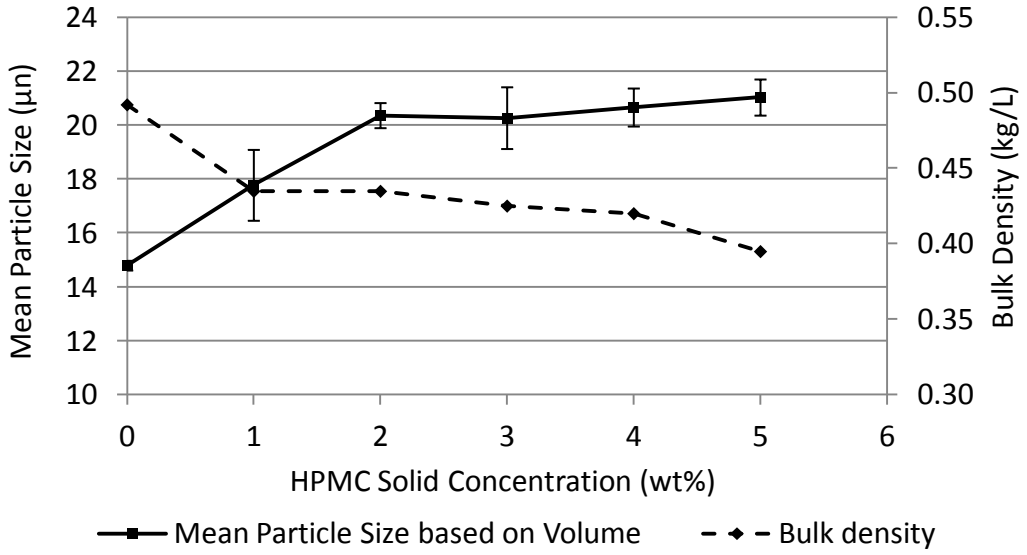

Figure 6.14: Mean particle size and bulk density measurements for composite powders with varying HPMC (22kDa) concentration: lactose/HPMC/Na-Cas=95/0/5, 94/1/5, 93/2/, 92/3/5, 91/4/5, 90/5/5 wt%.

Figure 6.15 shows the effect of HPMC molecular weight on the bulk density of the lactose/HPMC/Na-Cas powders with bulk concentrations of 92/3/5 wt%. A clear decrease in bulk density with an increase in HPMC molecular weight can be seen. This is consistent with the results of Part A of this chapter, and suggests the larger HPMC polymers have a higher flexibility that results in higher particle wall elasticity and thus greater particle expansion during spray drying.

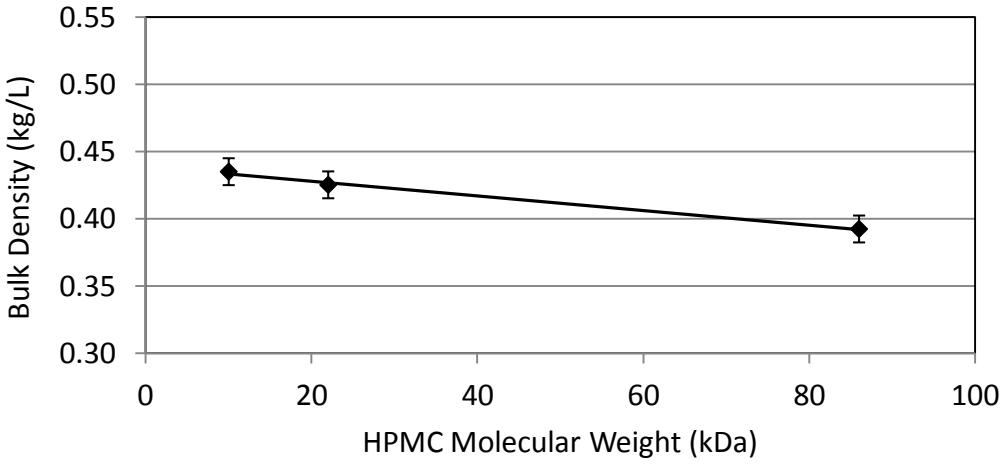

Figure 6.15: Bulk density of lactose/HPMC/Na-Cas=92/3/5 wt% powders with varying M_W of the HPMC.

Powder flowability

Lactose/Na-Cas/HPMC powders had significantly greater flowability than lactose/Na-Cas (95/5 wt%) powders, and this improvement was seen at HPMC bulk concentrations as low as 1 wt% (Figure 6.16). However, there was little change in the flowability when HPMC bulk concentrations were increased above 1 wt%, most probably because the spray-dried powders showed no significant changes in particle size (Figure 6.14) or surface composition (Figure 6.11) with increasing HPMC bulk concentration. The experiments described in Chapter 5 (Part A) also revealed improved powder flow for HPMC-containing lactose powders compared with Na-Cas-containing lactose powders.

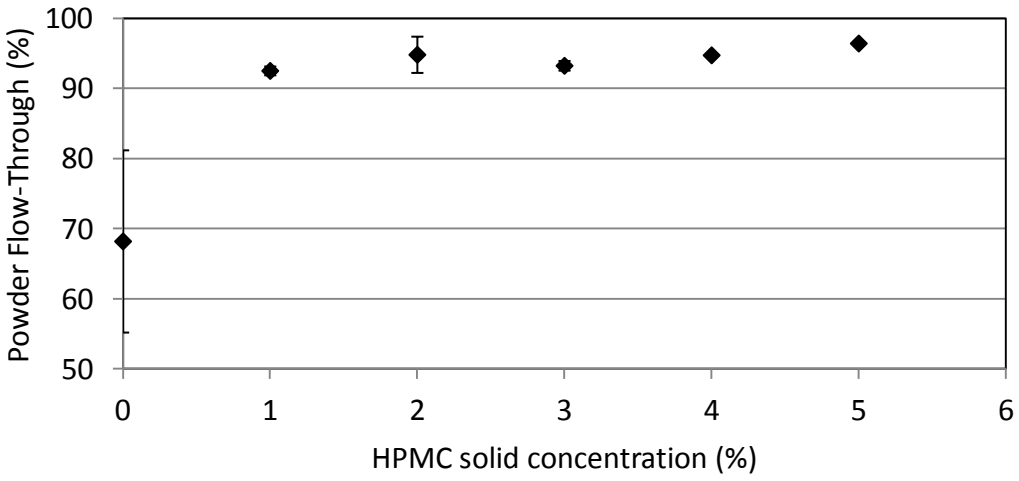

Figure 6.16: Flowability of composite powders with varying HPMC (22kDa) concentration: lactose/HPMC/Na-Cas=95/0/5, 94/1/5, 93/2/, 92/3/5, 91/4/5, 90/5/5 wt%.

Dissolution tests

Figure 6.17 shows the dissolution profiles of spray-dried lactose/Na-Cas (95/5 wt%) (without any HPMC) and lactose/HPMC(22kDa)/Na-Cas powders with the same protein bulk concentration (5wt%) but different HPMC bulk concentrations (2wt% and 5wt%). As the particulates dissolved, protein was released into solution and this can be seen in Figure 6.17 by a rise in the dissolved protein concentration for increasing mixing times, up to a point where all particles were dissolved, resulting in a 100% protein dissolution.

There was a clear dissolution delay of Na-Cas from the powder when HPMC was added. While the plateau (total protein dissolution) of a lactose/Na-Cas (95/5 wt%) powder was already achieved between 4 and 6 minutes, significantly longer times were required in the

presence of 2wt% HPMC (~ 10 minutes) and 5 wt% HPMC (~20 minutes) to achieve a complete protein dissolution. There were inconsistencies in the powder distribution on the water surface and powder agglomeration, both of which clearly affected the powder dissolution. Furthermore, the low bulk density of the powder interfered with wetting by hindering the sinking of the particulates beneath the water surface during stirring, thus causing longer dissolution times and higher time constants. However, Figure 6.14 shows that the powder bulk density did not change appreciably at HPMC bulk concentrations above 1 wt%. Thus, the increase in dissolution times of the various powders with increasing HPMC bulk concentrations were most likely affected by a thicker and more viscous polymer gel forming around the dispersed particles upon wetting, which delayed the dissolution of the powder and thus delayed the release of the proteins. This is supported by the work of Ishikawa et al. (2000), who reported that the thickness of this gel layer is relative to the HPMC concentration, and that this is the reason for the longer delays in drug release from HPMC-coated tablets with higher HPMC concentrations.

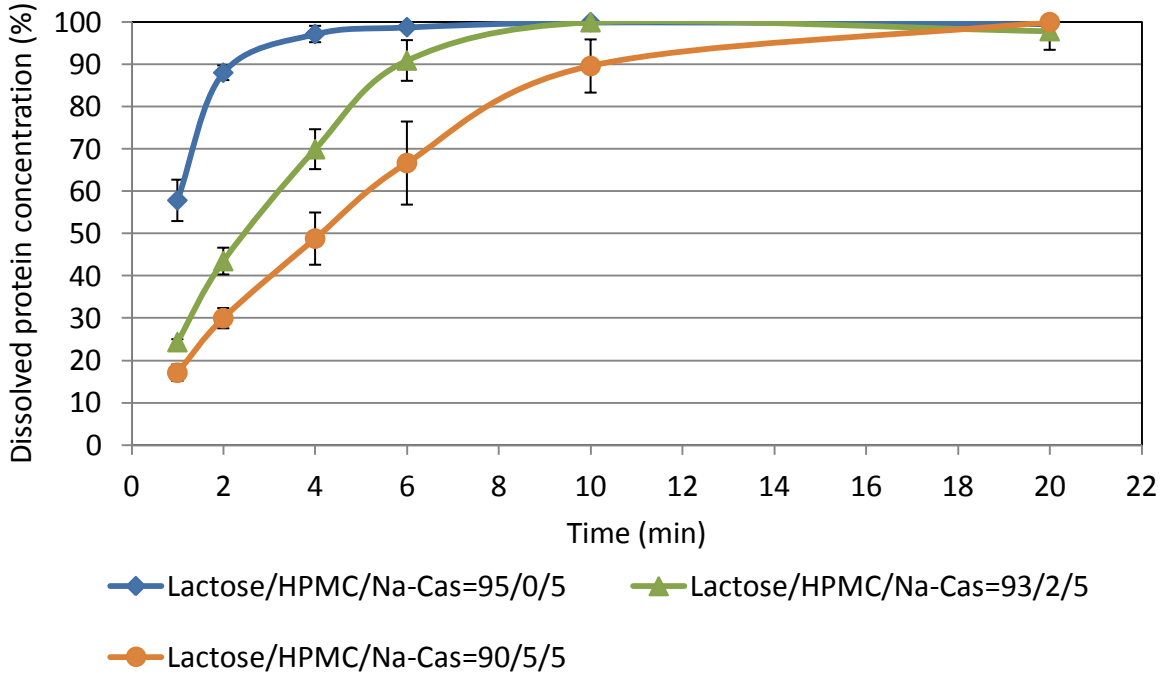

Figure 6.17: Dissolution profiles of Na-Cas protein, dissolved from lactose/Na-Cas=95/5 wt% and lactose/HPMC/Na-Cas powders with various HPMC (22kDa) bulk concentrations.

Figure 6.18 shows the effect of the M_W of the HPMC polymer on the protein dissolution with time. A clear delay in the protein dissolution time was measured when the M_W of the polymer was increased from 10 to 86 kDa. This is consistent with the results in Part A of this

study, where longer wetting times were measured for lactose/HPMC powder containing HPMC of higher M_W. Firstly, the decrease in bulk density of powders containing a higher-molecular-weight HPMC (Figure 6.15) was likely to have contributed to poorer wetting and thus longer dissolution times of the powders. Secondly, researchers such as Morrow et al. (2011), Ishikawa et al. (2000) and Gao et al. (1996) clearly showed a correlation between drug release rates and the molecular weight of HPMC molecules, which they explain is due to a thicker, more viscous polymer gel forming around the particles upon wetting, which delays the dissolution of the particles.

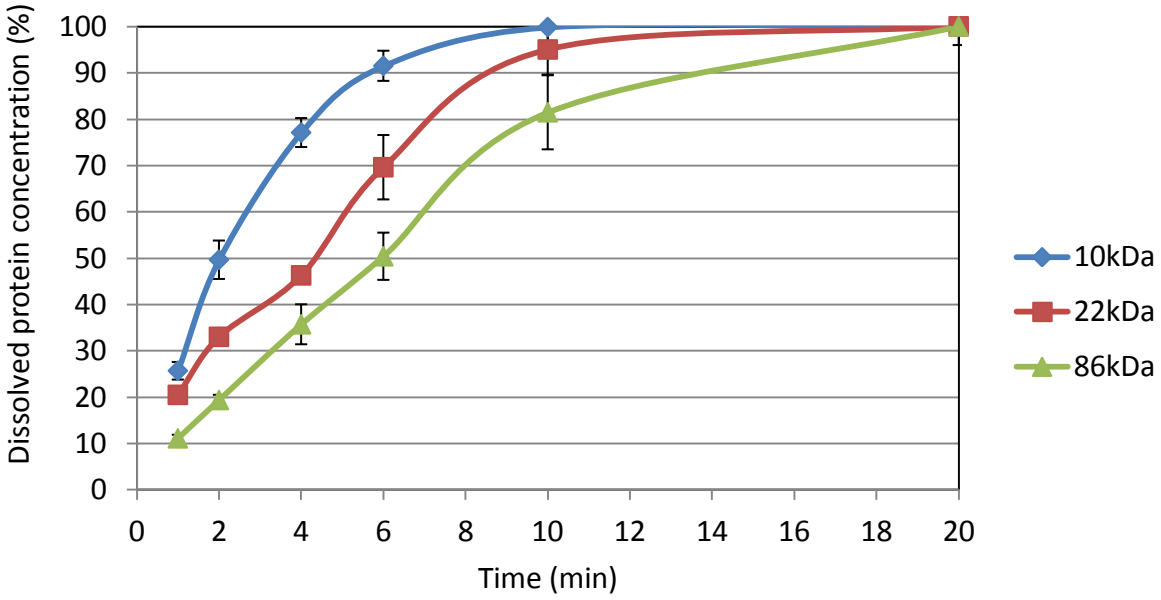

Figure 6.18: Dissolution profiles of Na-Cas proteins with powders of composition 92/3/5 wt% (lactose/HPMC/Na-Cas) with varying HPMC molecular weight.

This data is consistent with the data from Gao et al. (1996), who performed dissolution profiles using HPMC- coated tablets. This shows that it is indeed possible to use a one-step spray drying process for the production of coated composite particles that might offer an alternative method of producing tablets with a delayed drug release. Moreover, process and material costs might be reduced due to the lower number of process steps required. Further research is needed to establish the correct proportions of HPMC/lactose and API, and to show whether tablets produced by this alternative process offer comparable results with regards to pelletizing, tablet strength and retardation of drug release.

6.4. CONCLUSION

Part A:

This study investigated the effect of the molecular weight (M_W) of HPMC polymers on surface accumulation of the polymers during spray drying and its correlation to changes in powder yield, particle surface properties, powder functional properties and powder caking. Surface accumulation of the HPMC was independent of the M_W of the polymer, because the polymers all had similar surface activities and there was sufficient time during spray drying for even the largest of them to fully saturate the droplet surface.

Powder yields clearly decreased as the M_W of the polymer increased, even though the larger HPMC molecules would be expected to raise the glass transition temperature at the particulate surface more than the smaller ones. Likewise, lower yields were seen with higher bulk concentrations of polymer. These lower powder yields were likely to be because the cyclone has a poor separation efficiency with powders of very low bulk densities, as are obtained when using high M_W polymers or high polymer concentrations. The lower powder bulk densities, observed upon increasing the polymer bulk concentration or the polymer M_W, correlated with the measured increase in the average particle sizes. This was caused by an increase in total particle wall elasticity and thus particle expansion due to A) higher relative amounts of HPMC polymers at and beneath the particle surface and B) the higher flexibility of polymers of higher M_W. The texture of the particulate surface was largely unaffected by changes in the M_W of the polymer. Moreover, polymer bulk concentrations as low as 1 wt% resulted in a highly folded particle structure, similar to that of particles containing 10 wt% polymer bulk concentrations. This suggests that even low concentrations of low M_W polymers can induce a great enough increase in particle wall elasticity to promote extensive particle deformation during spray drying.

Powder flow could also be significantly increased by adding small amounts (1 wt %) of a low M_W polymer (10 kDa HPMC). The flowability of spray-dried lactose/HPMC powders was largely unaffected by changes in either polymer M_W or increases in polymer bulk concentration above 1 wt %. Wetting times were significantly increased with increasing polymer bulk concentration as well as with increasing polymer M_W. This is mainly due to A) the lowering of the powder bulk density and B) a thicker gel layer developing around the particles upon powder dissolution for lactose/HPMC powders containing either higher polymer bulk concentrations or a higher M_W polymer.

Crystallized powders containing only 1 wt% of HPMC showed extensive surface crystals and a partial loss of particulate structure, while 10 wt% of HPMC was sufficient to retain the particulate structure without the appearance of visible crystals at the surface of particles. This prevented the powders from transforming into a hard, brittle cake, as occurred for the ones containing only 1 wt% of HPMC. Soft, pliable cakes were formed from the lactose/HPMC (90/10 wt%) powders containing 10 kDa or 22 kDa HPMC, while those containing 86 kDa HPMC remained free flowing upon lactose crystallization.

Part B:

Surface composition measurements of lactose/HPMC/Na-Cas and HPMC/Na-Cas composite particles showed that Na-Cas can be completely encapsulated by HPMC at HPMC/Na-Cas ratios as low as 1:4, irrespective of the presence of lactose within the powder matrix. This proves the high efficiency of HPMC to encapsulate an active drug such as a protein in order to protect it from loss of molecular activity, which can occur should the drug/protein denature at the surface. The presence of HPMC causes an increase in particle size and a lowering of the powder bulk density, while powder flow is improved. Particle size and powder bulk density can be further controlled by the M_W of the HPMC, with larger particles of lower average density being produced in the presence of larger polymers.

Dissolution times were found to be strongly affected by the HPMC bulk concentration as well as the M_W of the polymer. Increases in either the M_W of HPMC or its bulk concentration caused a delay in powder dissolution and thus a delay in drug release, which was due to HPMC forming a gel network around the particle that was thicker when the polymer was present in higher bulk concentrations or when a polymer of higher M_W was used. The reduction in bulk density with increasing polymer bulk concentrations may have further contributed to the longer powder dissolution times. Due to the improved release-control capability of the higher grade (high-molecular-weight) HPMC polymers, they are the preferred choice as a coating material when a slow, sustained release of the drug is required. Using a higher grade HPMC also reduces material costs because of the lower amounts required to achieve the same delay in dissolution.

7. CONCLUSIONS AND RECOMMENDATIONS

A one-step spray coating process was successfully developed to produce coated, stabilized lactose powders with improved functional properties for food and/or pharmaceutical applications using the concept of *in-situ coating*. The work exploited the surface activity of the coating additives Na-Cas, WPI, HPMC, gelatine and lecithin, as well as the ability of milk fat to accumulate at the droplet surface during spray drying. These spray-dried coated powders were analyzed with regards to spray dryer yield, powder flow, wetting time, particle size and powder bulk density, surface crystallization, powder caking and overall crystallization delay upon moisture sorption. Using Na-Cas as coating additive, spray drying parameters, such as drying air temperature and atomization pressure, as well as feed conditions, such as TS and pH, were investigated with regards to protein surface accumulation and powder functional properties.

Further studies compared the surface enrichment of surface active additives in two different drying systems (drying droplets and drying thin films) in order to investigate various mechanisms of solute segregation, such as surface activity, moisture concentration gradients and Peclet number effect. For one of these studies, a numerical model was developed to calculate moisture concentration gradients within aqueous lactose/protein films produced and dried in the laboratory. The surface compositions of the dried films were then compared with those of spray-dried particles, and this allowed important conclusions to be drawn about solute segregation mechanisms. In another study, which explored competitive adsorption phenomena for different drying systems, solutions containing two surface active additives (HPMC and Na-Cas/WPI/lecithin; lecithin and Na-Cas/WPI) were used to prepare both dried films and spray-dried powders. This study also provided insight into how the presence of two different additives might be exploited to tailor the functional particulate properties of spray-dried lactose powders. Various grades of HPMC were used in further experiments to investigate the effect of the polymer's molecular weight on its accumulation at the drying droplet surface and to find correlations between polymer molecular weight and powder functional properties including powder stickiness and caking. Moreover, the one-step spray coating process was implemented to produce protein/lactose powders encapsulated by HPMC, and these were tested for delayed powder dissolution and ability to retard the release

of the protein into water, with a view to possible usage in pharmaceutical applications such as tablet production.

7.1. ACCUMULATION OF (SURFACE ACTIVE) ADDITIVES

All tested additives (Na-Cas, WPI, gelatine, HPMC, lecithin and milk fat) accumulated at the particulate surface when spray-dried at solid ratios of 1/9 with lactose. The highest accumulation on the particulate surface after spray drying (around 85 to 90%) was seen with HPMC, most likely due to it having the highest surface activity. The surface concentrations of the other additives were in a similar range (around 65 to 75%). Higher final surface protein (Na-Cas) concentrations were measured for spray-dried particles, compared with dried films of the same composition. Surface activity appeared to be the sole mechanism by which surface active additives such as proteins, polymers or phopholipids saturated the air-water interface during film-drying, while during spray drying other effects also affected the solute segregation and therefore final powder composition. During spray drying, the receding surface area was likely to have caused a further packing of adsorbed proteins at the droplet surface above their saturation limit. Furthermore, by using a mathematical model, moisture gradients within drying films were shown to exist, and their existence within dried droplets has been shown by other authors. These moisture concentration gradients had no effect on solute segregation between protein and lactose within drying films. Pe numbers below and above unity were calculated for Na-Cas proteins during film and spray drying, respectively, and this may have further contributed to the accumulation of proteins at and beneath the droplet surface to form protein multi-layers, due to the surface moving faster inwards than the dissolved proteins can diffuse away. Some of these protein layers may have been out of the detectable range of the surface composition analysis via XPS (~10 nm thick surface layer).

Lowering the TS of the spray-dried solution affected an increase in the total protein concentration at the surface of spray-dried lactose/protein (Na-Cas) particles, as did adjusting solution pH to be closer to the isoelectric point (pI) of the protein. In contrast, for dried films these effects were less pronounced (in the case of pH) or not clear (in the case of TS). Changes in other parameters, such as drying air temperatures (for particles and films) or atomization pressures (for particles) did not have an obvious effect on the accumulation of proteins, which suggests that enough time was given for proteins to accumulate at the surface of the droplet or film, and that it occurred well before a dried particle or film was formed.

The use of different sugars, such as lactose, sucrose or maltose, also did not have on obvious effect on protein accumulation during spray drying, and no sugar crystallization was observed for any of the sugars tested. This implies that during spray drying protein mobility was possible well above the solubility of the sugar, before a high-viscous glass was formed.

7.2. COMPETITIVE ADSORPTION OF SURFACE ACTIVE ADDITIVES

When droplets or films containing lactose plus two different surface active additives were dried, competitive adsorption between the surface active species was observed. HPMC was the only additive capable of displacing other surface active additives, such as Na-Cas, WPI or lecithin, almost completely from the surface of both films and droplets. This was most likely due to 1) the higher surface activity of HPMC, measured by a lower surface tension and/or 2) a steric effect, caused by long, flexible, adsorbed polymer molecules. The exclusion effect of HPMC was exploited to spray dry a compound powder of lactose/protein/polymer via a one-step spray coating process to produce polymer-coated lactose/protein (Na-Cas) particles with delayed powder dissolution. This powder may have possible applications in drug formulations, for example in pharmaceutical tablets, where lactose, used as excipient, is usually blended together with an active pharmaceutical ingredient (for example, a protein) before being compressed into a tablet and then coated by a suitable coating substance, such as HPMC, to affect a sustained drug release. The one-step spray coating process presented in this thesis may offer an alternative, simplified process for the production of coated pharmaceutical powders to be used in tablets or capsules.

When Na-Cas and lecithin were competing for the droplet or film surface during drying, higher surface lecithin concentrations were observed for dried particles, while in contrast, higher surface protein concentrations were measured for dried films. This suggests that the more surface active protein displaced the lecithin during film drying, when sufficient time for adsorption was given, while during spray drying, there may not have been sufficient time for the protein to exclude the smaller lecithin from the droplet surface. When WPI and lecithin were competing for the interface during drying, protein surface concentrations were higher for particles, while for films, the opposite occurred and lecithin dominated the surface. These competitive adsorption results suggest that for film drying, surface activity controls the surface competition between surface active species, while during spray drying other factors

also seem to play a role, such as limitation in the drying time or a possible Peclet number effect.

7.3. POWDER FUNCTIONAL PROPERTIES

The presence of various surface active molecules in a spray-dried lactose particle changed the properties of the powders significantly, with the effects depending on the size and flexibility of the additive. Large, low-density particles were formed when the flexible molecules Na-Cas, gelatine or (particularly) HPMC, which conferred elasticity to the particle walls, were present. The accumulation of large molecules, such as proteins or polymers, at the droplet surface of a lactose solution during drying increased the glass transition temperature of the particulate surface, which resulted in increased spray dryer yield and improved powder flow. Indeed, Na-Cas proteins and HPMC polymers significantly improved powder flow when present at bulk concentrations of just 1 wt%, while other additives with a lower molecular weight, such as lecithin, caused no significant improvement in powder flow. Changes in the TS and pH of the solution, both of which affected the Na-Cas surface accumulation, as well as in the drying air temperature, did not have a clear effect on powder flow, powder caking or lactose crystallization, probably due to the surface composition not being significantly different for the powders produced using these different parameters. A decrease in the atomization pressure during spray drying or the use of a larger spray dryer (pilot-scale) resulted in improved powder flow, due to larger particles being produced.

Wetting times were delayed significantly when additives such as HPMC or proteins accumulated at the particulate surface because their adsorption makes the surface less polar, and/or because these coated particles were of lower density than pure spray-dried lactose. The presence of fat caused poor powder wetting, poor powder flow and very low spray dryer yields due to its high degree of stickiness and its hydrophobic nature. Due to its excellent wetting abilities, lecithin was the only additive which caused the coated lactose powder to wet instantly, in a similar way to pure spray-dried lactose powder. Changes in the pH of the solution did not have a significant effect on the wetting of lactose/protein powders, while an increase in the TS or in the atomization pressure resulted in slightly improved powder wetting, due to differences in the surface composition (for the former) or surface to volume ratios of particles (for the latter). A larger scale spray dryer (pilot-scale) produced lactose/protein powders with significantly improved wetting due to powders with larger,

heavier particles and possibly more agglomeration being produced. The additional presence of a wetting agent such as lecithin within a spray-dried lactose/HPMC or lactose/protein solution, was shown to significantly improve powder wetting due to small fractions of lecithin at the particulate surface. This could be exploited to tailor powder functional properties, for example to produce lactose powders containing two different surface active species, such as lecithin and HPMC, that possess both a good powder flow and good powder wetting.

7.4. LACTOSE CRYSTALLIZATION AND POWDER CAKING

Lactose crystallization could be delayed (but not prevented) when using additives such as proteins or polymers, although none of the tested additives delayed moisture sorption into the particle. Gelatine was the most promising additive with regards to delaying lactose crystallization, most likely because of its abundance of polar parts, which increases its affinity for lactose and enables it to bind to lactose to form larger compounds with a higher glass transition temperature. Thus, polar, hygroscopic additives can be used as additives to increase the total glass transition temperature of a lactose compound powder with a resulting delay in lactose crystallization. In addition, the presence of a protein (Na-Cas or WPI) or a polymer (HPMC) throughout the bulk of the particles helped to maintain the particle's structural integrity when lactose crystallized upon moisture sorption, probably due to the additive forming a network throughout the whole particle. Without the protein or polymer, lactose particles lost their form entirely during crystallization and merged together. Other additives such as lecithin, milk fat or gelatine could not (or could only partly) prevent the particulate collapse. The additional presence of lecithin within a spray-dried lactose/HPMC powder was shown to destabilize the particulate structure upon lactose crystallization, perhaps due to interactions with the polymer that prevented an efficient network formation within the particle.

Excessive powder caking, which is initiated by lactose crystallization at the particle surface, could be minimized by a suitable choice of coating material, such as Na-Cas or (particularly) HPMC. HPMC was clearly the most promising additive with regards to minimizing caking of the lactose compound powder, with approximately 10 wt% of a high-molecular-weight polymer (86 kDa HPMC) required to completely prevent the powder from caking and therefore retain powder flowability. Although lactose crystallization still occurred

in the bulk of these particle, as shown by DSC, the polymer coat formed a protective coating on the surface of the lactose particles, which prevented lactose crystallization at the particulate surface, shown by SEM. This was due to 1) the high surface activity of HPMC, leading to significant accumulation of these polymers at the droplet surface, 2) the superior encapsulation and binding properties of long, flexible HPMC polymers, which are capable of forming a dense protective layer at the particulate surface, making HPMC an excellent wall material, and 3) the increase in glass transition temperature at the surface due to the presence of HPMC. Powder caking could also be prevented by the use of Na-Cas as additive, however higher bulk concentrations (≥20wt%) were required to achieve this, probably due to the protein giving lower surface accumulation and being a less protective wall material, compared with HPMC.

7.5. APPLICATIONS AND LIMITATIONS

7.5.1. Applications

The one-step spray coating process, the development of which is described within this thesis, was found to be successful for the production of coated lactose powder with significantly higher spray dryer yields and better powder flowability, compared with pure lactose powder. These improved properties were achieved by using small fractions (around 1 wt%) of Na-Cas or HPMC as coating additive to lactose, with the latter being particularly effective. Higher additive concentrations (> 1wt%) are recommended to further improve powder flow, delay lactose crystallization and minimize powder caking. While a lactose powder with only 1 wt% additive (for example: lactose/HPMC with a bulk composition of 99/1wt% or lactose/HPMC/lecithin with one of 99/0.5/0.5wt%) could have a market in food and pharmaceutical products as "lactose powder" with improved functionality (purity of 99% required), a lactose powder with additive concentrations >1wt% ("lactose/Na-Cas", "lactose/HPMC" or "lactose/HPMC/ lecithin" powder) could have possible applications in food and/or pharmaceutical products where a higher concentration of protein or polymer is desired (for example, in protein/energy bars or pharmaceutical powders, respectively).

7.5.2. Limitations

The use of proteins or polymers as additives, such as Na-Cas, WPI, gelatine or HPMC, affected the wettability and dispersability of the spray-dried lactose powders negatively. However, the additional presence of lecithin within the powder was shown to counteract the poorer wetting of protein- or polymer-coated lactose powder. Moreover, as mentioned before, the use of a larger-scale spray dryer would also improve powder wetting significantly, mostly due to more agglomerated powders with larger, heavier particles being produced. While lactose crystallization could be significantly delayed by adding increasing concentrations of proteins (Na-Cas or gelatine) or HPMC, it could not be completely prevented at additive concentrations ≤ 20 wt%. This was mostly due to the fact that none of the tested additives acted as moisture barrier to prevent the glass transition temperature of the lactose from falling below the product temperature upon moisture sorption of the powder. Moreover, it was not possible to prevent coated lactose powder from caking when the additive concentration was below 10 wt% (for HPMC) or 20 wt% (for Na-Cas). Although a 100% coating of additive on the particles was not achieved, this work shows that such a coating is not required to prevent the powder from caking.

7.6. RECOMMENDATIONS

Due to the poor solubility of lactose, this work used only low TS, in the range 5 to 20 wt%. To successfully implement an economic commercial-scale spray drying process, TS needs to be increased significantly (≥50 wt%). This can be more easily realised when spray drying an aqueous solution of a more soluble solute such as sucrose, which would benefit from *in-situ coating* during spray drying to minimize droplet and powder stickiness and therefore increase the spray dryer yield.

Pe number and moisture content gradients during spray drying could not be investigated directly within this work because radial solute/solvent concentration gradients in the drying droplet or in the dried particle could not be measured. Further research is required here to enable such an analysis by using direct measurements. This would help to separate Pe number and moisture content gradients from other effects on solute segregation, such as surface activity, molecular size of the solutes and a reducing surface area. This will give the technologists of the future better control over the final surface composition of spray-dried

powders, and enable them to adjust particle properties and therefore improve powder functional properties.

Another area which invites further research is competitive adsorption amongst various surface active species with varying physicochemical properties and molecular sizes, such as WPI and lecithin, in order to better understand the impacts of surface activity, drying time and inter- or intra-species intermolecular interactions on the competitive adsorption behaviour. This would allow a better prediction of how these properties impact on surface competition in different drying systems. Competitive adsorption could be exploited to develop powders with a two-component coating or a double coating via a one-step spray drying process. This spray coating process could then be implemented in the food or pharmaceutical industries to produce coated powders with improved properties.

The use of a one-step spray coating process to produce pharmaceutical HPMC-coated lactose/protein powders to be used for direct pelletizing should also be further investigated. Compressibility, tablet hardness and tablet dissolution could be tested and the results compared with those obtained with conventional tablets coated in a post-treatment process with HPMC. The optimal choice of polymer molecular weight and bulk polymer concentration should be established in order to create a tablet with the desired properties. Tablet storage tests in different humidity conditions should be also performed to investigate whether lactose crystallization occurs within the tablets over time and what effects this has on the tablet properties.

Coated lactose powders, produced via the one-step spray coating process, need to be tested in different foods, such as dry powder soups or drinks, to investigate their stability within the food system, for example, to find out how they contribute to the powder flow of the mixture, the caking of the powder upon moisture sorption or the dissolution of the powder mix into cold or hot water. Long-term storage tests of the powder mixture should be performed at different humidities and temperatures to explore the storage conditions required for powder stability. Ideally, a comparison of the powder stability and powder dissolution of lactose powders with various coatings should be made in order to assess their suitability for use in different product types. Depending on the end-use of the powder and its requirements within the product, a suitable lactose powder with one or multiple coatings could be tailored by using the mechanism of *in-situ coating* via spray drying.

Other alternative coating mechanisms should be compared with the *in-situ spray coating* process with regards to coating effectiveness and powder stability as well as process cost and scalability. A fluidized bed coating might offer a possible alternative that would achieve a complete coating of the lactose and therefore prevent powder caking, perhaps with lower coating concentrations than those currently required to achieve a coating during spray drying alone. The design of a three-fluid nozzle or other nozzle type with separate inlet and outlet streams for lactose and coating solution, and a means of efficiently mixing both streams at different ratios prior to or during atomization, might be another option for coating lactose particles during spray drying.

REFERENCES

Adhikari, B., Howes, T., & Bhandari, B. (2007a). Use of solute fixed coordinate system and method of lines for prediction of drying kinetics and surface stickiness of single droplet during convective drying. *Chemical Engineering and Processing: Process Intensification, 46*(5), 405-419.

Adhikari, B., Howes, T., Bhandari, B., & Langrish, T. (2009a). Effect of addition of proteins on the production of amorphous sucrose powder through spray drying. *Journal of Food Engineering, 94*(2), 144-153.

Adhikari, B., Howes, T., Bhandari, B., & Truong, V. (2001). Stickiness in foods: a review of mechanisms and test methods. *International Journal of Food Properties, 4*(1), 1-33.

Adhikari, B., Howes, T., Shrestha, A., & Bhandari, B. (2007b). Development of stickiness of whey protein isolate and lactose droplets during convective drying. *Chemical Engineering and Processing, 46*(5), 420-428.

Adhikari, B., Howes, T., Wood, B., & Bhandari, B. (2009b). The effect of low molecular weight surfactants and proteins on surface stickiness of sucrose during powder formation through spray drying. *Journal of Food Engineering, 94*(2), 135-143.

Adler, M., Unger, M., & Lee, G. (2000). Surface composition of spray-dried particles of bovine serum albumin/trehalose/surfactant. *Pharmaceutical research, 17*(7), 863-870.

Amefia, A. E., Abu-Ali, J. M., & Barringer, S. A. (2006). Improved functionality of food additives with electrostatic coating. *Innovative Food Science & Emerging Technologies, 7*(3), 176-181.

Arakawa, T., & Timasheff, S. N. (1982). Stabilization of protein structure by sugars. *Biochemistry, 21*(25), 6536-6544.

Arboleya, J.-C., & Wilde, P. J. (2005). Competitive adsorption of proteins with methylcellulose and hydroxypropyl methylcellulose. *Food Hydrocolloids, 19*(3), 485-491.

Arvanitoyannis, I. S., Nakayama, A., & Aiba, S.-i. (1998). Chitosan and gelatin based edible films: state diagrams, mechanical and permeation properties. *Carbohydrate polymers, 37*(4), 371-382.

Atkinson, P. J., Dickinson, E., Horne, D., & Richardson, R. M. (1995a). Neutron reflectivity of adsorbed protein films. *Proteins at interfaces ii, 602*, 311-320.

Atkinson, P. J., Dickinson, E., Horne, D. S., & Richardson, R. M. (1995b). Neutron reflectivity of adsorbed β-casein and β-lactoglobulin at the air/water interface. *J. Chem. Soc., Faraday Trans., 91*(17), 2847-2854.

Belyakova, L. E., Antipova, A. S., Semenova, M. G., Dickinson, E., Matia Merino, L., & Tsapkina, E. N. (2003). Effect of sucrose on molecular and interaction parameters of sodium caseinate in aqueous solution: relationship to protein gelation. *Colloids and Surfaces B: Biointerfaces, 31*(1), 31-46.

Berlin, E., Anderson, B., & Pallansch, M. (1968). Comparison of water vapor sorption by milk powder components. *Journal of dairy science, 51*(12), 1912-1915.

Bhandari, B., & Burel, B. (2007). Prediction of lactose crystals present in supersaturated lactose and whey solutions by measuring the water activity. *International Journal of Food Properties, 10*(1), 163-171.

Bhandari, B., & Howes, T. (1999). Implication of glass transition for the drying and stability of dried foods. *Journal of Food Engineering, 40*(1-2), 71-79.

Bigi, A., Cojazzi, G., Panzavolta, S., Rubini, K., & Roveri, N. (2001). Mechanical and thermal properties of gelatin films at different degrees of glutaraldehyde crosslinking. *Biomaterials, 22*(8), 763-768.

Blomqvist, B. R., Wärnheim, T., & Claesson, P. M. (2005). Surface rheology of PEO-PPO-PEO triblock copolymers at the air-water interface: Comparison of spread and adsorbed layers. *Langmuir, 21*(14), 6373-6384.

Bodvik, R., Dedinaite, A., Karlson, L., Bergström, M., Bäverbäck, P., Pedersen, J. S., Claesson, P. M. (2010). Aggregation and network formation of aqueous methylcellulose and hydroxypropylmethylcellulose solutions. *Colloids and Surfaces A: Physicochemical and Engineering Aspects, 354*(1), 162-171.

Brash, J. L., & Horbett, T. A. (1995). Proteins at interfaces. An Overview, *American Chemical Society*, 1-25.

Brech, M., Nijdam, J. J., Pearce, D., & Bagga, P. (2013). Improved Lactose Powder Properties by In-situ Coating with Additives during Spray Drying. *Journal of Medical and Bioengineering Vol, 2*(3).

Bronlund, J., & Paterson, T. (2004). Moisture sorption isotherms for crystalline, amorphous and predominantly crystalline lactose powders. *International Dairy Journal, 14*(3), 247-254.

Buma, T. (1968). A correlation between free fat content and moisture content of whole milk spray powders. *Neth. Milk Dairy J, 22*, 22–28.

Bushill, J., Wright, W., Fuller, C., & Bell, A. (1965). The crystallisation of lactose with particular reference to its occurrence in milk powder. *Journal of the Science of Food and Agriculture, 16*(10), 622-628.

Caessens, P. W. J. R., De Jongh, H. H. J., Norde, W., & Gruppen, H. (1999). The adsorption-induced secondary structure of [beta]-casein and of distinct parts of its sequence in relation to foam and emulsion properties. *Biochimica et Biophysica Acta (BBA)-Protein Structure and Molecular Enzymology, 1430*(1), 73-83.

Champion, D., Le Meste, M., & Simatos, D. (2000). Towards an improved understanding of glass transition and relaxations in foods: molecular mobility in the glass transition range. *Trends in food science & technology, 11*(2), 41-55.

Charlesworth, D., & Marshall Jr, W. (1960). Evaporation from drops containing dissolved solids. *AIChE Journal, 6*(1), 9-23.

Chen, X. D., & Özkan, N. (2007). Stickiness, functionality, and microstructure of food powders. *Drying technology, 25*(6), 959-969.

Chen, X. D., Sidhu, H., & Nelson, M. (2011). Theoretical probing of the phenomenon of the formation of the outermost surface layer of a multi-component particle, and the surface chemical composition after the rapid removal of water in spray drying. *Chemical Engineering Science, 66*(24), 6375-6384.

Chiou, D., Langrish, T., & Braham, R. (2008). The effect of temperature on the crystallinity of lactose powders produced by spray drying. *Journal of Food Engineering, 86*(2), 288-293.

Costantino, H. R., Andya, J. D., Nguyen, P. A., Dasovich, N., Sweeney, T. D., Shire, S. J., . . . Maa, Y. F. (1998). Effect of mannitol crystallization on the stability and aerosol performance of a spray-dried pharmaceutical protein, recombinant humanized anti-IgE monoclonal antibody. *Journal of pharmaceutical sciences, 87*(11), 1406-1411.

Crank, J. (1979). *The mathematics of diffusion*: Oxford university press.

Dee, K. C., Puleo, D. A., & Bizios, R. (2003). Protein-Surface Interactions. *An introduction to tissue-biomaterial interactions*, 37-52.

Dee, K. C., Puleo, D. A., & Bizios, R. (2004). An Introduction to Tissue-Biomaterial Interactions. *MRS BULLETIN*, 419.

Desai, K. G. H., & Jin Park, H. (2005). Recent developments in microencapsulation of food ingredients. *Drying technology, 23*(7), 1361-1394.

Dickinson, E. (1999). Adsorbed protein layers at fluid interfaces: interactions, structure and surface rheology. *Colloids and Surfaces B: Biointerfaces, 15*(2), 161-176.

Dickinson, E. (2001). Milk protein interfacial layers and the relationship to emulsion stability and rheology. *Colloids and Surfaces B: Biointerfaces, 20*(3), 197-210.

Dickinson, E. (2003). Hydrocolloids at interfaces and the influence on the properties of dispersed systems. *Food Hydrocolloids, 17*(1), 25-39.

Dickinson, E. (2008). Interfacial structure and stability of food emulsions as affected by protein–polysaccharide interactions. *Soft Matter, 4*(5), 932-942.

Dickinson, E. (2011). Mixed biopolymers at interfaces: Competitive adsorption and multilayer structures. *Food Hydrocolloids, 25*(8), 1966-1983.

Dickinson, E., Rolfe, S. E., & Dalgleish, D. G. (1988). Competitive adsorption of α< sub> s1</sub>-casein and β-casein in oil-in-water emulsions. *Food Hydrocolloids, 2*(5), 397-405.

Elversson, J., & Millqvist-Fureby, A. (2006). In situ coating--An approach for particle modification and encapsulation of proteins during spray-drying. *International journal of pharmaceutics, 323*(1-2), 52-63.

Elversson, J., & Millqvist-Fureby, A. (2005). Particle size and density in spray drying—effects of carbohydrate properties. *Journal of pharmaceutical sciences, 94*(9), 2049-2060.

Euston, S. E., Singh, H., Munro, P. A., & Dalgleish, D. G. (1995). Competitive Adsorption Between Sodium Caseinate and Oil-Soluble and Water-Soluble Surfactants in Oil-in-Water Emulsions. *Journal of food science, 60*(5), 1124-1131.

Fäldt, P., & Bergenståhl, B. (1994). The surface composition of spray-dried protein--lactose powders. *Colloids and Surfaces A: Physicochemical and Engineering Aspects, 90*(2-3), 183-190.

Fäldt, P., & Bergenståhl, B. (1995). Fat encapsulation in spray-dried food powders. *Journal of the American Oil Chemists' Society, 72*(2), 171-176.

Fäldt, P., & Bergenståhl, B. (1996). Spray-dried whey protein/lactose/soybean oil emulsions. 1. Surface composition and particle structure. *Food Hydrocolloids, 10*(4), 421-429.

Farkye, N. (2006). Significance of milk fat in milk powder. *Advanced Dairy Chemistry Volume 2 Lipids*, 451-465.

Fitzpatrick, J., Iqbal, T., Delaney, C., Twomey, T., & Keogh, M. (2004). Effect of powder properties and storage conditions on the flowability of milk powders with different fat contents. *Journal of Food Engineering, 64*(4), 435-444.

Flink, J. M. (1983). Structure and structure transitions in dried carbohydrate materials.

Foster, K. D., Bronlund, J. E., & Paterson, A. (2005). The prediction of moisture sorption isotherms for dairy powders. *International Dairy Journal, 15*(4), 411-418.

Fox, P. F. (1985). *Developments in dairy chemistry. 3. Lactose and minor constituents* (Vol. 3): Elsevier Applied Science Publshers Ltd.

Freudig, B., Hogekamp, S., & Schubert, H. (1999). Dispersion of powders in liquids in a stirred vessel. *Chemical Engineering and Processing: Process Intensification, 38*(4), 525-532.

Gaiani, C., Morand, M., Sanchez, C., Tehrany, E. A., Jacquot, M., Schuck, P., . . . Scher, J. (2010). How surface composition of high milk proteins powders is influenced by spray-drying temperature. *Colloids and Surfaces B: Biointerfaces, 75*(1), 377-384.

Gaiani, C., Mullet, M., Arab-Tehrany, E., Jacquot, M., Perroud, C., Renard, A., & Scher, J. (2011). Milk proteins differentiation and competitive adsorption during spray-drying. *Food Hydrocolloids, 25*(5), 983-990.

Gaiani, C., Scher, J., Ehrhardt, J. J., Linder, M., Schuck, P., Desobry, S., & Banon, S. (2007). Relationships between dairy powder surface composition and wetting properties during storage: Importance of residual lipids. *Journal of agricultural and food chemistry, 55*(16), 6561-6567.

Ganzle, M. G., Haase, G., & Jelen, P. (2008). Lactose: crystallization, hydrolysis and value-added derivatives. *International Dairy Journal, 18*(7), 685-694.

Gao, P., Skoug, J. W., Nixon, P. R., Robert Ju, T., Stemm, N. L., & Sung, K. C. (1996). Swelling of hydroxypropyl methylcellulose matrix tablets. 2. Mechanistic study of the influence of formulation variables on matrix performance and drug release. *Journal of pharmaceutical sciences, 85*(7), 732-740.

Gharsallaoui, A., Roudaut, G., Chambin, O., Voilley, A., & Saurel, R. (2007). Applications of spray-drying in microencapsulation of food ingredients: An overview. *Food Research International, 40*(9), 1107-1121.

Gibbs, Selim Kermasha, Inteaz Alli, Catherine N. Mulligan, & Bernard. (1999). Encapsulation in the food industry: a review. *International Journal of Food Sciences and Nutrition, 50*(3), 213-224.

Gohel, M., & Jogani, P. D. (2005). A review of co-processed directly compressible excipients. *J Pharm Pharm Sci, 8*(1), 76-93.

Gonnissen, Y., Remon, J. P., & Vervaet, C. (2007). Development of directly compressible powders via co-spray drying. *European journal of pharmaceutics and biopharmaceutics, 67*(1), 220-226.

Gordon, M., & Taylor, J. S. (1952). Ideal copolymers and the second-order transitions of synthetic rubbers. i. non-crystalline copolymers. *Journal of Applied Chemistry, 2*(9), 493-500.

Graham, D. E., & Phillips, M. C. (1979a). Proteins at liquid interfaces: I. Kinetics of adsorption and surface denaturation. *Journal of colloid and interface science, 70*(3), 403-414.

Graham, D. E., & Phillips, M. C. (1979b). Proteins at liquid interfaces: II. Adsorption isotherms. *Journal of colloid and interface science, 70*(3), 415-426.

Graham, D. E., & Phillips, M. C. (1979c). Proteins at liquid interfaces: III. Molecular structures of adsorbed films. *Journal of colloid and interface science, 70*(3), 427-439.

Haque, M. K., & Roos, Y. H. (2004a). Water Plasticization and Crystallization of Lactose in Spray-dried Lactose/Protein Mixtures. *Journal of food science, 69*(1), FEP23-FEP29.

Haque, M. K., & Roos, Y. H. (2004b). Water Sorption and Plasticization Behavior of Spray-dried Lactose/Protein Mixtures. *Journal of food science, 69*(8), E384-E391.

Haque, M. K., & Roos, Y. H. (2005). Crystallization and X-ray diffraction of spray-dried and freeze-dried amorphous lactose. *Carbohydrate Research, 340*(2), 293-301.

Haynes, C. A., & Norde, W. (1994). Globular proteins at solid/liquid interfaces. *Colloids and Surfaces B: Biointerfaces, 2*(6), 517-566.

Hecht, J. P., & King, C. J. (2000). Spray drying: Influence of developing drop morphology on drying rates and retention of volatile substances. 1. Single-drop experiments. *Industrial & Engineering Chemistry Research, 39*(6), 1756-1765.

Holsinger, V., & Kligerman, A. (1991). Applications of lactase in dairy foods and other foods containing lactose. *Food technology, 45*.

Ibach, A., & Kind, M. (2007). Crystallization kinetics of amorphous lactose, whey-permeate and whey powders. *Carbohydrate Research, 342*(10), 1357-1365.

Incropera, F. P., Lavine, A. S., & DeWitt, D. P. (2011). *Fundamentals of heat and mass transfer*: John Wiley & Sons.

Ishikawa, T., Watanabe, Y., Takayama, K., Endo, H., & Matsumoto, M. (2000). Effect of hydroxypropylmethylcellulose (HPMC) on the release profiles and bioavailability of a poorly water-soluble drug from tablets prepared using macrogol and HPMC. *International journal of pharmaceutics, 202*(1), 173-178.

Islam, M., & Langrish, T. (2010). An investigation into lactose crystallization under high temperature conditions during spray drying. *Food Research International, 43*(1), 46-56.

Islam, M., Langrish, T., & Chiou, D. (2010a). Particle crystallization during spray drying in humid air. *Journal of Food Engineering, 99*(1), 55-62.

Islam, M., Sherrell, R., & Langrish, T. (2010b). An investigation of the relationship between glass transition temperatures and the crystallinity of spray-dried powders. *Drying technology, 28*(3), 361-368.

Jayasundera, M., Adhikari, B., Adhikari, R., & Aldred, P. (2010a). The Effect of Food-Grade Low-Molecular-Weight Surfactants and Sodium Caseinate on Spray Drying of Sugar-Rich Foods. *Food Biophysics, 5*(2), 128-137.

Jayasundera, M., Adhikari, B., Adhikari, R., & Aldred, P. (2010b). The effect of protein types and low molecular weight surfactants on spray-drying of sugar-rich foods. *Food Hydrocolloids*.

Jayasundera, M., Adhikari, B., Aldred, P., & Ghandi, A. (2009). Surface modification of spray dried food and emulsion powders with surface-active proteins: a review. *Journal of Food Engineering, 93*(3), 266-277.

Jelen, P. (2009). *Dried Whey, Whey Proteins, Lactose and Lactose Derivative Products*: Wiley-Blackwell.

Jouppila, K., & Roos, Y. (1994a). Water sorption and time-dependent phenomena of milk powders. *Journal of dairy science, 77*(7), 1798-1808.

Jouppila, K., & Roos, Y. H. (1994b). Glass Transitions and Crystallization in Milk Powders. *Journal of dairy science, 77*(10), 2907-2915.

Kachel, S., Scharfer, P., & Schabel, W. (2013). Sorption isotherms of mixtures of polymers, proteins and electrolytes—Measurement data and model predictions. *Chemical Engineering and Processing: Process Intensification, 68*, 45-54.

Kato, A., Matsuda, T., Matsudomi, N., & Kobayashi, K. (1984). Determination of protein hydrophobicity using sodium dodecyl sulfate binding method. *Journal of agricultural and food chemistry, 32*(2), 284-288.

Kelly, J., Kelly, P. M., & Harrington, D. (2002). Influence of processing variables on the physicochemical properties of spray dried fat-based milk powders. *Le Lait, 82*(4), 401-412.

Kim, E. H., Chen, X. D., & Pearce, D. (2005a). Melting characteristics of fat present on the surface of industrial spray-dried dairy powders. *Colloids and Surfaces B: Biointerfaces, 42*(1), 1-8.

Kim, E. H. J., Chen, X. D., & Pearce, D. (2002). Surface characterization of four industrial spray-dried dairy powders in relation to chemical composition, structure and wetting property. *Colloids and Surfaces B: Biointerfaces, 26*(3), 197-212.

Kim, E. H. J., Chen, X. D., & Pearce, D. (2003). On the mechanisms of surface formation and the surface compositions of industrial milk powders. *Drying technology, 21*(2), 265-278.

Kim, E. H. J., Chen, X. D., & Pearce, D. (2005b). Effect of surface composition on the flowability of industrial spray-dried dairy powders. *Colloids and Surfaces B: Biointerfaces, 46*(3), 182-187.

Kim, E. H. J., Chen, X. D., & Pearce, D. (2009a). Surface composition of industrial spray-dried milk powders. 1. Development of surface composition during manufacture. *Journal of Food Engineering, 94*(2), 163-168.

Kim, E. H. J., Chen, X. D., & Pearce, D. (2009b). Surface composition of industrial spray-dried milk powders. 2. Effects of spray drying conditions on the surface composition. *Journal of Food Engineering, 94*(2), 169-181.

Kim, E. H. J., Chen, X. D., & Pearce, D. (2009c). Surface composition of industrial spray-dried milk powders. 3. Changes in the surface composition during long-term storage. *Journal of Food Engineering, 94*(2), 182-191.

Landström, K., Alsins, J., & Bergenståhl, B. (2000). Competitive protein adsorption between bovine serum albumin and [beta]-lactoglobulin during spray-drying. *Food Hydrocolloids, 14*(1), 75-82.

Landström, K., Arnebrant, T., Alsins, J., & Bergenståhl, B. (2003). Competitive protein adsorption between [beta]-casein and [beta]-lactoglobulin during spray-drying: effect of calcium induced association. *Food Hydrocolloids, 17*(1), 103-116.

Lee, J. C., & Timasheff, S. N. (1981). The stabilization of proteins by sucrose. *Journal of Biological Chemistry, 256*(14), 7193-7201.

Lifran, E., Hourigan, J., Sleigh, R., & Johnson, R. (2000). New wheys for lactose. *Food Australia, 52*(4), 120-136.

Listiohadi, Y. D., Hourigan, J., Sleigh, R. W., & Steele, R. (2005). Properties of lactose and its caking behaviour. *Australian Journal of Dairy Technology, 60*(1), 33-52.

Luo, H., Cardinal, C. M., Scriven, L., & Francis, L. F. (2008). Ceramic nanoparticle/monodisperse latex coatings. *Langmuir, 24*(10), 5552-5561.

Magdassi, S. (1996). *Surface activity of proteins: chemical and physicochemical modifications*: CRC.

Masters, K. (1972). *Spray drying: an introduction to principles, operational practice and applications*: L. Hill.

Masters, K. (1979). Spray drying handbook. *Spray drying handbook.*(Ed. 3).

Masters, K. (2002). *Spray drying in practice*: SprayDryConsult.

Matsuno, R., & Adachi, S. (1993). Lipid encapsulation technology-techniques and applications to food. *Trends in food science & technology, 4*(8), 256-261.

McSweeney, P., & Fox, P. F. (2009). *Advanced dairy chemistry: volume 3: lactose, water, salts and minor constituents*: Springer.

Meerdink, G., & van't Riet, K. (1995). Modeling segregation of solute material during drying of liquid foods. *AIChE Journal, 41*(3), 732-736.

Millqvist-Fureby, A., & Smith, P. (2007). In-situ lecithination of dairy powders in spray-drying for confectionery applications. *Food Hydrocolloids, 21*(5-6), 920-927.

Morrow, R. J., Woolfson, A. D., Donnelly, L., Curran, R., Andrews, G., Katinger, D., & Malcolm, R. K. (2011). Sustained release of proteins from a modified vaginal ring device. *European journal of pharmaceutics and biopharmaceutics, 77*(1), 3-10.

Mujumdar, A. S. (2006). *Handbook of industrial drying*: CRC Press.

Mulvihill, D., & Fox, P. (1989). Physico-chemical and functional properties of milk proteins. *Developments in dairy chemistry. 4. Functional milk proteins.*, 131-172.

Muñoz, M. G., Monroy, F., Ortega, F., Rubio, R. G., & Langevin, D. (2000). Monolayers of symmetric triblock copolymers at the air-water interface. 1. Equilibrium properties. *Langmuir, 16*(3), 1083-1093.

Nijdam, J., & Langrish, T. (2005). An investigation of milk powders produced by a laboratory-scale spray dryer. *Drying technology, 23*(5), 1043-1056.

Nijdam, J., & Langrish, T. (2006). The effect of surface composition on the functional properties of milk powders. *Journal of Food Engineering, 77*(4), 919-925.

Nikiforow, I., Adams, J. r., König, A. M., Langhoff, A., Pohl, K., Turshatov, A., & Johannsmann, D. (2010). Self-stratification during film formation from latex blends driven by differences in collective diffusivity. *Langmuir, 26*(16), 13162-13167.

Norde, W. (1992). Energy and entropy of protein adsorption. *Journal of dispersion science and technology, 13*(4), 363-377.

Park, H. J., & Chinnan, M. S. (1995). Gas and water vapor barrier properties of edible films from protein and cellulosic materials. *Journal of Food Engineering, 25*(4), 497-507.

Paulsson, M., & Dejmek, P. (1992). Surface film pressure of β-lactoglobulin, α-lactalbumin and bovine serum albumin at the air/water interface studied by Wilhelmy plate and drop volume. *Journal of colloid and interface science, 150*(2), 394-403.

Peniche, C., Argüelles-Monal, W., Peniche, H., & Acosta, N. (2003). Chitosan: An attractive biocompatible polymer for microencapsulation. *Macromolecular bioscience, 3*(10), 511-520.

Pisecky, J. (1997). Handbook of milk powder manufacture. *Recherche, 67*, 02.

Prescott, J. K., & Barnum, R. A. (2000). On powder flowability. *Pharmaceutical technology, 24*(10), 60-85.

Rahman, M. S. (2008). *Food properties handbook*: CRC press.

Ré, M. (1998). Microencapsulation by spray drying. *Drying technology, 16*(6), 1195-1236.

Ribeiro, A. C., Ortona, O., Simoes, S. M., Santos, C. I., Prazeres, P. M., Valente, A. J., . . . Burrows, H. D. (2006). Binary mutual diffusion coefficients of aqueous solutions of sucrose, lactose, glucose, and fructose in the temperature range from (298.15 to 328.15) K. *Journal of Chemical & Engineering Data, 51*(5), 1836-1840.

Rodríguez Patino, J. M., & Pilosof, A. M. (2011). Protein–polysaccharide interactions at fluid interfaces. *Food Hydrocolloids, 25*(8), 1925-1937.

Roos, Y., & Karel, M. (1991a). Plasticizing effect of water on thermal behavior and crystallization of amorphous food models. *Journal of food science, 56*(1), 38-43.

Roos, Y., & Karel, M. (1991b). Water and molecular weight effects on glass transitions in amorphous carbohydrates and carbohydrate solutions. *Journal of food science, 56*(6), 1676-1681.

Roos, Y. H. (2002). Importance of glass transition and water activity to spray drying and stability of dairy powders. *Le Lait, 82*(4), 475-484.

Roudaut, G., Simatos, D., Champion, D., Contreras-Lopez, E., & Le Meste, M. (2004). Molecular mobility around the glass transition temperature: a mini review. *Innovative Food Science & Emerging Technologies, 5*(2), 127-134.

Sarkar, N. (1984). Structural interpretation of the interfacial properties of aqueous solutions of methylcellulose and hydroxypropyl methylcellulose. *Polymer, 25*(4), 481-486.

Shawqi Barham, A., Haque, K., Roos, Y. H., & Kieran Hodnett, B. (2006). Crystallization of spray-dried lactose/protein mixtures in humid air. *Journal of crystal growth, 295*(2), 231-240.

Shrestha, A. K., Howes, T., Adhikari, B. P., & Bhandari, B. R. (2007). Water sorption and glass transition properties of spray dried lactose hydrolysed skim milk powder. *LWT-Food Science and Technology, 40*(9), 1593-1600.

Sober, H. A. (1968). Handbook of biochemistry.

Sollohub, K., & Cal, K. (2010). Spray drying technique: II. Current applications in pharmaceutical technology. *Journal of pharmaceutical sciences, 99*(2), 587-597.

Sugiyama, Y., Larsen, R. J., Kim, J.-W., & Weitz, D. A. (2006). Buckling and crumpling of drying droplets of colloid-polymer suspensions. *Langmuir, 22*(14), 6024-6030.

Suttiprasit, P., Krisdhasima, V., & McGuire, J. (1992). The surface activity of α-lactalbumin, β-lactoglobulin, and bovine serum albumin: I. Surface tension measurements with single-component and mixed solutions. *Journal of colloid and interface science, 154*(2), 316-326.

Tahara, K., Yamamoto, K., & Nishihata, T. (1995). Overall mechanism behind matrix sustained release (SR) tablets prepared with hydroxypropyl methylcellulose 2910. *Journal of controlled release, 35*(1), 59-66.

Takeuchi, H., Yasuji, T., Hino, T., Yamamoto, H., & Kawashima, Y. (1998). Spray-dried composite particles of lactose and sodium alginate for direct tabletting and controlled releasing. *International journal of pharmaceutics, 174*(1), 91-100.

Takeuchi, H., Yasuji, T., Yamamoto, H., & Kawashima, Y. (2000). Temperature-induced crystallization and compactibility of spray dried composite particles composed of amorphous lactose and various types of water-soluble polymer. *CHEMICAL AND PHARMACEUTICAL BULLETIN-TOKYO-, 48*(4), 585-587.

Teunou, E., Fitzpatrick, J. J., & Synnott, E. C. (1999). Characterisation of food powder flowability. *Journal of Food Engineering, 39*(1), 31-37.

Thompson, A., Boland, M., & Singh, H. (2009). *Milk Proteins: From Expression to Food*: Academic Press.

Tomas, J. (2004). Fundamentals of cohesive powder consolidation and flow. *Granular Matter, 6*(2-3), 75-86.

Trueman, R., Lago Domingues, E., Emmett, S., Murray, M., & Routh, A. (2012). Auto-stratification in drying colloidal dispersions: A diffusive model. *Journal of colloid and interface science, 377*(1), 207-212.

Uedaira, H., & Uedaira, H. (1969). Diffusion coefficients of xylose and maltose in aqueous solution. *Bull. Chem. Soc. Jpn, 42*(8), 2140-2142.

Vega, C., & Roos, Y. (2006). Invited Review: Spray-Dried Dairy and Dairy-Like Emulsions--Compositional Considerations. *Journal of dairy science, 89*(2), 383-401.

Vehring, R. (2008). Pharmaceutical particle engineering via spray drying. *Pharmaceutical research, 25*(5), 999-1022.

Vehring, R., Foss, W. R., & Lechuga-Ballesteros, D. (2007). Particle formation in spray drying. *Journal of aerosol science, 38*(7), 728-746.

Vignolles, M. L., Jeantet, R., Lopez, C., & Schuck, P. (2007). Free fat, surface fat and dairy powders: interactions between process and product. A review. *Le Lait, 87*(3), 187-236.

Vrentas, J., & Vrentas, C. (1993). A new equation relating self-diffusion and mutual diffusion coefficients in polymer-solvent systems. *Macromolecules, 26*(22), 6129-6131.

Wan, L. S., Heng, P. W., & Chia, C. G. (1992a). Spray drying as a process for microencapsulation and the effect of different coating polymers. *Drug development and industrial pharmacy, 18*(9), 997-1011.

Wan, L. S. C., Heng, P. W. S., & Chia, C. G. H. (1992b). Plasticizers and their effects on microencapsulation process by spray-drying in an aqueous system. *Journal of microencapsulation, 9*(1), 53-62.

Wang, S., & Langrish, T. (2010). The Use of Surface Active Compounds as Additives in Spray Drying. *Drying technology, 28*(3), 341-348.

Wang, S., Langrish, T., & Leszczynski, M. (2010). The Effect of Casein as a Spray-Drying Additive on the Sorption and Crystallization Behavior of Lactose. *Drying technology, 28*(3), 422-429.

Wu, W. D., Liu, W., Gengenbach, T., Woo, M. W., Selomulya, C., Chen, X. D., & Weeks, M. (2014). Towards spray drying of high solids dairy liquid: Effects of feed solid content on particle structure and functionality. *Journal of Food Engineering, 123*, 130-135.

Yampolskaya, G., & Platikanov, D. (2006). Proteins at fluid interfaces: Adsorption layers and thin liquid films. *Advances in colloid and interface science, 128*, 159-183.

Ye, A., Anema, S. G., & Singh, H. (2007). Behaviour of homogenized fat globules during the spray drying of whole milk. *International Dairy Journal, 17*(4), 374-382.

APPENDICES

APPENDIX 1. COMMISSIONING OF THE SPRAY DRYER

A.1.1. Temperature trends and heat loss

The spray dryer *Niro Atomizer* was successfully commissioned to ensure full functionality of all installed measurement devices. For the measurement of the relative humidity of the outlet air, a HOBO probe (HAMA GmbH & Co KG, Germany) was installed at the exhaust pipe, together with a thermo couple. Water and energy balances were performed to determine if possible condensation of water on exhaust pipes and energy losses through the dryer walls and exhaust pipes were a problem. Temperature runs without and with additional water feeding can be seen in Figures A1 and A2. The first runs were performed by varying the water feed rate, atomizing air pressure and air inlet temperatures to see the overall efficiency of the dryer regarding heat losses and to determine the mass balances around the system. Air inlet temperatures of 160°C to 240°C were tested with water feed rates of 1 kg/h to 3 kg/h, and the resulting chamber outlet air temperatures and relative humidities were recorded. The air velocity was measured using a pitot tube at different positions along the exhaust pipe to calculate the overall air flow rate. It was discovered that the air flow is not always constant, but depends on the air temperature. Higher air outlet temperatures lead to lower air flows, probably due to a lower efficiency of the fan.

A large amount of heat loss (38 to 57%) from the spray drying system was observed, especially within the dying chamber and along the exhaust pipes, and when increasing the feed rate (Table A1). Hence we chose to insulate the exhaust pipes to reduce the heat loss and to enhance the overall efficiency of the dryer. However, the additional insulation did not result in either better performance or decreased heat loss. Generally, it takes a long time for the outlet data to reach a constant steady state (up to 1 ½ hours), as can be seen in Figure A3.

Table A1. Calculation of energy losses of spray dryer *Niro Atomizer* at various conditions.

AIR, IN		Air,out				Water, in	Water,out (Vapor)	Energy loss (within dryer, exhaust pipes and cyclone)
T [°C]	RH [%]	T,chamber out [°C]	T,exhaust out [°C]	RH[%]	M,air [kg/h]	M,wat [kg/h]	M,wat [kg/h]	[%]
220	42	106.5	78.2	3.4	102	1.0	0.4 +-1.3	56.7
220	42	91.7	69.8	10.8	102	2.0	1.6+-0.8	47.3
220	42	76.4	61.5	24	102	3.0	2.8 +-0.5	38
200	42	100.5	75.4	3.8	102	1.0	0.35 +-1.0	54.3
200	42	86	67.4	12.3	102	2.0	1.7 +-0.7	42.8

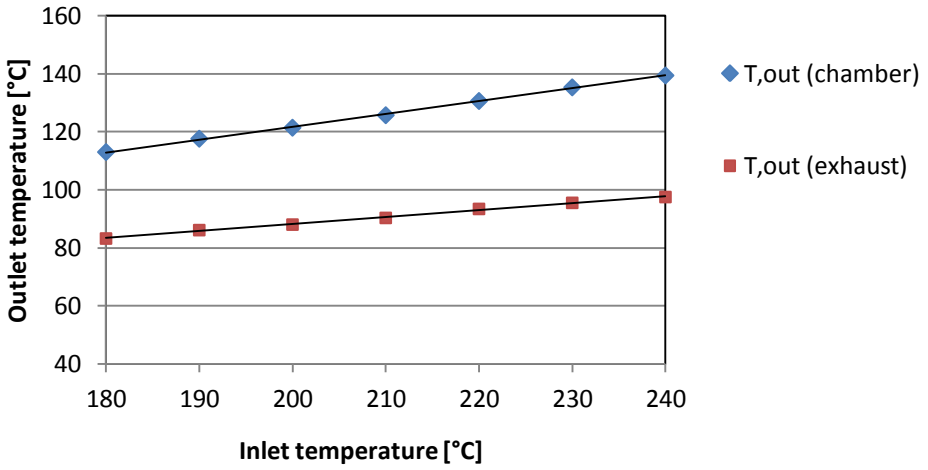

Figure A1: Temperature trend of inlet and outlet temperatures without water evaporation.

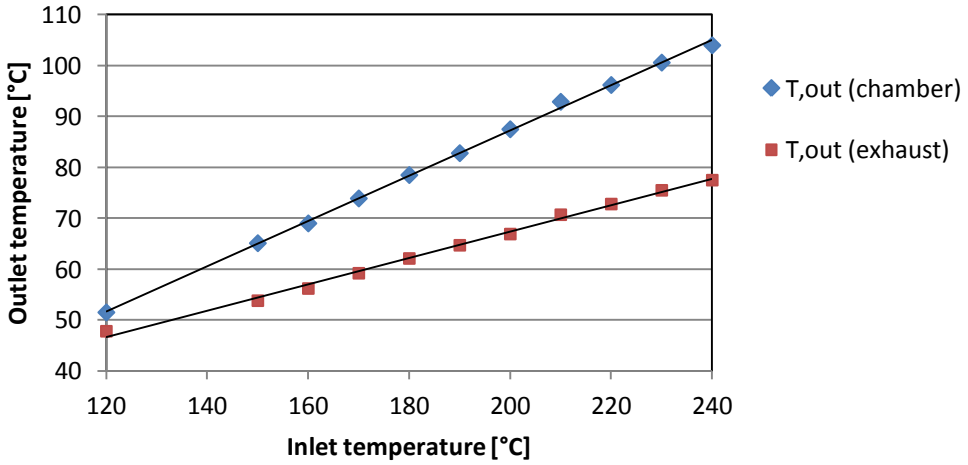

Figure A2: Temperature trends of inlet and outlet temperatures (pure water droplets; 2.2kg/h feed).

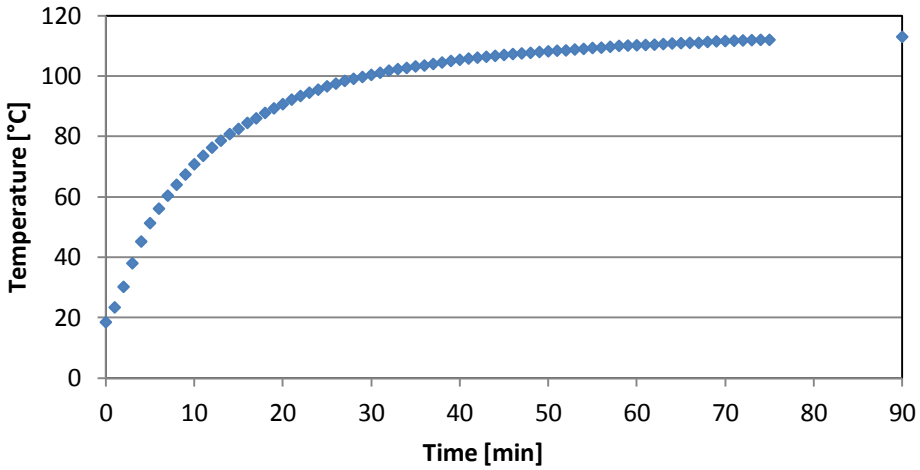

Figure A3: Start-up of the spray dryer at 180°C.

A.1.2. Spray drying studies of whole milk powder (WMP) and skim milk powder (SMP)

Test runs with WMP and SMP were performed to analyze different powders regarding stickiness, residual water content and particle size distribution. The 2-fluid nozzle and rotary atomizer were used in these experiments. The first successful test-runs with milk solution, prepared from WMP, were performed using a solid content of 30 to 50% (w/w), feed rates of 2 to 4 kg/h, air inlet temperatures of 160°C to 240 °C and compressed air pressures for atomization of 0.2 to 1.5 bar. It was discovered that the 2-fluid nozzle atomizer produced very fine particles, even at low air pressures (0.2 bar), which adhered strongly to the spray dryer wall during the drying process. For WMP, this was probably due to high fat content of the surface of the particles, which resulted in very low overall powder yields, as can be seen in Figure A6.

Particle size analysis of the final powder was performed by *Laser Light Diffraction* to determine the effect of the atomizing air pressure on the final particle size. Higher atomization air pressures clearly resulted in finer particles being produced (Figure A4). Water contents of the spray-dried powders were measured using a heat balance (Sartorius) at 85 °C. The weight loss of a thin layer of powder sample was measured until no further water evaporation occurred, and the final weight loss was recalculated to give the water content (dry basis) of the powder sample. Results of the water content measurements can be seen in Figure A5. Higher inlet temperatures resulted in dryer powder particles due to the greater

energy supply. Higher atomization pressures result in smaller particles, and it was therefore expected that powders would have a lower water content due to the higher ratio of droplet surface area to droplet volume and thus faster drying rate. This trend cannot be clearly observed in Figure A4. A possible explanation might be that the particles might reabsorb moisture from the wet air, when collected in the glass jar, especially at higher relative humidities of the outlet air, and thus equilibrate with the humid air. Smaller particles, in particular, re-equilibrate faster due to their higher surface area, compared to larger particles.

A) Particle size analysis by *Laser Light Diffraction*

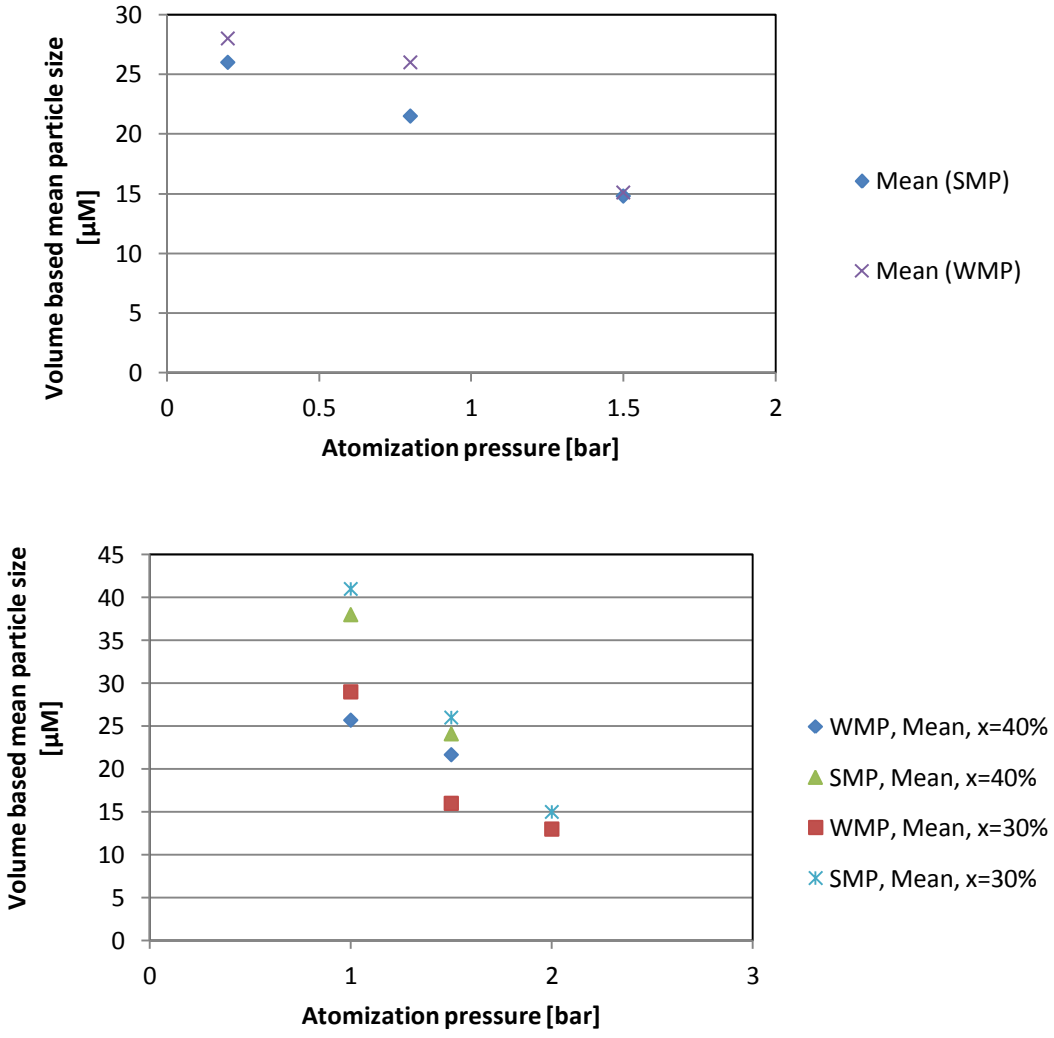

Figure A4: Particle size distribution of spray-dried milk powder at different atomization pressure (top: 2-fluid nozzle; bottom: rotary atomizer)

B) Water content measurements using a heat balance (Sartorius)

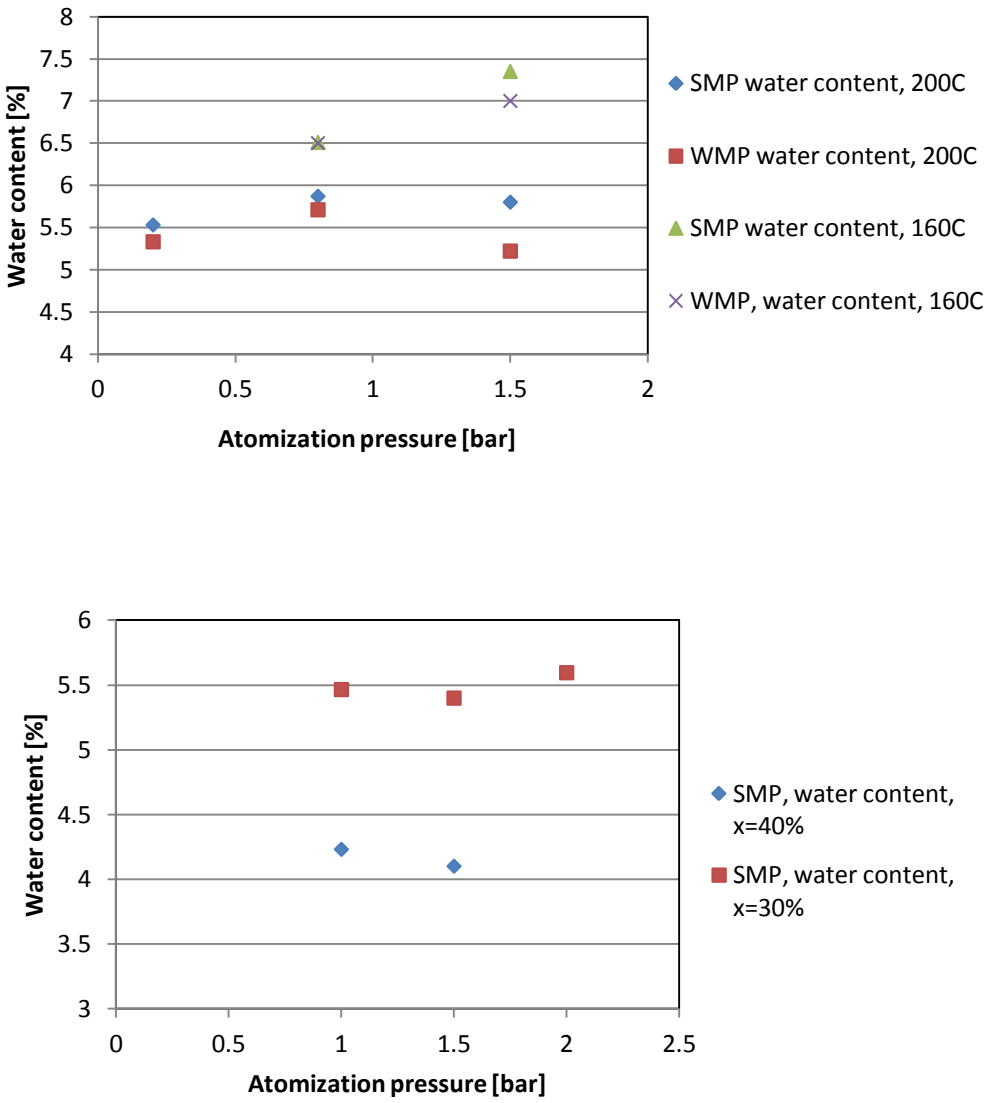

Figure A5: Water content measurements of spray-dried milk powder at different atomization pressures (top: 2-fluid nozzle; bottom: rotary atomizer)

C) Powder yield after spray drying (without banging with hammer)

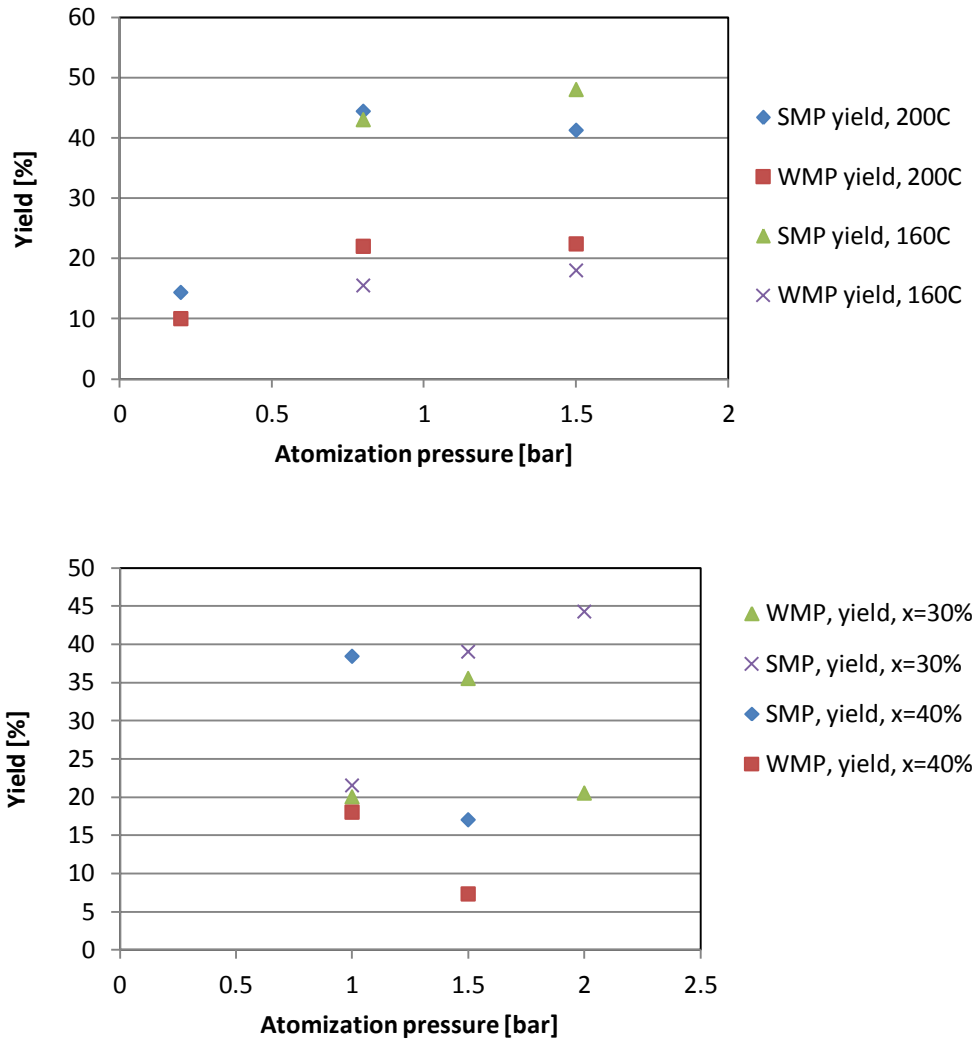

Figure A6: Yield measurements of spray-dried milk powder at different atomization pressures (top: 2-fluid nozzle; bottom: rotary atomizer)

A.1.3. Comparative study of 2-fluid nozzle and rotary atomizer

A detailed comparative study was performed between the 2-fluid nozzle (2FN) and the rotary atomizer (RA). Results are only described here in short.

Operational conditions:

- T_{in} = 200°C
- T_{out} = 80 +/- 2°C
- Relative humidity $(RH)_{out}$ = 22 +/- 1%
- $p_{atomization}$ = 1.0 bar (2FN), 1.5 bar (RA)
- Solid content = 30% (w/w)
- Feed rate = 2.8 kg/h
- Air flow = 120 +/- 5 kg/h

Particle Size

Particle sizes with a volume based median of 17 to 20 µm were spray-dried under the conditions mentioned above. It was observed that the rotary atomizer produced larger SMP particles than WMP particles, while the 2-fluid nozzle produced larger WMP particles than SMP particles. Possible reasons for this could be that the rotary atomizer produces WMP particles with higher free fat content than the 2-fluid nozzle, which results in a lower surface tension during atomization. Given the higher measured viscosity of WMP solution compared to SMP solution, the WMP particles should be considerably larger than SMP particles, if fat was not present on the emulsion droplets after leaving the atomizer. Therefore, the emulsion droplets leaving the atomization advice could have had free fat on their surfaces, which might have reduced the surface tension of the droplets, so that the WMP particles became smaller than the SMP particles. The centrifugal force of the rotary atomizer might have been responsible for that effect.

Particle Size Distribution (PSD)

When WMP particles were spray-dried, no obvious differences in particle size distributions were observed between powders produced using the rotary atomizer and those produced using the 2-fluid nozzle. However, the rotary atomizer produced a broader particle size distribution of SMP particles compared to the 2-fluid nozzle.

Energy consumption

It was observed that the rotary atomizer required a higher compressed air pressure (1.5 bar) for atomization than did the 2-fluid nozzle (1.0 bar) to achieve the same final particle sizes.

Water contents of final powder

There was no observable difference in the residual water contents of spray-dried powders produced using the rotary atomizer and those produced using the 2-fluid nozzle. Generally, SMP particles showed slightly higher water contents compared to WMP particles. This might be due to the hygroscopic behaviour of proteins and lactose on the surface of SMP particles causing the powder to absorb moisture when collected in the glass jar. The surfaces of WMP particles are mainly covered by fat that does not tend to absorb as much moisture due to its hydrophobic character. Enhanced drying of the droplets using the rotary atomizer, which produces droplet trajectories different to those produced by a two-fluid nozzle, could not be observed.

Yield

It could be observed that the 2-fluid nozzle produced slightly higher yields than the rotary atomizer. One possible explanation is that the rotary atomizer creates a wider spray angle that favours the interaction of the droplets with the chamber wall, resulting in greater powder build-up within the spray dryer.

Spray drying performance

It could be observed that the rotary atomizer was very sensitive to solution conditions, such as high viscosity, induced by a high solid content of the spray-dried solution. A reduction of the rotation speed was noticed during spray drying, probably due to the very sticky solution within the cavities of the atomization device. In contrast, the 2-fluid nozzle showed a higher flexibility, was easier to operate and could also be used with solutions of higher solid content without complications. Only at solid contents of 50% (w/w) and higher was there a strong risk of nozzle blockage.

APPENDIX 2. THE USE OF SURFACE ACTIVE MILK PROTEINS AS FUNCTIONAL COATINGS FOR SPRAY-DRIED LACTOSE POWDER

A.2.1. XPS - calculation of surface composition using a matrix (Fäldt et al., 1993)

Method A (considering C, N and O)

<u>3-component system, e.g. lactose-protein-fat</u>

The elemental composition (%C, %N, %O) of 3 pure components (here: lactose ("Lac"), protein ("Pro"), fat ("Fat")) are measured individually by XPS and can be written in form of a matrix A, as follows:

$$A = \begin{matrix} Lac(\%C) & Pro(\%C) & Fat(\%C) \\ Lac(\%N) & Pro(\%N) & Fat(\%N) \\ Lac(\%O) & Pro(\%O) & Fat(\%O) \end{matrix}$$

The measured elemental composition of the powder analyzed by XPS can be written in form of a vector b, as follows:

$$b = \begin{matrix} \%C \\ \%N \\ \%O \end{matrix}$$

Now, we can write:

$$A.c = b \qquad \text{(A1)}$$

where c represents the percentages of solids in the surface layer of around 10 nm thickness (measured by XPS), as follows:

$$c = \begin{matrix} \%Lac \\ \%Pro \\ \%Fat \end{matrix}$$

which results in:

(1) %C = [Lac(%C). %Lact+ Prot(%C). %Prot+ Fat(%C). %Fat]

(2) %N= [Lac(%N). %Lact+ Prot(%N). %Prot+ Fat(%N). %Fat]

(3) %O= [Lac(%O). %Lact+ Prot(%O). %Prot+ Fat(%O). %Fat]

Equation A1 needs to be transformed in order to calculate the vector c, as follows:

$$c(\%) = A^{-1}.b.100\%$$

where A^{-1} is the inverse of Matrix A.

2-component system, e.g. lactose-protein

The elemental composition (%C, %N, %O) of 2 pure components (here: lactose ("Lac") and protein ("Pro") are measured individually by XPS and can be written in form of a matrix A, as follows:

$$A = \begin{matrix} Lac(\%C) & Pro(\%C) \\ Lac(\%N) & Pro(\%N) \\ Lac(\%O) & Pro(\%O) \end{matrix}$$

The measured elemental composition of the analyzed powder by XPS can be written in form of a vector b, as follows:

$$b = \begin{matrix} \%C \\ \%N \\ \%O \end{matrix}$$

We want to calculate the solid composition at the particulate surface c:

$$c = \begin{matrix} \%Lac \\ \%Pro \end{matrix}$$

When using Equation A2, we have an over-determined system, because we have 3 known parameter but only 2 un-known parameters. Since there is no exact solution, the *least-square* approximation has to be used to calculate the solid composition of the surface layer of around 10 nm thickness (c), as follows:

$$\| A.c - b \| \approx 0 \ (as\ small\ as\ possible)$$

$$A^T.A.c = A^T.b \qquad \text{(A2)}$$

where A^T is the transpose of the matrix A.

Equation A2 can now be transformed to

$$c = [(A^T.A)^{-1}.A^T].b$$

Method B (considering only N)

2-component system, e.g. lactose-protein

The elemental composition (%C, %N, %O) of 2 pure components (here: lactose ("Lac") and protein ("Pro") are measured individually by XPS and can be written in form of a matrix A, as follows:

$$A = \begin{matrix} Lac(\%C) & Pro(\%C) \\ Lac(\%N) & Pro(\%N) \\ Lac(\%O) & Pro(\%O) \end{matrix}$$

The measured elemental composition of the analyzed powder by XPS can be written in form of a vector b, as follows:

$$b = \begin{matrix} \%C \\ \%N \\ \%O \end{matrix}$$

Because Lac(%N)=0, the percent nitrogen (%N), which was measured by XPS, can be used to calculate the percentages of lactose and protein, as follows:
Using Equation A1, we can write:

$$\%Pro = \frac{\%N}{Pro(\%N)} .100\% \quad \text{(A3)}$$

$$\%Lac = 100\% - \%Pro \quad \text{(A4)}$$

A comparison of method A and B was performed, as illustrated in Figure A11. Data are all within experimental uncertainty at Na-Cas bulk concentration ≥ 1wt%. A relative uncertainty of ± 5 wt% was estimated here, based on 3 repeat measurements.

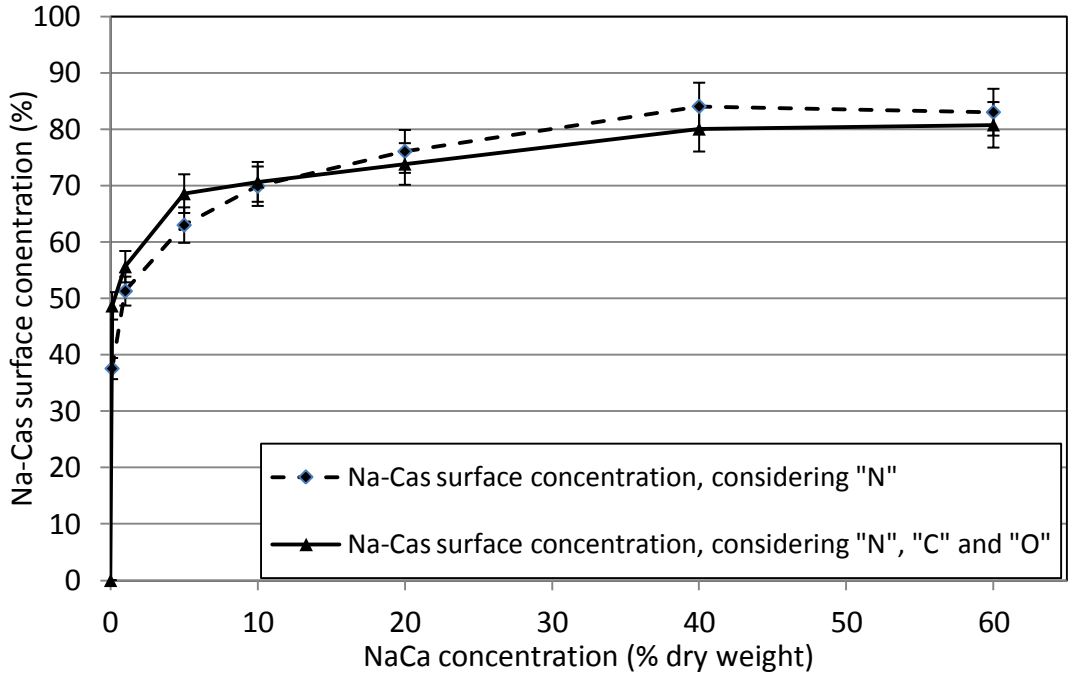

Figure A11: Calculated Na-Cas surface concentration of spray-dried lactose/Na-Cas powders (at pH7, TS=10 wt%, varying lactose/Na-Cas total ratios), using Method A (solid line) and Method B (dashed line).

A.2.2. XRD results of spray-dried sucrose, lactose and maltose powders

Figure A12 shows the diffraction patterns of several maltose, lactose, lactose/Na-Cas and sucrose/Na-Cas powders, spray-dried under various spray drying conditions to show that no crystallization occurred for any of the sugars during spray drying.

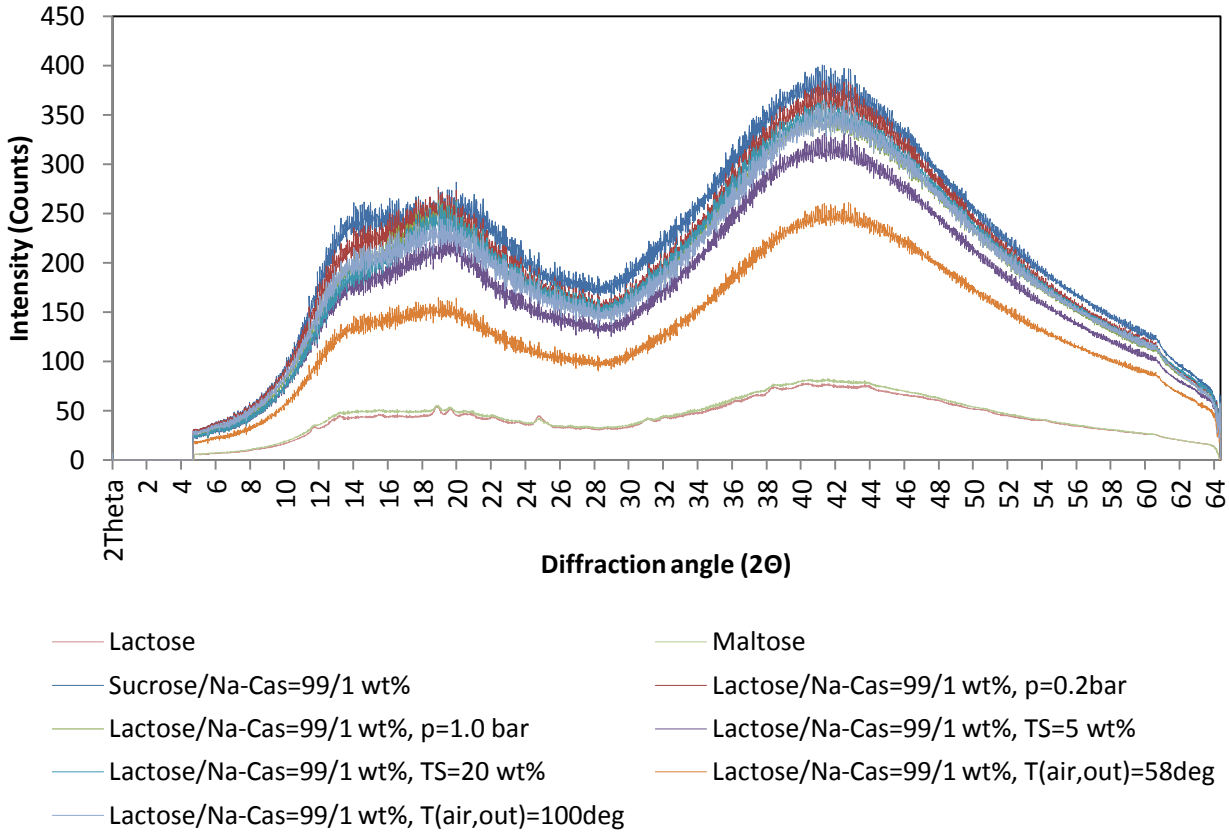

Figure A12: XRD diffraction pattern of several maltose, lactose, lactose/Na-Cas and sucrose/Na-Cas powders.

A.2.3. DSC measurements of lactose and lactose/additive=9/1 wt% powders

Figure A13 shows DSC profiles of pure lactose and lactose/Na-Cas powders with 1, 10 and 20 wt% of Na-Cas, respectively. Powders were equilibrated in a closed desiccator containing a super-saturated LiCl-solution at 30°C, which resulted in a relative humidity of around 11.4% within the desiccator. After equilibration, 5 to 12 mg aliquots of powder were weighed and transferred into 50 µL aluminium pans (Perkin Elmer, BO14-3017) and hermetically sealed. Samples were heated up from 50 to 200°C with a 50°C/min heating rate, using an Elmer DSC8000 instrument (Perkin Elmer, USA). A high heating rate was chosen due to the higher recorded sensitivity for the glass transition temperature. PYRIS Software was used to calculate onset and peak temperatures for the glass transition and crystallization. A clear increase in the crystallization temperatures, as observed by an exothermic heat flow peak, occurred with increasing protein concentrations. This was caused by a binding of lactose with proteins, resulting in increasing glass transition temperatures and delayed crystallization.

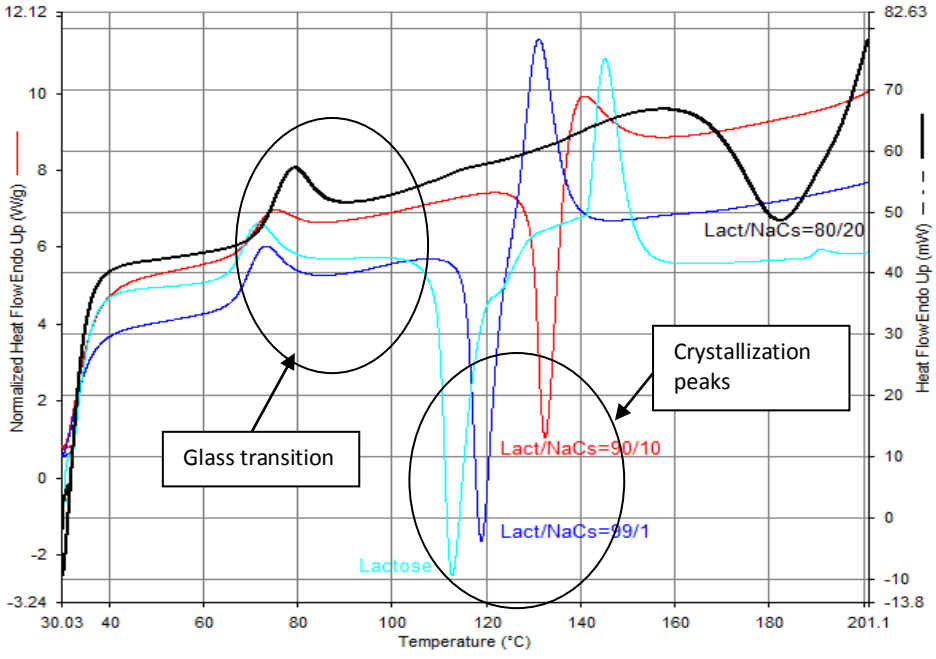

Figure A13: DSC profiles of pure lactose and lactose/Na-Cas=99/1; 90/10; 80/20 wt% powders.

A.2.4. Powder flowability tests of spray-dried lactose/WPI powders

Figure A10 shows the powder flows of spray-dried lactose/WPI powders, with varying WPI bulk concentrations, through a vibrating sieve. Powder flowability was significantly increased in the presence of protein, even when protein represented just 0.1 wt% of total solids. This is due to the increase in glass transition temperature upon protein adsorption, which results in less agglomerated powders. Compared to lactose/Na-Cas powders, lactose/WPI powders gave slightly improved powder flows through the vibrating sieve (for protein bulk concentrations between 0.1 and 5 wt%).

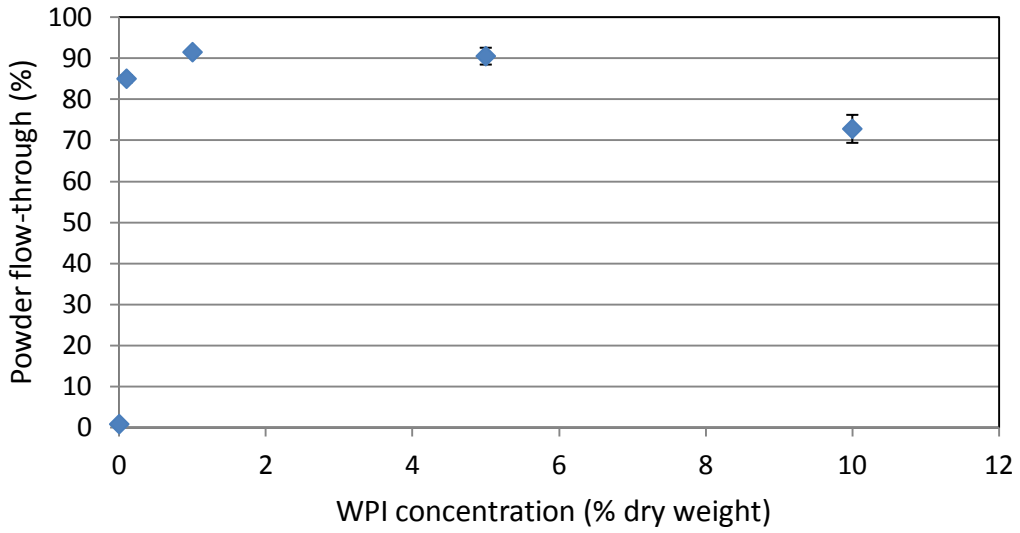

Figure A14: Powder flows of spray-dried lactose/WPI powder with varying WPI bulk concentration through a vibrating sieve.

A.2.5. Effect of pH on particle size, bulk density and powder morphology and powder functional properties of spray-dried Na-Cas and WPI powders

Table A2 shows the measured particle sizes and powder bulk densities of Na-Cas and WPI powders spray-dried at various solution pHs. Figure A15 and A16 show the effect of the pH on the particulate morphology of spray-dried Na-Cas and WPI powders. Spray-dried WPI powders had poorer powder flows than spray-dried Na-Cas powders, probably due to the WPI particles being considerably smaller (Table A2). Wetting times were significantly longer for pure Na-Cas powders, compared to WPI powers, irrespective of the pH. The lower bulk density of Na-Cas powder would have contributed towards it having longer wetting times than the WPI powder (Table A2), as would its presumably higher surface hydrophobicity (Na-Cas is more flexible than WPI and has a distinctive hydrophobic region, which allows it to orientate higher amounts of non-polar residues towards the air-water interface, as described in Section 2.2.4. (Thompson et al, 2008)).

Table A2: Particle size and powder bulk density of Na-Cas and WPI powders, spray-dried at various solution pHs.

	Vol. based particle size (µm)		**Powder bulk density (kg/L)**	
pH	Na-Cas	WPI	Na-Cas	WPI
8.5	24 ± 1	13 ± 1	0.23 ± 0.02	0.31 ± 0.03
7.0	23 ± 1	13 ± 1	0.22 ± 0.02	0.33 ± 0.03
6.0	25 ± 1	14 ± 1	0.21 ± 0.02	0.28 ± 0.03
	Flowability (%)		**Wetting time (min)**	
pH	Na-Cas	WPI	Na-Cas	WPI
8.5	90 ± 2	4 ± 1	24 ± 5	10 ± 1
7.0	77 ± 1	1 ± 1	31 ± 8	9 ± 1
6.0	33 ± 4	1 ± 1	60 ± 4	8 ± 2

Differences in particle size and bulk density between spray-dried WPI and Na-Cas particles can be explained by the higher flexibility of Na-Cas proteins, which cause a higher particle wall elasticity and thus a stronger expansion of particulates during drying. This results in Na-Cas particles being larger with lower density, compared to spray-dried WPI particles. This is further supported by the SEM micrographs showing larger particles with larger invasions of the particle wall for Na-Cas powder (Figure A11). A high number of WPI particles seemed to have a collapsed particle structure, which may be caused by a too high internal pressure within the internal vacuole (Figure A12). The particle walls of WPI-containing lactose particles seemed too weak or simply not elastic enough to expand in a similar way to the walls of Na-Cas-containing lactose particles, and thus may have collapsed at the weakest point. The collapsed particle structure was also shown by Vehring (2008), for glycoproteins spray-dried at higher Pe numbers.

Vehring (2008) provides another possible explanation for the formation of large, low density particles in the presence of flexible molecules such as proteins or polymers. He assumes that the earlier in the spray drying process that the particle surface formation occurs, the more likely it is that particles of lower density will be produced, due to a "sink-hole" developing after surface formation and further moisture loss during spray drying. Due to its higher surface activity and lower solubility, Na-Cas was likely to form a shell earlier than WPI and thus formed larger particles of lower average density. However, Na-Cas also gave very large, smooth particles, which seemed to be "blown-up" by an internal vacuole and solidified before becoming deflated by the vacuole, thus we assume that vacuole formation was very likely to have occurred here. Additionally, a faster formation of the surface of Na-Cas particles might have contributed towards the particle walls being less resistant to vacuole-induced deformations.

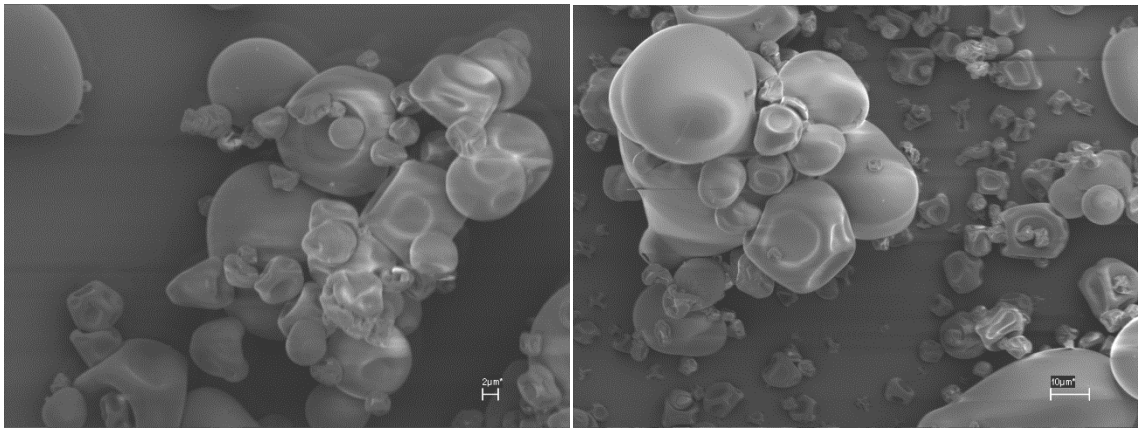

Figure A15: Na-Cas powder, spray-dried at a solution pH of 8.5 (left) and pH6 (right).

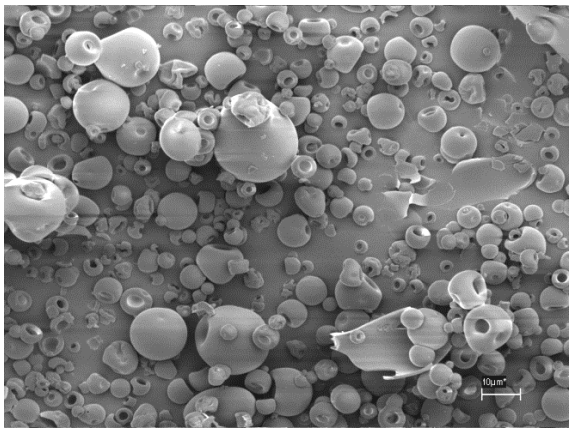

Figure A16: WPI powder, spray-dried at a solution pH of 7.

APPENDIX 3. INVESTIGATION OF SOLUTE SEGREGATION BETWEEN LACTOSE AND NA-CAS FOR DIFFERENT DRYING SYSTEMS

A.3.1. Matlab code (for calculation of moisture content gradients during film-drying (lactose/Na-Cas=9/1 wt%, 10wt% TS, T(drying air)=40 °C)

```
%Drying of a thin film in warm air_Numerical approach
%Determination of moisture gradients within the drying film
v_air=1.1; %m/s
L_film=125*10^-6; % m, film thickness
L=0.1; %m length of interfacial film
A=0.09*0.09; %Surface area of drying film
V=A*L_film;
x_s0=0.1; %kg solids/(kg water+solids)=initial solids content
X_w0=9; %kg water/kg solids=initial water conten(dry basis)
x_w0=X_w0/(1+X_w0) %kg water/(kgwater+solids)=initial water content (wet
basis)
x_lactose=0.09;
x_NaCas=0.01;
x_lactsol=0.9;
x_NaCassol=0.1;
Xin=9; %kg water/kg dry
Xfin=0.05; %kg water/kg tot
T_air=40; %deg
T_film=24.3; %deg
T_int=(T_air+T_film)/2; %deg
RH_air=28; %%
X_air=0.013 %kg water/kg dry air
k_air=0.0264; %W/(mK)
k_H2O=0.68; %W/(mK)
roh_air=(1.205+1.127)/2; %30deg
roh_H2O=1000; %kg/m^3
roh_lactose=1525; %kg/m^3
roh_NaCas=1250; %kg/m^3
roh_solids=1/(x_lactsol/roh_lactose+x_NaCassol/roh_NaCas);
roh_sol=1/((x_w0/roh_H2O)+(x_lactose/roh_lactose)+(x_NaCas/roh_NaCas))
%kg/m^3

m_film=V*roh_sol %initial mass and density of solution
msol=(1-Xin)*m_film;
```

```
mwat=Xin*m_film;
h=580.85;
D=2.1*10^(-9); %m^2/s (22deg)
D_air=2.77*10^-5; %m^s/s (air)
D_vap=2.42*10^-5; %m^2/s, moisture in air
p_sat_Tfilm=exp(23.161004868-3792.404857/((T_film+273.15)-47.19962873));
p_sat_Tair=exp(23.161004868-3792.404857/((T_air+273.15)-47.19962873));
p_air=p_sat_Tair*RH_air/100;
p_atm=1.01325*10^5; %Pa
R=8.314; %J/(mol K) = kg m^2/(s^2 mol K)
M_water=18; %g/mol

Re=v_air*L*roh_air/mueh_air;
Sc=mueh_air/(roh_air*D_air);
Sh_ave=0.664*Re^0.5*Sc^(1/3); %Correlation for laminar flow above flat
plate

k_c=0.0215; % m/s convective mass transfer coefficient
dn_dt=k_c*p_atm/((R*1000)*(273.15+T_int))*log((p_atm-p_air)/(p_atm-
p_sat_Tfilm)) %kmol/*m^2s)
dm_dt=dn_dt*M_water; % area specific mass flux water from film into air
kg/m^2/s

D_upper=5.7E-10;%m^2/s
D_cent=1.4E-10;
D_lower=7.0E-11;

IE=1; %Isotropy component
L_filmdry=(roh_sol*x_s0)*L_film/roh_solids;
SVOL_0=(roh_H2O/(roh_solids*Xin+roh_H2O))
DC_0_upper=(D_upper*SVOL_0^(1+1/IE));
DC_0_cent=(D_cent*SVOL_0^(1+1/IE));
DC_0_lower=(D_lower*SVOL_0^(1+1/IE));



j=90001;
i=11;
deltax=L_filmdry/10; %m
deltat=0.005; %s
```

```
%Bi=k_c*deltax/D
%Fo=D*deltat/deltax^2

A_upper=zeros(j,i);
A_upper(1,:)=[Xin Xin Xin Xin Xin Xin Xin Xin Xin Xin Xin];

A_cent=zeros(j,i);
A_cent(1,:)=[Xin Xin Xin Xin Xin Xin Xin Xin Xin Xin Xin];

A_lower=zeros(j,i);
A_lower(1,:)=[Xin Xin Xin Xin Xin Xin Xin Xin Xin Xin Xin];

SVOL_upper=zeros(j,i); %Volume fraction
SVOL_upper(1,:)=[SVOL_0 SVOL_0 SVOL_0 SVOL_0 SVOL_0 SVOL_0 SVOL_0 SVOL_0
SVOL_0 SVOL_0 SVOL_0];

SVOL_cent=zeros(j,i); %Volume fraction
SVOL_cent(1,:)=[SVOL_0 SVOL_0 SVOL_0 SVOL_0 SVOL_0 SVOL_0 SVOL_0 SVOL_0
SVOL_0 SVOL_0 SVOL_0];

SVOL_lower=zeros(j,i); %Volume fraction
SVOL_lower(1,:)=[SVOL_0 SVOL_0 SVOL_0 SVOL_0 SVOL_0 SVOL_0 SVOL_0 SVOL_0
SVOL_0 SVOL_0 SVOL_0];

DC_upper=zeros(j,i); %Varying diffusion coefficients
DC_upper(1,:)=[DC_0_upper DC_0_upper DC_0_upper DC_0_upper DC_0_upper
DC_0_upper DC_0_upper DC_0_upper DC_0_upper DC_0_upper DC_0_upper];

DC_cent=zeros(j,i);
DC_cent(1,:)=[DC_0_cent DC_0_cent DC_0_cent DC_0_cent DC_0_cent DC_0_cent
DC_0_cent DC_0_cent DC_0_cent DC_0_cent DC_0_cent];

DC_lower=zeros(j,i);
DC_lower(1,:)=[DC_0_lower DC_0_lower DC_0_lower DC_0_lower DC_0_lower
DC_0_lower DC_0_lower DC_0_lower DC_0_lower DC_0_lower DC_0_lower];

CELL=zeros(j,i); %Shrinking nodes
CELL(1,1)=(deltax/2/SVOL_upper(1,1));
CELL(1,11)=(deltax/2/SVOL_upper(1,11));
```

```
CELL(1,2:10)=(deltax./SVOL_upper(1,2:10));

i=11; %nodes Sitance steps
j=90001; %Time steps

%Calculating the average moisture contents
L_dry=[L_filmdry/20 L_filmdry/10 L_filmdry/10 L_filmdry/10 L_filmdry/10
L_filmdry/10 L_filmdry/10 L_filmdry/10 L_filmdry/10 L_filmdry/10
L_filmdry/20]



for j=1:90001
    for i=1

A_upper(j+1,i)=2*deltat/deltax^2*(DC_upper(j,i)+DC_upper(j,i+1))/2*(A_upper
(j,i+1)-A_upper(j,i))+A_upper(j,i);
        SVOL_upper(j+1,i)=roh_H2O/(roh_solids*A_upper(j+1,i)+roh_H2O);
        DC_upper(j+1,i)=D_upper*SVOL_upper(j+1,i)^(1+1/IE);
        CELL_upper(j+1,i)=deltax/2/SVOL_upper(j+1,i);
        CELLSUM_upper(j,i)=0;



A_cent(j+1,i)=2*deltat/deltax^2*(DC_cent(j,i)+DC_cent(j,i+1))/2*(A_cent(j,i
+1)-A_cent(j,i))+A_cent(j,i);
        SVOL_cent(j+1,i)=roh_H2O/(roh_solids*A_cent(j+1,i)+roh_H2O);
        DC_cent(j+1,i)=D_cent*SVOL_cent(j+1,i)^(1+1/IE);
        CELL_cent(j+1,i)=deltax/2/SVOL_cent(j+1,i);
        CELLSUM_cent(j,i)=0;



A_lower(j+1,i)=2*deltat/deltax^2*(DC_lower(j,i)+DC_lower(j,i+1))/2*(A_lower
(j,i+1)-A_lower(j,i))+A_lower(j,i);
        SVOL_lower(j+1,i)=roh_H2O/(roh_solids*A_lower(j+1,i)+roh_H2O);
        DC_lower(j+1,i)=D_lower*SVOL_lower(j+1,i)^(1+1/IE);
        CELL_lower(j+1,i)=deltax/2/SVOL_lower(j+1,i);
        CELLSUM_lower(j,i)=0;

        %AV(j,i)=(A(j,i)*L_dry(i)); %Average moisture content
```

```
    end
    for i=2:10

A_upper(j+1,i)=deltat/deltax^2*((DC_upper(j,i)+DC_upper(j,i+1))/2*(A_upper(
j,i+1)-A_upper(j,i))-(DC_upper(j,i)+DC_upper(j,i-1))/2*(A_upper(j,i)-
A_upper(j,i-1)))+A_upper(j,i);
        SVOL_upper(j+1,i)=roh_H2O/(roh_solids*A_upper(j+1,i)+roh_H2O);
        DC_upper(j+1,i)=D_upper*SVOL_upper(j+1,i)^(1+1/IE);
        CELL_upper(j+1,i)=deltax/SVOL_upper(j+1,i);
        CELLSUM_upper(j,i)=(sum(CELL_upper(j,2:i)));


A_cent(j+1,i)=deltat/deltax^2*((DC_cent(j,i)+DC_cent(j,i+1))/2*(A_cent(j,i+
1)-A_cent(j,i))-(DC_cent(j,i)+DC_cent(j,i-1))/2*(A_cent(j,i)-A_cent(j,i-
1)))+A_cent(j,i);
        SVOL_cent(j+1,i)=roh_H2O/(roh_solids*A_cent(j+1,i)+roh_H2O);
        DC_cent(j+1,i)=D_cent*SVOL_cent(j+1,i)^(1+1/IE);
        CELL_cent(j+1,i)=deltax/SVOL_cent(j+1,i);
        CELLSUM_cent(j,i)=(sum(CELL_cent(j,2:i)));


A_lower(j+1,i)=deltat/deltax^2*((DC_lower(j,i)+DC_lower(j,i+1))/2*(A_lower(
j,i+1)-A_lower(j,i))-(DC_lower(j,i)+DC_lower(j,i-1))/2*(A_lower(j,i)-
A_lower(j,i-1)))+A_lower(j,i);
        SVOL_lower(j+1,i)=roh_H2O/(roh_solids*A_lower(j+1,i)+roh_H2O);
        DC_lower(j+1,i)=D_lower*SVOL_lower(j+1,i)^(1+1/IE);
        CELL_lower(j+1,i)=deltax/SVOL_lower(j+1,i);
        CELLSUM_lower(j,i)=(sum(CELL_lower(j,2:i)));

        %AV(j,i)=(A(j,i)*L_dry(i));
    end

    for i=11
        A_upper(j+1,i)=(-dm_dt/roh_solids-(DC_upper(j,i)+DC_upper(j,i-
1))/2*(A_upper(j,i)-A_upper(j,i-1))/deltax)/deltax*2*deltat+A_upper(j,i);
        SVOL_upper(j+1,i)=roh_H2O/(roh_solids*A_upper(j+1,i)+roh_H2O);
        DC_upper(j+1,i)=D_upper*SVOL_upper(j+1,i)^(1+1/IE);
        CELL_upper(j+1,i)=deltax/2/SVOL_upper(j+1,i);
        CELLSUM_upper(j,i)=(sum(CELL_upper(j,1:i)));
```

```
        A_cent(j+1,i)=(-dm_dt/roh_solids-(DC_cent(j,i)+DC_cent(j,i-
1))/2*(A_cent(j,i)-A_cent(j,i-1))/deltax)/deltax*2*deltat+A_cent(j,i);
        SVOL_cent(j+1,i)=roh_H2O/(roh_solids*A_cent(j+1,i)+roh_H2O);
        DC_cent(j+1,i)=D_cent*SVOL_cent(j+1,i)^(1+1/IE);
        CELL_cent(j+1,i)=deltax/2/SVOL_cent(j+1,i);
        CELLSUM_cent(j,i)=(sum(CELL_cent(j,1:i)));

        A_lower(j+1,i)=(-dm_dt/roh_solids-(DC_lower(j,i)+DC_lower(j,i-
1))/2*(A_lower(j,i)-A_lower(j,i-1))/deltax)/deltax*2*deltat+A_lower(j,i);
        SVOL_lower(j+1,i)=roh_H2O/(roh_solids*A_lower(j+1,i)+roh_H2O);
        DC_lower(j+1,i)=D_lower*SVOL_lower(j+1,i)^(1+1/IE);
        CELL_lower(j+1,i)=deltax/2/SVOL_lower(j+1,i);
        CELLSUM_lower(j,i)=(sum(CELL_lower(j,1:i)));

        %AV(j,i)=(A(j,i)*L_dry(i));
    end
    %AVE(j)=sum(AV(j,1:11))/L_filmdry;
    %AVER(j,1:11)=[AVE(j) AVE(j) AVE(j) AVE(j) AVE(j) AVE(j) AVE(j) AVE(j)
AVE(j) AVE(j) AVE(j)];
end

%Connecting Endpoints
%X_surf=[A(1,11) A(4001,11) A(20001,11) A(40001,11) A(60001,11) A(70001,11)
A(80001,11) 0];
%y_surf=[CELLSUM(1,11) CELLSUM(4001,11) CELLSUM(20001,11) CELLSUM(40001,11)
CELLSUM(60001,11) CELLSUM(70001,11) CELLSUM(80001,11) L_filmdry];



% Simplified analytical model

t_dry=[0:10:450]; %s
t=[0:0.005:450];

X_w=9;



X_w=Xin-dm_dt.*t_dry/(x_s0*roh_sol*L_film);
x_w=X_w./(1+X_w);
t_drying=Xin/dm_dt*x_s0*roh_sol*L_film; %s
```

```
t_drying=t_drying/60 %min



plot(t_dry,X_w,'r-')
xlabel('Time (s)')
ylabel('Moisture content (kg/kg)')
title('Moisture content of drying film (numerical solution)','fontsize',12)
axis ([0 800 0 9])
legend('Analyt.Model')
figure

%plot(t,AVE,'b-')
xlabel('Time (s)')
ylabel('Moisture content (kg/kg)')
title('Moisture content of drying film (numerical solution)','fontsize',12)
axis ([0 800 0 9])
%legend('Numer.Model')
figure



plot(CELLSUM_upper(2,:),A_upper(2,:),'-r')
xlabel('Distance (m)')
ylabel('Moisture content (kg H2O/kg solid)')

title('Moisture content profiles within a drying film at
T(air)=60deg','fontsize',12)
hold on



%plot(CELLSUM(20001,:),AVER(20001,:),'-k*')

plot(CELLSUM_upper(10001,:),A_upper(10001,:),'-g')
plot(CELLSUM_cent(10001,:),A_cent(10001,:),'--g')
plot(CELLSUM_lower(10001,:),A_lower(10001,:),'--g')
%plot(CELLSUM(40001,:),AVER(40001,:),'-k*')



plot(CELLSUM_upper(30001,:),A_upper(30001,:),'-r')
plot(CELLSUM_cent(30001,:),A_cent(30001,:),'--r')
```

```
plot(CELLSUM_lower(30001,:),A_lower(30001,:),'--r')
%plot(CELLSUM(70001,:),AVER(70001,:),'-k*')


plot(CELLSUM_upper(50001,:),A_upper(50001,:),'-b')
plot(CELLSUM_cent(50001,:),A_cent(50001,:),'--b')
plot(CELLSUM_lower(50001,:),A_lower(50001,:),'--b')
%plot(CELLSUM(60001,:),AVER(60001,:),'-k*')

plot(CELLSUM_upper(70001,:),A_upper(70001,:),'-b')
plot(CELLSUM_cent(70001,:),A_cent(70001,:),'--b')
plot(CELLSUM_lower(70001,:),A_lower(70001,:),'--b')
%plot(CELLSUM(60001,:),AVER(60001,:),'-k*')

plot(CELLSUM_upper(90001,:),A_upper(90001,:),'-b')
plot(CELLSUM_cent(90001,:),A_cent(90001,:),'--b')
plot(CELLSUM_lower(90001,:),A_lower(90001,:),'--b')
%plot(CELLSUM(60001,:),AVER(60001,:),'-k*')


%plot(y_surf,X_surf,'-k')
axis([0 1.1E-4 0 9.5])
legend('0s','50s','100s','200s','300s','350s','400s');
hold off
```

A.3.2. Stability check: Differences in calculated water contents along the drying films with m nodes and at different times (n)

Table A3 shows the calculated water contents within the drying lactose/Na-Cas=9/1wt% film (initial TS of 10 wt%) at increasing drying times (n) and at different nodes (m) throughout the film. Time steps and number of nodes were varied in this numerical model in order to investigate numerical stability. A grid and time-step sensitivity analysis was performed, where the number of spaces was doubled and time-steps were halved. This resulted in differences in the water contents of <0.1% for any the water contents calculated throughout the film thickness.

Table A3: Calculated moisture content X_W within a drying lactose/Na-Cas=9/1wt% films, illustrated in form of a matrix A(n,m) where n=time and m= film distance

Film Drying: Δt=0.01s, Δx=L_Film/10 (10 nodes)

n \ m										
8.9988	8.9979	8.9947	8.9861	8.9660	8.9224	8.8367	8.6844	8.4425	8.1021	7.6765
8.4119	8.3855	8.3069	8.1779	8.0016	7.7828	7.5278	7.2444	6.9409	6.6256	6.3061
6.8723	6.8504	6.7857	6.6810	6.5410	6.3710	6.1774	5.9661	5.7429	5.5130	5.2808
5.2847	5.2714	5.2321	5.1682	5.0817	4.9755	4.8527	4.7166	4.5703	4.4170	4.2593
3.7509	3.7439	3.7229	3.6886	3.6417	3.5834	3.5150	3.4379	3.3535	3.2633	3.1688
2.2693	2.2663	2.2573	2.2426	2.2222	2.1967	2.1662	2.1313	2.0925	2.0502	2.0049
1.1188	1.1178	1.1145	1.1092	1.1018	1.0925	1.0812	1.0681	1.0533	1.0370	1.0193

Δt=0.005s, Δx=L_Film/10 (10 nodes)

8.9988	8.9979	8.9947	8.9861	8.9660	8.9224	8.8367	8.6844	8.4426	8.1022	7.6765
8.4118	8.3855	8.3069	8.1779	8.0016	7.7828	7.5278	7.2444	6.9409	6.6256	6.3061
6.8723	6.8504	6.7857	6.6810	6.5410	6.3710	6.1774	5.9661	5.7429	5.5130	5.2808
5.2847	5.2714	5.2321	5.1682	5.0817	4.9755	4.8527	4.7166	4.5703	4.4170	4.2593
3.7509	3.7439	3.7229	3.6886	3.6417	3.5834	3.5150	3.4379	3.3535	3.2633	3.1688
2.2693	2.2663	2.2573	2.2426	2.2222	2.1967	2.1662	2.1313	2.0925	2.0502	2.0049
1.1188	1.1178	1.1145	1.1092	1.1018	1.0925	1.0812	1.0681	1.0533	1.0370	1.0193

Δt=0.01s, Δx=L_Film/20 (20 nodes)

8.9991	8.9989	8.9983	8.9972	8.9953	8.9921	8.9870	8.9790	8.9668	8.9486	8.9223
8.8853	8.8344	8.7666	8.6787	8.5683	8.4338	8.2746	8.0920	7.8884	7.6674	
8.4108	8.4042	8.3844	8.3514	8.3056	8.2471	8.1762	8.0935	7.9996	7.8949	7.7804
7.6569	7.5253	7.3866	7.2419	7.0921	6.9384	6.7818	6.6233	6.4638	6.3041	
6.8702	6.8647	6.8483	6.8212	6.7837	6.7362	6.6792	6.6133	6.5393	6.4578	6.3696
6.2754	6.1761	6.0724	5.9650	5.8546	5.7420	5.6276	5.5122	5.3962	5.2801	
5.2833	5.2800	5.2700	5.2536	5.2308	5.2018	5.1669	5.1264	5.0806	5.0298	4.9745
4.9150	4.8518	4.7853	4.7158	4.6438	4.5697	4.4938	4.4164	4.3380	4.2588	
3.7501	3.7484	3.7431	3.7343	3.7221	3.7066	3.6878	3.6659	3.6410	3.6133	3.5828
3.5498	3.5144	3.4769	3.4374	3.3960	3.3531	3.3086	3.2630	3.2162	3.1685	
2.2689	2.2682	2.2659	2.2622	2.2570	2.2503	2.2422	2.2328	2.2219	2.2098	2.1964
2.1817	2.1659	2.1490	2.1311	2.1121	2.0923	2.0715	2.0500	2.0277	2.0047	
1.1187	1.1184	1.1176	1.1163	1.1144	1.1120	1.1091	1.1057	1.1017	1.0973	1.0923
1.0869	1.0811	1.0748	1.0680	1.0608	1.0532	1.0453	1.0369	1.0282	1.0192	

Δt=0.005s, Δx=L_Film/20 (20 nodes)

8.9991	8.9989	8.9983	8.9972	8.9953	8.9921	8.9870	8.9790	8.9668	8.9486	8.9223
8.8853	8.8344	8.7666	8.6787	8.5684	8.4338	8.2746	8.0920	7.8884	7.6674	
8.4108	8.4042	8.3844	8.3514	8.3056	8.2470	8.1762	8.0935	7.9996	7.8949	7.7804
7.6569	7.5253	7.3866	7.2419	7.0921	6.9384	6.7818	6.6233	6.4638	6.3041	
6.8702	6.8647	6.8483	6.8212	6.7837	6.7362	6.6792	6.6133	6.5393	6.4578	6.3696
6.2754	6.1761	6.0724	5.9650	5.8546	5.7420	5.6276	5.5122	5.3962	5.2801	
5.2833	5.2800	5.2700	5.2536	5.2308	5.2018	5.1669	5.1264	5.0806	5.0298	4.9745
4.9150	4.8518	4.7853	4.7158	4.6438	4.5697	4.4938	4.4164	4.3380	4.2588	
3.7501	3.7484	3.7431	3.7343	3.7221	3.7066	3.6878	3.6659	3.6410	3.6133	3.5828
3.5498	3.5144	3.4769	3.4374	3.3960	3.3531	3.3086	3.2630	3.2162	3.1685	
2.2689	2.2682	2.2659	2.2622	2.2570	2.2503	2.2422	2.2328	2.2219	2.2098	2.1964
2.1817	2.1659	2.1490	2.1311	2.1121	2.0923	2.0715	2.0500	2.0277	2.0047	
1.1187	1.1184	1.1176	1.1163	1.1144	1.1120	1.1091	1.1057	1.1017	1.0973	1.0923
1.0869	1.0811	1.0748	1.0680	1.0608	1.0532	1.0453	1.0369	1.0282	1.0192	

A.3.3. Calculation of Peclet numbers

According to Vehring et al. (2007), drying temperatures between 100 and 150 ^{o}C resulted in evaporation rates of 6 to 10 μm^2/ms for pure water droplets (in dry stagnant air). Evaporation rates of a similar order can be expected during spray drying, because once fine droplets have left the atomizer they attain the velocity of the surrounding air, as stated by Masters (2002). Assuming a droplet temperature of 80^{o}C during spray drying, the diffusion coefficients of lactose and Na-Cas (β-casein) were estimated at 1.67x10^{-9} m^2/s and 2.06x10^{-10} m^2/s, respectively. Equation 2.7 (Chapter 2) was used to calculate *Pe* numbers during spray drying for Na-Cas and lactose, according to Vehring et al. (2007): 6.07 and 0.75, respectively.

Pe numbers for drying films (lactose/Na-Cas90/10 wt%, 10 wt% TS, 80 °C drying air temperature) were calculated using Equation 4.25 and the following parameters: an initial and final approximated film thickness of 125 and 9 μm (the latter calculated using Equations 4.9 and 4.10), a drying time of approximately 7 minutes (estimated from Figure 4.), solution viscosity of 0.677 mPa.s (for a wet bulb temperature of 35°C) and hydrodynamic radii of 0.436 nm for lactose (Ribeiro et al., 2006) and 3.54 nm for Na-Cas (calculated using the Stokes Einstein equation - Equation A5). The calculation yielded *Pe* numbers of 0.2 and 0.02 for Na-Cas and lactose, respectively, in a film drying system at 80 °C.

$$D_W = \frac{K_B T}{6\pi\mu R_i} \qquad \text{(A5)}$$

where D_W is the Fickian diffusion coefficient, K_B is the Boltzmann constant, R_i is the hydrodynamic radius of the solute i, T is the solvent temperature and μ is the dynamic viscosity of the solution.

APPENDIX 4. THE USE OF HYDROXYPROPYL-METHYLCELLULOSE AS A FUNCTIONAL COATING FOR SPRAY-DRIED PHARMACEUTICAL LACTOSE

A.4.1. UV/VIS spectroscopy: Calibration curves of Na-Cas, lactose and HPMC

Figure A13 shows the UV_280nm calibration curves of dissolved lactose, Na-Cas and HPMC. A linear relationship between solid concentration and absorbance can be seen. According to the *Lambert Beer Law* the concentration of the dissolved solute can be calculated, as follows:

$$A_{280} = a\lambda \,.\, b \,.\, c_{protein} \qquad \text{(A6)}$$

where $a\lambda$ is a wavelength-dependent absorptivity coefficient, b is the path length and $c_{protein}$ is the concentration of dissolved protein in solution.

The absorbance of Na-Cas proteins at 280 nm was significantly higher than the absorbance of lactose or HPMC. Thus, it was assumed that the UV/Vis absorption at 280nm was influenced only by the presence of Na-Cas in the solution, and that the presence of lactose and HPMC did not affect the measured absorbance.

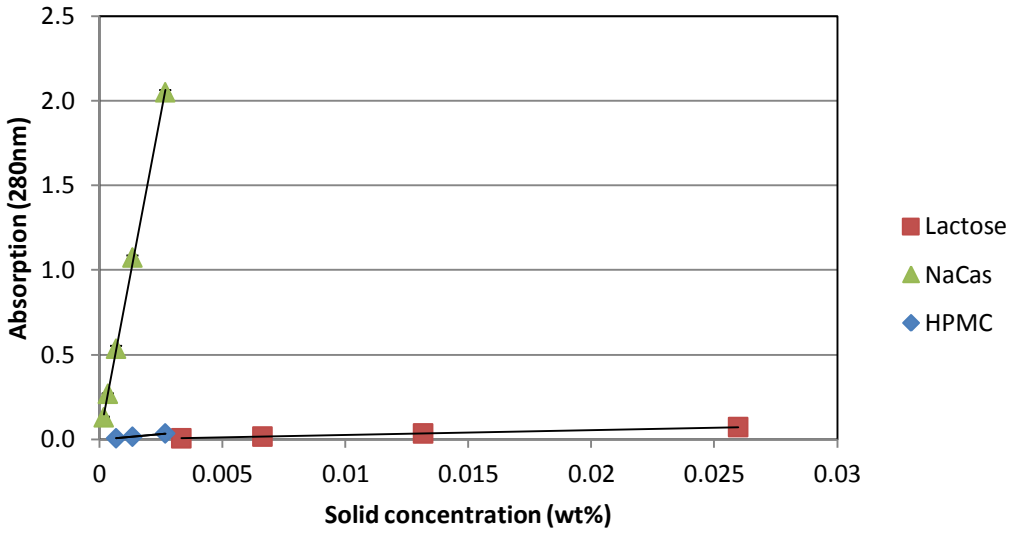

Figure A13: Calibration curves of aqueous lactose, Na-Cas and HPMC solutions - UV absorbance at 280nm versus weight concentration of the solute.